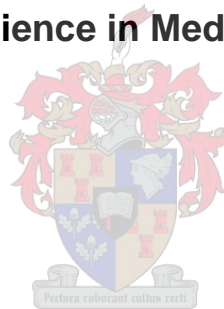# ROLE OF GLYCOGEN SYNTHASE KINASE 3 (GSK-3) AND ITS SUBSTRATE PROTEINS IN THE DEVELOPMENT OF CARDIOMYOPATHY ASSOCIATED WITH OBESITY AND INSULIN RESISTANCE.

Thabile Brian Flepisi

Thesis presented in partial fulfillment of the requirements for the degree

Master of Science in Medical Sciences

Department of Biomedical Sciences

Division of Medical Physiology

University of Stellenbosch

Supervisor: Prof. B Huisamen

Co-Supervisor: Prof. A Lochner

March 2011

Declaration

By submitting this thesis electronically, I declare that the entirety of the work contained therein is my own, original work, that I am the sole author thereof (save to the extent explicitly otherwise stated), that reproduction and publication thereof by Stellenbosch University will not infringe any third party rights and that I have not previously in its entirety or in part submitted it for obtaining any qualification.

March 2011

ABSTRACT

INTRODUCTION: Glycogen synthase kinase-3 (GSK-3) is a serine-threonine protein kinase that was first discovered as a regulator of glycogen synthase thus playing a role in glycogen synthesis (Embi et al. 1980). GSK-3 has also been shown to down regulate the expression of SERCA-2a (a calcium ATPase pump) thus playing a role in myocardial contractility (Michael et al. 2004). However, SERCA-2a activity is regulated by phospholamban (PLM) and sarcolipin (SLN) (Asahi et al. 2003). GSK-3 is constitutively active in cells and can be acutely inactivated by insulin through phosphorylation by PKB/Akt. However, GSK-3 is known to phosphorylate and inhibit IRS-1 protein, thus disrupting insulin signaling (Eldar-Finkelman et al. 1996). In addition, abnormally high activities of GSK-3 protein has been implicated in several pathological disorders which include type 2 diabetes, neuron degenerative and affective disorders (Eldar-Finkelman et al 2009). This led to the development of new generations of inhibitors with specific clinical implications to treat these diseases (Martinez 2008). GSK-3 inhibition has been shown to improve insulin and blood glucose levels and to be cardioprotective during ischemia/reperfusion (Nikoulina et al. 2002; Kumar et al. 2007).

AIMS: To determine whether myocardial GSK-3 protein and its substrate proteins are dysregulated in obesity and insulin resistance, and whether a specific GSK-3 inhibitor can prevent or reverse the cardiovascular pathology found in obese and insulin resistant animals.

OBJECTIVES: To correlate the alterations in expression and activation of GSK-3 protein in a well characterised rat model of obesity coupled to insulin resistance with: i) myocardial contractile dysfunction and an inability of hearts to withstand ischemia/reperfusion, ii) the activation and expression of phospholamban and SERCA-2a in the sarcoplasmic reticulum, iii) the activation of intermediates (IRS-1, IRS-2 and PKB/Akt) that lie upstream in the activation pathway of GSK-3 and iv) to determine the effects of inhibition of GSK-3 on the abovementioned parameters.

METHODS: Age and weight matched male Wistar rats (controls and diet induced obese (DIO) animals) were used in the present study. Controls were fed normal rat chow, while DIOs were fed a rat chow diet supplemented with sucrose and condensed milk, for 8 or 16 weeks. Half of each group of animals were treated with the GSK-3 inhibitor for 4 weeks (from 12 to 16 weeks). After the feeding and treatment period, animals were weighed, sacrificed, hearts removed and freeze clamped immediately or perfused with Krebs-Henseleit buffer and subjected to low flow ischemia (25 min) followed by 30 min reperfusion. Biometric (body weight, intraperitoneal fat, ventricular weight and tibia length) and biochemical (fasting blood glucose and insulin levels) parameters were determined. Expression of GSK-3, PKB/Akt, IRS-1, IRS-2, SERCA-2a and Phospholamban were determined by Western blotting. Ca^{2+} ATPase activity was determined spectrophotometrically.

RESULTS: At both 8 and 16 weeks DIO animals were significantly bigger than control animals and this was associated with increased intraperitoneal fat in DIOs. In DIO animals: IRS-1 was downregulated at 8 weeks and both IRS-1 and IRS-2 as well as PKB/Akt at 16 weeks. There was an increased tendency of GSK-3 expression at both 8 and 16 weeks in DIO animals while SERCA-2a was severely downregulated from 8 weeks onwards and associated with lower Ca^{2+}-ATPase activity. PLM expression was upregulated but its phosphorylation was attenuated. At 16 weeks, baseline heart rate (225 vs 275 in control, P<0.0001, n=6) and rate pressure product (21000 vs 30000 in control, P=0.019, n=6) were significantly lower in hearts from DIO animals. Functional recovery was unchanged but the time to ischemic contracture development was increased (11.6±0.4 control vs 16.2±0.5 min DIO, P<0.01, n=6). Treatment had no effect on total GSK-3 expression. However, GSK-3 phosphorylation was significantly increased in treated controls, while there was no significant difference in DIO animals. However, there was a tendency for an increased GSK-3 phosphorylation in treated DIO animals. GSK-3 inhibitor, improved hypertrophy in DIO animals, while it led to its development in control animals. GSK-3 inhibitor improved IRS-2 expression in both control and DIO animals while it had no effect on IRS-1 and SERCA-2a expression and activity. However, GSK-3 inhibition increased PKB/Akt and phospholamban phosphorylation in DIO animals.

CONCLUSION: These findings show that high calorie diet as well as imbalance between energy intake and expenditure lead to the development of obesity and insulin resistance in male Wistar rats. We showed that GSK-3 and its substrate proteins are dysregulated in obesity and insulin resistance. The reduced SERCA-2a expression at baseline may have a negative impact on cardiac function. By treating

the animals with GSK-3 inhibitor, we showed that GSK-3 protein may not be responsible for changes seen at baseline. The decreased IRS-1 and SERCA-2a expression may have been caused by a different mechanism other than the actions of GSK-3. However, according to this study, GSK-3 may play a role in regulation of IRS-2 expression but not in IRS-1. Increased PKB/Akt phosphorylation may contribute to the GSK-3 inhibition. In addition, GSK-3 inhibition may reverse cardiac hypertrophy in DIO animals, thus acting as a negative regulator of hypertrophy.

OPSOMMING

Inleiding: Glikogeen sintase kinase-3 (GSK-3), 'n serien/threonien proteïen kinase, is oorspronklik ontdek as 'n rolspeler in glikogeen sintese, aangesien dit 'n reguleerder van glikogeen sintase is (Embi *et al.*1980). Intussen is dit ook bevind dat GSK-3 die uitdrukking van SERCA-2a ('n kalsium ATPase pomp) kan afreguleer en dus sodoende 'n rol speel in miokardiale kontraktiliteit (Michael *et al.* 2004). Die aktiwiteit van SERCA-2a kan egter ook gereguleer word deur fosfolamban (PLM) en sarkolipin (Asahi *et al.* 2003). GSK-3 is deurgaans aktief, maar kan tydelik geïnaktiveer word onder kondisies van insulien stimulasie deur PKB/Akt gemedieerde fosforilering. Aan die ander kant is dit bekend dat GSK-3 die IRS-1 proteïen kan fosforileer om dus sodoende insulien sein-transduksie af te reguleer (Eldar-Finkelman *et al.* 1996). Daarmee saam is abnormaal hoë vlakke van GSK-3 aktiwiteit geassosieer met verskeie patologiese versteurings, insluitend tipe 2 diabetes, neuron degeneratiewe en affektiewe versteurings (Eldar-Finkelman *et al.* 2009). Daar is dus nuwe generasies GSK-3 inhibitore ontwikkel met die kliniese potensiaal om hierdie patologieë te behandel (Martinez 2008). Dit is al bevind dat GSK-3 inhibisie geassosieer kan word met beide die normalisering van plasma insulien- en glukose vlakke, asook kardiobeskerming in die konteks van iskemie/herperfusie (Nikoulina *et al.* 2002; Kumar *et al.* 2007).

Doelwitte: Om te bepaal of GSK-3 proteïen en sy substraat proteïene gedisreguleer is onder kondisies van obesiteit en insulien weerstandigheid, asook om vas te stel of 'n spesifieke GSK-3 inhibitor die kardiovaskulêre patologie wat gevind word in obese en insulien weerstandige diere kan verhoed of omkeer.

Mikpunte: Om veranderinge in uitdrukking en aktiwiteit van GSK-3 proteïen in 'n goed gekarakteriseerde rotmodel van obesiteit, gekoppel aan insulien weerstandigheid, te korreleer met die volgende: i) miokardiale kontraktiele disfunksie en onvermoë om kardiale iskemie/herperfusie besering te weerstaan, ii) aktivering en uitdrukking van PLM en SERCA-2a in die sarkoplasmiese retikulum, iii) die aktivering van intermediêres wat proksimaal geleë is in die insulienseintransduksiepad van GSK-3 (IRS-1, IRS-2 en PKB/Akt) en iv) om die effek van behandeling met 'n spesifieke inhibitor van GSK-3 op die bogenoemde punte te bepaal.

Metodes: Ouderdoms- en gewigsgepaarde manlike Wistar rotte (kontrole en dieet geïnduseerde obees (DIO) diere) is in die studie gebruik. Kontrole diere was normale rotkos gevoer, terwyl die DIO diere op 'n dieet van rotkos aangevul met sukrose en kondensmelk geplaas is vir 'n periode van 8 of 16 weke. Helfte van die diere van elke groep is behandel met die GSK-3 inhibitor vir 4 weke (vanaf week 12 tot 16). Na afloop van die voer- en behandelingsperiode is die diere geweeg, doodgemaak en die harte verwyder om dan of onmiddelik gevriesklamp te word, of retrograad geperfuseer te word met Krebs-Hensleit buffer. Ex vivo geperfuseerde harte is dan blootgestel aan 25 minute lae vloei iskemie gevolg deur 30 minute herperfusie. Biometriese (liggaamsgewig, intraperitoneale vet, ventrikulêre gewig en tibia lengte) en biochemiese (vastende bloedglukose en -insulien vlakke) parameters is telkens bepaal. Western klad tegnieke is gebruik om die uitdrukking en fosforilering van GSK-3, PKB/Akt, IRS-1, IRS-2, SERCA-2a en PLM te bepaal. Ca^{2+}-ATPase aktiwiteit is spektrofotometries bepaal.

Resultate: Na beide 8 en 16 weke was die DIO diere beduidend swaarder as die kontrole diere. Hierdie gewigstoename was geassosieer met meer intraperitoneale vet in die DIO diere. Verder, in die DIO diere was IRS-1 afgereguleer na 8 weke, terwyl beide IRS-1 en IRS-2 asook PKB/Akt afgereguleer was na 16 weke. GSK-3 uitdrukking het 'n neiging getoon om toe te neem na beide 8 en 16 weke in die DIO diere, terwyl SERCA-2a beduidend afgereguleer was reeds vanaf 8 weke, geassosieer met laer Ca^{2+}-ATPase aktiwiteit. PLM uitdrukking het toegeneem en die fosforilering daarvan was verlaag. Op 16 weke was die basale harttempo (225 vs 275 in die kontrole groep, P<0.0001, n=6) en tempo druk produk (21000 vs 30000 in die kontrole groep, P=0.019, n=6) betekenisvol laer in die DIO diere. Funksionele herstel het onveranderd gebly, alhoewel die tyd tot iskemiese kontraktuur toegeneem het in die DIO groep (kontrole: 11.6±0.4 min vs DIO: 16.2±0.5 min, P<0.01, n=6). Toediening van die inhibitor het geen effek op totale GSK-3 uitdrukking gehad nie. Fosforilering van GSK-3 was egter wel beduidend verhoog in die behandelde kontrole diere, terwyl daar geen verskille in die DIO groep was nie. Die fosforilering van GSK-3 het wel geneig na 'n toename in die behandelde DIO diere. Die GSK-3 inhibitor het kontrasterende effekte op hipertrofie gehad: dit het dit omgekeer in die DIO groep, maar veroorsaak in die kontrole diere. Daarmee saam het die inhibitor die uitdrukking van IRS-2 in beide DIO en kontrole diere gestimuleer, maar geen effek op IRS-1 en SERCA-2a uitdrukking en aktiwiteit gehad nie. GSK-3 inhibisie het wel PKB/Akt en PLM fosforilering in die DIO diere verhoog.

Gevolgtrekking: Hierdie bevindinge toon dat 'n hoë kalorie dieet, tesame met 'n wanbalans tussen energie inname en verbruiking, lei tot die ontwikkeling van obesiteit en insulien weerstand in manlike Wistar rotte. Die studie het ook getoon dat GSK-3 en sy substraat proteïene wel gedisreguleer is in obesiteit en insulien weerstandigheid. Die verlaagde basale uitdrukking van SERCA-2a mag dalk 'n negatiewe impak hê op kardiale funksie. Behandeling van die diere met 'n GSK-3 inhibitor het getoon dat GSK-3 moontlik nie verantwoordelik is vir die basislyn veranderinge nie. Die afname in IRS-1 en SERCA-2a uitdrukking kan moontlik toegeskryf word aan ander meganismes buiten die effekte van GSK-3. Hierdie studie toon wel dat GSK-3 moontlik 'n rol speel in die regulering van die uitdrukking van IRS-2, maar nie IRS-1 nie. Verhoogde PKB/Akt fosforilering mag dalk bydra tot die inhibisie van GSK-3. Daarmee saam blyk dit dat GSK-3 inhibisie hipertrofie kan omkeer in DIO diere, om dan sodoende op te tree as 'n negatiewe reguleerder van hipertrofie, maar in normale kontrole diere, hipertrofie in die hand werk.

ACKNOWLEDGEMENTS

I would also like to thank God for hearing me whenever I cry upon him.

TABLE OF CONTENTS

LIST OF FIGURES AND TABLES

LIST OF ABBREVIATIONS

Acetyl-coenzyme A	Acetyl-CoA
Action potential	AP
Adaptor protein with a PH and SH2 domain	APS domain
Adenosine Di-Phosphate	ADP
Adenosine Tri-Phosphate	ATP
Amino	NH_2
Ammonium persulfate	APS
Ampere	A
Analysis of variance	ANOVA
Arrythmogenic right ventricular cardiomyopathy	ARVC
Asparagine	Asp
Beats per minute	BPM
Body mass index	BMI
Body weight	BW
Bovine serum albumin	BSA
Ca^{2+} induced Ca^{2+} release	CICR
Calcium Chloride	$CaCl_2$
Calcium current	I_{Ca}
Calcium	Ca^{2+}
cAMP response element binding	CREB
Carbon dioxide	CO_2
Carboxy	COOH
Chirone	CHIR

Chloride	Cl^-
Copper sulphate	$CuSO_4$
Coronary artery disease	CAD
Coronary flow	CF
Cyclin dependent protein kinase	CDK
Dalton	Da
Diastolic pressure	DP
Diet induced obese	DIO
Dilated cardiomyopathy	DCM
Distilled Water	dH_2O
End ischemic diastolic pressure	EIDP
Endoplasmic reticulum	ER
Enhanced chemiluminescence	ECL
Enzyme linked immunosorbent assay	ELISA
Ethylenediamin tetraacetic acid	EDTA
Ethyline glycol tetraacetic acid	EGTA
Eukaryotic initiation factor-2 beta	eIF2B
Excitation-contraction coupling	ECC
Extracellular signal regulated kinase	ERK
Folin Ciocalteus	Folin C
Frequently rearranged during advanced T cell lymphomas	FRAT
Glucose transporter	GLUT
Glycine	GLY
Glycogen synthase kinase-3	GSK-3
Glycogen synthase	GS

Grams	g
Heart rate	HR
Heat shock transcription factor-1	HSF-1
Homeostasis model assessment	HOMA
Hydrogen	H^+
Hypertrophic cardiomyopathy	HCM
Hypertrophic cardiomyopathy association	HCA
Immunoglobin	Ig
Inorganic Phosphate	P_i
Insulin receptor substrate-1	IRS-1
Insulin receptor substrate-2	IRS-2
Intra-peritoneal	IP
Kilo Dalton	kDa
Kilo grams	kg
Kilo Joules	KJ
Krebs Heinseleit	KH
Left ventricle	LV
Left ventricular developed pressure	LVDevP
Lithium Chloride	LiCl
Lithium	Li^+
Litre	l
Low flow ischemia	LFI
L-type calcium channel	$I_{ca,L}$
Lysine	Lys
Magnesium sulphate	$MgSO_4$

Magnesium	Mg^{+2}
Maximum velocity	V_{max}
Messenger-Ribonucleic acid	mRNA
Micro litres	µl
Millimetres of mercury	mmHg
Milli-ampere	mA
Milli-litres	ml
Milli-Volts	mV
Minutes	Min
Molecular weight	MW
Myeloblastosis c	cMyb
N,N,N,N,-tetramethylethylenediamine	TEMED
Na^+/Ca^{2+} exchanger	NCX
Nano metres	nm
National heart, lung and blood institute	NHLBI
Neuronal Nitric Oxide Synthase	nNOS
Nicotinamide adenine dinucleotide	NADH
Nitric oxide	NO
Nonesterified fatty acids	NEFAs
Oxygen	O_2
Peak contracture diastolic pressure	PCDP
Phenylmethane sulfonyl fluoride	PMSF
Phenylmethylsulphonyl fluoride	PMSF
Phoshatidylinositol 3-kinase	PI3K
Phosphatase and tensin homolog	PTEN

Phosphoinositide dependent kinase	PDK
Phosphoinosityde	PI
Phospholamban	PLM
Phosphorylation/Total	P/T
Phosphotyrosine binding	PTB
Plasmalemmal Calcium ATPase	PMCA
Pleckstrin homology	PH
Polyvinyledene Fluoride	PVDF
Potasium Chloride	KCl
Potasium phosphate	KH_2PO_4
Potassium	K^+
Potassium current	I_K
Potassium DiHydrogen Phosphate	KH_2PO_4
Proline	Pro
Protein kinase A	PKA
Protein kinase B	PKB/Akt
Protein kinase C	PKC
Pyruvate dehydrogenase	PDH
Quality control	QC
Rate pressure product	RPP
Reduced flavin adenine dinucleotide	$FADH_2$
Reducing agent	RA
Restrictive cardiomyopathy	RCM
Revolutions per minute	rpm
Ryanodine receptor	RyR

Sarcolipin	SLN
Sarcoplasmic reticulum	SR
Sarcoplasmic/endoplasmic reticulum Calcium ATPase-2a	SERCA-2a
Sodium Bicarbonate	$NaHCO_3$
Sodium bisulphite	$Na_2S_2O_5$
Sodium Chloride	NaCl
Sodium current	I_{Na}
Sodium dodecyl sulphate	SDS
Sodium dodecyl sulphate-polyacrylamide gel electrophoresis	SDS-PAGE
Sodium hydroxide	NaOH
Sodium navoate	Na_2VO_3
Sodium sulphate	$NaSO_4$
Sodium	Na^+
Sodium/Potasium ATPase	Na^+/K^+ ATPase
Src homology collagen	Shc
SRC homology-2	SH2
Standard error of a mean	SEM
Sulphuric acid	H_2SO_4
Systolic pressure	SP
Threonine	Thr
Tibia length	TL
Time to onset of ischemic contracture	TOIC
Transverse tubules	T-tubules
Tricarboxylic acid	TCA
Tri-chloroacetic acid	T-CA

Tris buffered saline	TBS
Tris-Hydrochloric acid	Tris-HCl
Valine	Val
Ventricular weight	VW
Vesicle-associated membrane protein	VAMP
Volts	V
Water	H_2O
World health organization	WHO

CHAPTER 1

LITERATURE REVIEW

1.1 Definition of Obesity

Obesity is defined as a state or condition where body fat content is increased to an extent that poses a risk to develop chronic diseases such as cardiovascular, pulmonary (sleep apnea), metabolic (diabetes, insulin resistance and dyslipidaemia), osteoarticular diseases, common forms of cancer (cervical, uterus, breast, ovarian and kidney) and other serious psychological illnesses (Bray and Bourchard 2004; Grundy 2004; Sodjinou et al. 2008).

The adipose mass may be distributed around the body and these individuals are said to be apple shaped, or the fat mass may be distributed in certain areas of the body such as abdomen, thighs and hips resulting in a pear-shaped body (Jackson et al. 2003; Wells et al. 2008). Body fat mass exceeds its normal content, partly as a result of unhealthy eating habits and sedentary lifestyle (Grundy 2004; Hicks 2006). In adults, obesity is mostly determined by calculating the body mass index (BMI), which is weight in kilograms divided by height in square meters (kg/m^2). According to the World Health Organization (WHO) criteria, individuals whose BMI is between 18.5 and 25 kg/m^2 are classified as normal, those between 25 and 30 kg/m^2 as overweight, and above 30 kg/m^2 as obese (National Institute of Health (NIH) 1998; Hicks 2006).

1.1.1 **Prevalence of obesity**

Obesity is significantly and increasingly becoming a major public health problem in both affluent and developing countries with 33% of adults reported to be overweight or obese in 2005 (Medeiros et al. 2003; Kosti and Panagiotakos 2006; Kelly et al. 2008b). It is further estimated that by 2030, 57.8% of the world's adult population would be either overweight or obese (Kelly et al. 2008b). Higher prevalence of overweight and obesity have been reported in developed countries in comparison to developing ones (35.2% vs 19.6% overweight adult and 20.3% vs 6.7% of obese people) (NIH 1998; Kelly et al. 2008b). The lower prevalence observed in developing countries does not necessarily mean that less people are affected, but is rather more due to larger populations in these countries (Kelly et al. 2008b).

However, in the past decade, the prevalence of obesity has tripled in developing countries, particularly those that have adopted a Westernized lifestyle (i.e., overconsumption of energy-dense food and increased physical inactivity) (Jackson et al. 2003; Kelly et al. 2008a). This has been attributed to, among other factors, growth in population size, urbanization, changes in lifestyle that include consumption of energy-dense food and physical inactivity (Hill and Peters 1998; Grundy 2004; Hicks 2006). Today, obesity in countries such as Brazil, China and those in Sub-Saharan Africa including South Africa, is increasing rapidly and exceeding levels reported in affluent countries (Kelly et al. 2008a). According to the WHO report published in 2005, the prevalence of overweight or obesity in America was 26.6% in men and 32.2% in women (Hicks et al 2006; Kelly et al. 2008b). In 2002, the obesity epidemic in South Africa was as high as 29% in men and 56% in women (Puoane et al. 2002; Kelly et al. 2008b).

1.2 Definition of Insulin resistance (IR)

Insulin resistance is a pathological state in which cells (muscle, adipose tissue and liver) fail to respond to the normal concentrations of insulin (review by Mlinar et al. 2007; Saltiel 2001). Insulin is a hormone produced by pancreatic beta cells that is responsible for lowering blood glucose by promoting cellular uptake, for either glycogen storage or cellular utility (Lomedico et al. 1979; Toriumi and Imai 2002; DeFronzo and Ferranini 2001; review by Mlinar et al. 2007). IR results in an inability of insulin to provide normal glucose and lipid homeostasis (Wang et al. 2004; Eckel et al. 2005). Insulin resistant individuals need higher insulin levels than normal to control blood glucose levels and as a result, the pancreas produces more to keep up with this increased demand (Eckel et al. 2005; National Diabetes Information Clearinghouse (NDIC) 2008). Under this condition the pancreas eventually fails to meet the insulin demands of the body, resulting in increased plasma glucose levels to an extent where diabetes develops (Weir and Bonner-Weir 2004; NDIC 2008).

Insulin resistance may be caused by excess weight gain (obesity) and it has also been reported that there are certain genes that make people susceptible to this condition (Reaven 1988; Haffner et al. 1997). These individuals usually have, in addition to insulin resistance, high blood pressure, excess weight around the waist (central obesity) and high levels of unwanted triglycerides (lipids) and cholesterol in the blood, leading to the development of chronic diseases such as type 2 diabetes and cardiovascular diseases (Grundy et al. 2004). Insulin resistance also results in alteration of the insulin signaling pathway (section 1.7) (review by Frojdo et al. 2009).

1.3 **Definition of Diabetes**

Diabetes is a condition whereby the blood sugar (glucose) is increased above normal levels (8 mmol/L in the fasting state), due to an inability of the body to utilize it sufficiently to produce energy (NDIC 2008; review by Frojdo et al. 2009). This state develops prior to an inability of the body to produce enough insulin, which is responsible for the intake of energy from various food sources by the cells (NDIC 2008; review by Frojdo et al. 2009). As mentioned above, insulin is also responsible for the conversion of excess plasma glucose into its storage form glycogen (Toriumi and Imai 2002; DeFronzo and Ferranini 2001; NDIC 2008). Glycogen is then stored in adipose tissues, muscles and liver for later use (Grundleger and Thenen 1982; Henry et al. 1995).

There are three types of diabetes that exist in humans, type I, II and gestational diabetes (Alberti and Zimmet 1998; Chou 2004). Type I diabetes is an autoimmune disease, that leads to the failure of the body to produce adequate concentrations of insulin, because of a lack of pancreatic beta cells (Alberti and Zimmet 1998; Hunt and Garvy 1998; Chou 2004). Type I diabetes affects children, teenagers and young adults and is known as juvenile or insulin dependent diabetes (Alberti and Zimmet 1998; NDIC 2008). Individuals with type I diabetes survive by regular insulin injections (Alberti and Zimmet 1998; NDIC 2008). In type II diabetes, also known as adult onset or noninsulin-dependent diabetes, pancreatic beta cells produce enough insulin but the peripheral insulin sensitive cells fail to respond to normal levels of insulin, a state known as insulin resistance (section 1.2) (Alberti and Zimmet 1998; Herinksen and Dokken 2006; NDIC 2008). Gestational diabetes affects pregnant

women but it disappears after birth and it is normally caused by the shortage of insulin and hormones of pregnancy (NDIC 2008).

Altered expression, activity and function of all transporters involved in calcium regulation and excitation- contraction coupling (Sarcoplasmic/endoplasmic reticulum Calcium (Ca^{2+}) ATPase (SERCA), Na^+/ Ca^{2+}-exchanger (NCX), ryanodine receptors (RyR) and plasmalemmal Ca^{2+}-ATPase (PMCA)) have been reported in both type I and II diabetic rodent models (Golfman et al. 1998; Vetter et al. 2002). Thus, diabetes is strongly associated with the development of cardiovascular complications such as diabetic cardiomyopathy (Fonarow and Srikanthan 2006). These cardiovascular complications are the leading causes of morbidity and mortality in diabetic patients (Vetter et al. 2002; Cesario et.al. 2006).

1.4 **Definition of Cardiomyopathy**

Cardiomyopathy literally means cardiac muscle pathology (Kasper et al. 2005). It is defined as a chronic disease where the heart muscle (myocardium) is weakening prior to inflammation leading to deterioration of its function (Kasper et al. 2005; Thiene et al. 2008). It also refers to a heterogeneous group of diseases of the myocardium associated with the mechanical and electrical dysfunction that usually exhibit inappropriate ventricular hypertrophy or dilation (Maron and Salberg 2001; Barry et al. 2007; Hypertrophic Cardiomyopathy Association (HCA) 2009). There are multiple causes of this condition which include among others viral infections (Kasper et al. 2005; Elliott et al. 2008; review by Wexler et al. 2009; HCA 2009). Cardiomyopathy is classified as intrinsic (primary) or extrinsic (specific/secondary) according to the cause (review by Wexler et al. 2009; HCA 2009).

1.4.1 Intrinsic cardiomyopathy

Intrinsic cardiomyopathy refers to a weakness within the cardiomyocyte that is not based on manifested systemic pathophysiological characteristics which means, it cannot be linked to a specific cause such as high blood pressure, heart valve defects, artery and congenital heart defects (Richardson et al. 1996; Fonarow and Srikanthan 2006; review by Wexler et al. 2009). There are four main types of intrinsic cardiomyopathy i.e. dilated cardiomyopathy (DCM), hypertrophic cardiomyopathy (HCM), restrictive cardiomyopathy (RCM) and arrythmogenic right ventricular cardiomyopathy (ARVC) but other types that do not readily fit into any group (unclassified cardiomyopathies) have been recognized (Richardson et al. 1996; Fuster and Hurst 2004; Thiene et al. 2008).

1.4.1.1 Dilated cardiomyopathy

It is the most common form and affects about 5 in 100 000 adults and 1 in 200 000 children (review by Wexler et al. 2009; National heart, lung and blood institute (NHLBI) 2009). As the name proclaims, in this condition the cardiac ventricles are stretched, therefore enlarged (dilated) allowing more blood to enter (NHLBI 2009; Fatkin et al. 2010). Because the heart is weak it cannot pump the blood out as normal, leading to abnormal heart rhythms called arrhythmias and heart failure (Maron et al. 2006; NHLBI 2009). Also in a dilated heart and arteries, blood moves slowly and this may result in clot (thrombus) formation, hampering the blood circulation (NHLBI 2009; Fatkin et al. 2010). In adults, dilated cardiomyopathy may be caused by coronary artery diseases (CAD) (ischemic cardiomyopathy) and hypertension, but it can also be caused by viral myocarditis, valvular disease and genetic predisposition (Hunt et al. 2005; NHLBI 2009). In children, dilated

cardiomyopathy may be caused by neuromuscular diseases such as Duchenne muscular dystrophy, Becker muscular dystrophy and Barth syndrome (Kaski et al. 2007; NHLBI 2009).

1.4.1.2 Hypertrophic cardiomyopathy

This is a state where cardiac muscle mass of the left ventricle enlarges and become hypertrophic (HCA 2009; review by Boudina and Abel 2010). It is reported that enlarged left ventricular (LV) mass is an independent risk factor for heart failure and in type 2 diabetes it may occur without an increased arterial blood pressure and may also contribute to myocardial compliance reduction (Aneja et al. 2008; HCA 2009). It may be caused by 11 mutant genes consisting of more than 500 individual transmutations, in which the most common variant involve beta-myosin heavy chain and myosin binding protein C (Maron et al. 2003; HCA 2009).

1.4.1.3 Restrictive cardiomyopathy

In this state the myocardium of the ventricles hardens or become rigid, preventing the ventricles from filling and contracting per heart beat (review by Wexler et al. 2009; NHLBI 2009). Restrictive cardiomyopathy may be caused by infiltrative processes (Maron et al. 2006; NHLBI 2009). A rare form of restrictive cardiomyopathy known as obliterative cardiomyopathy has been reported, in this type the myocardium in the apex of the left and right ventricle thickens and become fibrotic thus decreasing the volume within the ventricles (Richardson et al. 1996; NHLBI 2009).

1.4.1.4 Arrythmogenic right ventricular cardiomyopathy

Arrythmogenic right ventricular cardiomyopathy is defined as an autosomal dominant disorder of the right ventricular muscle (review by Wexler et al. 2009; NHLBI 2009). In this condition, the myocardium is replaced by fatty and fibrous tissue mass which compromise cardiac function, leading to syncope, ventricular arrhythmias, heart failure and sudden death (Hulot et al. 2004; Buja et al. 2008).

1.4.2 Extrinsic (specific) cardiomyopathy

Extrinsic (specific) cardiomyopathy is attributed to specific causes located outside the myocardium, which may be diseases involving other organs and the heart i.e. ischemic, valvular, hypertensive, and diabetic cardiomyopathy (Fonarow and Srikanthan 2006; NHLBI 2009).

1.4.2.1 Diabetic cardiomyopathy

Diabetic cardiomyopathy is the term first introduced by Rubler et al in 1972 that refer to a clinical condition which develops in patients with diabetes (Fonarow and Srinkanthan 2006; Karnik et al. 2007; review by Boudina and Abel 2010). It denotes diabetes associated changes in structure of the plasma membrane, mitochondria, sarcoplasmic reticulum (SR) and the morphology of the cardiac interstitium (review by Adeghate 2004; Karnik et al. 2007; NHLBI 2009). It is also associated with changes in the function of the myocardium, resulting in dysfunctional ventricles without chronic diseases such as coronary atherosclerosis and hypertension (Poornima et al. 2006; Karnik et al. 2007; review by Boudina and Abel 2010). The etiology of diabetic cardiomyopathy is very complex, as a result, several factors have been implicated in its pathogenesis i.e. variations in cardiac metabolism, decreased

vascular sensitivity and abnormal reactivity to various ligands, increased ventricular wall stiffness and abnormalities of various ion channels that control ionic homeostasis across the cell membrane (Hayat et al. 2004; Cesario et.al. 2006;). Diabetic cardiomyopathy may be caused by increased triglycerides and nonesterified fatty acids (NEFAs) therefore hyperlipidemia (Poornima et al. 2006; Karnik et al. 2007) or increased plasma insulin levels above normal followed by the failure of pancreatic beta cells to produce insulin. Furthermore, this leads to increased blood glucose levels (hyperglycemia), that is known to cause reactive oxygen species and reactive nitrogen species release (review by Cai and Kang 2001, Poornima et al. 2006; Karnik et al. 2007). However, it may be functionally characterized by ventricular dilation (dilated cardiomyopathy), myocyte hypertrophy (hypertrophic cardiomyopathy), prominent fibrosis and decreased or preserved systolic function (Fonarow and Srikanthan 2006; NHLBI 2009).

1.5 Cardiac myocyte

Heart muscle is a highly organized tissue, composed of several cell types including smooth muscle cells, fibroblasts and cardiac myocytes (Zellner et al. 1991; review by Walker and Spinale 1999). A cardiac myocyte is the fundamental contractile cell of the myocardium that is responsible for force generation (Zellner et al. 1991; review by Walker and Spinale 1999). However, transduction of this force into mechanical pump performance depends on the interaction between the myocyte and extracellular matrix (Robinson et al. 1986; Zellner et al. 1991; review by Walker and Spinale 1999). Extracellular matrix ensures proper alignment of the myocyte during diastole, coordinates myocyte contraction during systole and also maintains capillary patency throughout the cardiac cycle (Buck and Horwitz 1987).

The myocyte consists of a basement membrane which forms a boundary between the extracellular and intracellular spaces (Timpl 1985; Zellner et al. 1991; review by Walker and Spinale 1999). Basement membranes are primarily composed of collagen IV, the glycoprotein, laminin, fibronectin, and proteoglycans (Timpl 1985; review by Martin and Timpl 1987; Junqueira et al. 1992). The basement membrane provides an interface to the collagen matrix of the extracellular space with anchoring fibers that attach basal lamina to the underlying collagen (Stanley et al. 1982; Junqueira et al 1992). The function of the basement membrane is to provide an initial barrier that influences the selective exchange of macromolecules between the extracellular space and the myocyte (Stanley et al. 1982; review by Walker and Spinale 1999). It also provides an interface for myocyte adhesion and continuity with the extracelluar matrix (Paulsson 1992) (figure 1.1).
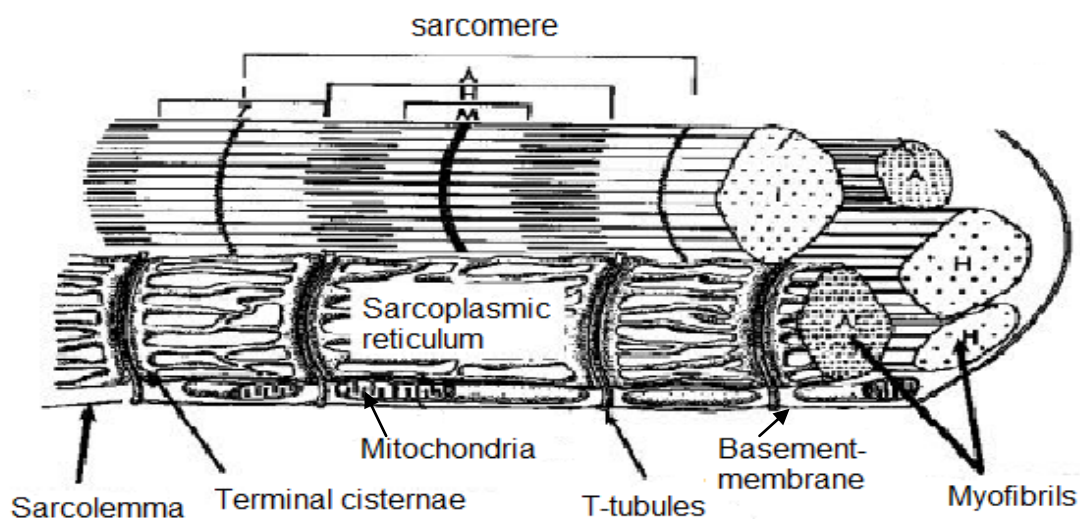
Figure 1.1: *Cardiac myocyte.* Shown are the myofibrils, basement membrane, T-tubules, mitochondrion, terminal cisternae, sarcolemma, sarcomere, z-lines and bands (A, H and M) (**Taken and edited from**: Griffin et al. 2004)

1.5.1 **Sarcolemma**

Myocytes also contain a specialized structure known as sarcolemma, which is a coalescence of the plasma membrane proper and the basement membrane (figure 1.1) (review by Walker and Spinale 1999). Sarcolemma is composed of a lipid bilayer that consists of hydrophilic heads (facing outside) and hydrophobic tails (inside), which allows it to interact with both intracellular and extracellular environment (Sachse et al. 2008). The hydrophobic core of the sarcolemma leads to the impermeability of sarcolemma to charged molecules (review by Walker and Spinale 1999). Sarcolemma invaginates into the cytosol forming a transverse tubular system (t-system) (Block et al. 1988).

1.5.1.1 **Intercalated discs and transverse tubules (T-tubules)**

Sarcolemmal extensions form two specialized regions of the myocyte i.e. the intercalated disks and the transverse tubular system (figure 1.1) (Brette and Orchard 2003). Intercalated disks are specialized cell-cell junctions that serve both as a strong mechanical linkage between myocytes and as a path of low resistance that allows for rapid conduction of the action potential (Katz 1992). Transverse tubules (T-tubules) are sarcolemmal invaginations into the myocytes that form a barrier between extracellular and intracellular space (Block et al. 1988). They bring L-type Ca^{2+} channels and the sarcoplasmic reticulum Ca^{2+} discharge system in close proximity (Bers 2002). The fundamental function of the sarcolemma is to provide a barrier for diffusion, thus it contains membrane proteins which include receptors, pumps and channels which are also important for the contractile process of the myocyte (review by Walker and Spinale 1999; Sachse et al. 2008).

1.5.1.2 **Sarcolemmal pumps and ion channels (Action potential)**

Ion channels are a diverse group of pore forming proteins that transverse the cell membrane to allow the selective passage of ions across it (Kass 2005). Ion channels and sarcolemmal pumps are the major transducers of intercellular physiologic signals in the heart (Cesario et al. 2006; Kass 2005). Sarcolemmal pumps and ion channels play an important role in the action potential, a process in which the electrical membrane potential of a cell propagates (Carmeleit 2004). The co-ordination of the action potential depends on several different ion channels within the sarcolemma (Carmeliet 2004; Cesario et al. 2006).

As shown in figure 1.2 below, there are four phases of the action potential (phases 0, 1, 2, 3 and 4) (Wahler 2001b). During the first phase of the action potential i.e. phase 4 also known as resting membrane potential, the sarcolemma is only permeable to K^+, therefore it is the K^+ equilibrium potential that determines the resting membrane potential (about -90 mV) of the myocyte (Barach and Wikswo 1991; Wahler 2001b). Phase 4 is maintained primarily by the inward K^+ rectifier channel which allows diffusion of K^+ into the myocyte and is secondarily influenced by the Na^+/Ca^{2+} exchanger and the sarcolemmal Ca^{2+} ATPase (review by Walker and Spinale 1999; Faber and Rudy 2000). The Na^+/K^+ ATPase, which is also a site for digitalis binding, generates a net outward current through the extrusion of three Na^+ ions for two K^+ ions (Barach and Wikswo 1991; Faber and Rudy 2000), while the Na^+/Ca^{2+} exchanger and the sarcolemmal Ca^{2+} ATPase provide a basis for Ca^{2+} extrusion from the myocytes (review by Walker and Spinale 1999; Faber and Rudy 2000). The Na^+/Ca^{2+} exchanger is a bidirectional channel that allows either ion to be carried across the membrane with the amount determined by the concentration gradient on

either side of the membrane (Philipson 1990; Faber and Rudy 2000). However, in myocytes the Na^+/Ca^{2+} exchanger is the primary system for Ca^{2+} efflux (Philipson 1990; Hryshko and Philipson 1997). Maintaining the balance between Ca^{2+} efflux and influx can contribute to the maintenance of the resting membrane potential (Philipson 1990; Hryshko and Philipson 1997).
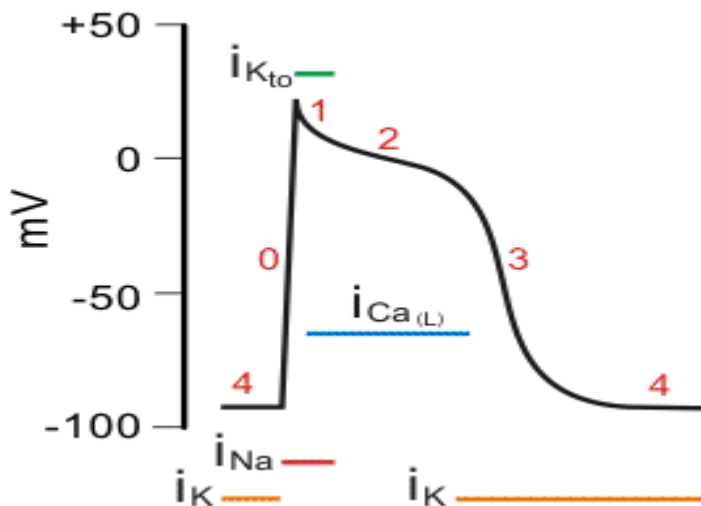
Figure 1.2: *Ventricular myocyte action potential.* Diagrammatic representation of an adult mammalian ventricular myocyte action potential (AP). Four phases of the action potential are labelled (0-4). $I_{Ca,}$(calcium current); I_K (potassium current) and I_{Na} (sodium current) (**Taken from**: Klabunde 1998-2010).

When the membrane potential reaches the predetermined threshold voltage of -70 mV, Na^+ channels (fast) are activated rapidly (<1 ms) and remain active for a duration of about 2 to 10 ms (review by Walker and Spinale 1999; Wahler 2001a). Na^+ channel activation allows Na^+ to flow into the cell followed by both electrical and chemical concentration gradients (Brown et al. 1981; Faber and Rudy 2000; Franco et al. 2006). This triggers other ionic processes responsible for the other phases (1, 2 and 3) of the action potential (review by Walker and Spinale 1999; Wahler 2001b).

Early repolarization is evidenced when rapid inactivation of the Na^+ channels and slower activation of two outward currents prevail (Ruben 2001; Wahler 2001b; Zaza 2010). This is then followed by a positive membrane potential, where a Cl^- concentration gradient and increased membrane permeability to Cl^- allows the entry of Cl^- into the cell (Wahler 2001b; Ruben 2001; Zaza 2010). In addition, a transient efflux of K^+ through specific channels takes place along with the K^+ electrochemical gradient (Wahler 2001b; Ruben 2001; Franco et al. 2006). These three events contribute to a brief and small repolarization occurring during the phase 1 of the action potential (Coraboeuf 1969; review by Walker and Spinale 1999).

When the membrane potential depolarizes to about -40 mV, L-type Ca^{2+} channels open, leading to the influx of Ca^{2+} (Wahler 2001b). Influx of Ca^{2+} through the L-type Ca^{2+} channels leads to a plateau phase (phase 2) of the action potential which is followed by a counter balancing outward K^+ current flowing through the K^+ rectifier (Coraboeuf 1969; Balke and Shorofky 1998; review by Mukherjee and Spinale 1998). These two channels are normally activated during the upstroke of the action potential and reach peak current during the plateau phase (Bers 2002a). Increased K^+ conductance through the delayed rectifier of the K^+ channels results in repolarization (phase 3) (Wahler 2001b). Towards the end of the plateau phase, K^+ channels are activated resulting in K^+ ions to flow along the concentration gradient (Barach and Wikswo 1991). During this phase all other inward currents such as Na^+ and Ca^{2+} are inactivated, therefore making the delayed rectifying K^+ current responsible for the restoration of the membrane potential to the resting state (Mazzanti and DeFelice 1990; Nanasi et al. 1998).

1.5.1.3 **Contractile apparatus**

The basic unit of contraction in the myocyte is a sarcomere (figure 1.1) which is composed of thick and thin filaments and has a resting length of about 1.8-2.4 µm (Berne and Levy 1997). The sarcomere also contains the regulatory components of the contractile apparatus which are myosin, actin, tropomyosin and troponin protein complex, figure 1.3 (Berne et al. 1997). When intracellular Ca^{2+} concentration is increased, myosin, actin, tropomyosin and troponin proteins interact with each other resulting in changes in physical and chemical dynamics, leading to the development of tension which is accompanied by the hydrolysis of ATP (Williams 1997; Tajsharghi 2008).

Thick filaments (myosin) are composed of a filamentous tail and a globular head region that contains the actin binding site and the catalyzing site for ATPase activity, figure 1.3 (Rayment et al. 1993; Hooper et al. 2008). Thin filaments are mainly composed of actin which has two isoforms, figure 1.3 (G and F) (Tajsharghi 2008). F-actin forms the backbone of the thin filaments while G-actin, which has two myosin binding sites, works as a stabilizing protein (Gordon et al. 2000). In the presence of ATP, the interaction between the myosin globular head and the G-actin monomer results in crossbridge formation and shortening of the sarcomere length (review by Walker and Spinale 1999; Craig and Lehman 2001). Also found in the thin filaments is the rigid α-helical protein (±40 nm long) molecule known as tropomyosin (Spudich et al. 1972; Perry 2001).
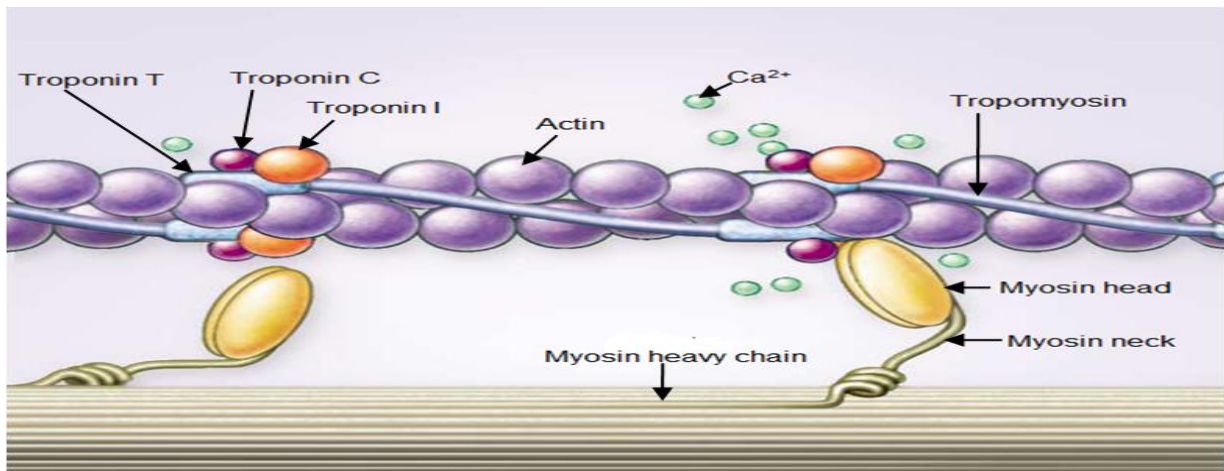
Figure 1.3: *Thick and thin filaments*. shown are proteins called myosin (thick filament), actin, tropomyosin, troponin I, troponin C and troponin T, which are arranged to form a filamentous complex (thin filament). (**Taken and edited from**: Kamisago et al. 2000).

Tropomyosin lies on either side of the actin, thus adding to the rigidity of the thin filaments and most importantly, it also influences the actin-myosin crossbridge formation by physically interdigitating between the actin-myosin cleft, therefore preventing Ca^{2+} binding (Katz et al. 1992; review by Walker and Spinale 1999). Also present in the thin filaments, is the troponin complex which is composed of three proteins i.e. troponin T, I and C, figure 1.3 (Davis et al. 2007). Troponin regulates the extent of crossbridge formation and contributes greatly to the structural integrity of the sarcomere (Lehman et al. 2009). Troponin T binds the troponin complex to the thin filament while phosphorylated troponin I weakens the affinity of Ca^{2+} for troponin C (Tikunova et al. 2002; Lehman et al. 2009). Binding of Ca^{2+} to troponin C results in conformational change of the complex with actin-myosin interaction that initiates crossbridge formation and power-stroke (Tikunova et al. 2002).

1.6 Myocardial energetics

Energy metabolism is essential for normal contraction of the myocyte, as the heart uses between 3-5kg of ATP per day to keep pumping (Taegtmeyer 2002; Shah et al. 2003; Doenst et al. 2008). At normal heart rates (~60 beats per minute) which take place when the body is at rest, a vast amount of energy is utilized by excitation-contraction coupling (ECC) (Bers 2001; Maack and O'Rourke 2007). It has been shown that the myosin ATPase, plasmalemmal Na^+/K^+-ATPase and sarcoplasmic reticulum Ca^{2+}-ATPase are the main consumers of cellular energy in cardiomyocytes (Bers 2001; Doenst et al. 2008). In each normal heart beat ~2% of cellular ATP pool is consumed, while the whole ATP pool is turned over within couple of seconds during maximal workload (Harris and Das 1991; Mootha et al. 1997; Balaban 2002).

It has been reported that the mitochondrion is the main site of energy production in cardiomyocytes (Balaban 2002; review by Maack and O'Rourke 2007). Mitochondria are located in close vicinity to the main sites of energy consumption (myofilaments, SR and T-tubules) and occupy about one third (30%) of the cardiomyocyte space (figure 1.1) (Territo et al. 2001; Ormerod et al. 2008). The omnivorous cardiomyocyte can metabolise a wide variety of energy producing molecules such as lactate, ketone bodies and ethanol but under normal conditions the majority of ATP is supplied by fatty acids (60-90%) and glucose (10-40%) (Gertz et al. 1988; Young et al. 2002; review by Maack and O'Rourke 2007). However, the heart normally responds to large variations in both substrate availability and energy demand, but has limited capacity for energy storage (Botker et al. 1994; Stanley et al. 2005). The β-oxidation (fatty acid metabolism to form acetyl-CoA) and glycolysis (glucose metabolism to form pyruvic acid) pathways are reciprocally controlled and overall ATP produced is

closely coupled to myofibrillar contraction (Stanley et al. 2005). Under normal physiological conditions, glucose is transformed to pyruvate, which then enters mitochondria and is further transformed by pyruvate dehydrogenase (PDH) to acetyl-coenzyme A (acetyl-CoA) (Stanley et al. 2005). Fatty acids are converted to fatty acyl-CoA in the cytosol and transported into the mitochondria via the carnitine-acyltranslocase (Grynberg and Demaison 1996). Mitochondrial acyl-CoA molecules are then broken down, resulting in the production of acetyl-CoA, reduced nicotinamide adenine dinucleotide (NADH) and reduced flavin adenine dinucleotide (FADH$_2$) (Garland and Randle 1964; Goodwin et al. 1998b).

Acetyl-CoA from both glycolysis and β-oxidation enters the tricarboxylic acid (TCA) cycle, leading to the formation of NADH and FADH$_2$ (electron carriers) (Garland and Randle 1964; Taegtmeyer et al. 1980). Electrons from NADH and FADH$_2$ flow through the electron transport chain to oxygen, during which energy is released and used to pump H$^+$ ions across the inner mitochondrial membrane (Garland and Randle 1964; Taegtmeyer et al. 1980). The mitochondrial membrane contains various enzyme complexes that drive the synthesis of ATP from ADP and Pi (Stanley et al. 2005; review by Maack and O'Rourke 2007). However, in pathological states such as diabetic cardiomyopathy, myocardial energy efficiency i.e. the ratio between cardiac work load and myocardial oxygen consumption is decreased, due to an increased reliance of the myocardium on fatty acid oxidation as an energy substrate (Boudina and Abel 2006).

1.7 **Insulin signaling pathway**

Insulin, as mentioned above is a multifunctional peptide hormone that is composed of 51 amino acids with a molecular weight of about 5808 Da (Daltons) (Lomedico et al. 1979; Toriumi and Imai 2002). It is produced by pancreatic β-cells of the islets of Langerhans and its structure varies between animal species (Lomedico et al. 1979; Toriumi and Imai 2002). Insulin has a profound effect in metabolism by promoting the uptake of glucose, fatty acids and amino acids from the blood by the cells to be used or stored as glycogen, lipids and proteins (Lomedico et al. 1979; Cherrington 1999; Saltiel and Kahn 2001). When administered or endogenously released from the pancreas, insulin inhibits glucose production by hepatic cells and stimulates its utility by peripheral cells, therefore it is a primary regulator of glucose metabolism (review by Goalstone and Draznin 1997; Saltiel and Kahn 2001).

Insulin also prohibits the use of fatty acids as energy source in the presence of excess plasma glucose by stimulating lipogenesis and diminishing lipolysis (review by Omerod et al. 2008). In addition, it is reported that insulin regulates gene transcription and increases amino acid transport into cells (Saltiel and Kahn 2001). Any disruption in the action of insulin such as in insulin resistance or deficiency, results in dysregulation of the above mentioned processes (Shulman et al. 1990; Cline 1994). There are several stimuli that may trigger the release of insulin by the pancreas, some of which are ingested proteins and glucose from digested food sources (Parker et al. 1983).

1.7.1 **Glucose metabolism**

After a meal, blood glucose concentration increases drastically leading to the release of insulin from pancreatic β-cells (DeFronzo and Ferrannini 2001; De Myets and Whittaker 2002; Henriksen and Teachery 2007). Insulin binds onto its receptor located in the plasma membrane of the insulin sensitive cells (figure 1.4) (De Myets and Whittaker 2002; review by Frojdo et al. 2009). The insulin receptor is a glycosylated homodimer linked by disulfide bonds (Ring 2003; Hooper et al. 2007). It consist of two monomers each made up of an extracellular α-subunit and a β-subunit that spans the cell membrane (Sparrow et al. 1997; Hooper et al. 2007). The α-subunits consist of insulin binding elements, while the β-subunit contains a protein-tyrosine kinase domain in its intracellular portion and other domains involved in signal transduction pathways (Sparrow et al. 1997). Insulin binds to the α-subunits which induces a conformational change leading to autophosphorylation of tyrosine residues in the β-subunit (Van Obberghen et al 2001).

Phosphotyrosine binding (PTB) domains, in proteins such as insulin receptor substrates (IRS) recognise these residues, bind to them and are activated (White 2002). The activated IRS proteins then activate Src homology collagen (Shc) and adaptor protein with a pleckstrin homology (PH) and SRC homology-2 (SH2) domain (APS) (Alessi and Downes 1998; Hooper et al. 2007). These phosphorylated proteins stimulate downstream effector molecules, which then further activate different signaling pathways such as extracellular signal regulated kinase (ERK) pathway involved in growth (Van Obberghen et al. 2001). For metabolic effects of insulin the phoshatidylinositol 3-kinase (PI3K) is activated through IRS-1 (White 2002; Gual et al 2005). IRS-1 is a tyrosine phosphorylated protein that belongs to the

IRS family of adaptor molecules, (section 1.7.2) (Kim et al. 1999; White 2002; Bouzakri et al. 2003). Activated PI3K enzyme phosphorylate inositol phospholipids in the plasma membrane, thus increasing the levels of phoshatidylinositol 3, 4, 5-trisphosphate (PIP3) (Alessi and Downes 1998; review by Frojdo et al. 2009). This enables the recruitment and activation of serine/threonine kinase and phosphoinositide-dependent protein kinase (PDK1) which binds phospholipids through their PH domain (Van haesebroeck and Alessi 2000; Simpson et al. 2001; Beeson et al. 2003). PDK1 further phosphorylates and activates protein kinase C (PKC) and protein kinase B isoforms (PKB/Akt) (figure 1.4) (Van haesebroeck and Alessi 2000; Simpson et al. 2001). PKB/Akt will be discussed in section 1.7.3. PKC is involved in translocation of GLUT-4 (glucose transporter isoform), through phosphorylation of vesicle-associated membrane protein (VAMP)-2 protein located on GLUT-4 vesicles (Beeson et al. 2004). This results in GLUT-4 translocation to the plasma membrane, where GLUT-4 facilitates the import of glucose into the cell (Henriksen and Dokken 2006). Once inside the cell glucose is either used to produce energy or stored as glycogen for later usage (Henriksen and Dokken 2006). Glycogenesis is triggered by the rate limiting enzyme glycogen synthase and deactivated by glycogen synthase kinase-3 (GSK-3) through phosphorylation of glycogen synthase, therefore inhibiting it (figure 1.4) (Brady et al. 1998; Henriksen and Dokken 2006).
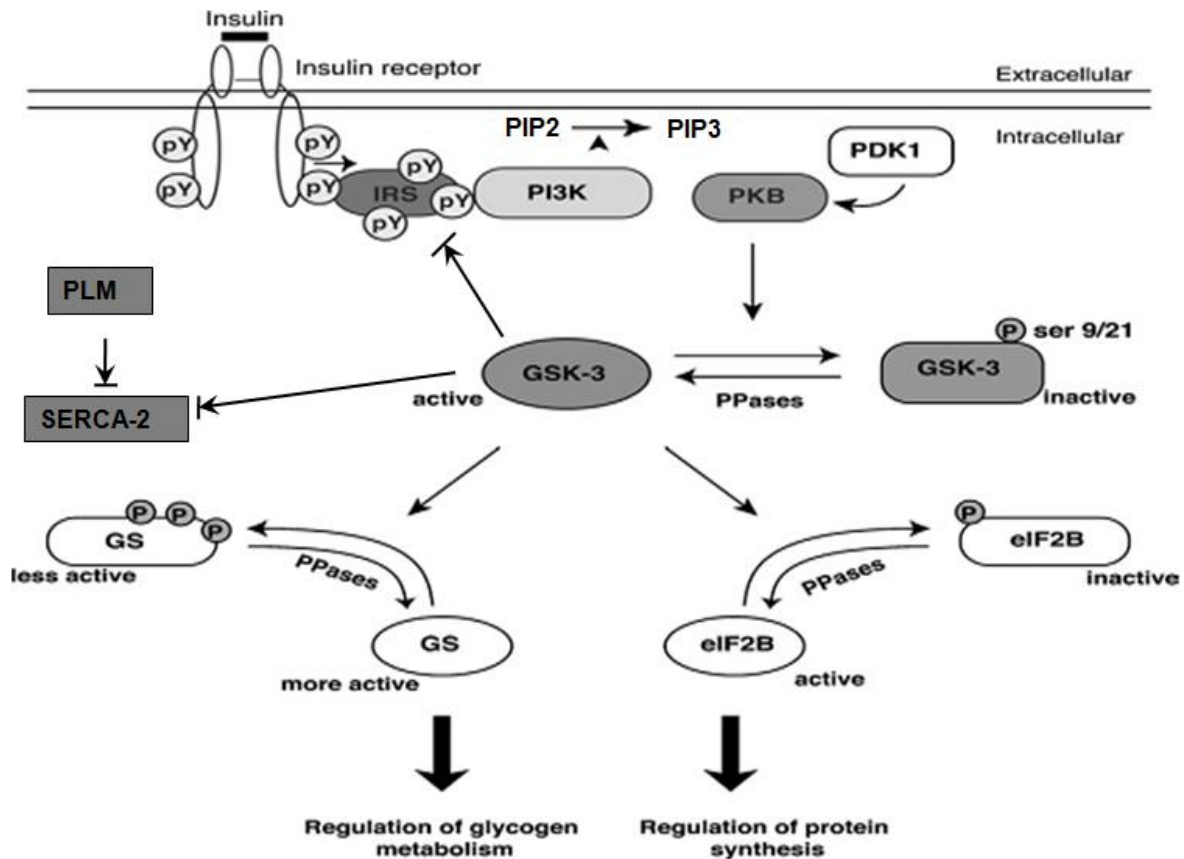
Figure 1.4: *Insulin signaling pathway.* Insulin initiates a signaling cascade that results in PKB/Akt-induced phosphorylation and inactivation of GSK-3β leading to the regulation of glycogen metabolism and protein synthesis (Grimes et al. 2001, Patel et al. 2004*)*. IRS, insulin receptor substrate; PI3K, phosphatidylinositol 3 kinase; PIP2, phosphatidylinositol-4,5-bisphosphate; PIP3, phosphatidylinositol-3,4,5-trisphosphate; PDK1, phosphoinositide-dependent kinase-1; PKB/Akt , protein kinase B; GSK-3, glycogen synthase kinase-3; SERCA-2, Sarcoplasmic/endoplasmic reticulum Calcium (Ca^{2+}) ATPase; PLM, phospholamban; eIF2B, eukaryotic initiation factor-2 beta. (**Taken and edited from**: Patel et al. 2004).

1.7.2 **Insulin receptor substrate (IRS) proteins**

Insulin receptor substrates are tyrosine kinase proteins that mediate a variety of signaling pathways and their activities are induced by insulin, insulin like growth factors and cytokines (Kim et al. 1999; Kabuta et al. 2008). There are four members of IRS family namely IRS-1, IRS-2, IRS-3 and IRS-4 which range in order of their discovery (Kim et al. 1999; Vollenweider et al. 2002; Bouzarki et al. 2003). These proteins are best distinguished as docking or adaptor proteins for they couple the receptor to proteins containing a SH2 domain (Myers et al. 1995). First evidence for these substrate specific proteins came from studies done by White et al 1985, and IRS-1 was the first to be purified (Rothenberg et al. 1991; Myers et al. 1994; Waters et al. 1996). The open reading frame of the cDNA of IRS-1 protein has a molecular weight of ~131 kDa, while on SDS-PAGE it migrates between 165-180 kDa due to its high serine phosphorylation state (White et al. 1985; Myers et al. 1994).

It is reported that IRS-1 has about 50 potential serine/threonine phosphorylation sites and 21 putative tyrosine phosphorylation sites located in the carboxy (COOH) terminal domain and these serve as binding sites for various SH2 containing proteins such as the p85 regulatory subunit of PI3K (Myers et al. 1995; Whitehead et al. 2000; Gual et al. 2005). All four IRS proteins have a conserved domain structure with PH and phosphotyrosine binding (PTB) domains in the amino (NH_2) terminus, enabling them to couple with the insulin receptor (Whitehead et al. 2000). For the purpose of the study, we will concentrate more on IRS-1 and IRS-2.

1.7.2.1 Regulation and specificity of IRS-1/2 proteins

As mentioned above, IRS-1 and IRS-2 function as a link for the insulin receptor to its downstream molecules, thereby inducing biological actions, figure 1.4 (Kerouz et al. 1997; Patel et al. 2004; Sherpherd 2005). This link is achieved through a series of intermediate effectors that bind to the tyrosine-phosphorylated motifs in IRS proteins via SH2 domains (Kerouz et al. 1997; Saltiel and Pessin 2003; Sherpherd 2005). PI3K is one of the examples of an SH2 domain containing protein (Vollenweider et al. 2002; Bousakri 2003.). PI3K plays an important role in several biological processes including growth and metabolism (Kerouz et al. 1997; Kim et al 1999; Bouzakri et al. 2003.). In metabolism, PI3K is involved in glucose transport, glycogen synthesis and inhibition of the key enzymes of gluconeogenesis (Cheatham and Kahn 1995; Sherpherd 2005). It has been shown that PI3K consists of a regulatory p85 subunit to which IRS-1 and IRS-2 bind via SH2 domains, and a 110 kDa catalytic subunit which phosphorylates phosphoinositidyl (PI) protein, and its 4' and 4', 5' phosphorylated derivatives in the D-3 position of the inositol ring (Endemann et al 1990; Kerouz et al. 1997). In addition, it has been reported that IRS-1 is directly regulated by the insulin receptor (IR) which is stimulated by insulin (Cheatham and Kahn 1995; Vollenweider et al. 2002; White 2002). However, it has also been reported that IRS-1 is inhibited by GSK-3 through serine phosphorylation thus regulating it (Eldar-Finkelman and Krebs 1997).

1.7.2.2 **Role of IRS-1/2 proteins in metabolism**

Evidence show that IRS-1 and IRS-2 play a direct role in insulin signaling especially in its metabolic actions but the exact role of IRS-3 and IRS-4 is poorly understood (Whitehead et al. 2000). However it is reported that IRS-3 and 4 overexpression in adipocytes may stimulate some of the activities of insulin (Whitehead et al. 2000). As mentioned previously, IRS-1 and IRS-2 are responsible for transmitting insulin signals from the insulin receptor to downstream intracellular effectors in the presence of glucose to maintain its homeostasis, figure 1.4 (Nandi et al. 2004; Thirone et al. 2006).

1.7.3 **Protein kinase B/Akt (PKB/Akt)**

Protein kinase B also known as Akt is a serine/threonine protein kinase with a molecular weight of 57 kDa (Hajduch et al. 2001). It was discovered more than 10 years ago and since then it has emerged as a critical signaling node in all eukaryotic cells and has been considered as the most important and versatile protein kinase in human physiology and diseases (Manning and Cantley 2007). PKB/Akt was so named because of its high homology with protein kinase A and C (PKA and PKC) (Hajduch et al. 2001). PKB/Akt was also called Akt due to the product of murine oncogene, v-Akt (Akt8 retrovirus) which turned out to be its cellular homologue (c-Akt) (Coffer et al. 1998; Hanada et al. 2004).

There are three PKB/Akt isoforms i.e. PKB/Akt1, PKB/Akt2 and PKB/Akt3 (α, β and γ) present in higher eukaryotes and each posess an amino terminal PH domain, a kinase domain and a carboxy terminal regulatory domain (Coffer et al. 1998; Hajduch et al. 2001). It is reported that α and β isoforms are ubiquitously expressed,

while the γ-isoform is relatively highly expressed in brain and testis only (Hanada et al. 2004).

1.7.3.1 **Regulation and specificity of PKB/Akt**

PKB/Akt is actively stimulated in response to insulin and growth factors through PI3K in a two step process, figure 1.4 (Hajduch et al. 2001). As shown in figure 1.4, the first step involves the stimulation of IRS proteins by insulin, which then activate PI3K resulting in the production of phosphoinositides PIP_2 and PIP_3 that are known to bind to the PH domain of PKB/Akt, therefore altering its conformation, leading to its phosphorylation and activation (Andjelkovic et al. 1997; Hajduch et al. 2001). PKB/Akt phosphorylation takes place at Threonine 308 (Thr308) of the kinase domain and Serine 473 (Ser473) of the C-terminal domain (Coffer et al. 1998; Vanhaesebroeck and Alessi 2000; Dong and Liu 2005). It is reported that PDK1 is responsible for the phosphorylation of PKB/Akt at Thr308 and PDK2 at Ser473 (Alessi et al. 1997; Stokoe et al. 1997).

Little is known about the mechanism in which PKB/Akt is inactivated, but it is stated that tumor suppressor PTEN (phosphatase and tensin homolog) acts as a phosphatase to dephosphorylate PIP_3 back to PIP_2, while PHLPP (PH domain and Leucine rich repeat Protein Phosphatases) directly dephosphorylate PKB/Akt isoforms (Stokoe et al. 1997; Lawrence and Roach 1997; Patel et al. 2004). This results in delocalization of PKB/Akt from the plasma membrane back to the cytosol decreasing the rate of its activation (Bayascas and Alessi 2005). It is also stated that PKB/Akt is the effector of PI3K signaling pathways in all cells including B cells where stimulated B cell receptor (BCR) can phosphorylate both PI3K and PKB/Akt (Ma et

al. 2008). All PKB/Akt isoforms are members of the AGC kinase family as they contain extensive homology to protein kinases A, G, and C (Manning and Cantley 2007).

1.7.3.2 **Role of PKB/Akt in cells**

PKB/Akt-α is predominantly expressed in skeletal muscle, while PKB/Akt-β is the predominant isoform in adipocytes, but PKB/Akt-γ is active neither in skeletal muscles nor adipocytes (Hajduch et al. 2001). PKB/Akt is well established as the effector of PI3K signaling pathway in all cells (Fruman and Cantley 2002). As mentioned above, PKB/Akt is activated via PIP_3, (figure 1.4) and when activated, it phosphorylates and controls the activities of several proteins involved in regulating cellular functions i.e. metabolism, growth, proliferation and cell survival (Yang et al. 2004; Bayascas and Alessi 2005).

In cell survival, PKB/Akt phosphorylate the BH3 domain-containing BAD protein which is a pro-apoptotic protein of Bcl-2 family (Clarke et al. 1994; review by Hajduch et al. 2001). BAD phosphorylation leads to its dissociation from Bcl-2/Bcl-X complex thus losing its pro-apoptotic effect (Wang et al. 1999; Cheatham et al. 1994; Faissner et al. 2006). PKB/Akt also regulates IkB kinase (IKK) and indirectly activates NF-kB resulting in pro-survival gene transcription (Cheatham et al. 1994; Faissner et al. 2006). In glucose metabolism PKB/Akt is involved in translocation of glucose transporters (mainly GLUT 4) to the plasma membrane, thereby promoting glucose intake by the cells (Clarke et al. 1994; Wang et al. 1999; Hajduch et al. 2001). Once plasma glucose is available in excess, PKB/Akt phosphorylates GSK-3 which normally phosphorylates and inhibits the glycogen synthase, a rate limiting enzyme

of glycogenesis (Figure 1.4) (Lawrence and Roach 1997). Inhibition of GSK-3 by PKB/Akt favors glycogen synthesis and storage in muscles, liver and adipose tissues (Lawrence and Roach 1997; Hajduch et al. 2001).

1.7.4 Glycogen Synthase Kinase-3 (GSK-3)

The GSK-3 is a serine/threonine protein kinase that was discovered in the early 1980s as an enzyme involved in regulation of glucose metabolism (Park et al. 2003). Its involvement in glucose metabolism increased researcher's interest and since then, it has been extensively researched especially in the context of metabolic actions of insulin (Woodgett, 2001; review by Huisamen and Lochner 2010). Studies have shown that GSK-3 phosphorylates and inhibits glycogen synthase and insulin receptor substrate-1 (IRS-1) activity thereby impairing insulin signaling (Eldar-Finkelman et al. 1996).

It has been discovered that GSK-3 is not only involved in glucose metabolism, but is a multifunctional protein kinase that performs a role in several signaling pathways such as in the regulation of cell fate, including Wnt (wingless) and Hedgehog signal transduction, protein synthesis, mitosis and apoptosis (review by Forde and Dale 2007). GSK-3 has been implicated, when dysregulated, in the development of human diseases such as diabetes, Alzheimer's disease, bipolar disorder and cancer (review by Doble and Woodgett 2003). GSK-3 was originally identified in mammals, but other homologues have been discovered in all eukaryotes (Rylatt et al. 1980). All GSK-3 homologues share a significant degree of sequence homology ranging from species as distant as humans and drosophila that share over 80% similarity within the kinase domains (review by Ali et al. 2001).

1.7.4.1 **GSK-3 isoforms**

In humans, two GSK-3 isoforms have been identified, GSK-3α with a molecular weight of ~51 kDa and GSK-3β with a molecular weight of ~47 kDa (figure 1.5) (Woodgett 1990; Ciaraldi et al 2007). These isoforms are encoded by two distinct genes located on chromosomes 19q13.1-2 and 3q13.3-q21. As a result they exhibit a high degree of sequence similarity in their catalytic domains (Ciaraldi et al 2007; Markou et al. 2008). Exact cytological locations of these isoforms have been identified using chromosomal mapping, i.e. GSK-3α is located at 19q13.2 and GSK-3β maps to 3q13.3 (Shaw et al. 1998; review by Ali et al. 2001). They exhibit about 98% homology in their kinase domains, but they share only about 36% identity in the last 76 C-terminal amino-acid residues (figure 1.5) (Woodgett 1990).
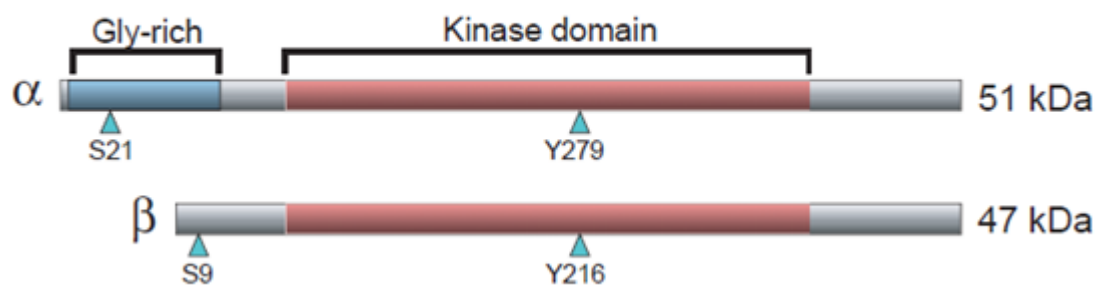
Figure 1.5: *Schematic representations of GSK-3α and GSK-3β isoforms.* Blue arrow-heads indicate sites of serine and tyrosine phosphorylation. A glycine-rich N terminal domain of GSK-3α and a conserved kinase domain from both GSK-3α/β are highlighted (**Taken from**: Doble and Woodgett 2003)

Although these isoforms are structurally similar, their expression patterns, substrate preferences and cellular functions are not identical (Woodgett 2001; review by Doble and Woodgett 2003). Hoeflich et al. 2000 reported that mice embryos carrying homozygous deletions of exon 2 of the GSK-3β isoform suffer from a massive liver degeneration caused by extensive hepatocyte apoptosis, leading to death at around embryonic day 16. GSK-3α isoform was unable to take over the function of GSK-3β in these GSK-3β null mice, indicating that the degenerative liver phenotype develops specifically from the loss of GSK-3β isoform (review by Doble and Woodgett 2003).

1.7.4.2 Regulation and specificity of glycogen synthase kinase-3 (GSK-3)

1.7.4.2.1 Regulation of GSK-3 protein

GSK-3 is, unlike most other protein kinases, active in the resting state and deactivated when cells are stimulated (Woodgett 1994; Hirotani et al 2007). The most well defined mechanism of GSK-3 regulation is the phosphorylation of Serine 9 (Ser9) in GSK-3β and Ser21 in the GSK-3α isoform (Markou et al. 2008; Miron 2008). This is accomplished by hormones such as insulin, endothelial growth factor and platelet growth factor (Ciaraldi et al. 2007). In cells, insulin stimulates glycogen synthesis both by inhibiting GSK-3 and dephosphorylation of glycogen synthase (Ali et al. 2001). PKB/Akt (PI3K pathway), some isoforms of protein kinase C (PKC), PKA, p90[RSK] and p70S6 kinase may all be responsible for phosphorylation of GSK-3 on serine residues located at the N-terminus, thus inactivating it (Murphy and Steenbergen 2005). GSK-3 is also inhibited by cardiac hypertrophic stimuli, including endothelin-1, Fas, and pressure overload, possibly through the PI3K-PKB/Akt pathway (Haq et al. 2000; Badorff et al. 2002).

It has been demonstrated that a phosphor-peptide based on the N-terminus of GSK-3β acts as a competitive inhibitor of the primed GSK-3 substrates (Dajani et al. 2001). These findings led to the suggestion that the phosphorylated N-terminus of GSK-3 protein auto-inhibits its activity by looping back into its active site (review by Forde and Dale 2007). Phosphorylated N-terminus also serve as a pseudo-substrate that binds to the positively charged pocket, consisting of Arg[96], Arg[180], and Lys[205], therefore competing with primed substrates for binding to the catalytic groove (Miron 2008). In contrast to inactivation via serine phosphorylation, GSK-3 can also be phosphorylated on tyrosine residues resulting in its activation, i.e. tyr-279 of GSK-3α and tyr-216 of the GSK-3β isoform (Murphy and Steenbergen 2005). This means GSK-3 tyrosine phosphorylation results in facilitative autophosphorylation while serine phosphorylation is regulatory (Markou et al. 2008). The kinase responsible for tyrosine phosphorylation of GSK-3 protein is poorly understood but it has been reported that calcium sensitive protein-tyrosine kinase-2 might be responsible (Hartigan and Johnson 1999).

GSK-3 activity can also be regulated by protein interactions, e.g. it is usually complexed with β-catenin, axin and adenomatous polyposis coli (APC) proteins (Murphy and Steenbergen 2005). Disruption of such a complex by displacement of axin by other proteins such as dishevelled and frequently rearranged during advanced T cell lymphomas (FRAT), a.k.a. GSK-3 binding protein, blocks GSK-3β association with β-catenin, resulting in reduction of β-catenin phosphorylation (Hinoi et al. 2000). Other mechanisms resulting in GSK-3 regulation besides phosphorylation have been employed, one of which is the control of subcellular localization (Miron 2008). That is, specific substrate phosphorylation may be

regulated by targeting GSK-3β to a specific location or binding partner (Murphy and Steenbergen 2005). GSK-3β can be targeted by different stimuli to the nucleus or mitochondria where it acts on a subset of cellular substrates (Juhaszova et al. 2004). For example, during the G1 phase of the cell cycle, GSK-3β is predominantly cytoplasmic, but during the S phase, a significant fraction enters the nucleus promoting its ability to phosphorylate cyclin D1 in the nucleus (Diehl et al. 1998; Miron 2008).

In cardiomyocytes, GSK-3β has been shown to be present in both nucleus and cytosol under normal, unstimulated conditions (Murphy and Steenbergen 2005). It has been reported that nuclear localisation of GSK-3β is enhanced by endothelin (Morisco et al. 2001). Upstream kinases such as PKB/Akt can also be targeted to GSK-3 in specific locations (Morisco et al. 2001). However, the export of GSK-3β from the nucleus is achieved by addition of isoprenaline (Morisco et al. 2001). In addition to that, GSK binding protein (FRAT) has also been shown to enhance nuclear export of GSK-3β (Franca-koh et al. 2002).

1.7.4.2.2 **Specificity of GSK-3 protein**

When activated, GSK-3 preferentially targets the proteins that are pre-phosphorylated at a priming residue located four residues C- terminal to the GSK-3 phosphorylation site (Eldar-Finkelman 2002; Patel et al. 2004). It has been reported that priming phosphorylation of most of GSK-3 substrates enhances the efficiency of their phosphorylation and provide a means for GSK-3 to integrate multiple signaling pathways (Patel et al. 2004; Murphy and Steenbergen 2005).

GSK-3 is considered as a selective serine/threonine kinase that recognizes and phosphorylates the consensus sequence T/SXXXT/S(P) or S^1xxxS^2(p) where 'X' is any amino acid and '(P)' is the phosphorylatable residue in certain proteins (Fiol et al 1990; Patel et al. 2004). The S^2(p) represents the priming site. However, certain substrates such as c-Jun, c-Myc and c-Myb do not follow the S^1xxxS^2(p) motif and do not require pre-phosphorylation (Plyte et al. 1992). Whether the substrate is pre-phosphorylated or not, its phosphorylation by GSK-3 attenuates its function (Eldar-Finkelman 2002).

1.7.4.3 **Targets of GSK-3**

GSK-3 does not only target glycogen synthase but there are a number of other substrates identified, including translation initiation factor eIF2B(epsilon), PKA, phosphatase subunit RGI and ATP-citrate lyase (Woodgett et al. 1993). In addition, GSK-3 also phosphorylates several transcription factors which include CREB, c-Jun, c-Myc, c-Myb as well as heat shock transcription factor HSF-1 (Xavier et al. 2000; Ali et al 2001). Some of the targets of GSK-3 are brain associated proteins such as amyloid precursor protein, Tau and neurofilament proteins (Plyte et al. 1992). It is reported that phosphorylated Tau has a lower affinity for microtubules and when hyper-phosphorylated it seems to promote association into paired helical filaments which is a pathological feature of Alzheimer's disease (Spittaels et al. 2000). In addition GSK-3 is also known to phosphorylate IRS-1 thus inhibiting insulin signaling (Eldar-Finkelman and Krebs 1997). Furthermore, GSK-3 substrate phosphorylation is generally inhibitory to its substrate, meaning that GSK-3 is a suppressor of these target proteins (Miron 2008).

1.7.4.4 GSK-3 and myocardial contractility (Calcium homeostasis)

It has been reported that GSK-3 protein plays an important role in the regulation of calcium homeostasis in the heart (Michael et al. 2004; Omar et al. 2010). In cardiomyocytes, calcium homeostasis is directly regulated by sarcoplasmic/endoplasmic reticulum Calcium (Ca^{2+}) ATPase (SERCA)-2a, also known as calcium ATPase pump (section 1.7.5) (Takeda 2010). However, it has been reported that GSK-3 down regulates the expression of the SERCA-2a protein, by acting directly on its promoter to lower the mRNA levels (Michael et al 2004). The attenuation of SERCA-2a expression in the heart may lead to contractile abnormalities such as systolic and diastolic dysfunction (Dutta et al. 2002; Michael et al. 2004; Wold et al. 2005). GSK-3β is also known to play a role in the regulation of cardiac growth and hypertrophy (Haq et al. 2000; Bardorf et al 2002). Cardiac hypertrophy can be physiological or pathological (review by Huisamen and Lochner 2010).

The association between pathologic hypertrophy and activation of neuro-humoral pathways i.e. endothelin I, angiotensin II and catecholamines, that lead to the release of calcium from the sarcoplasmic reticulum (SR), has been reported (Blankesteijn et al. 2008; review by Huisamen and Lochner 2010). The calcium released from the SR will then eventually activate the calcium dependent phosphatase called calcineurin, which regulates alterations in gene expression associated with hypertrophy (Blankesteijn et al. 2008). Pathologic hypertrophy of the cardiomyocytes may result in heart failure, a leading cause of death in developed countries (Haq et al. 2000). By using adenovirus-mediated gene transfer of GSK-3β containing a ser-9 to alanine mutation, Haq and colleagues demonstrated that the

inactivation of GSK-3β protein is required in order for the cardiomyocyte to undergo hypertrophy. They suggested that GSK-3β regulates the hypertrophic response, by modulating the nuclear/cytoplasmic partitioning of a member of the nuclear factor of activated T cell family of transcription factors (Haq et al. 2000).

1.7.4.5 **GSK-3 in diabetes and insulin resistance**

Diabetes mellitus is the most common metabolic disorder, affecting about 150 million people worldwide and is expected to double within the next 20 years (Cohen and Goedert 2004). Type II diabetes develops when the insulin sensitive tissues are resistant to insulin, thus hindering glucose transport and metabolism (Meijer et al. 2004). It has been reported that insulin decreases GSK-3 mediated inhibition of glycogen synthase, and thereby increases the activity of the latter (Meijer et al. 2004). It has also been reported that GSK-3 is one of the factors associated with the reduction of insulin action in skeletal muscle, liver, and adipose tissues (Henriksen and Dokken 2006). Most studies reported that GSK-3 is upregulated in muscles of both obese rodents and obese, type II diabetic humans (review by Herinksen and Fokken 2006). In addition, it has been shown that in skeletal muscle of obese rodents and type II diabetic humans, activated GSK-3 impairs insulin signaling by serine phosphorylation of IRS-1, thereby negatively regulating glucose uptake (Eldar-Finkelman et al. 1997).

The evidence from a variety of obese rodent models and type II diabetic humans supports a role for GSK-3 overactivity in the development of insulin resistance of glucose transport and glycogen synthesis (Embi et al. 1980; Henriksen and Dokken 2006). In addition to insulin resistance, animal models overexpressing GSK-3 also

presented with attenuated SERCA-2a expression in the heart resulting in contractile abnormalities (Pearce et al. 2004; Michael et al. 2004). As mentioned earlier, GSK-3 regulates through phosphorylation the activity of several metabolic enzymes including glycogen synthase (Embi et al. 1980). It has been reported that pharmacological GSK-3 inhibition potentiates insulin action in skeletal muscle of insulin resistant rats (Henriksen at al. 2003).

1.7.4.6 **GSK-3 Inhibition**

Diseases such as diabetes, Alzheimer's disease and some cardiovascular disorders, are associated with abnormalities in phosphorylation of proteins involved in regulation of signaling pathways (Noble et al. 2004; Martinez 2008). As a result, pharmaceutical companies are more interested in the development of pharmacological inhibitors of kinases and phosphatases (Martinez 2008). GSK-3 is one of the kinases that flared the interest to develop new generations of inhibitors with specific clinical implications (Martinez 2008). It has been reported that, in the heart, GSK-3 inhibition plays a crucial role in the protection against ischemic damage at the level of mitochondrial functioning as it keeps the mitochondrial permeability transition pore in a closed conformation (Juhaszova et al. 2004). The opening of this pore leads to cell death (Juhaszova et al. 2004).

In addition, it has been shown that inhibition of GSK-3β by the PI3K/PKB/Akt pathway provides cardioprotection and it is an attractive target in ischemia-reperfusion injury (reviewed by Kumar et al. 2007). Other studies using highly selective GSK-3 inhibitors indicated that the overactivation of GSK-3 protein in obesity is indeed associated with enhanced IRS-1 phosphorylation, and defective

IRS-1 dependent signaling which results in reduced glucose transporter (GLUT)-4 translocation in skeletal muscle (Liberman and Eldar-Finkelman 2005; Henriksen et al. 2003).

There are three distinct regions of GSK-3 that are targeted by inhibitors to suppress its activity i.e. Metal ion (Mg^{+2}) binding site, substrate interaction domain and ATP binding pocket (Van Wauwe and Haefner 2003). However, most of the GSK-3 inhibitors are known to compete with ATP to bind to its pocket (Patel et al. 2007). There are several types of GSK-3 inhibitors reported, ranging from hymenialdisine, paullones and indirubins, but they are also known to inhibit other protein kinases related to GSK-3 such as Cyclin-Dependant protein kinases (CDKs) resulting in side effects (Meijer et al. 2003; Leost et al. 2000).

Lithium (Li^+) was the first GSK-3 inhibitor to be discovered and since then it has been widely used as a pharmacological inhibitor (Klein and Melton 1996; Meijer et al. 2004). Lithium was originally used as a mood stabilizer in the nineteenth century and was considered as an effective treatment for both acute and long-term phases of manic depression (Williams et al. 2004). Lithium chloride (LiCl) is the most commonly used GSK-3 inhibitor (Stambolic et al. 1996). It non-specifically inhibits both GSK-3α and GSK-3β isoforms *in vitro* and *in vivo* (Klein and Melton 1996). This is accomplished through competition for Mg^{2+} binding at a site distinct from the ATP binding pocket (Ryves et al. 2002). However, there are other specific, potent and selected cell permeable GSK-3 inhibitors, including SB-216763, SB-415286 and Chirone, CHIR118637 (CT20026) reported (Coghlan et al. 2000). The GSK-3 inhibitors that act in the distal part of the insulin signaling pathway might represent a

promising opportunity to treat insulin resistance and type II diabetes (Van Wauwe and Haefner 2003; Cohen and Goedert 2004).

1.7.5 Sarcoplasmic/endoplasmic reticulum Calcium (Ca^{2+}) ATPase (SERCA)

SERCA is an intracellular membrane bound enzyme that belongs to the "P" family of cation transport ATPases which include plasma Ca^{2+} ATPase (PMCA), Na^+/K^+ ATPase and H^+/K^+ ATPase (Sweadner and Donnet 2001; Inesi et al. 2005). P-type ATPases transfer the terminal phosphate of the ATP molecule to an aspartate residue in the catalytic domain, resulting in a reversible conformational change that helps the movement of ions across the biological membranes (Periasamy and Kalyanasundaram 2007). SERCA transports calcium (Ca^{2+}) ions from the cytoplasm into the sarcoplasmic reticulum (SR), against its concentration gradient through the use of free energy of ATP and it is therefore considered as a pump (Inesi et al. 2005). That is, two calcium ions are transported per ATP hydrolysis (Periasamy and Kalyanasundaram 2007).

SERCA pump is a single polypeptide of about 110 kDa, localized in both endoplasmic reticulum (ER) and sarcoplasmic reticulum (SR) (Periasamy and Kalyanasundaram 2007). Large domains in the cytoplasm contain both a phosphorylation site (Asp^{351}) and a nucleotide binding site, while residues in four (M4, M5, M6 and M8) of the 10 trans-membrane helices form a Ca^{2+} translocating pocket (MacLennan et al 1997). It has been identified in both prokaryotes and eukaryotes and is also known to be present in all living organisms, from yeast and plants to the mammalian system (Periasamy and Kalyanasundaram 2007).

1.7.5.1 **SERCA pump isoforms**

There are three distinct genes encoding SERCA-1, 2 and 3 that are known to produce more than 10 isoforms in vertebrates (Periasamy and Kalyanasundaram 2007). SERCA-1 is mainly expressed in fast-twitch skeletal muscle and is alternatively spliced to encode SERCA-1a (994 amino acids, adult) and SERCA-1b (1011 aa, fetal) (Brandl et al. 1987). SERCA-2 encodes three isoforms i.e. SERCA-2a, b and c. SERCA-2a consist of about 997 amino acid residues and is predominantly expressed in cardiac and slow twitch skeletal muscle (MacLennan et al. 1985). SERCA-2b, which is about 1042 amino acid sequence long, is expressed in all tissues at low levels including muscle and nonmuscle cells (Dode et al. 2002). Recently discovered SERCA-2c is 999 amino acids long and has been reported in cardiac muscle (Dally et al. 2006).

SERCA-3 isoforms are expressed in several nonmuscle tissues and appear to be a minor form in muscles (Wuytack et al. 1994). However, SERCA-3 is known to encode for 6 isoforms (3a-3f) in humans ranging between 999-1052 amino acids in length at the mRNA level and are expressed in multiple tissues and cell types (Bobe et al. 2005). At protein level, only SERCA-3a,b,c isoforms are evidenced and are known to be expressed at high levels in the hematopoietic cell lineages, platelets, epithelial cells, fibroblasts and endothelial cells (Anger et al. 1993). For the purpose of the study we will focus more on SERCA-2a isoform which is critical for cardiac functioning.

1.7.5.2 Role of SERCA-2a in cardiac muscle contraction and relaxation

As mentioned previously, SERCA-2 gene encodes three different protein isoforms, however in the current study we will focus on SERCA-2a which is muscle specific and a ubiquitously expressed SERCA-2b isoform (Periasamy and Kalyanasundaram 2007). These two isoforms differ at the C-terminal domain, where the last four amino acids of the expressed SERCA-2a are replaced by an extended tail of 49 amino acids in SERCA-2b isoform (Periasamy and Kalyanasundaram 2007). Precise control of cytosolic and SR Ca^{2+} concentration is important in maintaining both systolic and diastolic functions (Michael et al. 2004; Fang 2003; Cosson and Kevorkian 2003). In addition, a derangement in Ca^{2+} homeostasis is a primary cause of myocardial contractile abnormalities in heart failure (Dutta 2002; Wold et al. 2005; Shattock 2009). SR is an intracellular membranous network found in all muscle cells, which plays a major role in the contraction-relaxation cycling of the myocardium by regulating its intracellular Ca^{2+} concentrations (Lytton et al. 1992).

Intracellular calcium is stored and released from the SR and it serve as a critical determinant of myocardial contractility (Gyorke and Carnes 2008). The total SR Ca^{2+} content in the mammalian cardiomyocyte has been estimated to be in the range of 50-150 µmol/l in the cytosol (or 1.4-3 mmol/l of SR volume), considering that SR comprises 3.5% of the cell volume (Bers 2002a). As mentioned previously, sequestration of Ca^{2+} by the calcium pump (SERCA-2a) of the SR membranes accounts for the major portion of Ca^{2+} removed from the cytosol during myocardial relaxation (Negretti et al. 1993). Therefore SERCA-2a plays a pivotal role in the regulation of cardiac functioning i.e. it is a principal means by which cytoplasmic calcium is lowered during relaxation and it is also a principal determinant of the Ca^{2+}

concentration in the sarcoplasmic reticulum, which in turn, determines contractility due to its influence on the magnitude of Ca^{2+} release (Asahi et al. 2003). Therefore, factors that affect/regulate SR calcium pump (SERCA-2a) activity are expected to have a marked effect on the mechanical properties of the heart (Takeda 2010).

1.7.5.2.1 **Myocardial contraction**

Myocardial contraction and relaxation involves the movement of calcium ions into and out of the cytoplasm of each myocyte (Woodcock and Matkovich 2005; Peskoff and Langer 1998). Thus, intracellular calcium handling is the central co-ordinator of cardiac contraction and relaxation (Berridge 2003). Traditionally, myocardial contraction begins with excitation-contraction coupling, a process involving electrical excitation of the myocytes leading to contraction of the heart (Bers 2002b). During the cardiac action potential (AP) (section 1.5.1.2), voltage-gated Na^+-channels are activated, and the inward Na^+-current (I_{Na}) induces a rapid depolarization of the cell membrane (Maack and O'Rourke 2007). This results in opening of the voltage-dependent L-type Ca^+ channels ($I_{ca,L}$) and Ca^+ enters the cell (Asahi et al 2003; Maack and O'Rourke 2007).

Ca^+ influx triggers the opening of the ryanodine receptors (RyR2 subtype), which release even greater amounts of Ca^{2+} from the SR, a process called Ca^{2+} induced Ca^{2+} release (CICR) (Fabiato 1985; Bers 2001). The dydic or junctional cleft, a gap or space of typically ~10 nm found between the SR and the cell membrane is then flooded by the Ca^{2+} released from RyRs and which then cover a volume with a radius of about 200 nm (Peskoff and Langer 1998). This high junctional [Ca^{2+}] rapidly decays by diffusion into the submembrane space, then further into the bulk cytosol

(Weber et al. 2002). Increased cytosolic Ca^{2+} binds to troponin C in the myofilaments and induces conformational changes, which subsequently allow the globular myosin head to interact with actin-binding site of the thin filaments resulting in contraction of the left and right ventricle (Schmidt et al. 2002). This leads to the ejection of blood through the aortic and pulmonary valves of the heart respectively, and initiating systole (Maack and O'Rourke 2007).

1.7.5.2.2 **Myocardial relaxation**

Myocardial relaxation is achieved by diffusion of Ca^{2+} from the myofilaments back to the cytosol (Michael et al. 2004). The main mechanism of removing cytosolic Ca^{2+} (back to the SR) involves the SR Ca^{2+}-ATPase (SERCA-2a), sarcolemmal Na^+/ Ca^{2+}-exchanger (NCX) and the plasmalemmal Ca^{2+}-ATPase (PMCA) (Bers et al. 2002a). Ca^{2+} is predominantly re-sequestered into the SR lumen by SERCA-2a and the remaining amount is extruded from the cell by NCX and PMCA (Schmidt et al. 2002). SERCA-2a plays an important role in mammalian cardiac muscle relaxation by acting as a regulator of calcium homeostasis (Periasamy and Huke 2001). As mentioned above, SERCA-2a transports calcium (Ca^{2+}) ions from the cytoplasm into the sarcoplasmic reticulum (SR), against its concentration gradient through the use of free energy of ATP (Inesi et al. 2005).

1.7.5.3 Regulation of SERCA-2a

SERCA-2a activity is regulated by phospholamban (PLM) (figure 1.4) and its homologue protein, sarcolipin (SLN), through direct protein-protein interactions (Asahi et al. 2002). PLM inhibits SERCA-2a by lowering its affinity for Ca^{2+} (Asahi et al. 2002). SERCA-2a-PLM interaction is regulated by Ca^{2+} concentration i.e. elevation in Ca^{2+} concentration leads to the dissociation of the SERCA-2a-PLM complex while lower concentrations of Ca^{2+} results in SERCA-2a-PLM complex formation (James at al. 1989). Toyofuku et al. 1994, suggested that there are three sites of interaction between SERCA-2a and PLM. The first is a cytoplasmic interaction site that is formed by charged and hydrophobic amino acids in the IA domain of PLM and by amino acids Lys-Asp-Asp-Lys-Pro-Val402 in SERCA-2a (Toyofuku et al. 1994). The second is also a cytoplasmic interaction site formed by the PLM domain IB and the transmembrane domain M4 of SERCA-2a (Toyofuku et al 1994; Kimura et al. 1998). The third interaction site is between PLM domain II and SERCA-2a transmembrane helix M6 (Asahi et al. 1999).

It has been reported that a decrease in Ca^{2+} uptake is a central feature of heart failure in humans and animals (Sordahl et al. 1973; Whitmer et al. 1988). In addition, it has been shown that, a relative increase in PLM to SERCA-2a ratio is an important determinant of SR dysfunction in heart failure (Meyer et al. 1995; Hasenfuss 1998). Sarcolipin (SLN) is a 31 amino acid SR membrane protein that interacts with and inhibits SERCA-2a by lowering its Ca^{2+} affinity and V_{max} (Asahi et al. 2003). SLN is predominantly expressed in fast-twitch skeletal muscle in human and is less expressed in cardiac and slow-twitch skeletal muscle (Odermatt et al. 1997). However, SLN is more expressed in rat cardiomyocytes than in human cardiac

muscle (Gayan-Ramirez et al. 2000). In addition to lowering the Ca^{2+} affinity and reducing the V_{max} of SERCA-2a, SLN also enhances the inhibitory effects of PLM on SERCA-2a *in vitro* (Asahi et al. 2002; Asahi et al. 2003). This is because of its ability to bind directly to PLM and prevent PLM from polymerization, resulting in an increase in the active form of PLM (monomer) (Asahi et al 2003). However, it has been reported that PLM has a stronger affinity for the SERCA-2a binding site than SLN, but SLN may have additional interactions with the SERCA-2a-PLM complex (Asahi et al. 2003; Vittorini et al. 2007). In general, SLN can regulate SERCA-2a by inhibiting it through direct interaction with SERCA-2a or by stabilizing the SERCA-2a-PLM complex (Asahi et al 2003; Vittorini et al. 2007).

1.7.6 Phospholamban (PLM)

Phospholamban is a 52 amino acid integral membrane protein that regulates SERCA-2a in cardiac and skeletal muscle cells (Rodriguez and Kranias 2005). In vitro studies have shown that phospholamban structure appears as a pentamer, that is composed of 6000 Da subunits and it is located in the SR of cardiac, slow twitch skeletal and smooth muscles (Schmidt et al. 2002). It has been suggested that although PLM mainly exists as a homopentamer, its functionally active form is a monomer and the pentamer probably act as a reservoir (Zvaritch et al. 2000). There are currently no isoforms of phospholamban known and therefore it is considered as a single copy gene (Simmerman and Jones 1998). The structure of PLM is organized into two main domains (i.e. Domain I and II). Domain I (amino acids residues 1-30) is hydrophilic and it constitutes the cytoplasmic sector and it can be subdivided further into two motifs i.e. domain Ia (residues 1-20) which has been reported to form an α helical structure and domain Ib (residues 21-30) which usually

exists as a random coil (MacLennan et al. 1998; Simmerman and Jones 1998). Domain II (amino acids 31-52) consists of a hydrophobic membrane spanning part of the protein and it has also been proposed to have an α-helical structure which stabilizes the phospholamban pentamer (Kadambi and Kranias 1997; Simmerman and Jones 1998).

1.7.6.1 **Role and regulation of PLM**

PLM in its unphosphorylated state, is known to inhibit SERCA-2a activity, however, when phosphorylated it dissociate from SERCA-2a (Luo et al. 1998; Minamisawa et al. 1999). It has been reported that, under normal physiological conditions, PLM phosphorylation on its serine residue is the main predominant event that leads to increased rates of Ca^{2+} uptake into the SR and accelerated relaxation (Tada et al. 1982; Luo et al. 1998). In addition, it has recently been shown that PLM forms an integral part of the Na^+/K^+ pump complex and provides the link between kinase activation and modulation of pumps (Silverman et al. 2005). This binding of PLM to the Na^+/K^+ pump begins with β-adrenergic receptor stimulation in the intact heart which is chronotropic, inotropic and lusitropic (Shattock 2009). Inotropic and lusitropic effects are primarily due to the activation of the cAMP-dependent kinase (PKA) which takes place after the elevation of the second messenger cAMP (Shattock 2009).

In vitro studies, using purified cardiac SR membranes, have shown that PLM can be phosphorylated by PKA at serine-16, Ca^{2+}/ calmodulin-dependent protein kinase at Threonine-17 and PKC at Serine-10, thus inhibiting it (Simmerman et al. 1986; Silverman et al. 2005; Shattock 2009). PKA activation has four main consequences

i.e. 1) an increase in L-type Ca^{2+} current, 2) an increase in recycling of Ca^{2+} back into the SR which follows PLM phosphorylation, 3) an increased rate of Ca^{2+} dissociation from the myofilaments following phosphorylation of troponin I, and 4) an increase in intracellular Na^+ which is due to increased heart rate and changes in the control of intracellular Ca^{2+} via Na^+/Ca^{2+} exchanger (Shattock 2009). PLM plays an essential role in the protection of the heart from Na^+ and Ca^{2+} overload during β-receptor stimulation (Shattock 2009). In addition, studies have shown that an increase in heart rate in the absence of β-adrenergic stimulation can lead to phospholamban (PLM) phosphorylation at Threonine-17 (Thr-17) through a process that involves the generation of nitric oxide (NO) from nNOS (Zhao et al. 2004; Sears et al. 2004).

1.8 Motivation, aims and objectives of this study

1.8.1 Motivation

To understand the causes and aetiology of the development of the cardiovascular pathology (cardiomyopathy) in obesity, in the current study we have focused on the insulin signaling pathway. Previous studies conducted in our laboratory, demonstrated this pathway to be insensitive to insulin stimulation in hearts from a model of diet induced obese (DIO) rats (du Toit et al. 2008). One of the abnormalities observed in this pathway, is an inability of insulin to stimulate PKB/Akt, which is known to mediate the metabolic effects of insulin such as glycogen synthesis and glucose uptake (unpublished results). The cardiomyocytes from these diabetic hearts also present with an inability to take up glucose on insulin stimulation (Patel et al. 2004). As mentioned previously, prior to the activation by insulin, PKB/Akt directly regulates the activity of GSK-3 (Lawrence and Roach 1997).

It has also been reported that GSK-3 protein is upregulated in muscles of both obese rodents and type II diabetic humans (review by Henriksen and Dokken 2006). This has been associated with decreased whole body insulin sensitivity and attenuated expression of the SERCA-2a protein in cardiomyocytes (Michael et al. 2004). However, in the context of protection via pre-conditioning, most studies focused more on GSK-3β than the GSK-3α isoform. As it is well known that the activity of PKB/Akt protein is suppressed in the insulin resistant state (Vollenweider et al. 2002; Bouzakri et al. 2003), we postulate that GSK-3 expression and activity will be upregulated in the hearts from obese rodents and that this may lead to the development of cardiomyopathy. As far as we understand, this has not yet been investigated.

In addition, a new range of selective and more specific GSK-3 inhibitors is currently under development (review by Henriksen and Dokken 2006). But the cardiovascular effects or long-term treatment effects of these inhibitors in obesity and insulin resistance have not been investigated. However, it has been shown that a 20 day treatment period of obese mice resulted in improved whole body insulin sensitivity (Rao et al. 2007). In addition, it is known that the inhibition of myocardial GSK-3 protein plays a role in the protection against ischemic damage at the level of mitochondrial functioning (Juhaszova et al. 2004). However, the expression, regulation or dysregulation and the intracellular compartmentalization of the GSK-3 protein in the heart, in states of obesity and insulin resistance is currently unknown. We therefore propose to use a selective GSK-3 inhibitor to elucidate the role of the GSK-3 protein in the development of the diverse detrimental myocardial effects resulting from obesity and insulin resistance.

1.8.2 Hypothesis

We hypothesize that GSK-3 protein and its substrate proteins play a role in the development of cardiomyopathy associated with obesity and insulin resistance. In addition, we also hypothesize that GSK-3 inhibition may improve cardiac functioning and insulin signaling in obese and insulin resistant animals.

1.8.3 **Aims**

The aims of the present study were to determine whether:

i) myocardial GSK-3 protein and its substrate proteins are dysregulated in obesity and insulin resistance,

ii) a specific GSK-3 inhibitor can prevent or improve the cardiovascular pathology found in obese and insulin resistant animals.

1.8.4 **Objectives**

Our objectives were to correlate the alterations in expression and activation of GSK-3 protein in a well characterised rat model of obesity coupled to insulin resistance with:

i) myocardial contractile dysfunction and an inability of hearts to withstand ischemia/reperfusion,

ii) the activation and expression of PLM and SERCA-2a in the SR

iii) the activation of intermediates (IRS-1, IRS-2 and PKB/Akt) that lie upstream in the activation pathway of GSK-3.

CHAPTER 2

MATERIALS AND METHODS

2.1 Materials

The reagents used in the current study were bought from different companies such as *Merck NT laboratory supplies* (PTY, LTD) (NaCl, KCl, CaCl$_2$, KH$_2$PO$_4$, NaHCO$_3$, MgSO$_4$, NaSO$_4$, d-glucose, Na$^+$ pyrophosphate, Folin Ciocalteus (Folin C), sodium dodecyl sulphate (SDS), tris (hydroxylmethyl) aminomethane, acrylamide), *Sigma-Aldrich Life Science* (ammonium persulfate (APS), pyruvate, mecarpto-ethanol, N,N,N,N,-tetramethylethylenediamine (TEMED), ponceau red, phenylmethylsulphonyl fluoride (PMSF), triton-X-100), *Millipore*, (Millipore Immobilon-p Polyvinyledene Fluoride (PVDF) microporous membrane and Linco Insulin enzyme linked immunosorbent assay (ELISA) kit), *Roche Diagnostics*, (bovine serum albumin (BSA)), *Amersham Biosciences*, (enhanced chemiluminescence (ECL) Western blotting detection reagents, anti-rabbit Ig, horseradish peroxidase linked whole secondary antibody), *Santa Cruz Biotechnology Inc.*, (SERCA-2a primary antibody), *Cell Signaling technology*, (IRS-1, IRS-2, GSK-3, PKB/Akt, PLM and β-Tubulin primary antibodies) and *Bayer-Bayer* (Euthanaze).

2.2 **Methods**

2.2.1 **Animals**

Age and weight matched male Wistar rats (animals) were used in the present study. At 4 weeks after birth, rats were weaned and placed on ad libitum diet i.e. free access to food (standard rat chow) and water. Rats were housed in cages (3 per cage) at constant environment of $22^{o}C$ temperature, 40% humidity and 12 hour artificial day/night cycle in the University of Stellenbosch Central Research facility. Throughout the study, the revised South African National Standard for the care and use of laboratory animals for scientific purposes was followed (SABS, SANS 10386, 2008). This study was approved by the Ethics committee of Stellenbosch University, Faculty of Health Science.

2.2.2 **Classification and selection of study groups**

Animals weighing between 160 and 180g were randomly selected and grouped into control and diet induced obese (DIO) groups. Controls were fed a normal rat chow diet supplying ~380 kJ of energy per day, while DIOs were fed a rat-chow diet supplemented with sucrose and condensed milk (~575 kJ energy per day) for a period of either 8 or 16 weeks (Table 2.1). The total number of rats used throughout the study was 80 and were divided into two groups of 40 controls and 40 DIOs (figure 2.1). These two groups were further subdivided into two subgroups of either 20 controls/DIO and 20 controls/DIO plus GSK-3 inhibitor (figure 2.1).
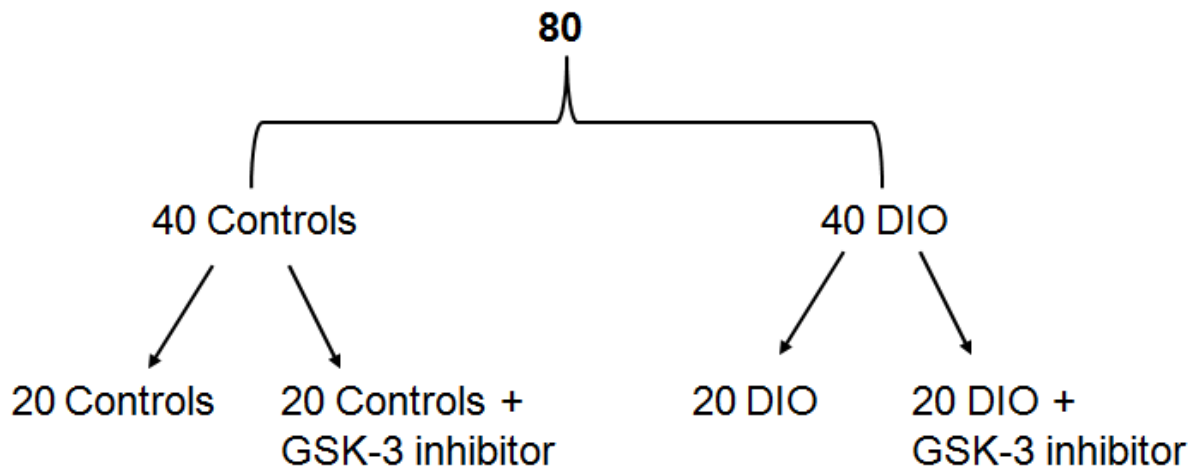
Figure 2.1: *Classification of animals into groups.* DIO, diet induced obese; GSK-3, glycogen synthase kinase-3.

Table 2.1: *Diet composition* (Controls and DIOs)

	Controls	DIOs
Carbohydrates:	60%	65%
Protein:	30%	19%
Fat:	10%	16%
KJ/day	~380	~575

2.2.3 Treatment with GSK-3 inhibitor

A GSK-3 inhibitor from Chirone, CHIR118637 (CT20026) was used in the current study. Chirone (CHIR118637) inhibitors are ATP competitive inhibitors and have been shown to be specific and to target both GSK-3α/β isoforms (Cline et al. 2002; Meijer et al. 2004). An amount of the inhibitor was weighed into each well of an ice cube container. 1 ml liquid jelly, made up of 2.5g Gelatin, 5g Jelly in 50 ml of water, was pipetted into each inhibitor containing wells, mixed thoroughly and allowed to solidify. Each rat (weighing about 300g) was given one jelly block according to its weight, two times per day (in the morning and afternoon) for four weeks (from week 12-16 of the diet period). The final dose was 30 mg/kg/day.

Following four weeks treatment, rats were anesthetized by intra-peritoneal injection of 160 mg/kg pentobarbitone sodium (Euthanaze), weighed and blood glucose concentration determined using a commercial glucometer. Hearts were then excised, weighed and freeze clamped in liquid nitrogen. Blood was collected into eppendorf tubes, allowed to clot on ice and centrifuged at 15000 revolutions per minute (rpm) for 15 minutes. The resultant plasma was then transferred into new eppendorfs and both freeze clamped hearts and plasma were stored at -80°C for later use. In addition, the intra-peritoneal fat mass and tibial lengths were measured. Protein expression and the SERCA-2a activity were then determined using the stored hearts. Results obtained after the treatment were then compared with the age-matched untreated animals.

2.3 **Experimental procedures**

2.3.1 **Western blot**

2.3.1.1 **Lysate preparation (GSK-3, PKB/Akt, IRS-1/2 and SERCA-2a)**

Both control and DIO animals were anesthetized with sodium pentobarbitone (Euthanaze). Hearts were then quickly excised, the atria removed and the ventricles rinsed with Krebs-Heinseleit (KH) buffer and freeze clamped in liquid nitrogen. Tissue stored in liquid nitrogen was homogenized in ice-cold lysis buffer (containing 20 mM Tris-HCl (pH 7.5), 1 mM EGTA, 1 mM EDTA, 150 mM NaCl, 1 mM Na_2VO_3, 1 mM β-glycerophosphate, 2.5 mM sodium-pyrophosphate, 0.3 mM PMSF, 1% (v/v) Triton X-100, 10 µg/ml leupeptin and 10 µg/ml aprotonin) with a polytron PT-10 homogenizer (2 x 4 seconds at setting 4). Following homogenization, samples were incubated on ice for 10 minutes and centrifuged in a microfuge at $4^{o}C$ for 15 minutes at $14^{o}000$ rpm. The resultant supernatants were transferred into new tubes to determine the protein content using the Bradford method (section 2.3.1.3).

2.3.1.2 **PLM lysate preparation**

Sarcoplasmic reticulum membranes were semi-purified using the method described in section 2.3.2.1. The protein content of the resultant semi-purified membrane samples was determined using Bradford method (section 2.3.1.3). Lysis buffer was added in order to dilute all samples to equal protein concentration. Then 3x Laemmli sample buffer with mercaptoethanol was also added. And the samples were incubated for 30 minutes at $37^{o}C$ and frozen for later use.

2.3.1.3 **Bradford protein determination**

Bradford protein determination method was used to determine the protein content of tissue lysates (Bradford 1976). Protein standards made up of a diluted bovine serum albumin (BSA) solution, that contained protein concentration of 1-20 µg in a volume of 100µl was pipetted into test tubes (duplicates). The volume pipetted into test tubes was (µl): 10, 20, 40, 60 and 80, then dH_2O was added into each tube to make a final volume of 100µl. 900µl of Bradford reagent (diluted 1:5) was also added, samples vortexed and incubated for 15-30 minutes. The absorbance values were measured using a spectrophotometer at 595 nm and the standard curve was plotted to determine the protein content of the unknown samples.

The samples (supernatants) from the above (section 2.3.1.1) were diluted 1:10 with dH_2O to dilute all detergents such as Triton-X present, which may interfere with the experiment. 5µl of each diluted sample (duplicates) was further diluted with 95µl of dH_2O to make a total volume of 100µl and 900µl Bradford reagent was added. All samples were vortexed thoroughly and incubated at room temperature for 15-30 minutes. The absorbance was measured with a spectrophotometer at 595 nm and the protein content was determined using the above mentioned standard curve. The standard curve generated saturates at ~20µg protein concentration per sample, therefore the necessary amount of samples were calculated and pipetted into Eppendorf tubes. Lysis buffer was added in order to dilute all samples to equal protein concentration. Then 3x Laemmli sample buffer with mercaptoethanol was also added. The samples were boiled for 5 minutes and stored at -20°C for later use.

2.3.1.4 Immunoblotting

2.3.1.4.1 Loading and separation of proteins

Following Bradford method, lysates were boiled for 5 minutes (excluding PLM lysates which were incubated at 37°C for 30 min), centrifuged and proteins (20-120μg) were separated by sodium dodecyl sulphate polyacrylamide gel electrophoresis (SDS-PAGE) using the standard BIO-RAD Mini-Protein III system. Throughout the study, 7.5% and 12% resolving gels were used, depending on the size of the protein and 4% stacking gel on top (table 2.2). The GSK-3, PKB/Akt and PLM proteins were separated with a 12% gel, while IRS-1, IRS-2 and SERCA-2a were separated with a 7.5% gel (table 2.3). The samples and molecular weight marker were loaded into the gel and the running buffer containing, 250mM Tris, 192mM glycine and 1% sodium dodecyl sulphate (SDS) was added, followed by electrophoresis. The gels were ran with 100 volts (V) and 200 milliampere (mA) for 10 minutes followed by 200V and 200 mA for 65 minutes. The molecular weight marker was used to locate each protein separated according to their molecular weights.

Table 2.2: *Gel composition*. Tris-HCl, trisaminomethane pH set with hydrochloric acid; SDS, sodium dodecyl sulphate; APS, ammonium persulfate; TEMED, tetramethylethylenediamine.

Reagent	Stock	7.5%	12%	4% (Stack gel)
dH$_2$O		5.525 ml	4.4 ml	3.05 ml
Tris-HCl (pH 8.8)	1.5 M	2.50 ml	2.50 ml	1.25 ml (0.5M Tris)
SDS	10%	100 µl	100 µl	50 µl
Acrylamide	40%	1.875 ml	3 ml	500 µl
APS	10%	50 µl	50 µl	50 µl
TEMED	99%	20 µl	20 µl	10 µl

2.3.1.4.2 Transfer of proteins

Following the separation technique, proteins were transferred (200V and 200mA) into a polyvinylidene flouride (PVDF) membrane using the electrotransfer system with a transfer buffer containing 25mM Tris-HCl, 192mM glycine and methanol (20% v/v) for 1 hour. After transfer, the membranes were washed with methanol for 30 seconds and left to dry for 15 minutes. These membranes were then stained with the reversible stain, Ponceau red to visualize the proteins and confirm if transferred satisfactorily.

The membranes were then washed with tris buffered saline-tween-20 (0.1%) (TBS-tween) to remove staining and the membrane blocked by incubating in TBS-tween or TBS-tween containing 5% fat free milk powder for ~1.5 hour. After ~1.5 hour, the membranes were washed with TBS-tween, incubated in the primary (1°) antibody that specifically recognize total or phosphorylated proteins and placed on a belly dancer, at 4^oC overnight. The primary antibodies used in the current study were total and phosphorylated GSK-3(α/β), total and phosphorylated PKB/Akt-α, total and phosphorylated PLM, total SERCA-2a, total IRS-1 and total IRS-2. These primary antibodies were either diluted with TBS-tween or 5% fat free milk in TBS-tween which varies according to the individual protein (table 2.3).

2.3.1.5 Secondary (2°) antibody and Immunodetection

The following day, the membranes were washed with TBS-tween and incubated in diluted secondary antibody for 1 hour at room temperature. The horseradish peroxidise-labelled secondary antibody (antirabbit for GSK-3, PKB/Akt, IRS-1/2 and PLM; or donkey-antigoat for SERCA-2a) was either diluted with TBS-tween or TBS tween containing 5% fat free milk powder (table 2.3). After an hour, the membranes were washed thoroughly with TBS-tween, covered with enhanced chemiluminescence (ECL) detection reagents (Amersham, Life Sciences) in the dark room and exposed to an autoradiography film (Hyperfilm ECL, RPN 2103-Amersham, Life Science) to detect light emission. The duration at which individual proteins were exposed differs from one to another (table 2.3).

2.3.1.6 Densitometry

Following exposure, the films were scanned and analysed with densitometry (UN-SCAN-IT, Silk Scientific Inc., Orema, Utah, USA). The protein values were then determined and expressed as the total and phosphorylated proteins.

2.3.1.7 Equal loading

To confirm if the proteins were equally loaded, all blots were stripped by washing them twice with distilled water (dH$_2$O) for 5 minutes each and incubated for another 5 minutes in 0.2M NaOH on the belly dancer at room temperature. After 5 minutes, membranes were washed twice again with dH$_2$O for 5 minutes each, blocked with TBS tween containing 5% fat free milk powder for ~1.5 hour and incubated with β-tubulin (Table 2.3) primary antibody overnight. Membranes were then washed, incubated with secondary antibody, exposed and developed as above. Bands from

the β-tubulin blott should have equal intensity and changes seen from the stripped

blott should not be present in the β-tubulin blott (figure 2.3).

A. Total IRS-1
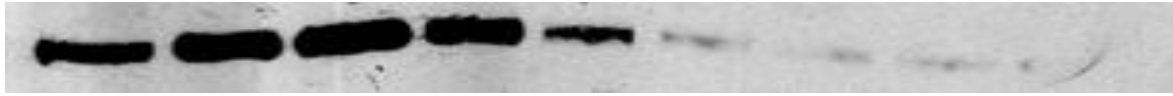
B. β-Tubulin

Figure 2.2: *Total IRS-1 and β-Tubulin*. Shown are the A. IRS-1 and B. β-Tubulin

blots, as an example confirming equal loading.

Table 2.3: Shown is the gel percentage, protein concentration, primary (1°) and

secondary (2°) antibodies and the exposure time for individual protein. TBS, tris-

buffered saline; MW, molecular weight; KDa, Kilo Daltons.

Proteins	MW (KDa)	Gel%	Protein loaded [µg]	1° Antibody dilution	2° Antibody dilution	Time (min) exposed
GSK-3	46	12	40	1:1000 TBS-Tween Milk- (5%)	1:4000 TBS-Tween Milk- (5%)	5
IRS-1	180	7.5	100	1:1000 TBS-Tween Milk- (5%)	1:4000 TBS-Tween Milk- (5%)	20
IRS-2	185	7.5	100	1:1000 TBS-Tween Milk- (5%)	1:4000 TBS-Tween Milk- (5%)	35
PKB/Akt	60	12	40	1:1000 TBS-Tween	1:4000 TBS-Tween Milk- (2.5%)	10
PLM	26	12	20	1:1000 TBS-Tween Milk- (5%)	1:4000 TBS-Tween Milk- (5%)	13
SERCA-2a	100	7.5	120	3µl/5ml TBS-Tween Milk- (5%)	1:4000 TBS-Tween Milk- (5%)	5
β-Tubulin	55	any	any	1:1000 TBS-Tween	1:4000 TBS-Tween	5

2.3.2 Enzyme Assays

2.3.2.1 Preparation of semi-purified sarcoplasmic reticulum membranes

Sarcoplasmic reticulum membranes were semi-purified using the method described by Feher and Davis 1991. After anesthesia, hearts were excised and cut finely with scissors in ice cold 0.9% NaCl and rinsed to remove all traces of blood. One heart was homogenized in 5 ml ice cold KCl- imidazole isolation buffer (1M KCl, 10mM imidazole, pH 7) with a Polytron (PT 10) homogenizer, 2 x 7 seconds at setting 6. The resultant homogenate was centrifuged for 20 minutes at 10 000xg using a Sorval SS 34 Rotor. The supernatant was discarded and the resultant pellet rehomogenized in 5 ml isolation buffer as described above. The homogenate was recentrifuged at 6 000xg for 20 minutes and pellet was discarded. Supernatant was centrifuged with a Beckman ultra-centrifuge at 27 000xg for 45 minutes. The resultant supernatant and fluffy layer on top of the pellet were transferred into a Potter-Elvehjem homogenizer and homogenized thoroughly.

2.3.2.2 Ca^{2+}-ATPase activity

Ca^{2+}-ATPase activity was defined as the difference in the amount of P_i produced in the absence or presence of 3mM $CaCl_2$ in a reaction medium containing 100mM KCl, 50mM Imidazole-HCl (pH 7.5), 5mM NaN_3, 3mM EGTA, 5mM $MgCl_2$, 2mM K^+-oxalate and 3mM ATP at pH 7.5. A volume of 900µl of the reaction medium (with or without $CaCl_2$) was added into 50 µl membrane fraction and incubated at 37^oC for 5 minutes. The reaction was initiated by adding 100µl ATP, incubated further for 10 minutes and stopped by adding 1 ml 10% tri-chloroacetic acid (TCA) at set time intervals. The reaction mixture was centrifuged at 4 000rpm for 15 minutes to remove chlorate precipitate.

To determine the amount of inorganic phosphate (P_i) liberated, 1 ml $5N$-H_2SO_4 and 1 ml Ammonium-molibdate (2.5g/100ml) were added into a 1 ml aliquot of the supernatant, vortexed thoroughly and incubated for 10 minutes. The complex formed was reduced by adding 100 µl reducing agent (RA) containing 0.239mM 1 Amino-2-Naphthol-4-Sulphonic acid, 0.19mM Sodium bisulphite ($Na_2S_2O_5$), 0.126mM Sodium Sulphite (Fiske and Subbarow 1925) and 6.9ml distilled water (dH_2O), vortexed and incubated for 10 minutes. Colour development was determined spectrophotometrically at 660nm.

2.3.2.3 Insulin enzyme linked immunosorbent assay (ELISA)

Insulin levels were determined from the previously stored plasma using an ELISA kit (Millipore). This assay is based on binding of insulin molecules from the samples to the wells of a microtiter plate, coated by a pre-titered amount of monoclonal mouse anti rat insulin antibodies and the binding of biotinylated polyclonal antibodies to the bound insulin (Millipore 2008). The 96 wells on the microtiter plate were divided into blanks (NSB) (x2), standards (x12), quality controls (QC) (x4) and samples (x78) and were all repeatedly washed three times with 300µl diluted (10X) wash buffer. Then 10µl assay buffer was added onto the non specific binding (NSB) wells. Followed by addition of 10µl Matrix solution to the NSB, standard and control wells. 10µl rat insulin standards were then added (duplicates) in order of ascending concentration. 10µl QC1 and QC2 were also added in to the appropriate wells in duplicates. In sample wells, 10µl sample was added sequentially in duplicates.

80µl Detection antibody was added into all wells, plates covered and incubated for two hours on an orbital microtiter plate shaker (400-500rpm) at room temperature. After 2 hours, the solution from the plate was decanted, plate tapped and washed 3 times with 10x diluted wash buffer (300µl). 100µl enzyme solution was added into each well, plate covered and incubated on shaker for 30 minutes at room temperature. Thereafter, the plate sealer was removed, solution decanted and the wells washed 6 times with 10x diluted wash buffer (300µl for each well per wash). 100µl substrate solution was then added into each well, plate covered and incubated on shaker for 15 minutes. When the blue colour had developed, 100µl stop solution was added and the plates shaked by hand to mix the solution (blue turned to yellow color). The absorbance was then read at 450 nm and 590 nm in a plate reader and insulin concentrations were calculated. Insulin sensitivity was also determined using homeostasis model assessment (HOMA) index, calculated using the equation ([Glucose] x [Insulin])/22.5.

2.3.3 Lowry Protein determination method

50µl homogenate from the above Ca^{2+}-ATPase activity assay (section 2.3.2.2) was pipetted into glass tubes, 1ml 10% Tri-chloroacetic acid (TCA) added and the mixture incubated on ice for 30 minutes or overnight at $4^{o}C$ to precipitate all proteins. Samples were then centrifuged at 2500rpm for 15 minutes at $4^{o}C$ and the resultant supernatant was carefully decanted and discarded. 500µl 1N NaOH was added and samples were heated in a water bath at $70^{o}C$ to dissolve the precipitate. 500µl dH_2O was then added to dilute the samples 1:1 to give a 0.5N NaOH solution and vortexed thoroughly. 50µl protein sample, standards (3 different BSA solutions with known protein concentration dissolved in 0.5N NaOH) and 0.5N NaOH (blank) was pipetted

into lucham tubes in triplicates. 1 ml Na^+K^+-Tartrate-$CuSO_4$ was added into the 50 µl samples, standards and blank from above at set time intervals and were vortexed and incubated at room temperature for 10 minutes. After 10 minutes, 0.1 ml of a 1:3 dilution of Folin Ciocalteus (Folin C) reagent was added at the same set time intervals, vortexed and incubated for 30 minutes. After 30 minutes, OD values were determined using a spectrophotometer at 750nm starting with the blank, standards and then samples. A standard curve was generated and the protein content of the samples was determined.

2.3.4 Heart Perfusion

Rats were anesthetized by intra-peritoneal injection of 160 mg/kg euthanaze. After deep anesthesia, as determined by a foot pinch, hearts were quickly excised and arrested in ice cold Krebs-Henseleit (KH) buffer containing 119 mM NaCl, 25 mM $NaHCO_3$, 4.7 mM KCl, 1.2 mM KH_2PO_4, 0.59 mM $MgSO_4 \cdot 7H_2O$, 0.59 mM Na_2SO_4, 1.25 mM $CaCl_2 \cdot 2H_2O$ and 11 mM glucose. Isolated hearts were then rapidly mounted on the aortic cannula and retrogradely perfused (Langendorff mode) at 37^oC with the KH buffer gassed with 95% O_2 and 5% CO_2 to maintain the pH at 7.4. Thermistor probe was inserted into the right coronary sinus to monitor the myocardial temperature. To monitor the function of the heart, a water (dH_2O) filled latex balloon was inserted into the left ventricle and inflated to establish a baseline pressure (diastolic) of 4-10 mmHg. The balloon was then connected to a pressure transducer (Mantaflex) to relay the pressure changes in the left ventricle via the amplifier to the powerlab/P200 (AD Instrument) which digitally displays the results on a computer.

2.3.4.1 **Perfusion protocol**

To determine functional perfomance, the hearts were stabilized for 30 minutes and subjected to low flow ischemia with a coronary flow rate of 0.2 ml/min for 25 minutes which then was followed by 30 minutes of reperfusion, figure 2.2. Throughout the experiment, changes in diastolic and systolic pressure were monitored. Coronary flow rate, heart rate (HR), time to onset of ischemic contracture (TOIC), peak contracture diastolic pressure (PCDP) and end ischemic diastolic pressure (EIDP) were also recorded. The rate pressure product (RPP) was then calculated from heart rate and the developed pressure. Baseline results were measured during stabilization.
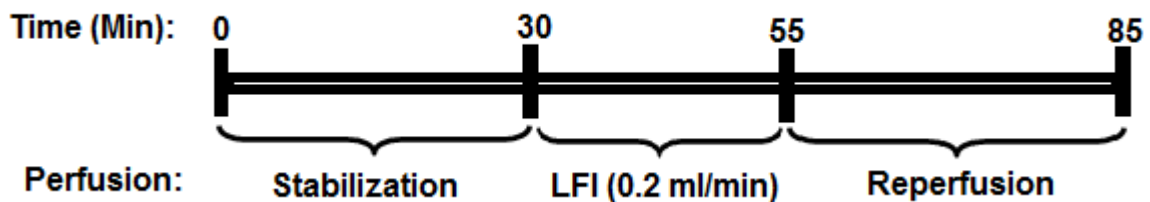

Figure 2.3: *Standard perfusion protocol*. Shown is the time at which the perfusion was started, duration of low flow ischemia (LFI), coronary flow rate (0.2 ml/min) and reperfusion period.

2.4 **Statistical analysis**

Results were statistically compared using Microsoft GraphPad Prism (version 5.0). Student's t-test was used to compare two variables, while one or two way analysis of variance (ANOVA) with Bonferroni post hoc test was used when comparing more than two variables. All values are expressed as the mean ± standard error of the mean (SEM) and p-value of less than 0.05 was considered statistically significant.

CHAPTER 3

RESULTS

3.1 8 weeks data (Baseline)

3.1.1 Biometric parameters

Following 8 weeks on diet, DIO animals were significantly bigger than control animals (*p<0.0001) (figure 3.1). This was associated with increased intra-peritoneal (IP) fat in DIO animals (**p<0.0001) (figure 3.2).
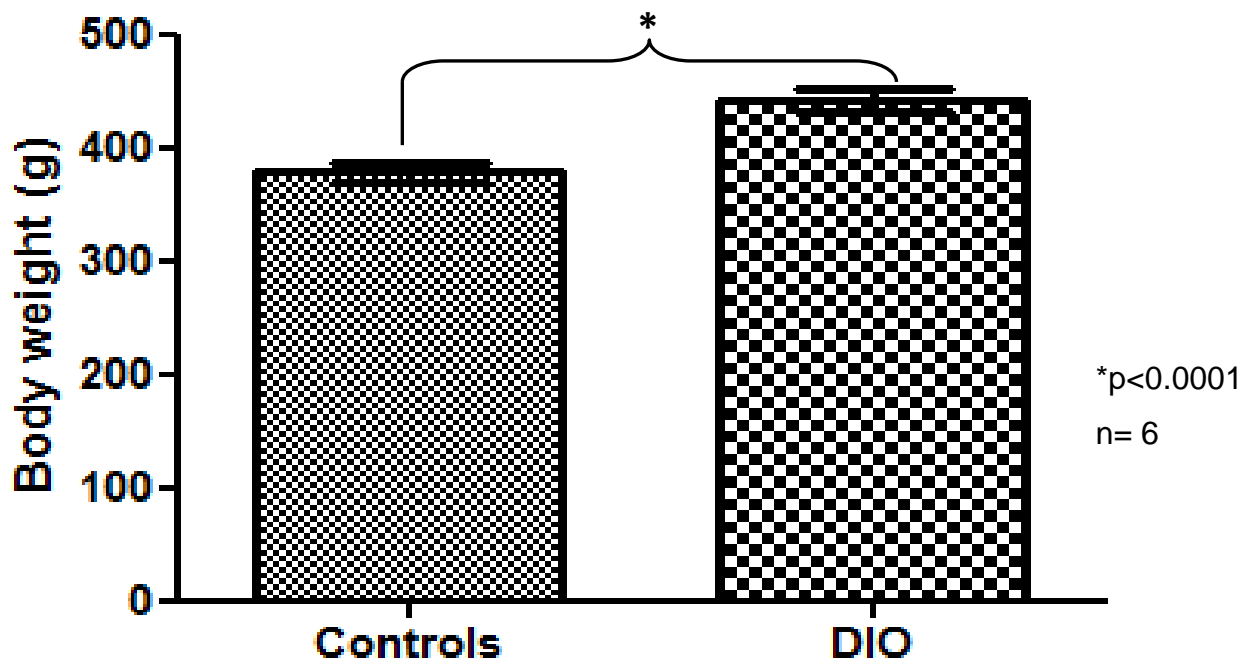

Figure 3.1: *Body weight (BW)*. Shown is the body weight measured in grams (g) of diet induced obese (DIO) and control animals (8 weeks).
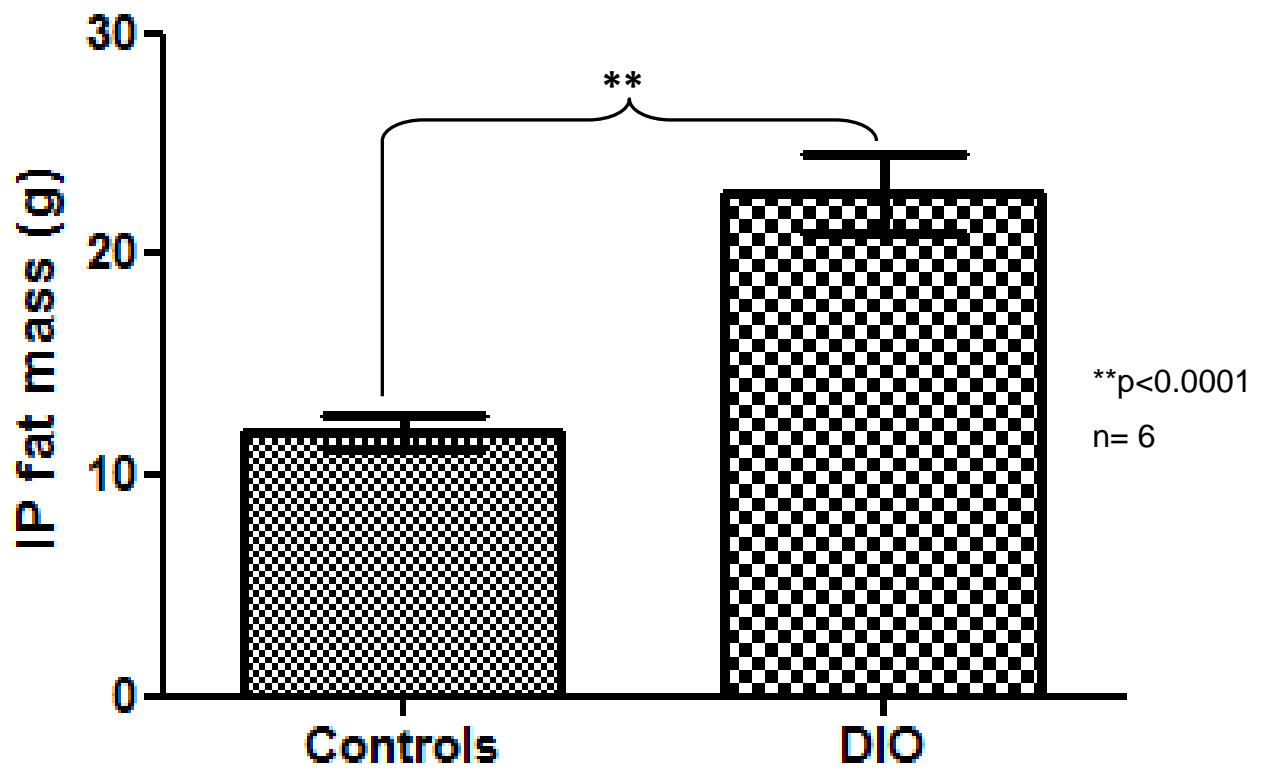
Figure 3.2: *Intra-peritoneal (IP) fat*: Shown is the IP fat mass measured in grams (g) of diet induced obese (DIO) and control animals (8 weeks).

3.1.2 Expression and phosphorylation of proteins (8 weeks)

3.1.2.1 GSK-3 protein

3.1.2.1.1 Total GSK-3

Following eight weeks on diet there was no significant difference in total GSK-3 protein expression between controls and DIO animals (figure 3.3). However, there was a trend towards increase in DIO animals.
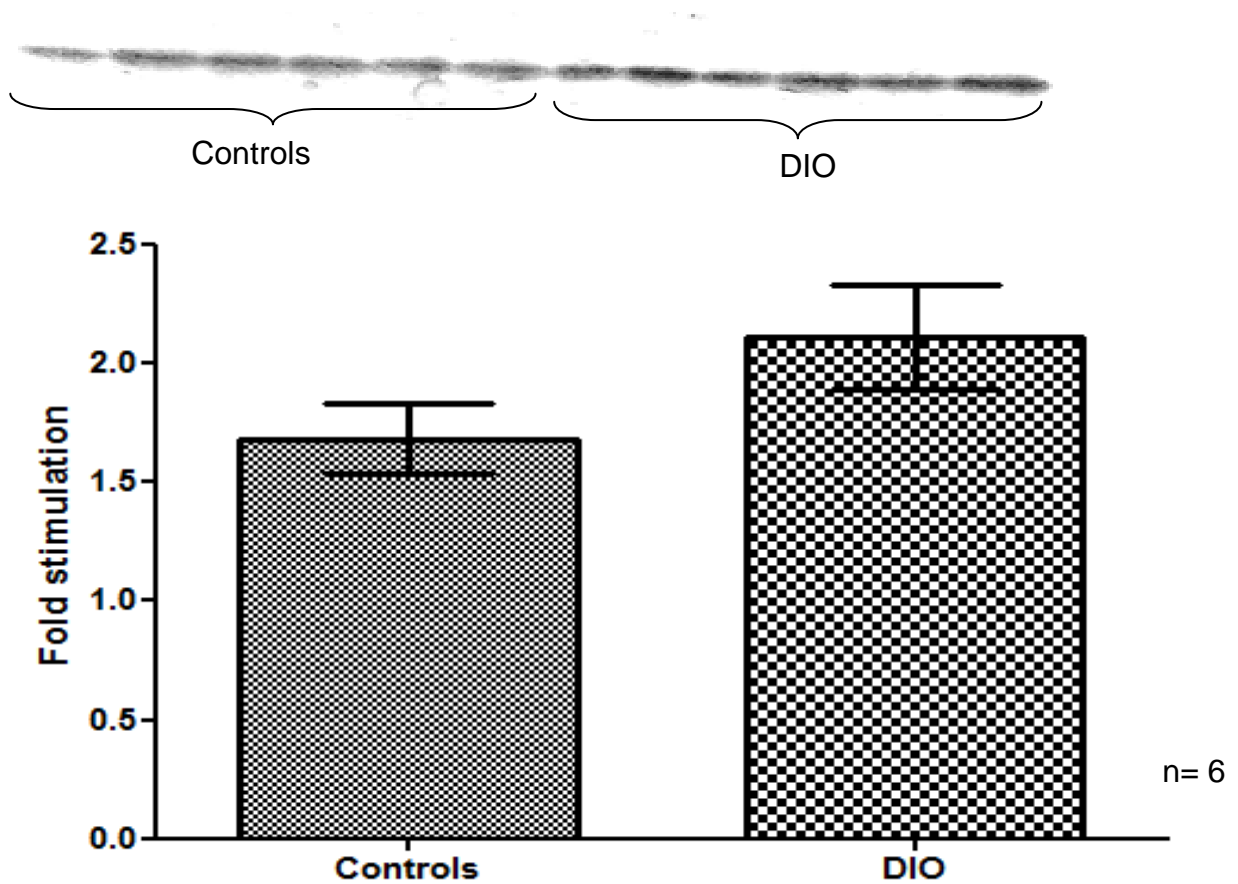

Figure 3.3: *Total Glycogen synthase kinase 3* (GSK-3). Shown is the Western blot for total GSK-3 protein and fold stimulation (compared to the first loaded control that was assigned a value of 1) graph comparing controls and diet induced obese (DIO) animals.

3.1.2.1.2 **Phosphorylated GSK-3α (Alpha)**

After eight weeks on diet, there was no significant difference in GSK-3α phosphorylation when controls and DIO animals were compared (figure 3.4). In addition, there was also no significant difference in phosphorylated (alpha)/total ratio between these two groups (figure 3.5).
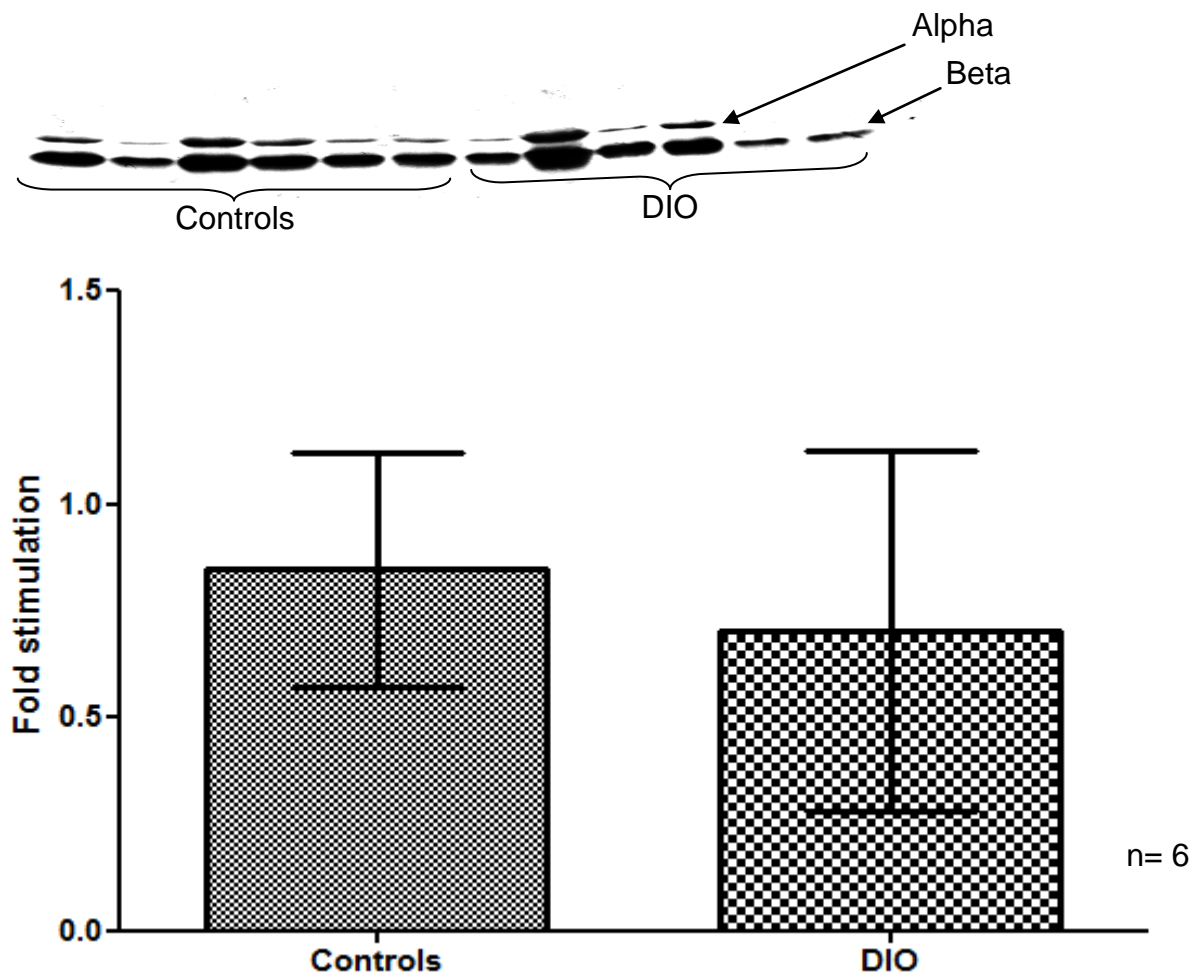

Figure 3.4: GSK-3α *(Alpha) phosphorylation.* Shown is the Western blot representing phosphorylated both GSK-3α and GSK-3β as well as a graph showing GSK-3α fold stimulation (compared to the first loaded control that was assigned a value of 1) comparing diet induced obese (DIO) and control animals.
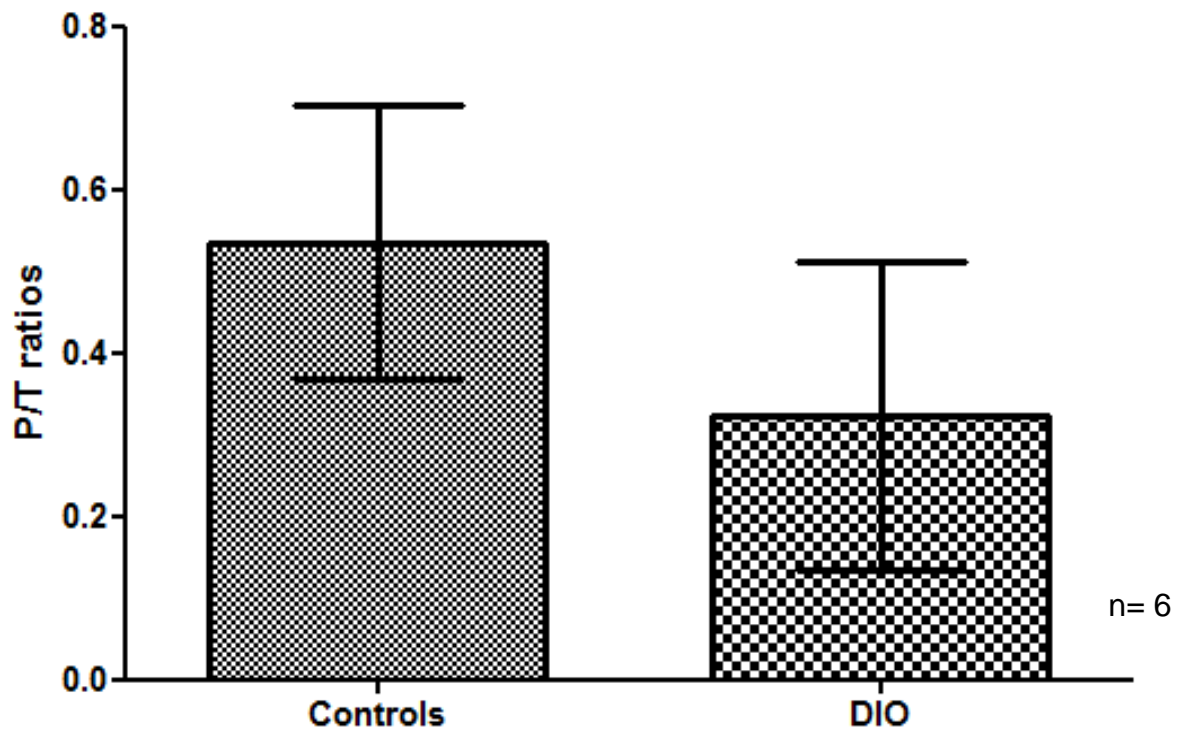
Figure 3.5: *Phospho (Alpha)/total ratios of GSK-3 protein*. Shown are the alpha

phospho/total ratio of both control and DIO animals.

3.1.2.1.3 **Phosphorylated GSK-3 Beta**

After eight weeks of feeding, there was no significant difference in phosphorylation of GSK-3β between controls and DIO animals (figure 3.6). In addition, there was also no significant difference in P/T ratio of GSK-3β (figure 3.7).

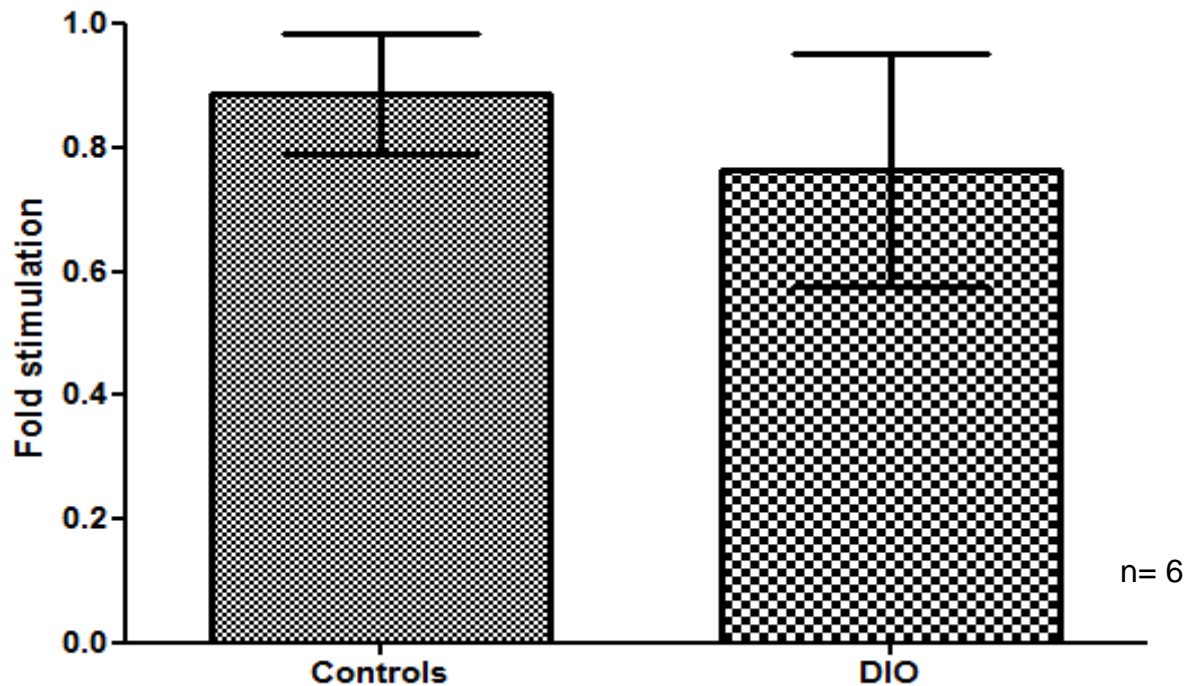
Figure 3.6: Beta phosphorylation of *Glycogen synthase kinase 3* (GSK-3β). Shown is the GSK-3β fold stimulation (compared to the first loaded control that was assigned a value of 1) comparing diet induced obese (DIO) and control animals.
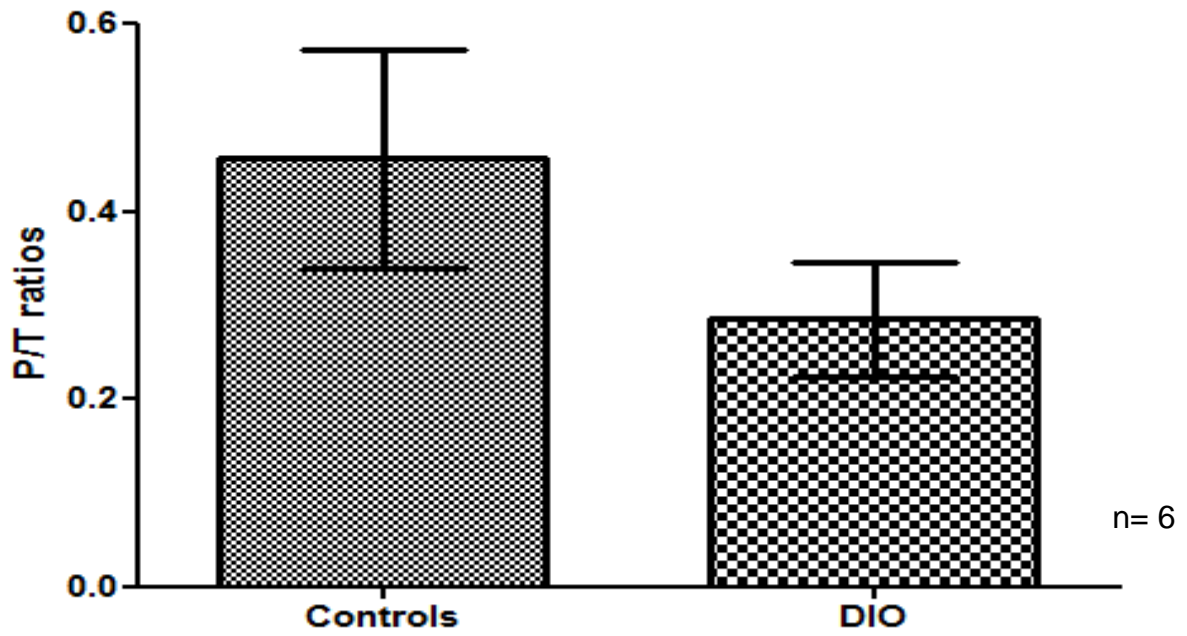
Figure 3.7: *Phospho (Beta)/total ratios of GSK-3 protein*. Shown are the beta

phospho/total ratios of both control and DIO animals.

3.1.2.2 **PKB/Akt protein**

3.1.2.2.1 **Total PKB/Akt protein**

Following eight weeks on diet, there was no significant difference in expression of total PKB/Akt when comparing controls and DIO animals (figure 3.8).
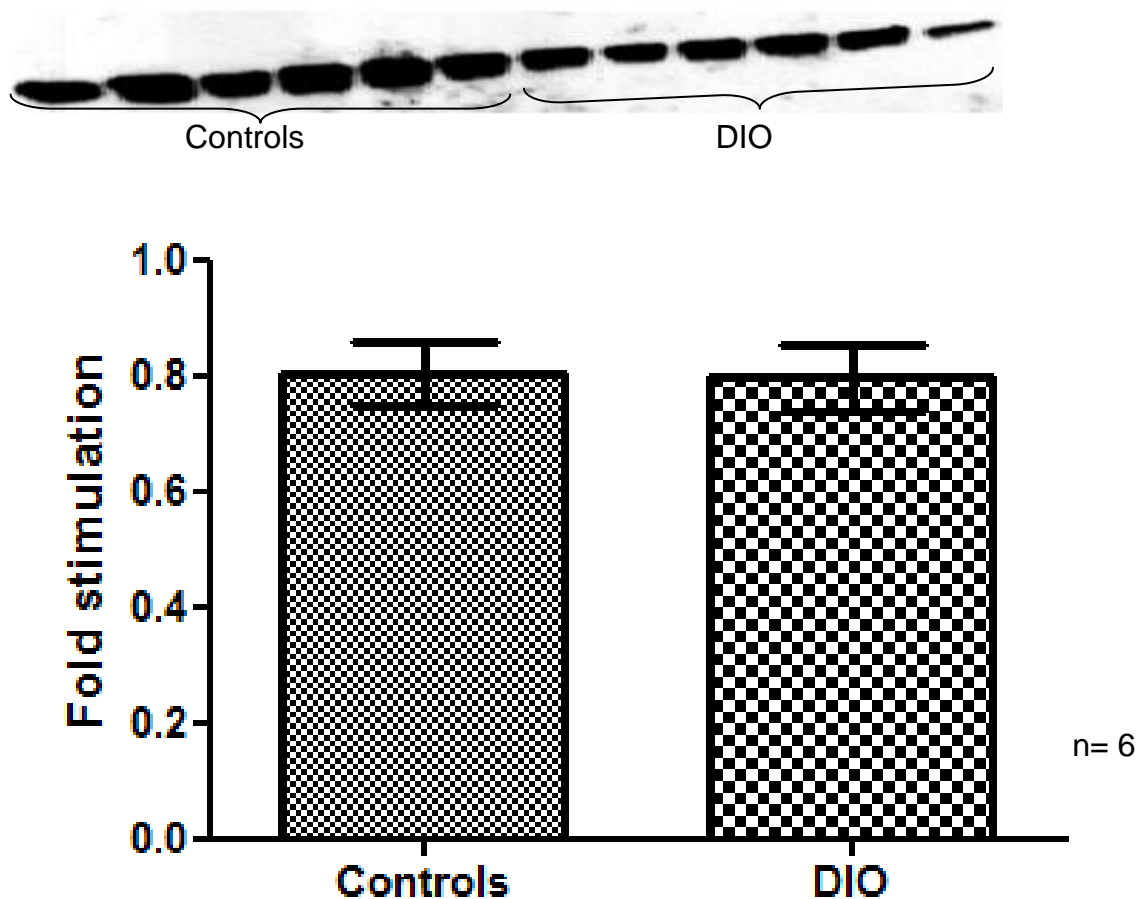

Figure 3.8: *Protein kinase B/Akt* (PKB/Akt). Shown is the Western blot representing total PKB/Akt as well as a graph showing its fold stimulation (compared to the first loaded control that was assigned a value of 1) in controls and diet induced obese (DIO) animals.

3.1.2.2.2 Phosphorylated PKB/Akt protein

Following eight weeks of diet, there was no significant difference in PKB/Akt phosphorylation when controls and DIO animals were compared (figure 3.9). There was also no significant difference in phospho/total ratios of PKB/Akt between control and DIO animals (figure 3.10).

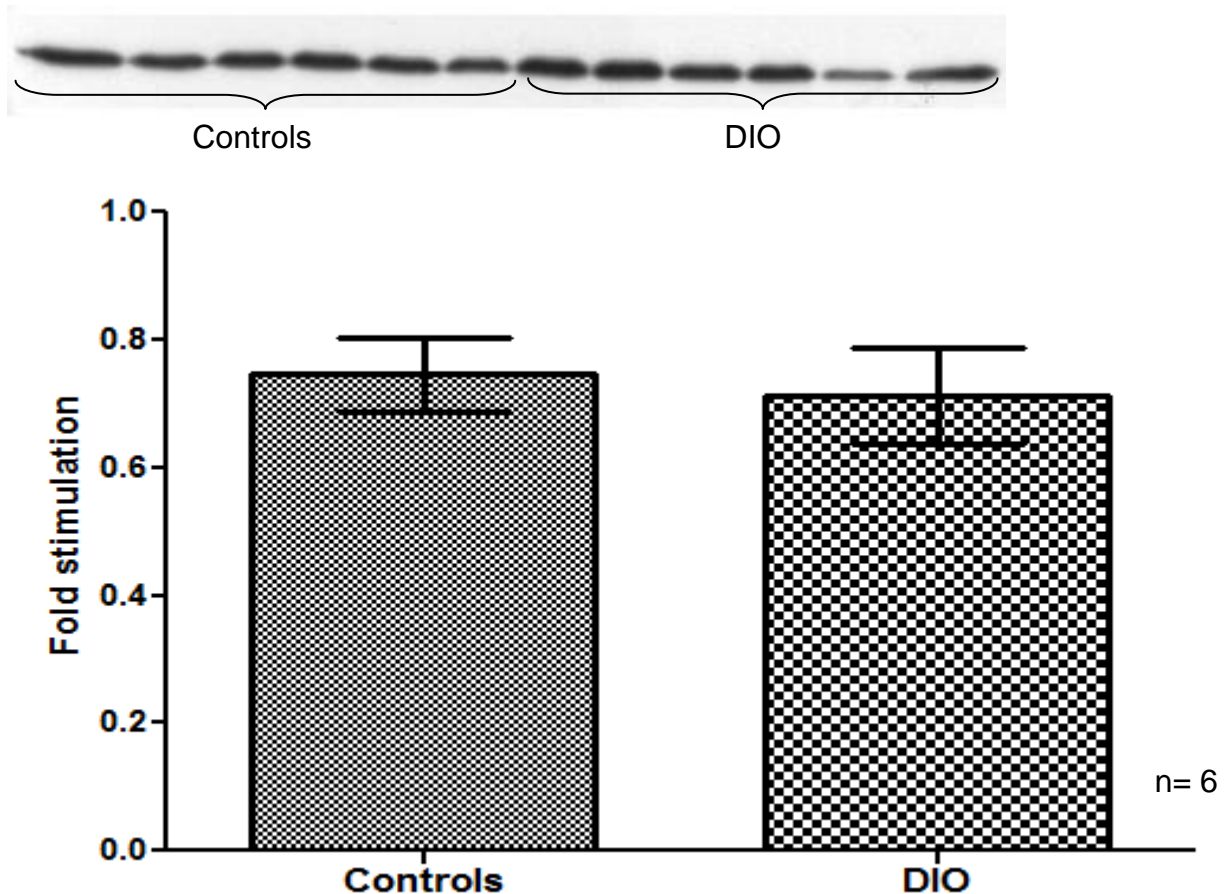**Figure 3.9**: *Protein kinase B/Akt* (PKB/Akt) *phosphorylation*. Shown is the Western blot representing PKB/Akt phosphorylation as well as a graph showing its fold stimulation (compared to the first loaded control that was assigned a value of 1) in controls and diet induced obese (DIO) animals.
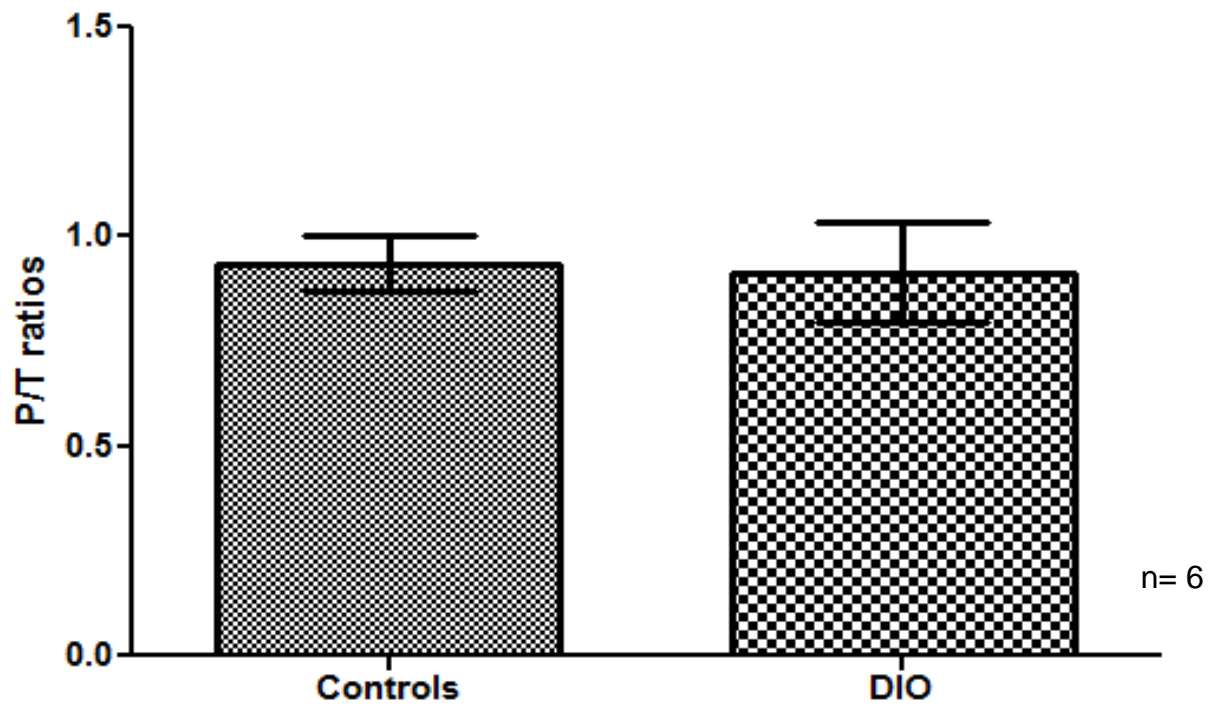
Figure 3.10: *Protein kinase B/Akt* (PKB/Akt). Shown are the phospho/total ratios of both control and DIO animals.

3.1.2.3 **Total IRS-1 protein**

After eight weeks on diet, IRS-1 protein was significantly downregulated in DIO animals when compared to their age matched controls (*p= 0.0002) (figure 3.11).
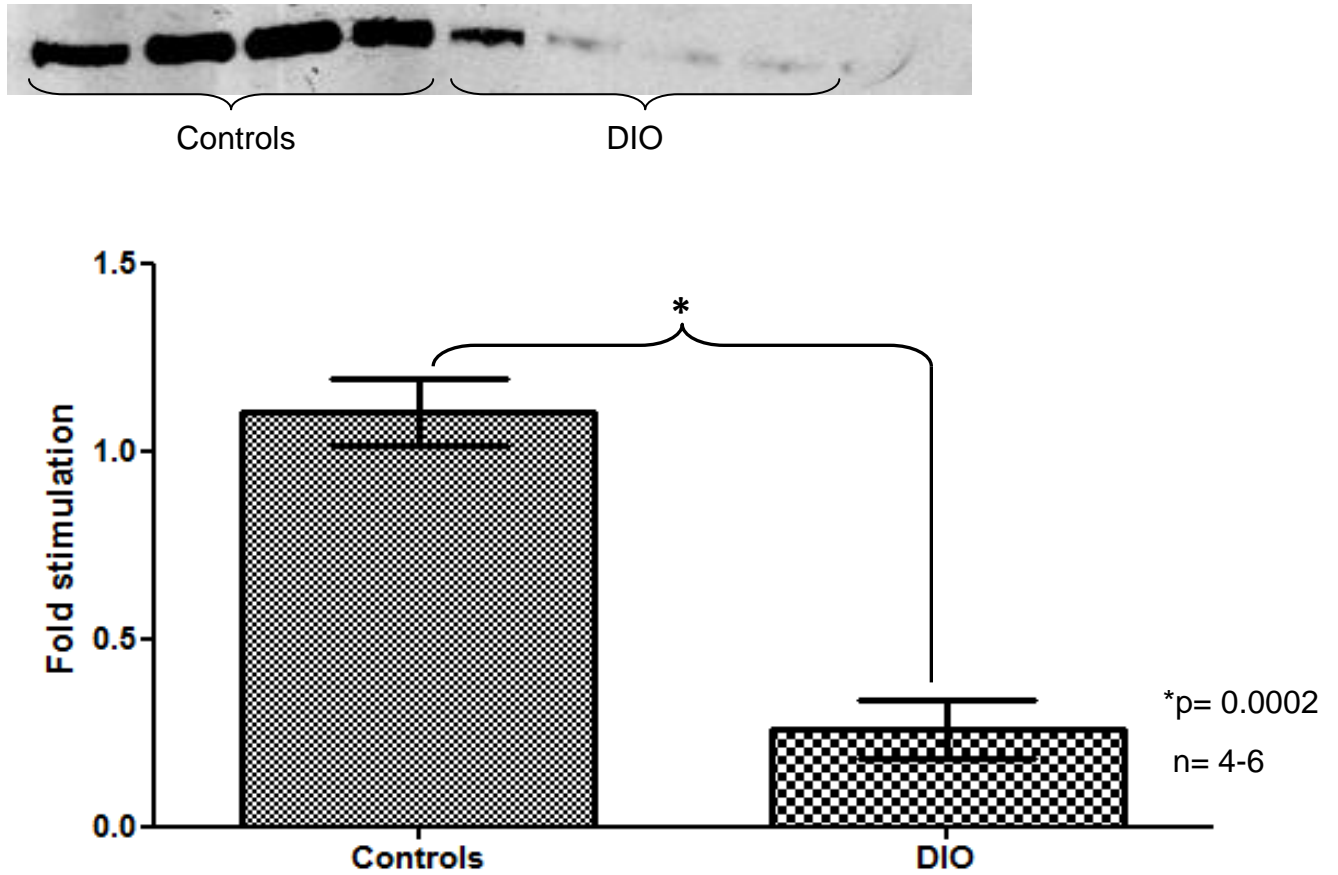
Figure 3.11: *Insulin receptor substrate-1* (IRS-1). Shown is the Western blot representing total IRS-1 expression and its fold stimulation (compared to the first loaded control that was assigned a value of 1) graph comparing controls and DIO animals.

3.1.2.4 **Total IRS-2 protein**

Following eight weeks on diet, there was no significant difference in expression of IRS-2 protein when comparing controls and DIO animals (figure 3.12).
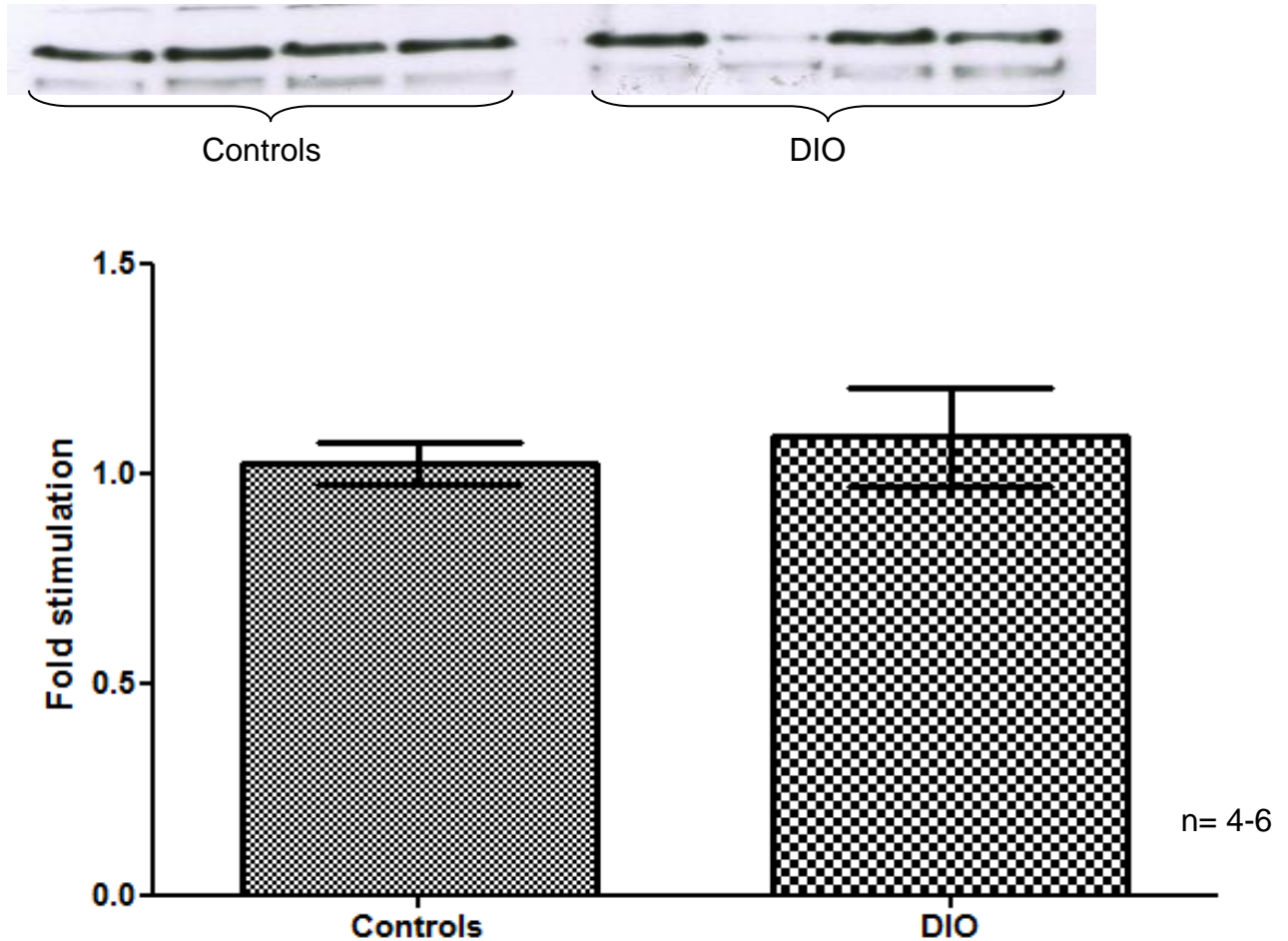
Figure 3.12: *Insulin receptor substrate-2* (IRS-2). Shown is the Western blot representing total IRS-2 expression and its fold stimulation (compared to the first loaded control that was assigned a value of 1) graph comparing controls and DIO animals.

### 3.1.2.5 Total SERCA-2a protein

After eight weeks on diet, DIO animals had a decreased SERCA-2a expression as compared to the age matched controls (*p= 0.0418) (figure 3.13).

Figure 3.13: *Total SERCA-2a*. Shown is the Western blot representing total SERCA-2a expression as well as fold stimulation (compared to the first loaded control that was assigned a value of 1) graph comparing controls and DIO animals.

3.2 Sixteen (16) weeks data (Baseline)

3.2.1 Biometric parameters

After 16 weeks on diet, the DIO animals were significantly bigger than their age matched control animals (*p=0.0009) (figure 3.14). This increased body weight was also associated with increased IP fat in DIO animals (*p=0.0002) (figure 3.15).
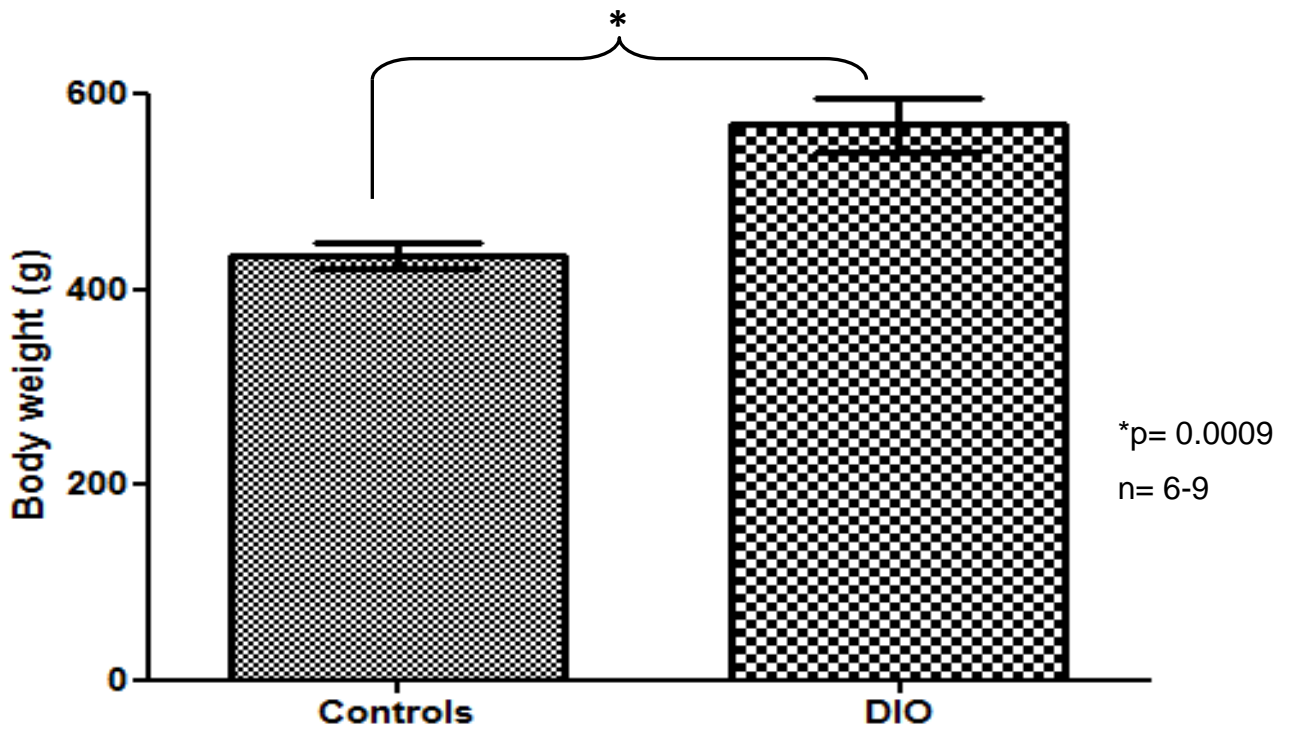
Figure 3.14: *Body weight (BW). Shown is the body weight measured in grams (g) of diet induced obese (DIO) and control animals (16 weeks).*
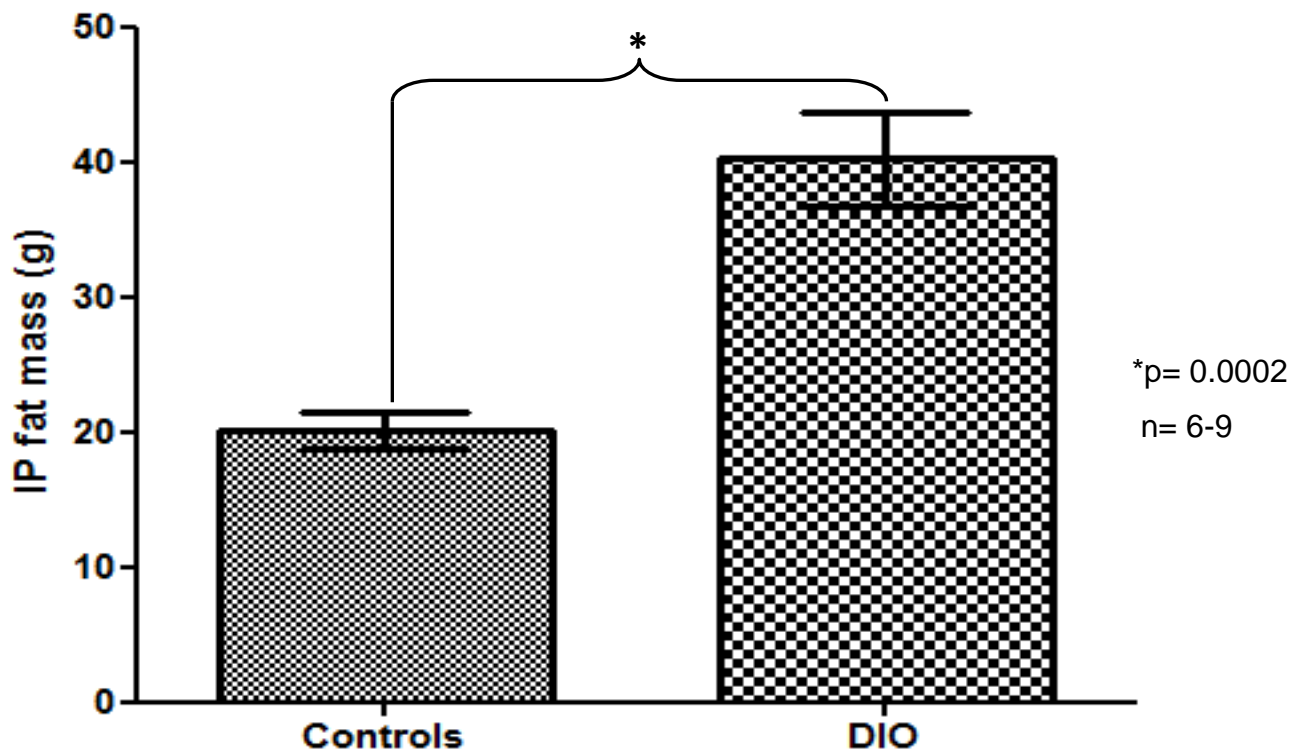
Figure 3.15: *Intra-peritoneal (IP) fat.* Shown is the IP fat mass measured in grams (g) of diet induced obese (DIO) and control animals (16 weeks).

3.2.2 Expression and phosphorylation of proteins (16 weeks)

3.2.2.1 GSK-3 protein

3.2.2.1.1 Total GSK-3

Following 16 weeks on diet, there was no significant difference in total GSK-3 expression when DIO animals were compared to their age matched controls (figure-3.16). However, there was a tendency towards elevated expression.
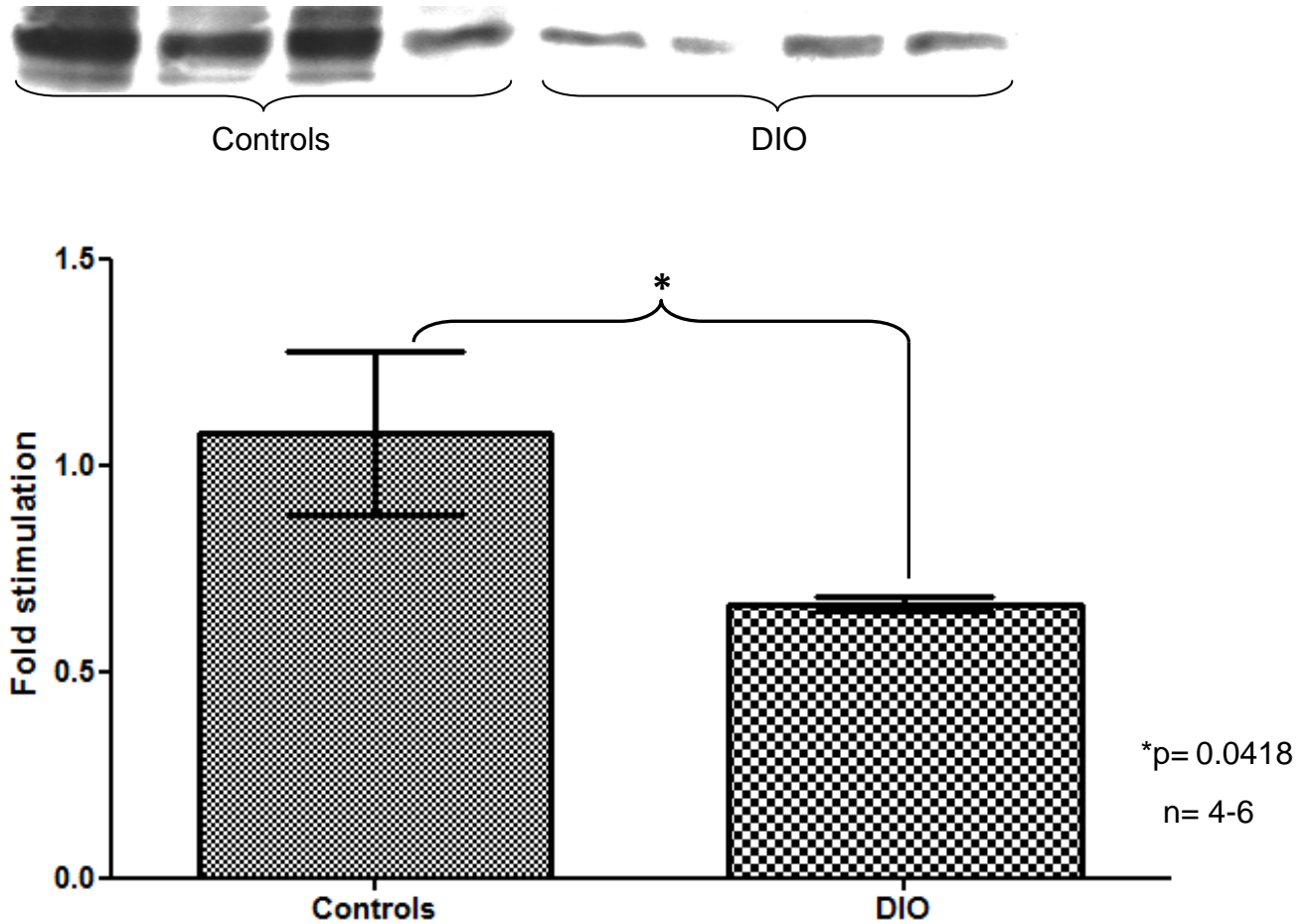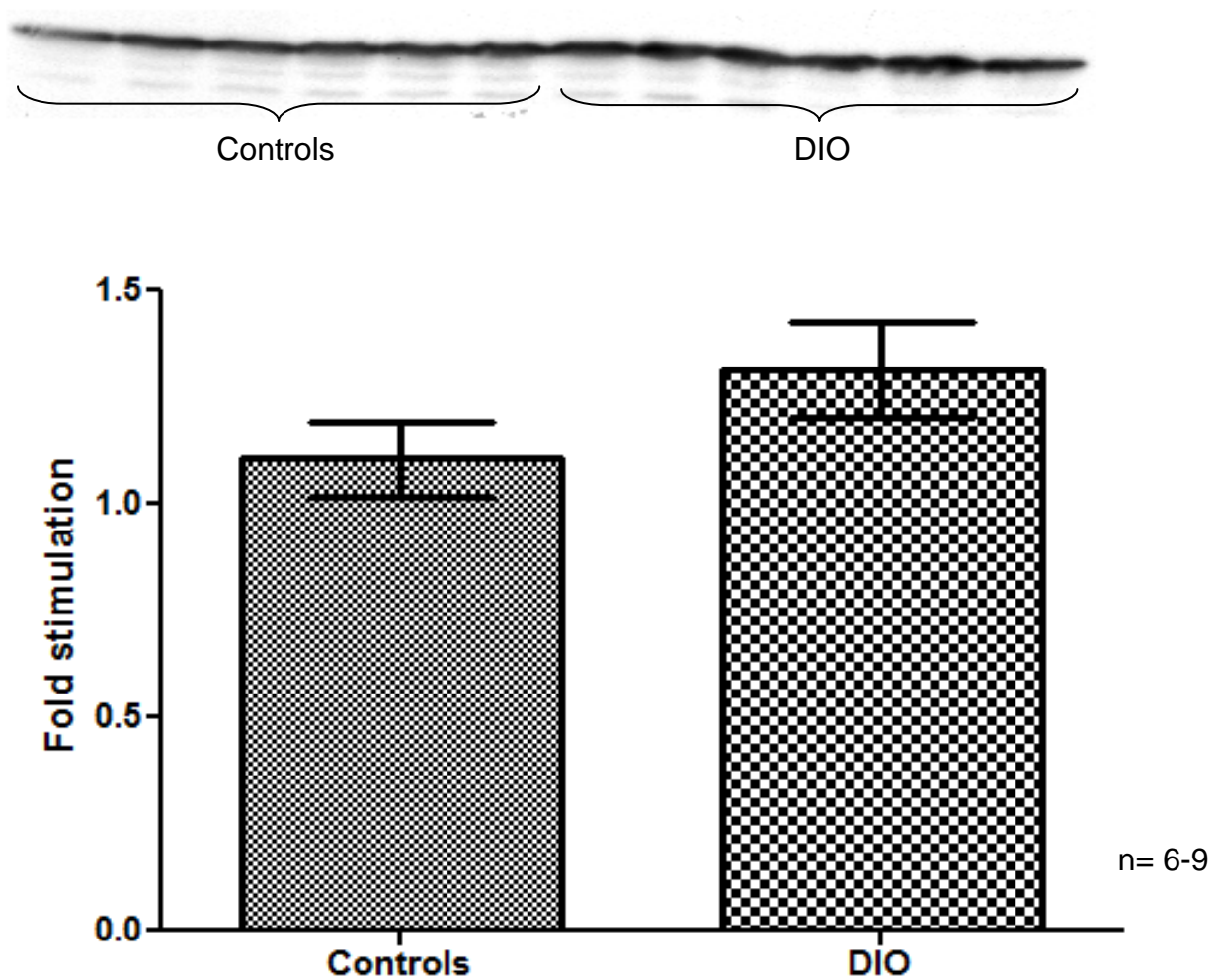

Figure 3.16: *GSK-3 protein*. Shown is the Western blot representing total GSK-3 expression as well as its fold stimulation (compared to the first loaded control that was assigned a value of 1) graph comparing controls and diet induced obese (DIO) animals.

3.2.2.1.2 **Phosphorylated GSK-3α**

After 16 weeks of diet, there was no significant difference in GSK-3α phosphorylation between controls and DIO animals (figure 3.17). In addition, there was also no significant difference in GSK-3α phospho/total (P/T) ratio between controls and DIO animals (figure 3.18).
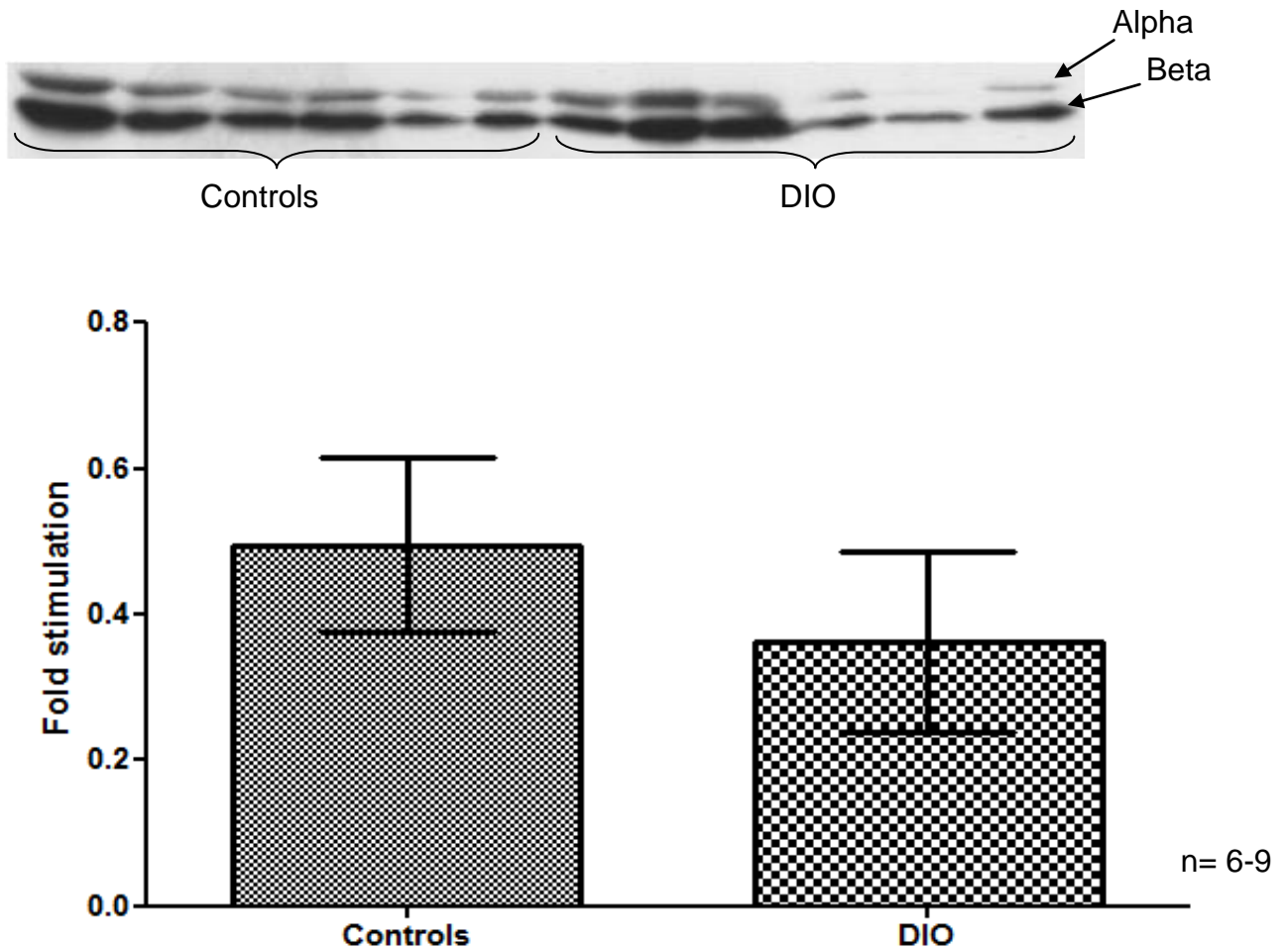
Figure 3.17: Phosphorylated *GSK-3α protein*. Shown is the Western blot representing both GSK-3α and GSK-3β phosphorylation. In addition, shown is the fold stimulation (compared to the first loaded control that was assigned a value of 1) graph of GSK-3α comparing controls and DIO animals.

n= 6-9
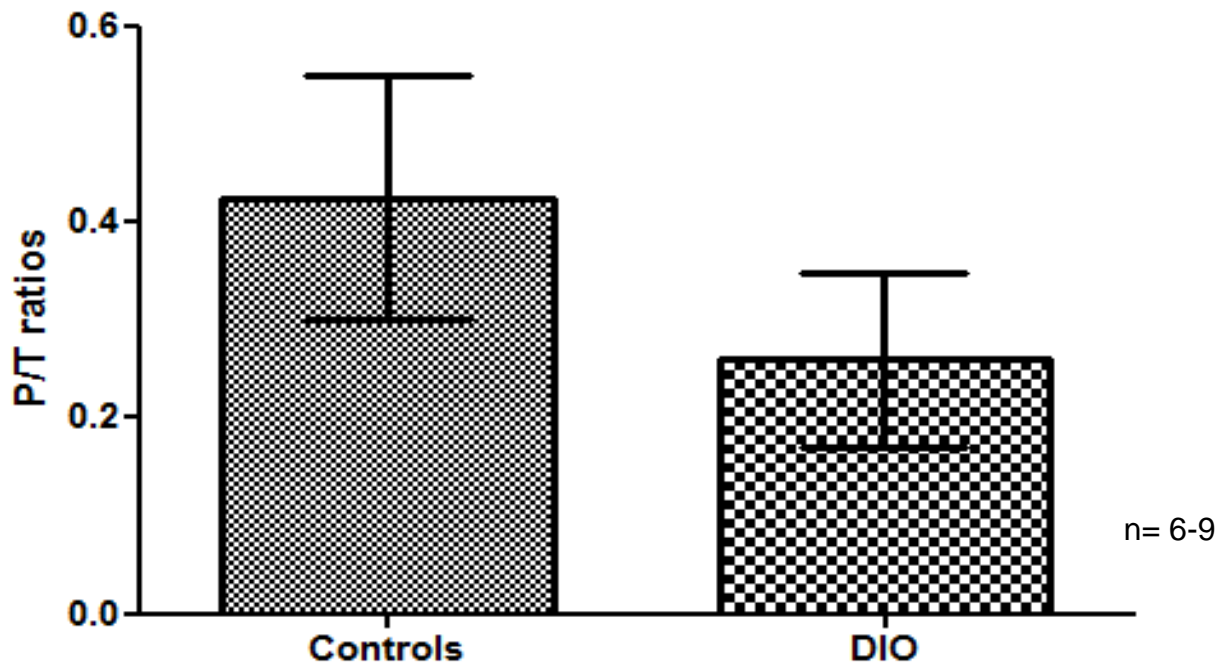
Figure 3.18: *GSK-3 P/T ratio*. Shown are the alpha phospho/total (P/T) ratios of both control and diet induced obese (DIO) animals.

3.2.2.1.3 **Phosphorylated GSK-3β**

Following 16 weeks on diet, there was no significant difference in phosphorylated GSK-3β between controls and DIO animals (figure 3.19). There was also no significant difference in P/T ratio of GSK-3β between these two groups (figure 3.20).
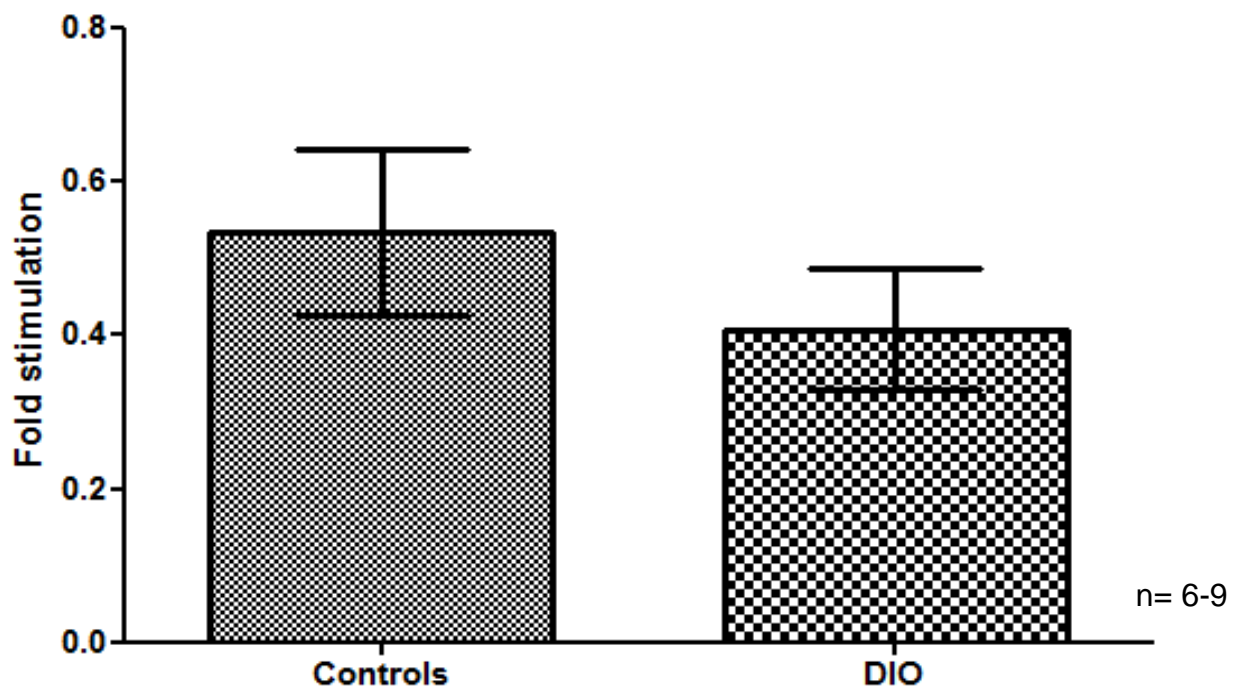
Figure 3.19: Beta phosphorylation of *Glycogen synthase kinase 3* (GSK-3β). Shown is the fold stimulation (compared to the first loaded control that was assigned a value of 1) graph of phosphorylated GSK-3β comparing controls and DIO animals.
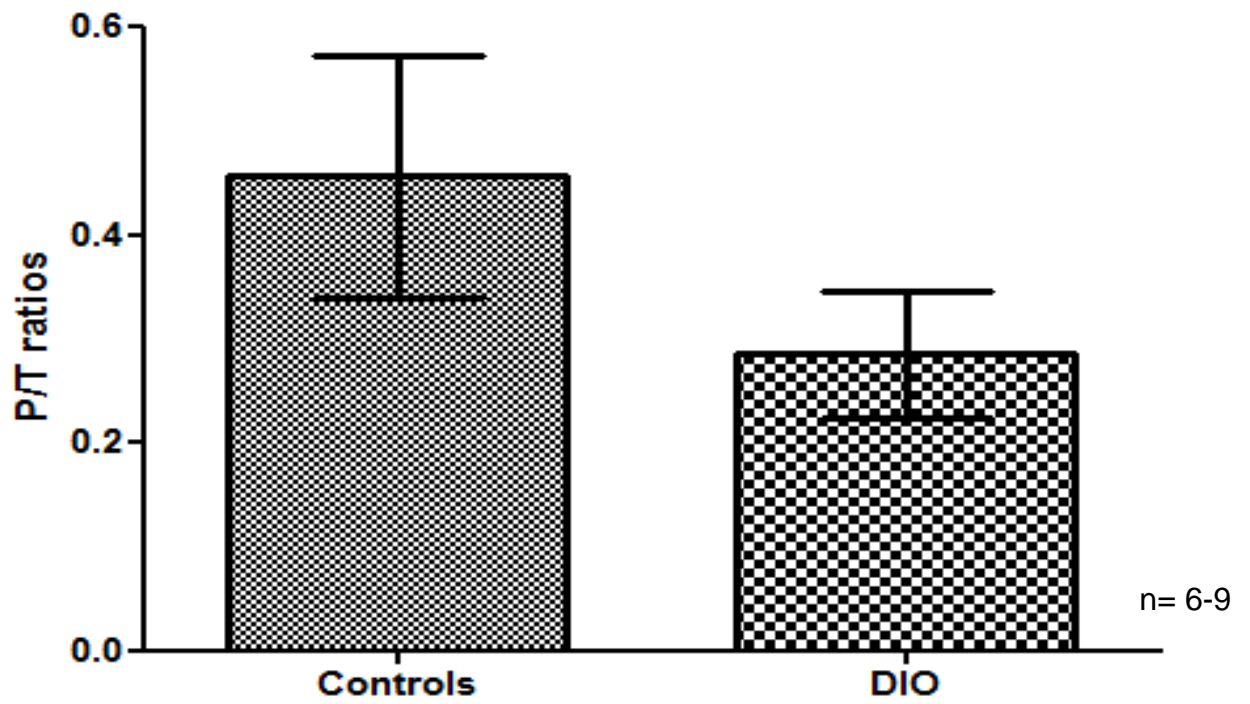
Figure 3.20: *GSK-3 P/T ratio*. Shown are the beta phospho/total ratios of both control and DIO animals.

3.2.2.2 Protein kinase B (PKB/Akt) protein

3.2.2.2.1 Total Protein kinase B (PKB/Akt)

Following 16 weeks on diet, total PKB/Akt expression was significantly down regulated in DIO animals when compared to their age matched controls (*p= 0.0425) (figure 3.21).

Figure 3.21: *Protein kinase B/Akt* (PKB/Akt). Shown is the Western blot representing total PKB/Akt as well as a graph comparing fold stimulation (compared to the first loaded control that was assigned a value of 1) between controls and diet induced obese (DIO) animals.

3.2.2.2.2 **Phosphorylated Protein kinase B (PKB/Akt)**

Following 16 weeks of diet, there was no significant difference in PKB/Akt phosphorylation when controls and DIO animals were compared (figure 3.22). There was also no significant difference in phospho/total ratios of PKB/Akt between control and DIO animals (figure 3.23).
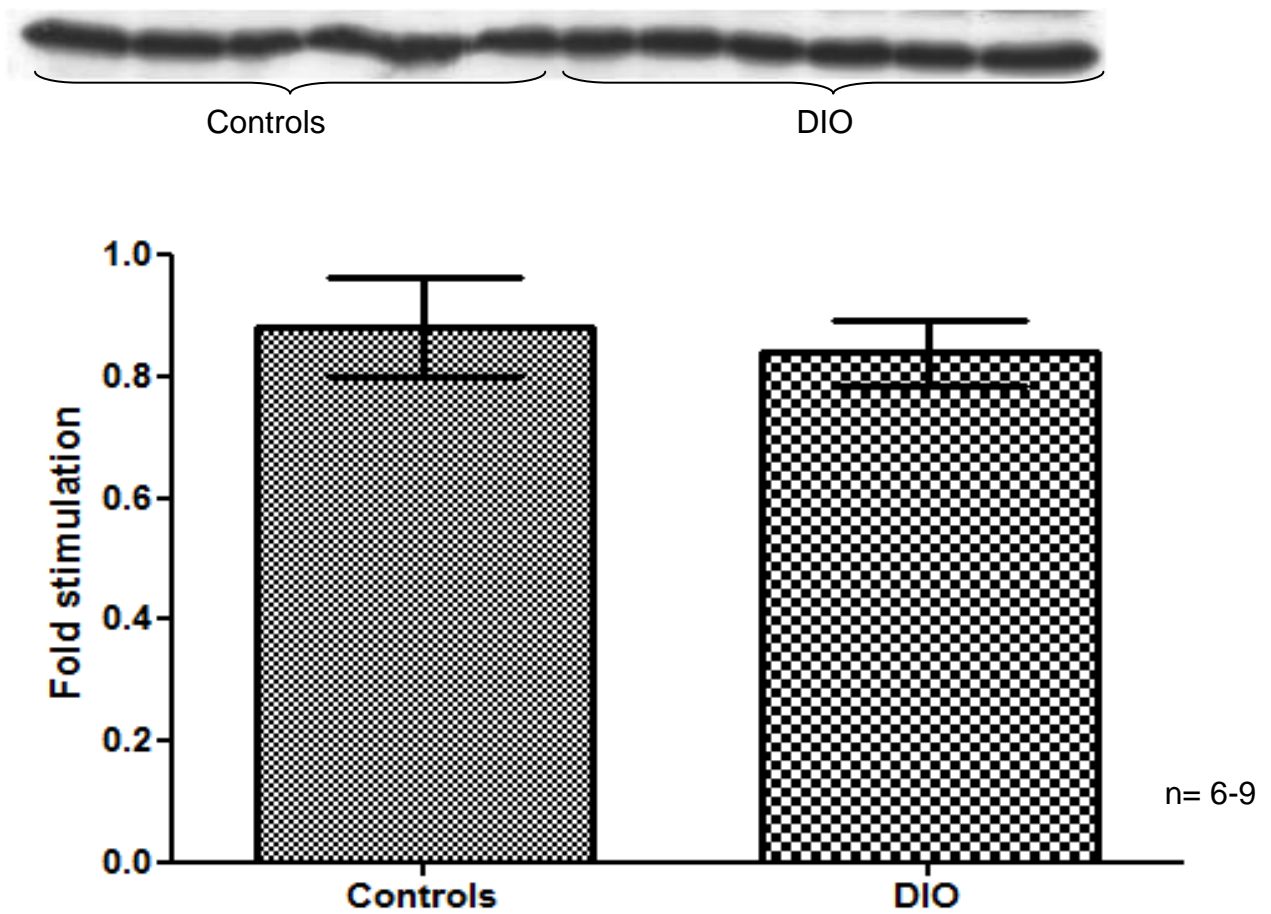
Figure 3.22: *Protein kinase B/Akt* (PKB/Akt) *phosphorylation*. Shown is the Western blot representing PKB/Akt phosphorylation as well as a graph showing its fold stimulation (compared to the first loaded control that was assigned a value of 1) in controls and diet induced obese (DIO) animals.
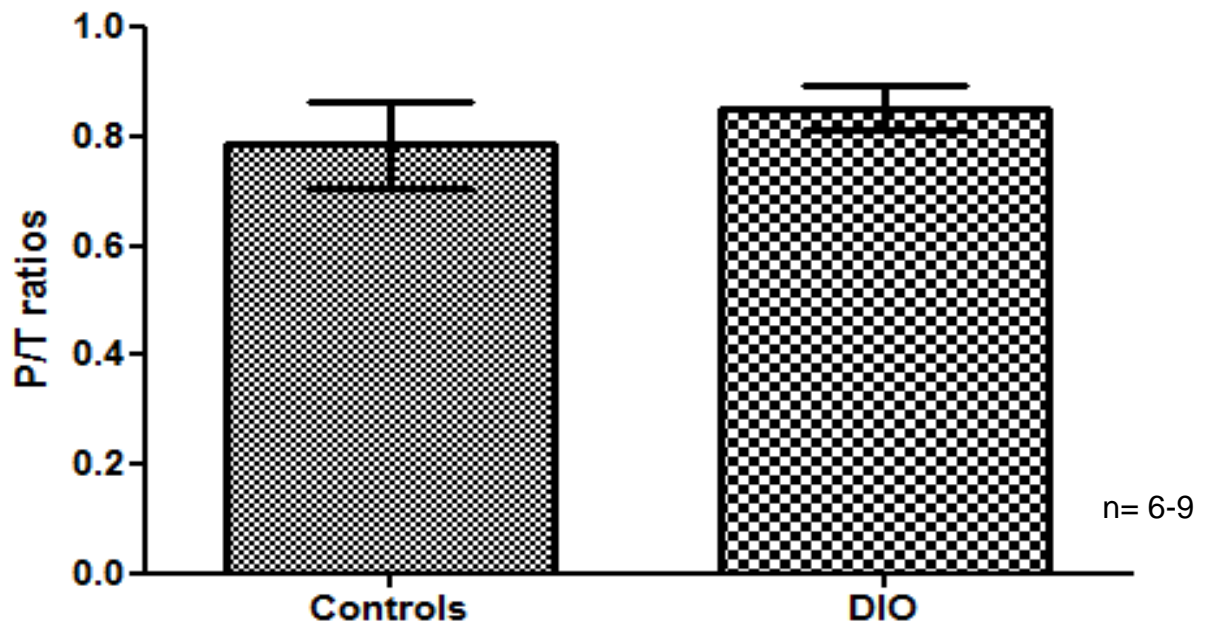
Figure 3.23: *PKB/Akt (P/T ratio).* Shown are the phospho/total ratios of both control

and diet induced obese (DIO) animals.

3.2.2.3 **Total IRS-1 expression**

After 16 weeks on diet, total IRS-1 protein was significantly downregulated in DIO animals as compared to their age matched controls (*p=0.0001) (figure 3.24).
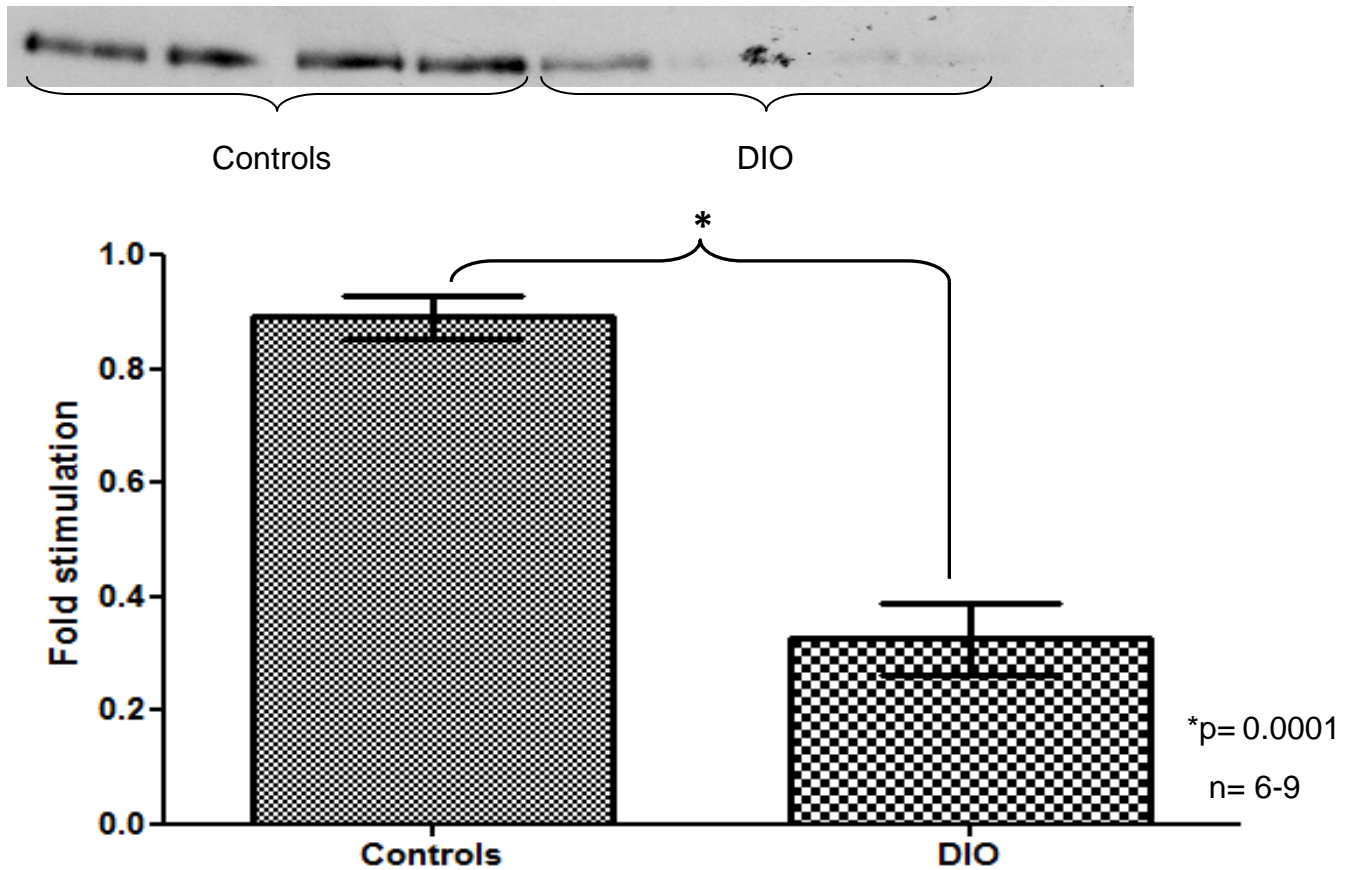
Figure 3.24: *Total IRS-1 protein*. Shown is the Western blot representing total IRS-1 expression as well as a graph showing its fold stimulation (compared to the first loaded control that was assigned a value of 1) in controls and diet induced obese (DIO) animals.

3.2.2.4 Total IRS-2 expression

Following 16 weeks on diet, IRS-2 protein was significantly downregulated in DIO animals as compared to the age matched control animals (*p=0.022) (figure 3.25).
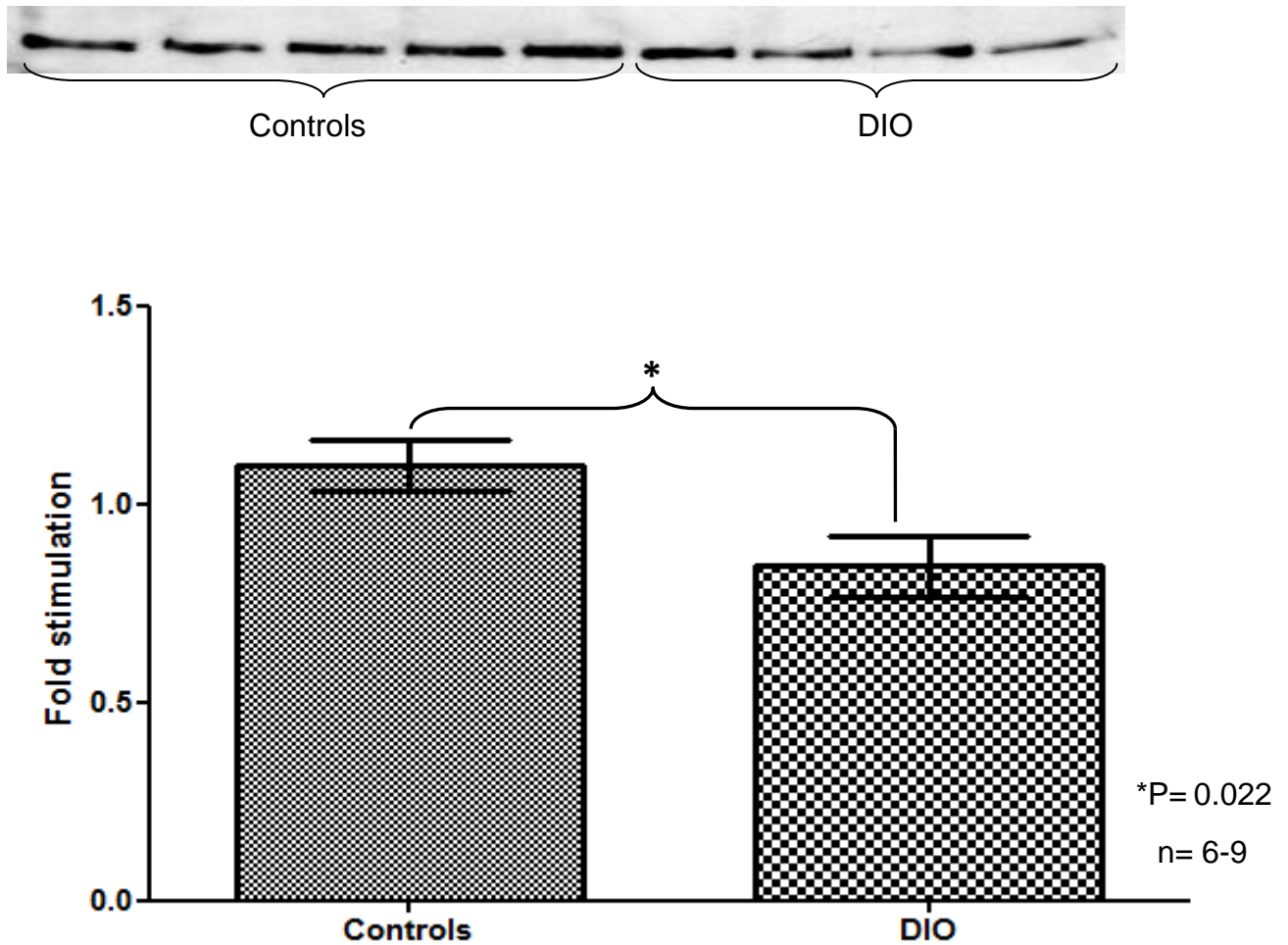
Figure 3.25: *Total IRS-2 protein.* Shown is the Western blot representing total IRS-2 expression as well as a graph showing its fold stimulation (compared to the first loaded control that was assigned a value of 1) in controls and diet induced obese (DIO) animals.

3.2.2.5 Total SERCA-2a expression

After 16 weeks on diet, DIO animals presented with decreased SERCA-2a expression as compared to the age matched controls (*p<0.0001) (figure 3.26).
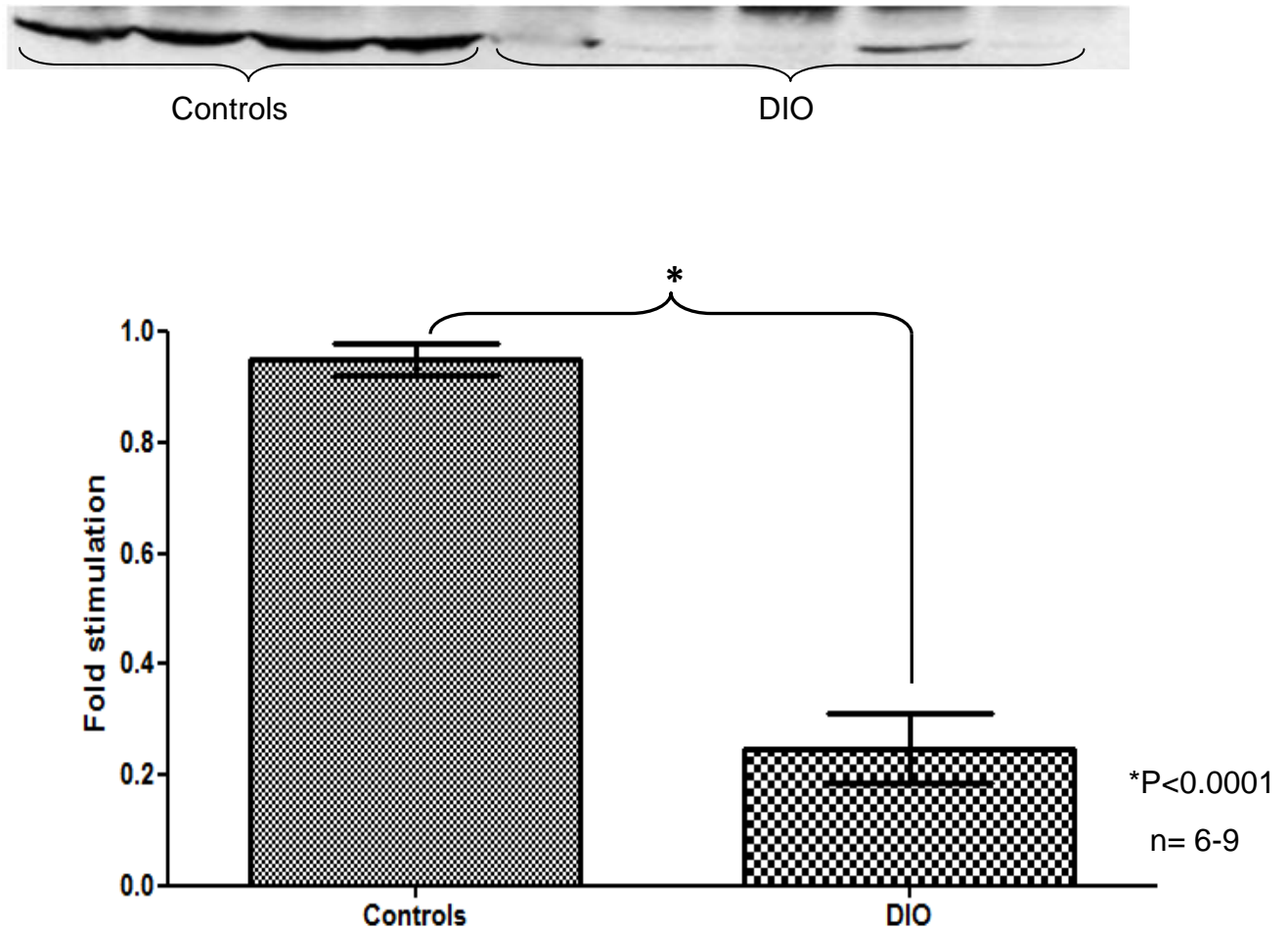
Figure 3.26: *Total SERCA-2a protein expression.* Shown is the Western blot representing total SERCA-2a expression as well as a graph showing its fold stimulation (compared to the first loaded control that was assigned a value of 1) in controls and diet induced obese (DIO) animals.

3.2.2.6 Phospholamban (PLM) protein

3.2.2.6.1 Total Phospholamban (PLM)

Following 16 weeks on diet, total PLM protein was significantly upregulated in DIO animals as compared to the age matched controls (*p= 0.0033) (figure 3.27).
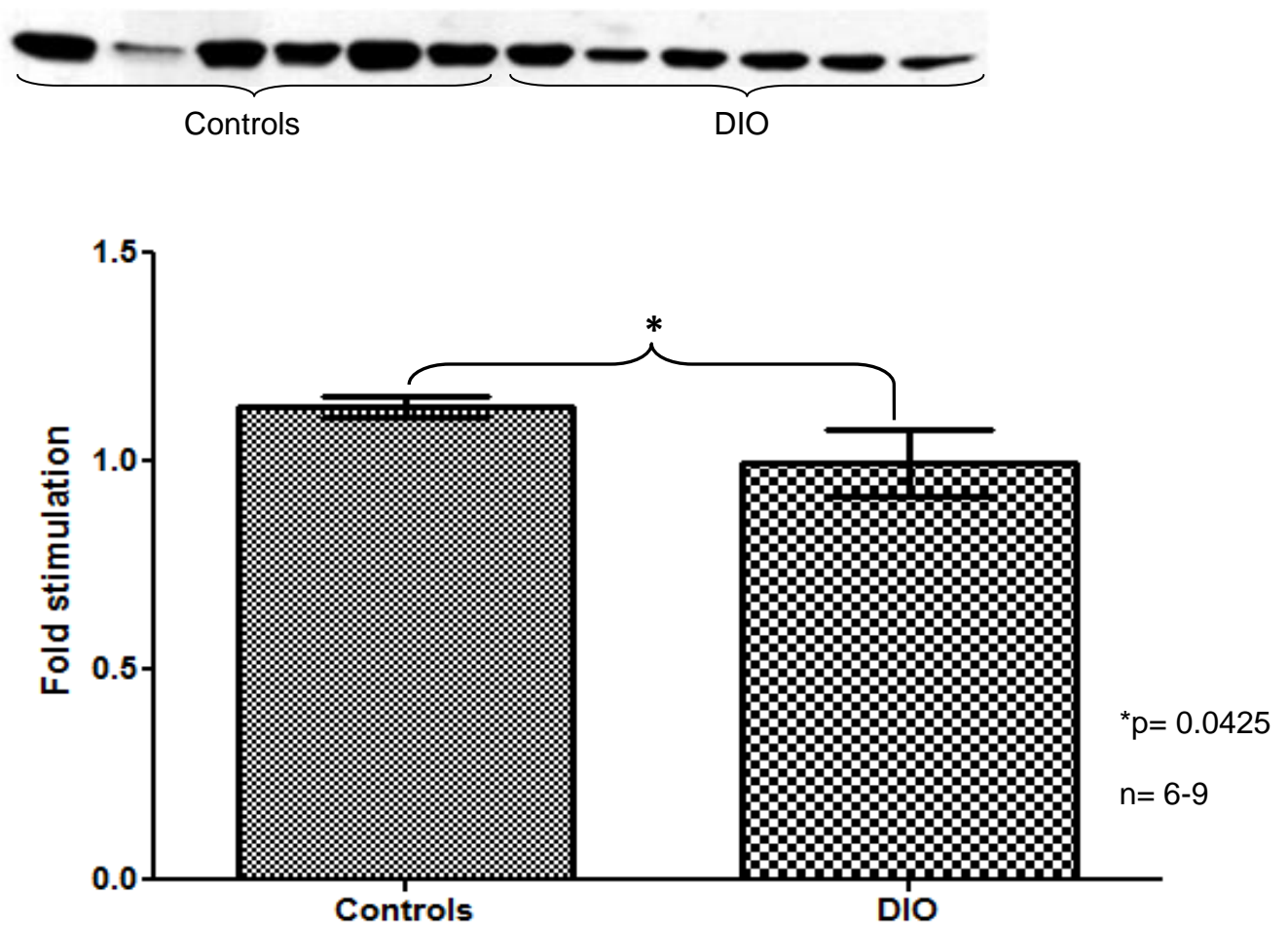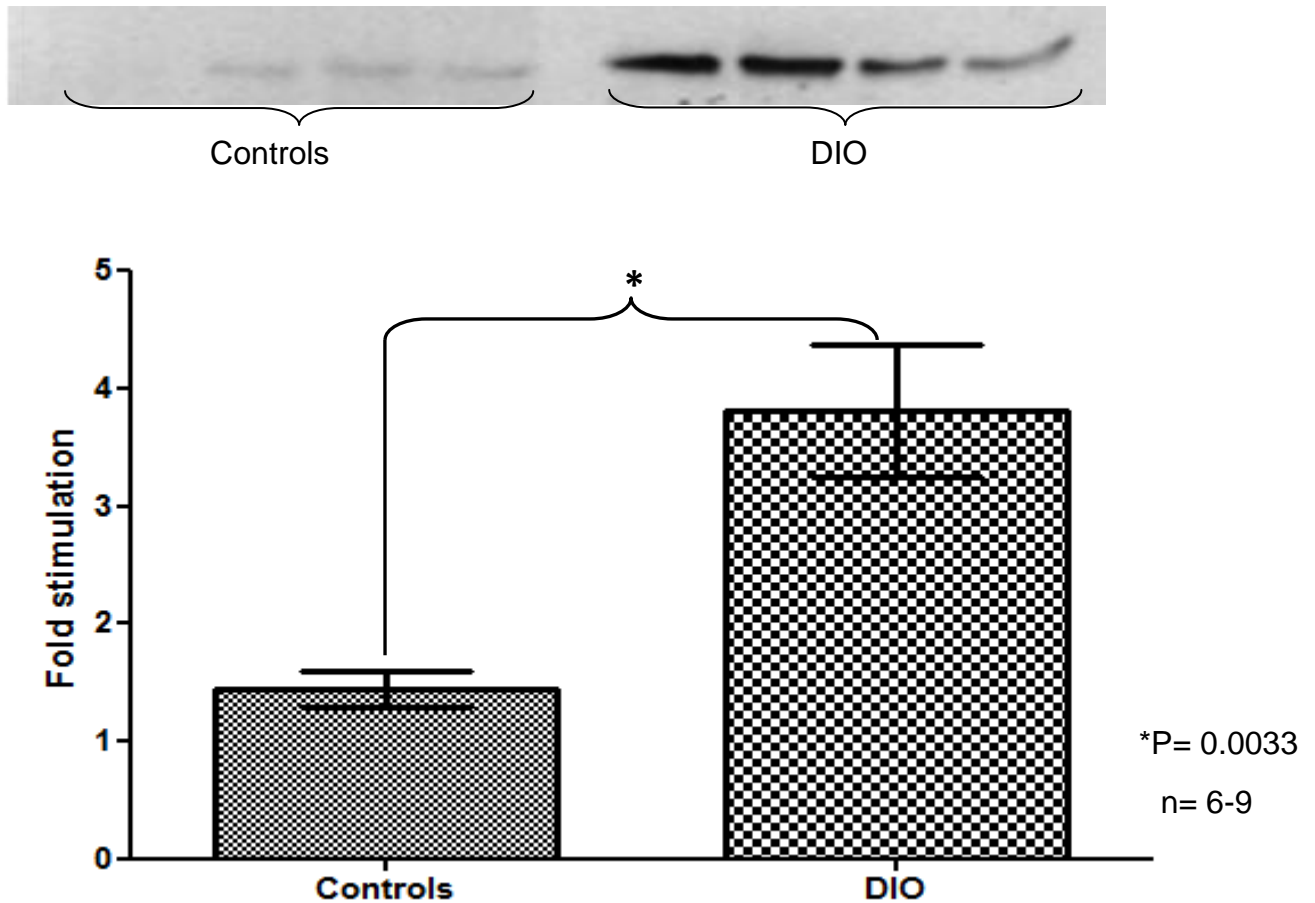

Figure 3.27: *Total PLM protein*. Shown is the Western blot representing total PLM protein expression as well as a graph showing its fold stimulation (compared to the first loaded control that was assigned a value of 1) in controls and diet induced obese (DIO) animals.

3.2.2.6.2 Phosphorylated PLM

After 16 weeks of diet, the PLM protein was significantly less phosphorylated in DIO animals as compared to the age matched controls (*p= 0.0095) (figure 3.28). In addition, the P/T ratios of PLM were significantly smaller in DIO animals (*p= 0.0018) (figure 3.29).
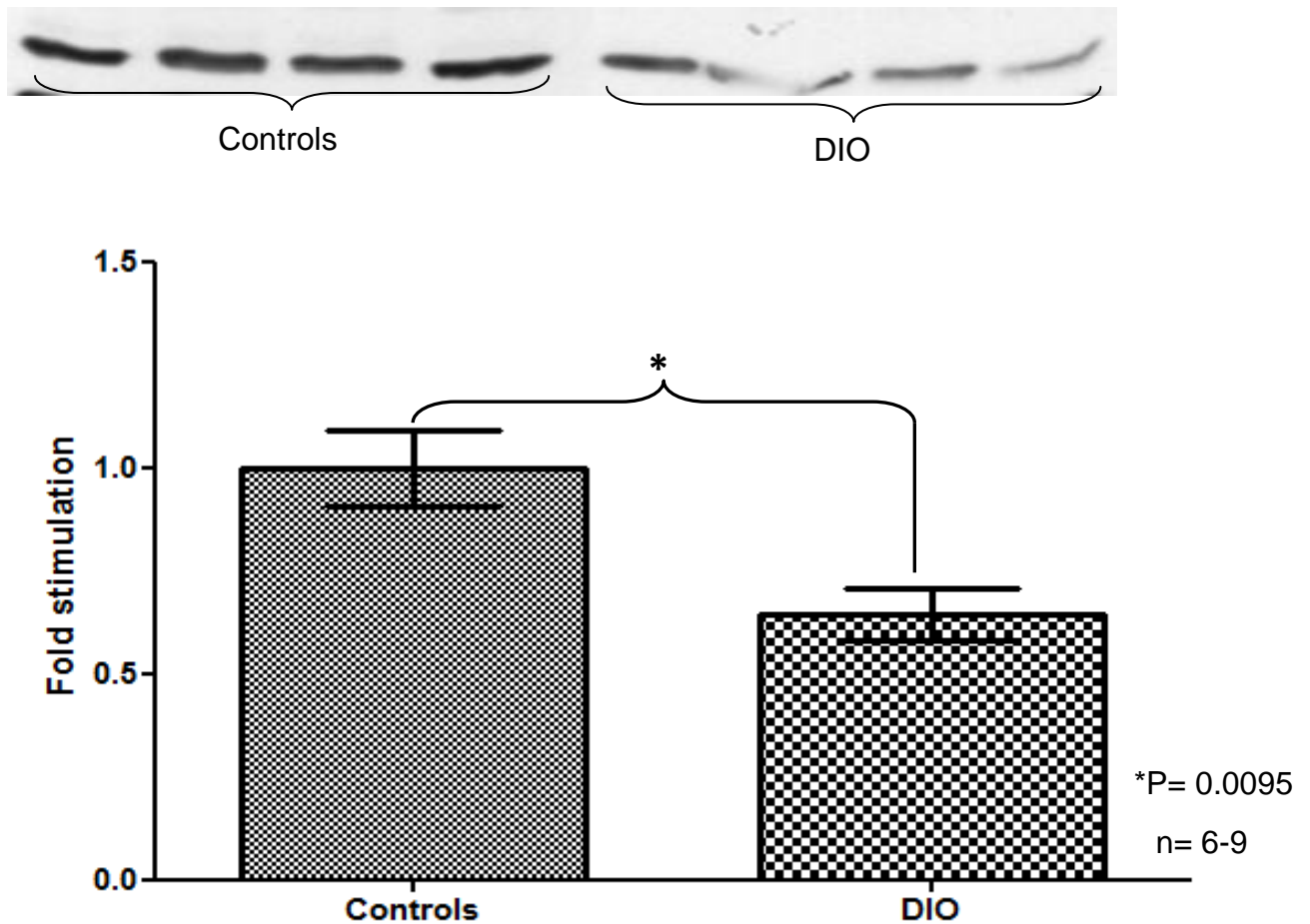
Figure 3.28: *Phosphorylation* of *Phospholamban* (PLM). Shown is the Western blot representing PLM phosphorylation as well as a graph showing its fold (compared to the first loaded control that was assigned a value of 1) in controls and diet induced obese (DIO) animals.
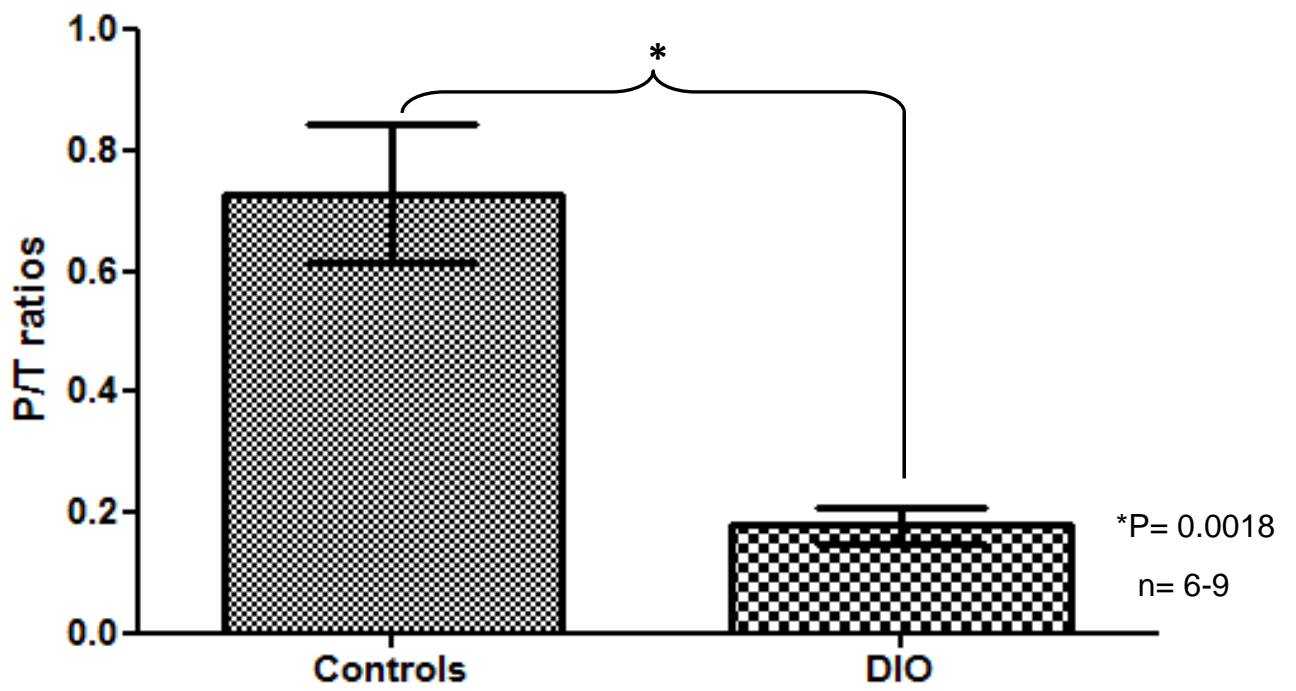
Figure 3.29: *PLM (*P/T *ratio)*. Shown are the phospho/total ratios of both controls and DIO animals (*p= 0.0018).

3.2.3 Calcium ATPase activity

After 16 weeks on diet, DIO animals presented with significantly decreased calcium ATPase activity as compared to the age matched control animals (*p= 0.0092) (figure 3.30).
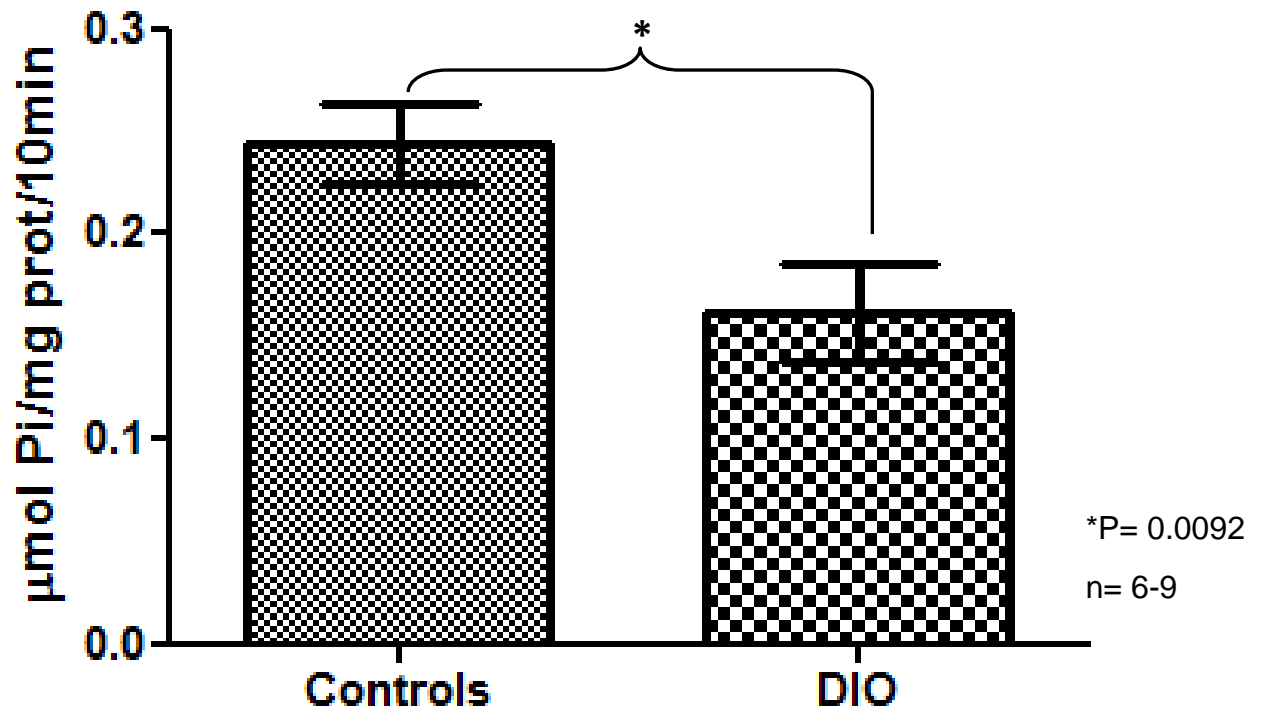
Figure 3.30: *Calcium ATPase activity.* Shown are the calcium ATPase activities in both controls and DIO animals as determined by the amount of inorganic phosphate (P_i) produced.

3.2.4 **Perfusion**

3.2.4.1 **Systolic pressure (SP)**

Following 16 weeks of diet, there was no significant difference in systolic pressure (SP) when comparing DIO and control animals at baseline (Figure 3.31A) and during reperfusion (figure 3.31B).

A. Systolic pressure (SP) at baseline perfusion
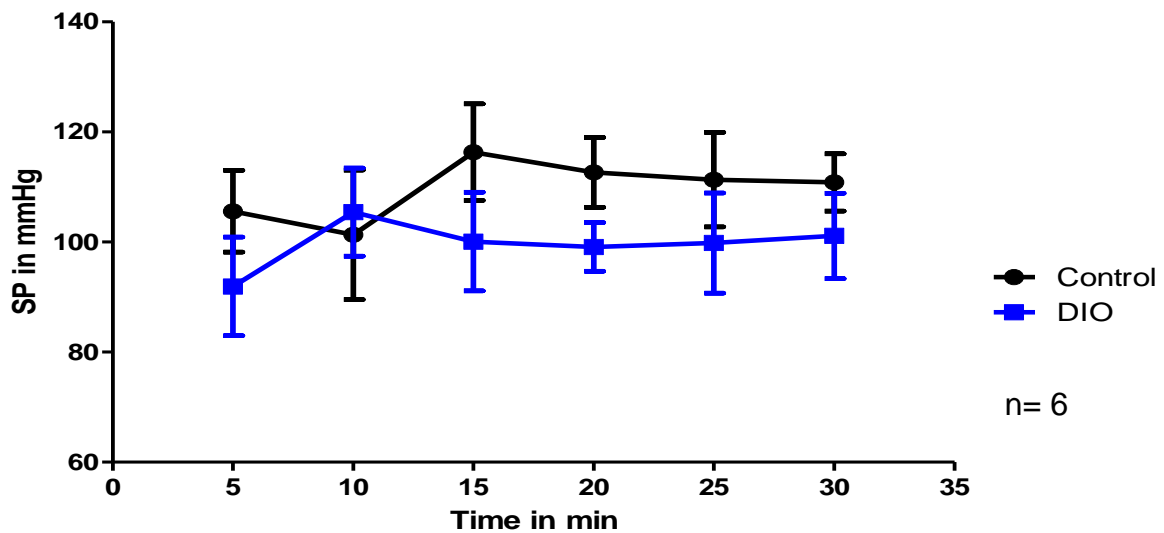
B. Systolic pressure (SP) at reperfusion
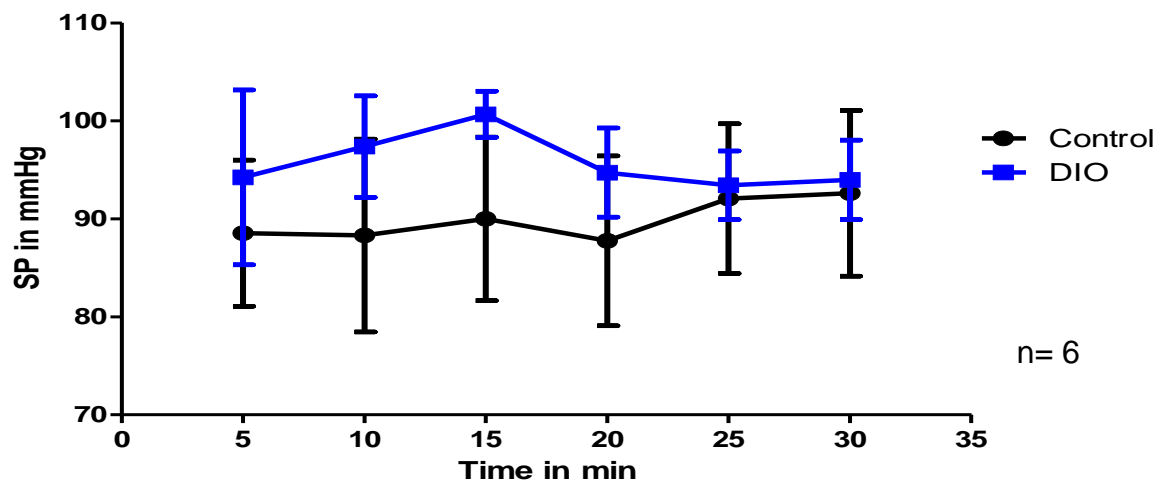
Figure 3.31: *Systolic pressure (SP). Shown is the systolic pressure at baseline (A) and during reperfusion (B).*

3.2.4.2 Diastolic pressure (DP)

After 16 weeks on diet, there was no significant difference in diastolic pressure (DP) when comparing DIOs and control animals at both baseline (figure 3.32A) and reperfusion (figure 3.32B).

A. DP at baseline
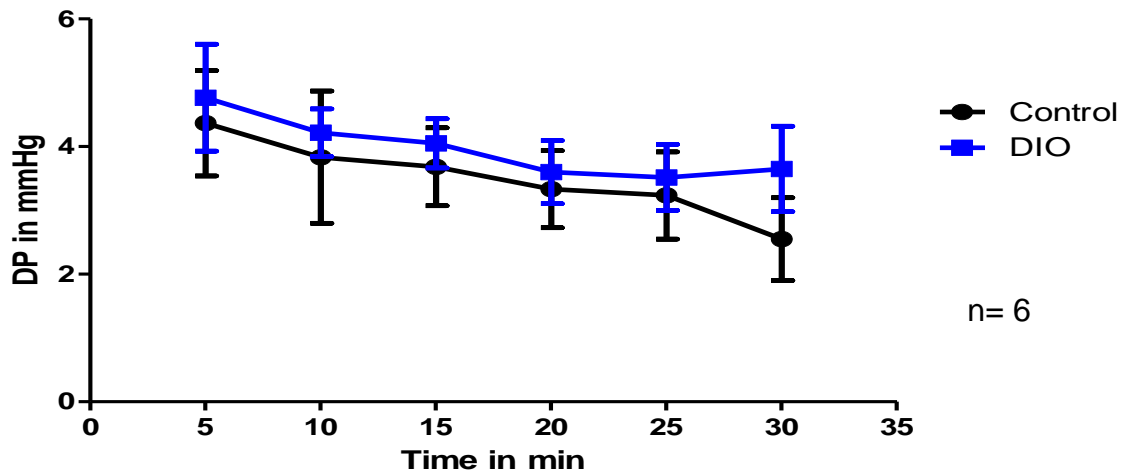
B. DP at reperfusion
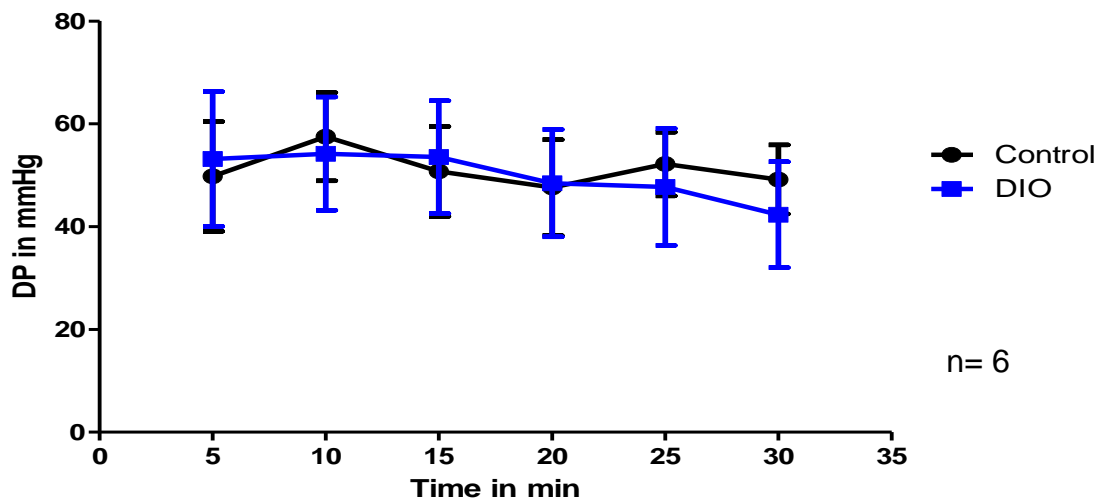
Figure 3.32: *Diastolic pressure (DP). Shown is the diastolic pressure at baseline (A) and during reperfusion (B).*

3.2.4.3 **Left ventricular developed pressure (LVDevP)**

Following 16 weeks on diet, there was no significant difference in left ventricular developed pressure when comparing DIO and control animals at both baseline (figure 3.33A) and reperfusion (figure 3.33B).

A. **Baseline LVDevP**
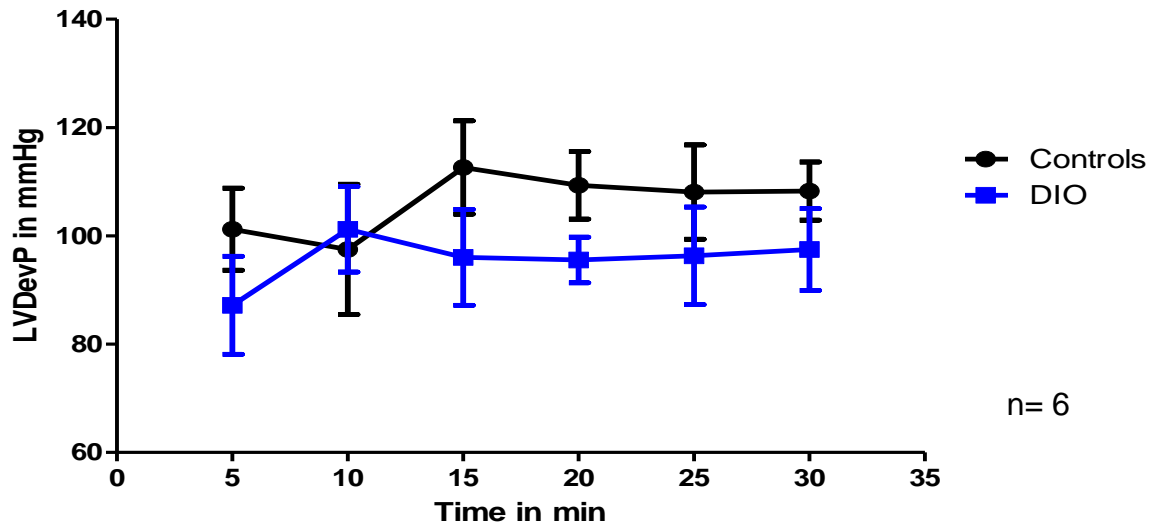
B. **LVDevP at reperfusion**
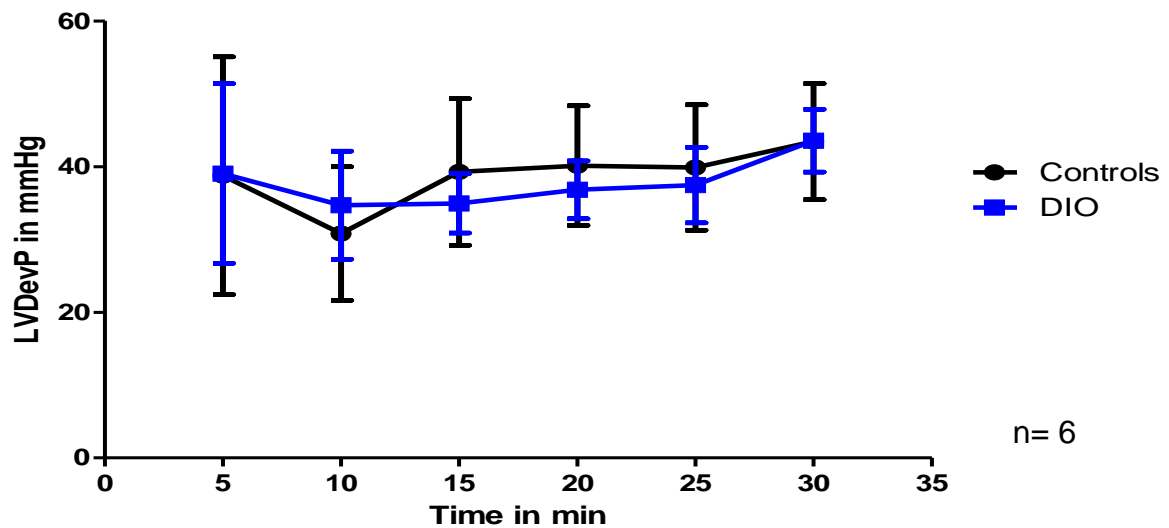
Figure 3.33: *Left ventricular developed pressure* (LVDevP). Shown is the left ventricular developed pressure at baseline (A) and during reperfusion (B).

3.2.4.4 **Heart rate (HR)**

After 16 weeks on diet, DIO animals had a significantly slower heart rate when compared to the age matched controls at baseline (*p<0.0001) (figure 3.34A). However, there was no significant difference in heart rates when controls and DIO animals were compared at reperfusion (figure 3.34B).

A. Heart rates at baseline
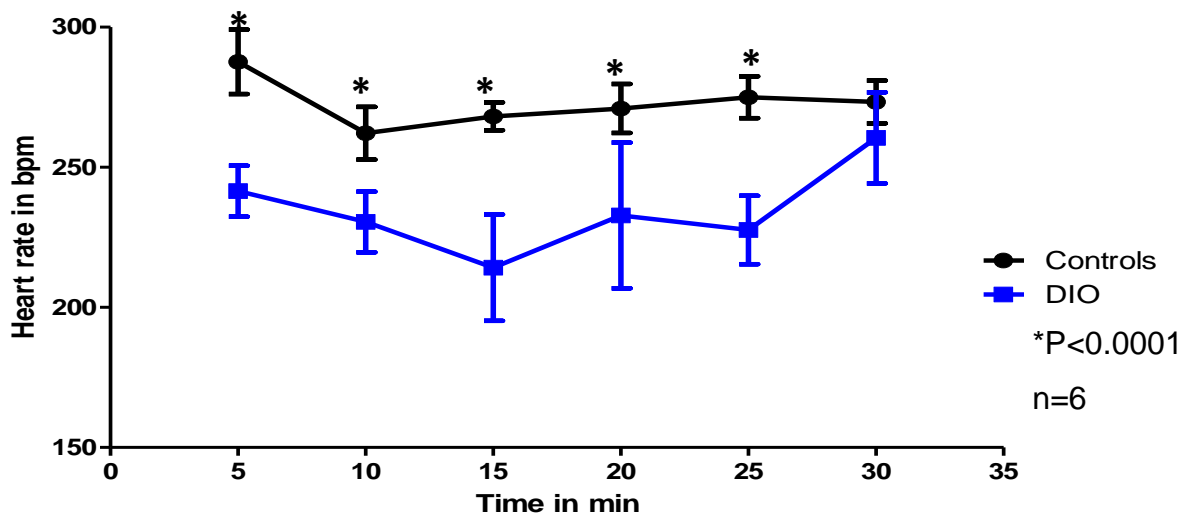
B. Heart rates at reperfusion
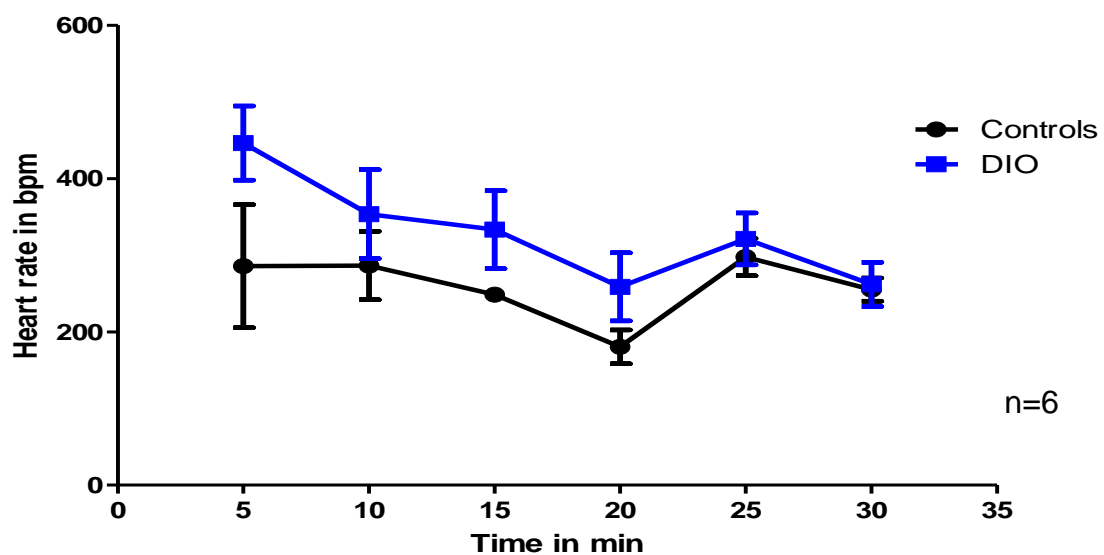
Figure 3.34: *Heart rate* (HR). Shown is the heart rate at baseline (A) and during reperfusion (B).

3.2.4.5 Rate pressure product (RPP)

Following 16 weeks on diet, DIO animals had significantly decreased rate pressure product when compared to control animals at baseline (*p<0.0001) (figure 3.35A). However, there was no significant difference between controls and DIO animals at reperfusion (figure 3.35B).

A. Rate pressure product at baseline
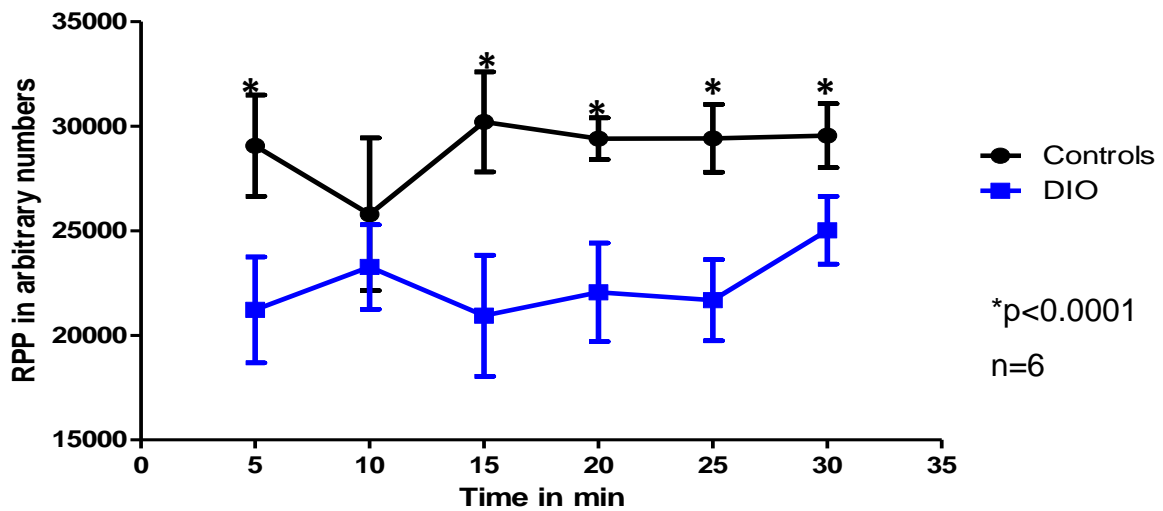
B. Rate pressure product at reperfusion
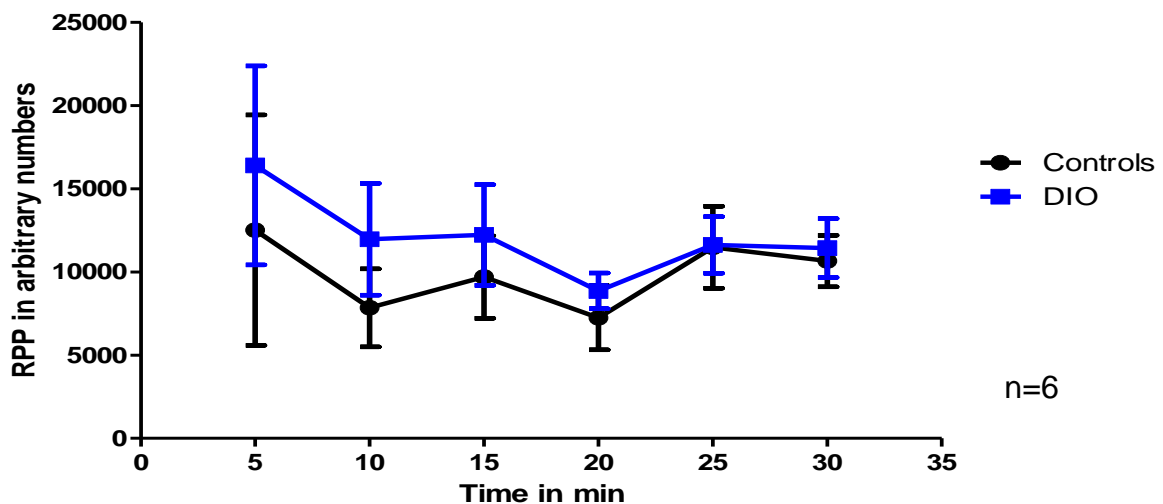
Figure 3.35: *Rate pressure product* (RPP). Shown is the RPP of both controls and DIO animals at baseline (A) and during reperfusion (B).

3.2.4.6 Low flow ischemia

During low flow ischemia (0.2 ml/min), DIO animals had a longer time to onset of ischemic contracture when compared to the age matched controls (*p= 0.0001) (figure 3.36). However, there was no significant difference in time to peak of contracture (TPC) (figure 3.37A), peak contracture diastolic pressure (PCDP) (figure 3.37B) and end ischemic diastolic pressure (EIDP) (figure 3.37C).

A. **Time to onset of ischemic contracture (TOIC)**

*p= 0.0001
n= 6
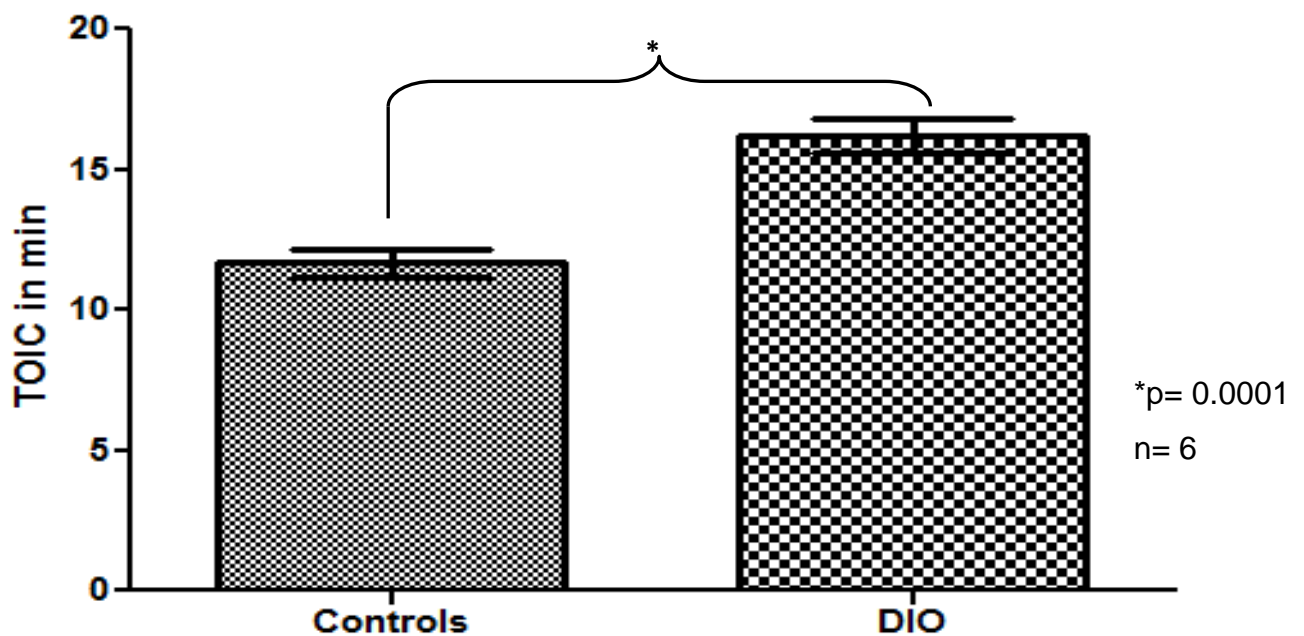
Figure 3.36: *Time to onset of ischemic contracture* (TOIC). Shown is the TOIC of both controls and DIO animals during low flow ischemia (25 min).

A. **Time to peak of contracture (TPC**)
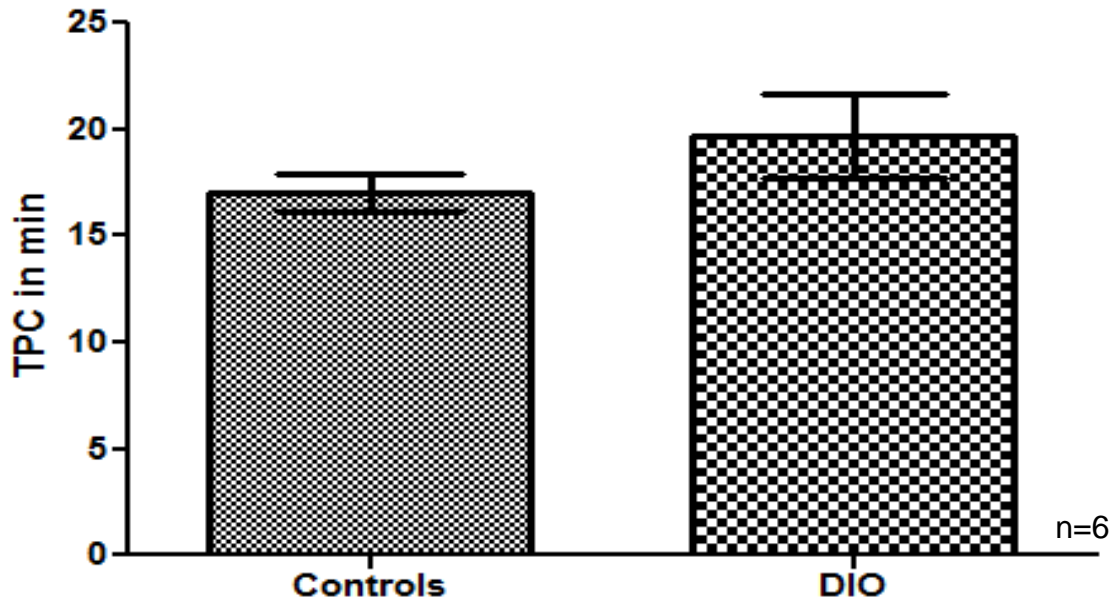
B. **Peak contracture diastolic pressure (PCDP)**
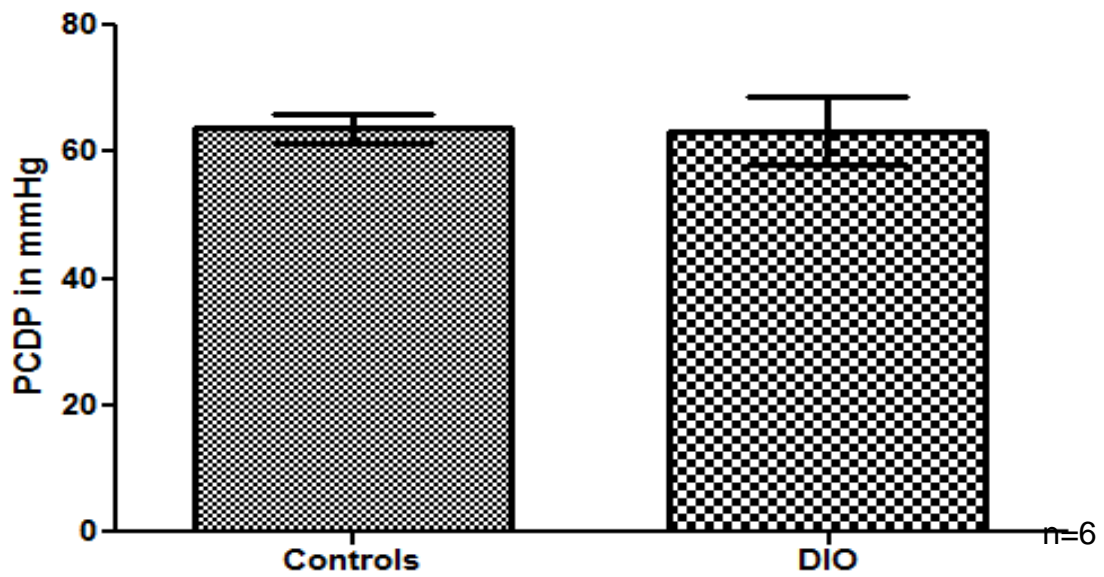
Figure 3.37A-B: *Time to peak of contracture* (A), *Peak contracture diastolic pressure*

(B). Shown is the TPC and PCDP of both controls and DIO animals.

C. **End ischemic diastolic pressures (EIDP)**
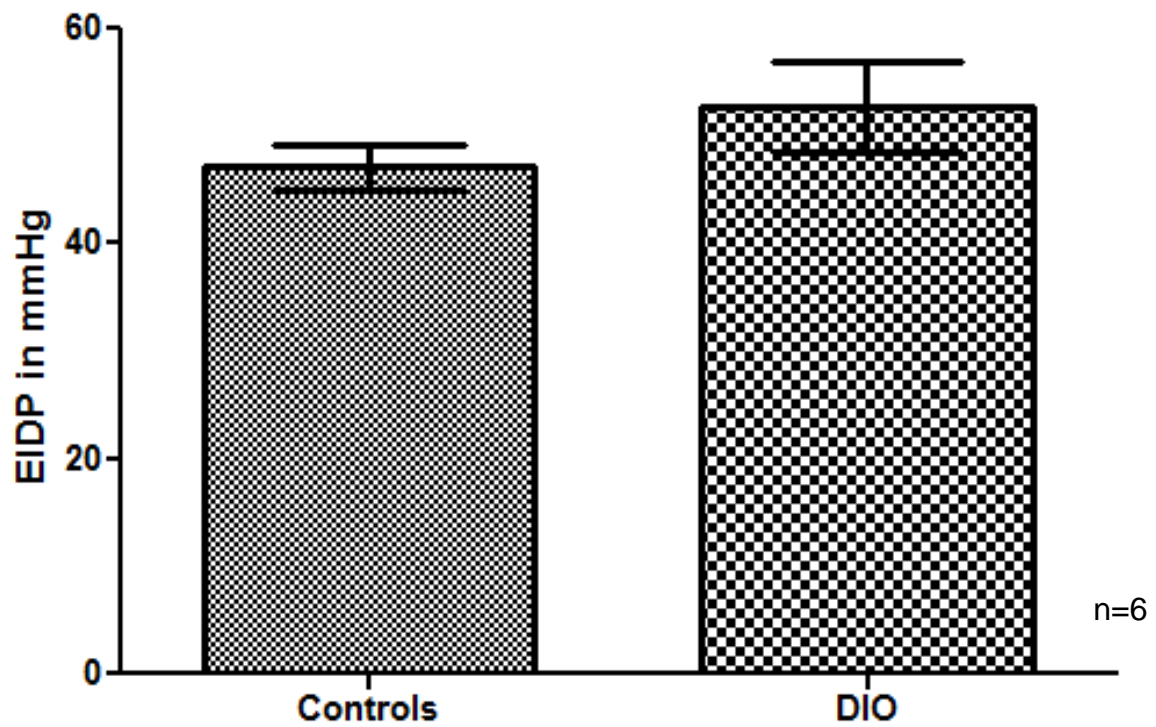
Figure 3.37C: *Time to peak of contracture* (A), *Peak contracture diastolic pressure* (B) and *End ischemic diastolic pressures* (C). Shown are TPC, PCDP and EIDP of both controls and DIO animals.

3.2.4.7 **Coronary flow rate (CF)**

The rate of coronary flow was also measured at baseline and during reperfusion. There was no significant difference in coronary flow rate when DIO and control animals were compared (figure 3.38).
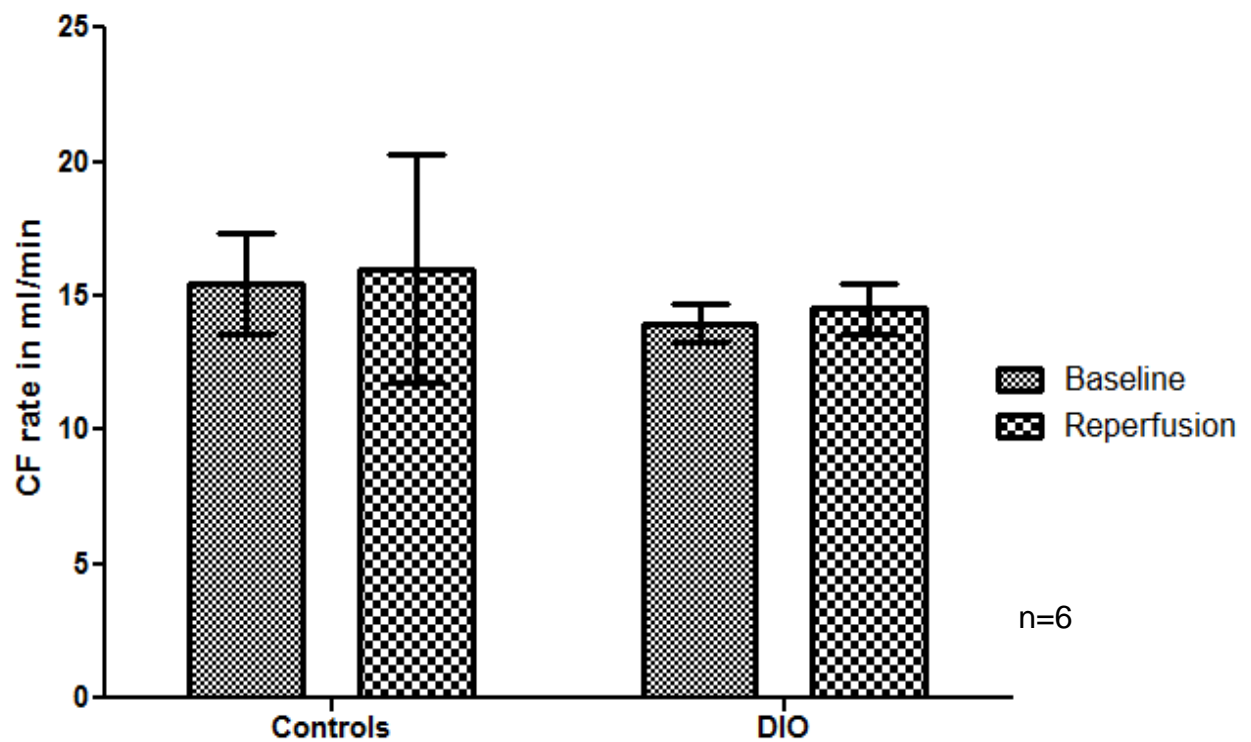
Figure 3.38: *Coronary flow rates*. Shown is the rate of coronary flow at baseline and at reperfusion.

3.3 Sixteen (16) weeks plus treatment data

3.3.1 The effect of GSK-3 inhibition on biometric and biochemical parameters

3.3.1.1 Effect on body weight and IP fat mass

3.3.1.1.1 Body weight (BW)

Following 16 weeks of diet, untreated DIO animals were significantly bigger than untreated controls (**p=0.0001) (figure 3.39). In addition, following 12 weeks of diet and the other four weeks on diet plus treatment with GSK-3 inhibitor, treated DIO animals were also significantly bigger than treated controls (##p= 0.0002). However, when comparing treated and untreated DIO animals, treated DIO animals gained less weight than untreated DIOs (#p= 0.0155) (figure 3.39), while the treated controls were significantly bigger than untreated control animals (*p= 0.0453) (figure 3.39).
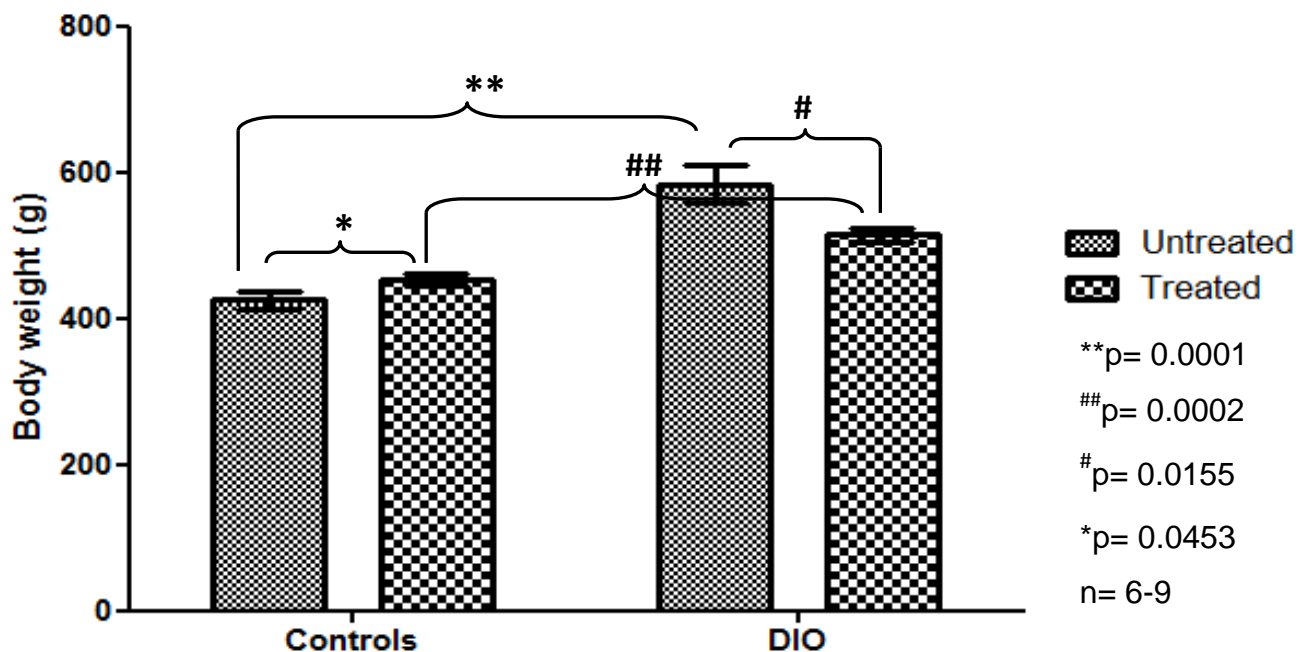
Figure 3.39: *Body weight (BW)*. Shown is the body weight measured in grams (g) of treated and untreated diet induced obese (DIO) and control animals after four weeks of treatment with GSK-3 inhibitor.

3.3.1.1.2 Intra-peritoneal (IP) fat mass

The untreated DIO animals had significantly more IP fat mass than untreated controls (**p= 0.0002). In addition, following 4 weeks of treatment with GSK-3 inhibitor, treated DIO animals also had more IP fat than treated controls (##p<0.0001) (figure 3.40). However, there was no significant difference in IP fat mass when treated and untreated DIO animals were compared as well as between treated and untreated control animals (figure 3.40).
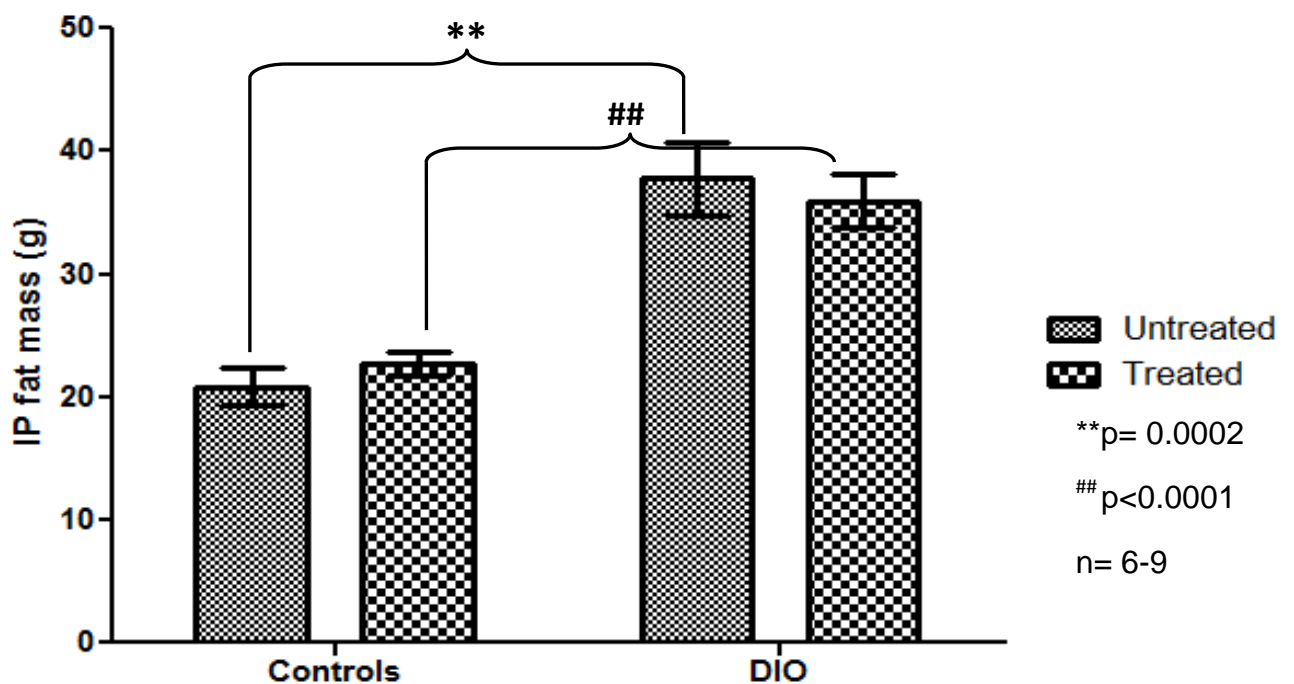
Figure 3.40: *Intra-peritoneal (IP) fat*. Shown is the IP fat mass measured in grams (g), of treated and untreated diet induced obese (DIO) and control animals after four weeks of treatment with GSK-3 inhibitor.

3.3.1.2 **Effect on ventricular weight (VW)**

The ventricles from untreated DIO animals were significantly larger than those coming from untreated controls (**p= 0.0003). In addition, following four weeks of treatment with GSK-3 inhibitor, treated DIO animals also had larger ventricles than treated controls (##p= 0.0140) (figure 3.41). However, when comparing treated and untreated DIO animals, the treated DIOs had significantly smaller ventricles than untreated DIO animals (#p= 0.0166). However, in control animals, treated controls had significantly larger ventricles than untreated controls (*p= 0.0072) (figure 3.41).
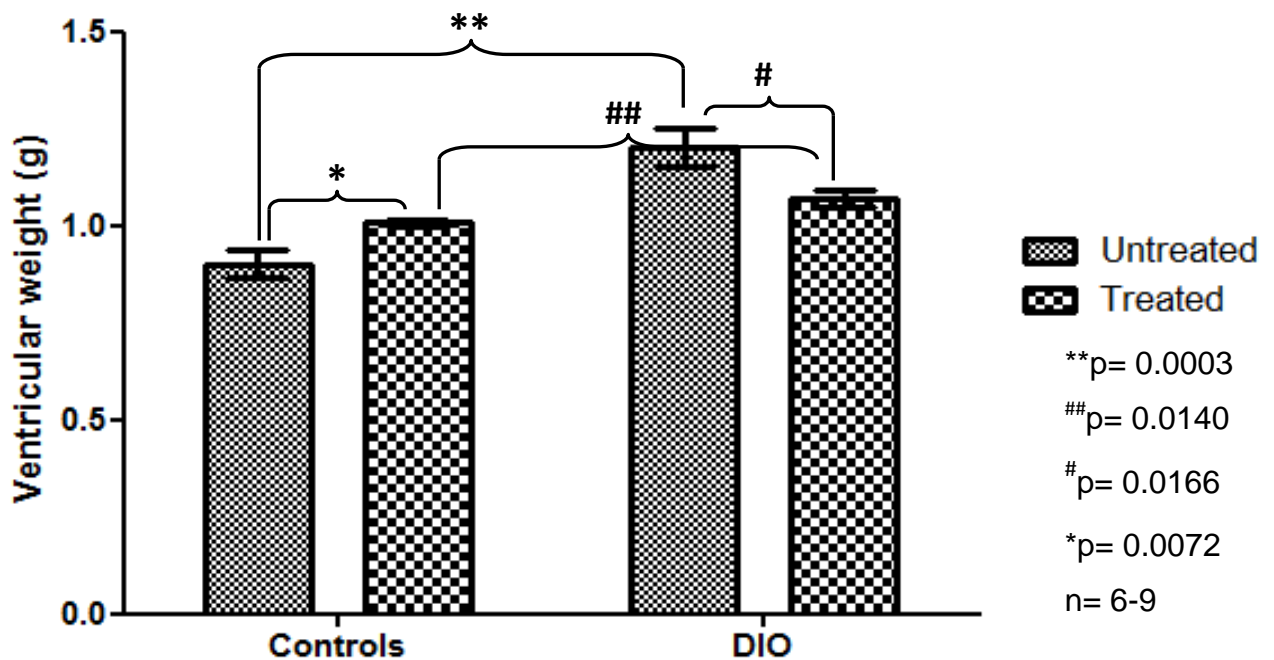
Figure 3.41: *Ventricular weight (VW)*. Shown are the ventricular weights measured in grams (g) of treated and untreated diet induced obese (DIO) and control animals after four weeks of treatment with GSK-3 inhibitor.

3.3.1.3 **Effect on tibia length**

Following 16 weeks on diet, there was no significant difference in tibia length between untreated DIOs and untreated controls as well as between treated DIOs and treated control animals (figure 3.42). There was also no significant difference in tibia length between treated and untreated DIOs as well as between treated and untreated control animals (figure 3.42).
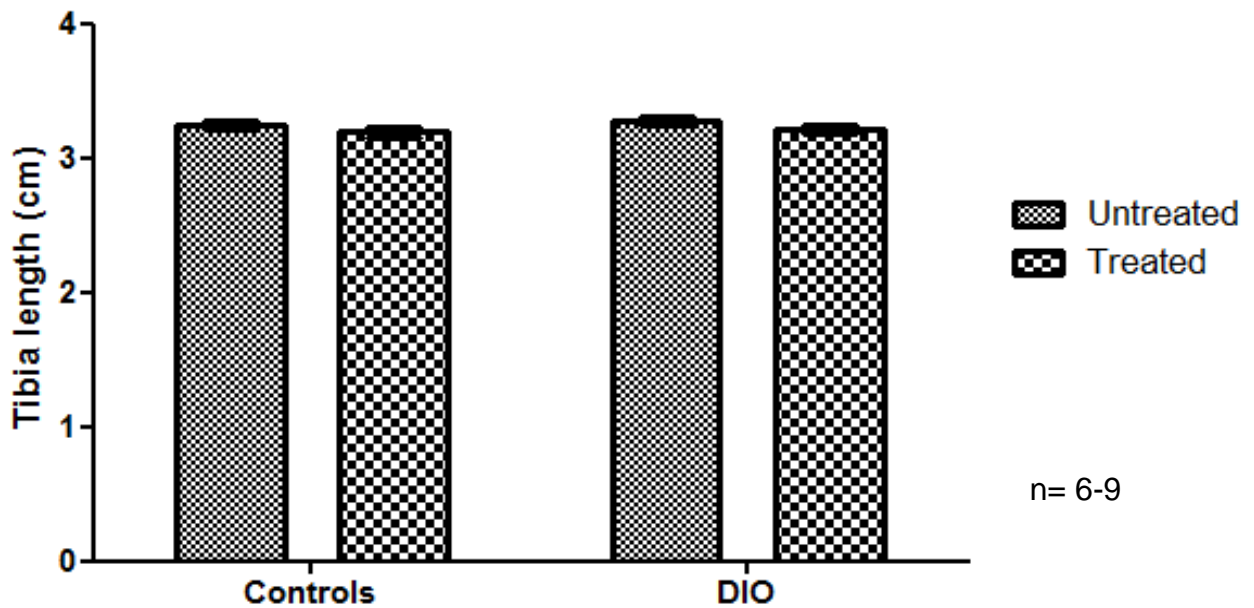
Figure 3.42: *Tibia length*. Shown are the tibia lengths measured in centimetres (cm) of treated and untreated diet induced obese (DIO) and control animals after four weeks of treatment with GSK-3 inhibitor.

3.3.1.4 Ventricular weight/tibia length (VW/TL) ratios

Following 16 weeks of diet, the VW/TL ratios were significantly higher in untreated DIO animals as compared to untreated controls (**p<0.0001) (figure 3.43). In addition, after four weeks of treatment with GSK-3 inhibitor,, the treated DIO animals also had higher VW/TL ratios than treated controls (##p= 0.0204). However, treated DIO animals had significantly lower VW/TL ratios as compared to untreated DIOs (#p= 0.0206), while treated controls had higher VW/TL ratio than untreated controls (*p= 0.0007) (figure 3.43).
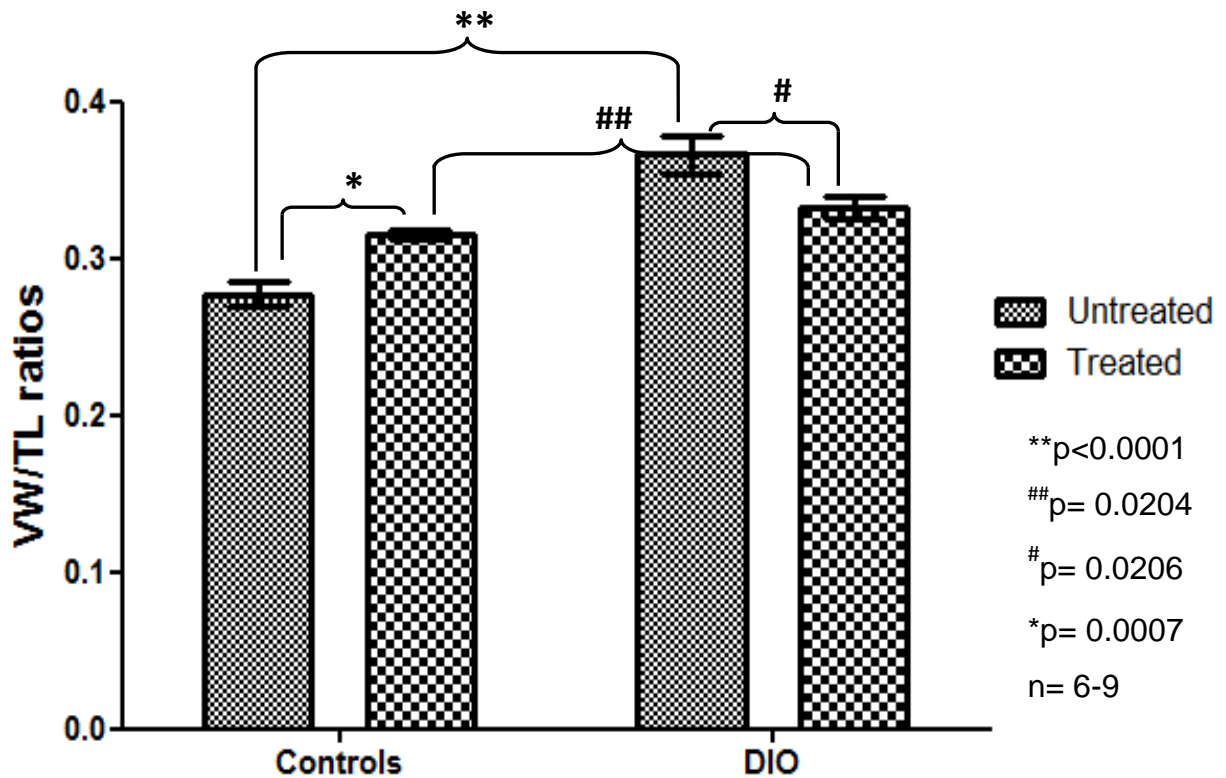
Figure 3.43: *Ventricular Weight (VW)/Tibia length (TL) ratios*. Shown are the VW/TL ratios of treated and untreated diet induced obese (DIO) and control animals after four weeks of treatment with GSK-3 inhibitor.

3.3.1.5 Effect on fasting blood glucose levels

Following 16 weeks on diet, fasting blood glucose levels were significantly higher in untreated DIOs than untreated control animals (*p= 0.0238) (figure 3.44). However, following four weeks of treatment with GSK-3 inhibitor, there was no significant difference in fasting blood glucose levels when treated DIOs and treated control animals were compared, as well as between treated and untreated DIOs, and treated and untreated control animals (figure 3.44).
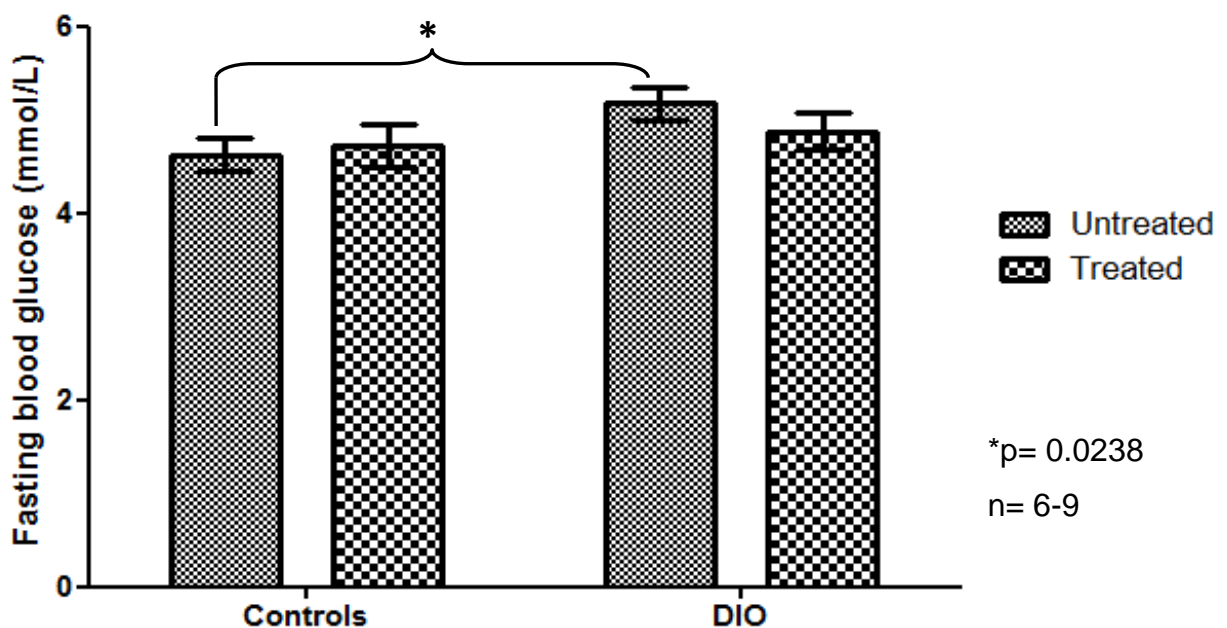
Figure 3.44: *Fasting blood glucose levels.* Shown are the fasting blood glucose levels of treated and untreated diet induced obese (DIO) and control animals after four weeks of treatment with GSK-3 inhibitor.

3.3.1.6 Effect on fasting plasma insulin levels

Following 16 weeks on diet, the levels of insulin were significantly higher in untreated DIOs than untreated control animals (**p=0.0313). In addition, following four weeks of treatment with GSK-3 inhibitor, treated DIOs were also significantly higher than treated control animals ([##]p= 0.0213) (figure 3.45). However, there was no significant difference in fasting plasma insulin levels when treated and untreated DIO animals were compared, as well as between treated and untreated control animals (figure 3.45).
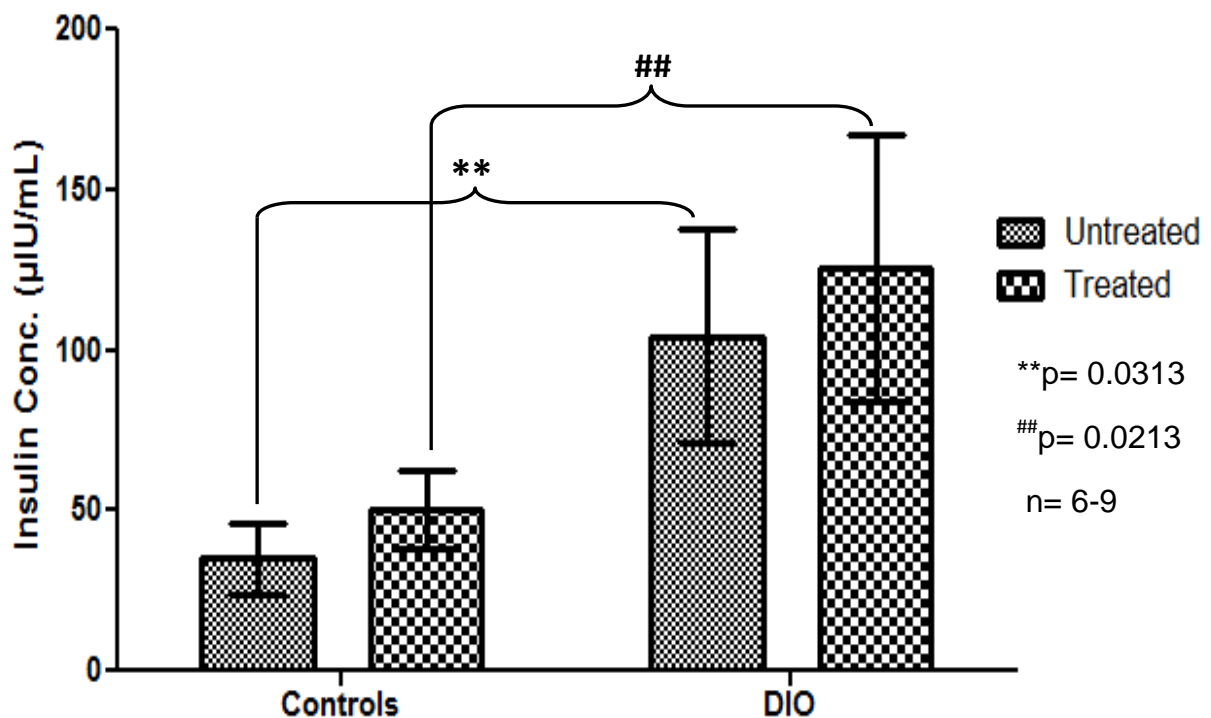
Figure 3.45: *Fasting plasma insulin levels*. Shown are the fasting plasma insulin levels of treated and untreated diet induced obese (DIO) and control animals after four weeks of treatment with GSK-3 inhibitor.

3.3.1.7 Homeostasis model assessment (HOMA) Index

There was no significant difference in HOMA index between untreated DIOs and untreated control animals, as well as between treated DIOs and control animals (figure 3.46). There was also no significant difference in HOMA index between treated and untreated DIOs as well as between treated and untreated controls (3.46).
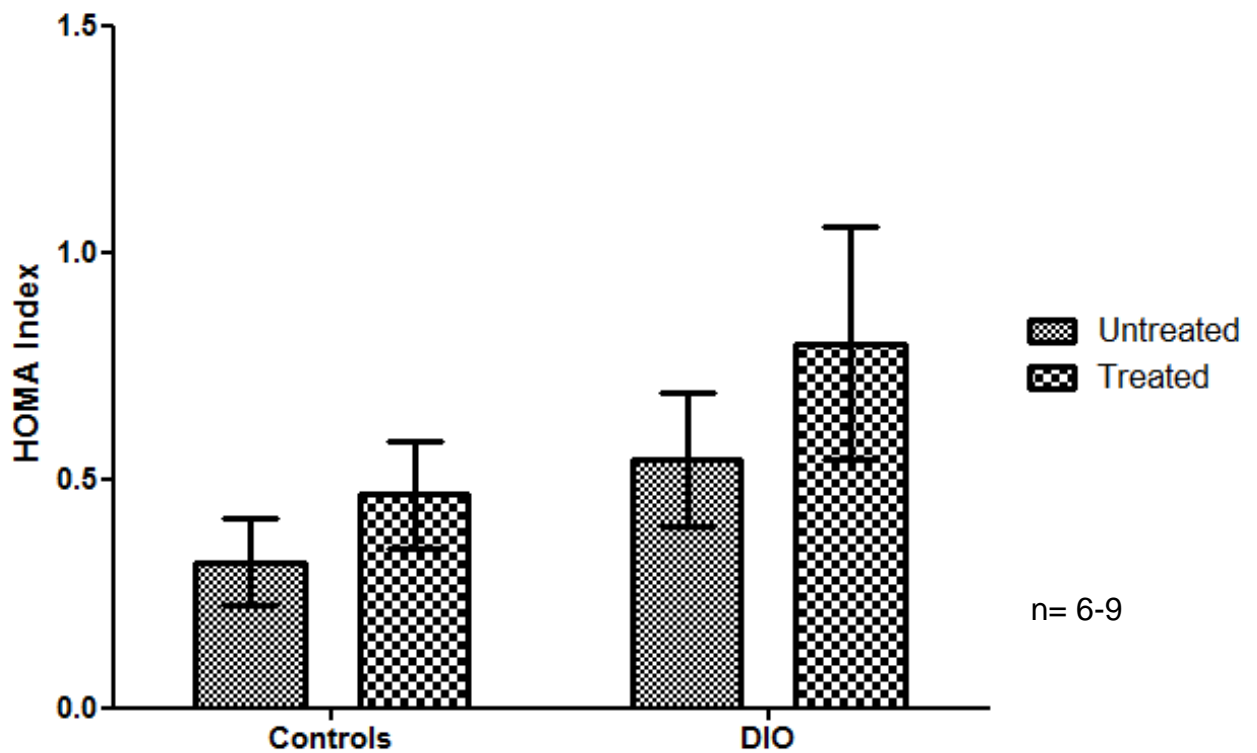
Figure 3.46: *Homeostasis model assessment (HOMA) Index.* Shown is the HOMA index of treated and untreated diet induced obese (DIO) and control animals after four weeks of treatment with GSK-3 inhibitor.

3.3.2 Effect of GSK-3 inhibition on protein expression and phosphorylation

3.3.2.1 Effect on GSK-3 protein

3.3.2.1.1 Total GSK-3

Following 16 weeks on diet, there was no significant difference in total GSK-3 when untreated DIOs and untreated controls were compared; however, there was a tendency towards increase in untreated DIO animals (not shown on the blot below). In addition, following the treatment with GSK-3 inhibitor, there was also no significant difference between treated DIOs and treated control animals (figure 3.47). There was also no significant difference in total GSK-3 protein when treated and untreated controls as well as treated and untreated DIOs were compared (figure 3.47).
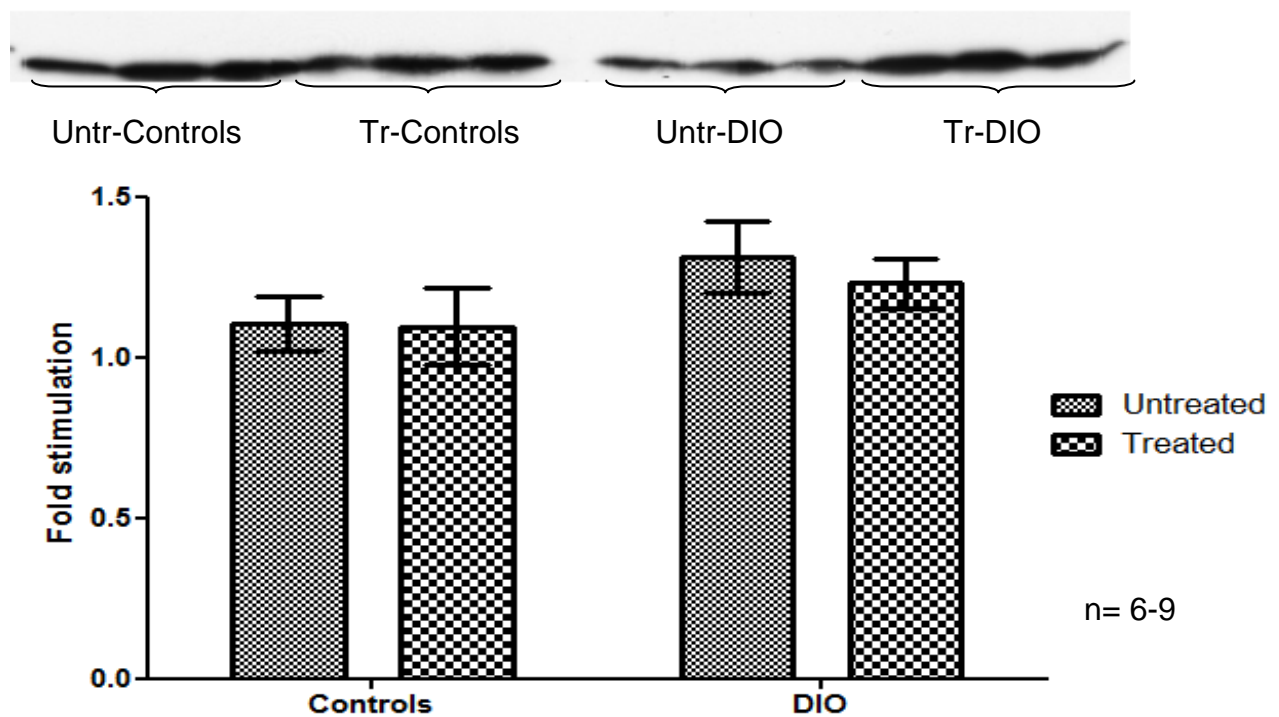
Figure 3.47: *Total GSK-3*. Shown is one of the Western blots representing total GSK-3 expression, as well as a graph showing its fold stimulation (compared to the first loaded control that was assigned a value of 1) in controls and diet induced obese (DIO) animals.

3.3.2.1.2 Effect on GSK-3 phosphorylation

After 16 weeks on diet, there was no significant difference in GSK-3β phosphorylation when untreated DIO animals were compared to untreated controls. However, after four weeks of treatment with GSK-3 inhibitor, treated DIO animals had less GSK-3 phosphorylation when compared to treated controls (##p= 0.0007) (figure 3.48). In addition, GSK-3 was more phosphorylated in treated than untreated controls (*p= 0.0008). However, there was no significant difference in GSK-3 phosphorylation between treated and untreated DIO animals (figure 3.48). GSK-3α was not phosphorylated in DIO animals.
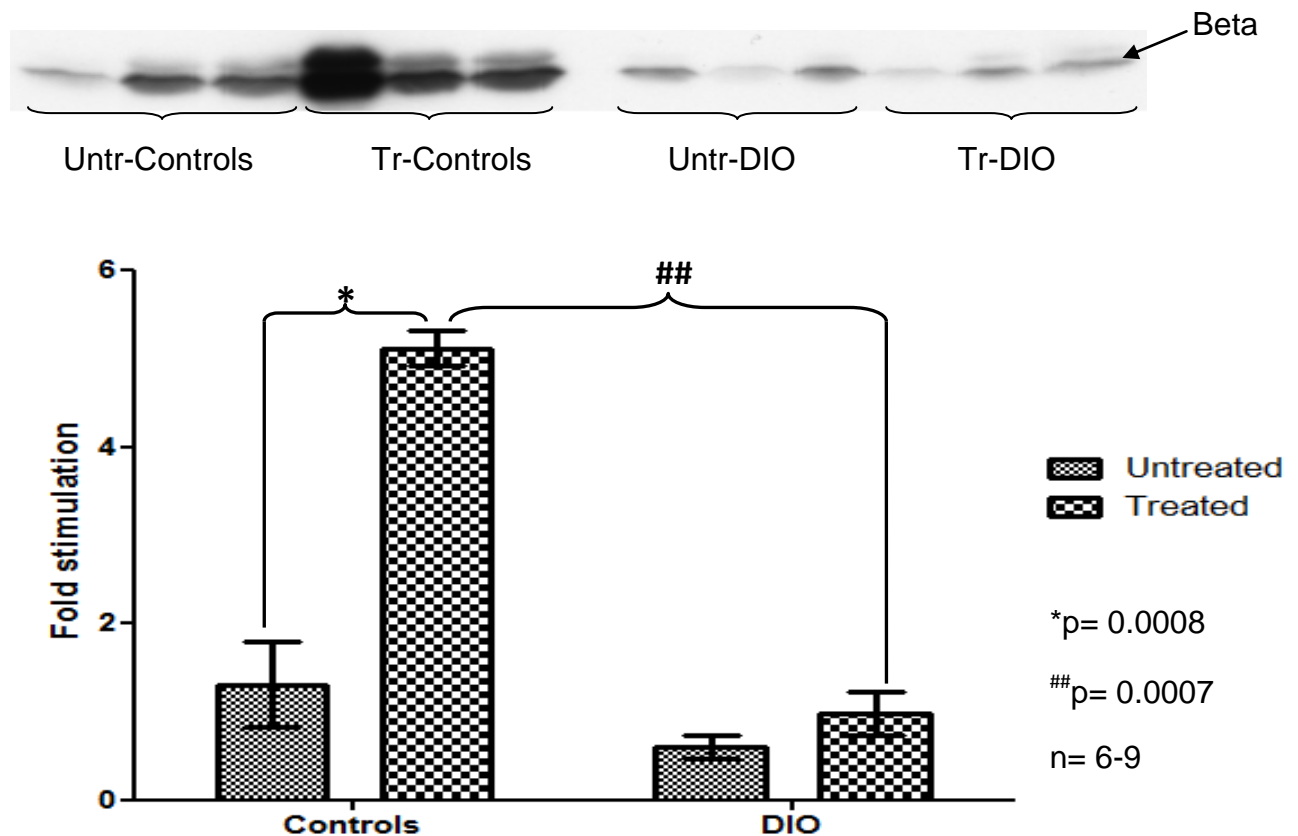
Figure 3.48: *GSK-3β phosphorylation*. Shown is the Western blot representing total GSK-3β phosphorylation, as well as a graph showing its fold stimulation (compared to the first loaded control that was assigned a value of 1) in controls and diet induced obese (DIO) animals.

3.3.2.1.3 Phospho/Total (P/T) ratios of GSK-3 protein

The P/T (GSK-3β) ratios were significantly lower in untreated DIO animals than untreated controls (**p= 0.0489) as well as when treated DIO animals and treated controls were compared (##p= 0.0020) (figure 3.49). In addition, treated controls had significantly higher P/T ratio than untreated control animals (*p= 0.0025). There was no significant difference between treated and untreated DIOs, but there was a trend towards increased P/T ratio in treated DIO animals (figure 3.49).
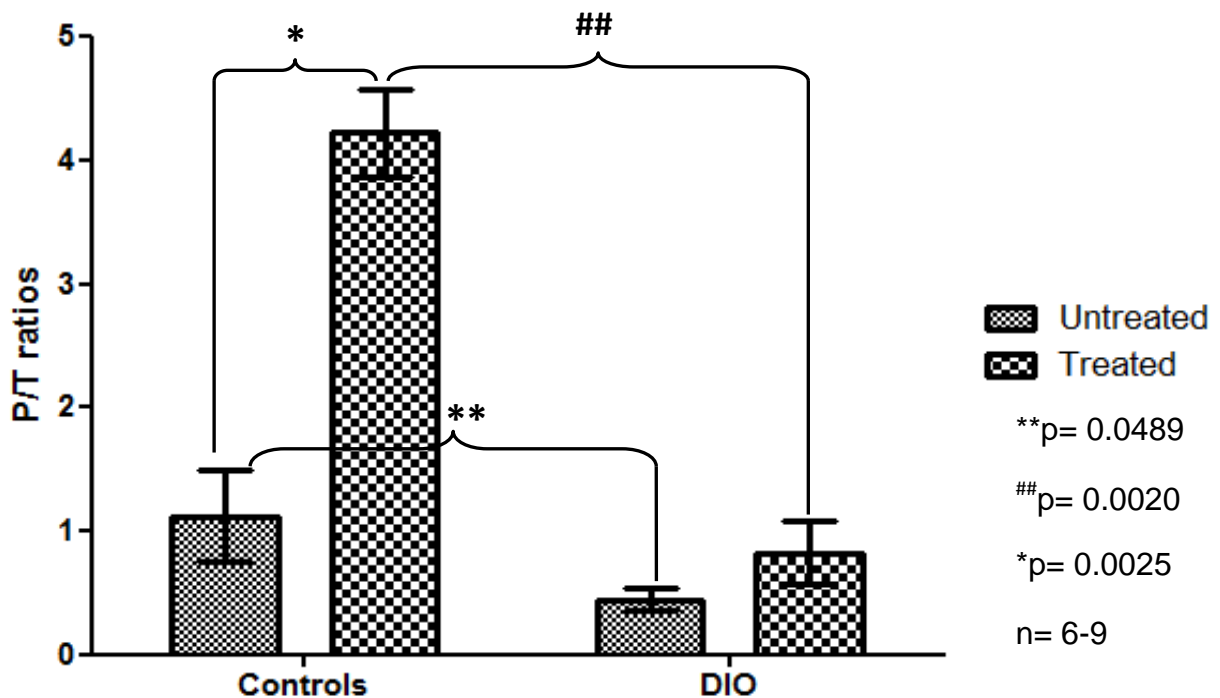
Figure 3.49: *GSK-3β P/T ratio*. Shown are the phospho/total ratios of both control and DIO animals.

3.3.2.2 Effect on PKB/Akt protein

3.3.2.2.1 Total PKB/Akt

After 16 weeks on diet, PKB/Akt was significantly downregulated in untreated DIO animals as compared to untreated controls (**p= 0.0417). In addition, following four weeks of treatment with GSK-3 inhibitor, PKB/Akt was also significantly downregulated in treated DIOs when compared to treated control animals ([##]p= 0.0026) (figure 3.50). Furthermore, total PKB/Akt was significantly downregulated in treated DIO animals as compared to untreated DIOs ([#]p= 0.0023). However, there was no significant difference in total PKB/Akt expression between treated and untreated control animals (figure 3.50).
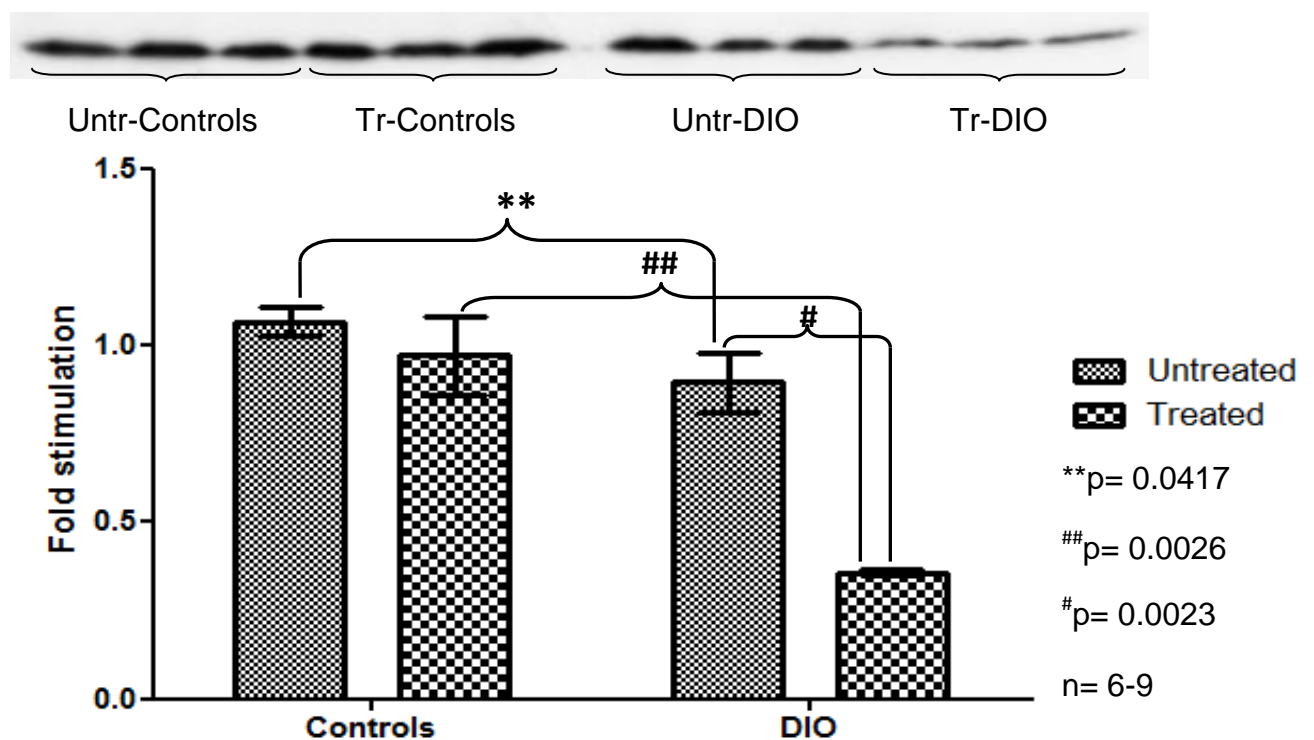
Figure 3.50: *Total PKB/Akt*. Shown is one of the Western blots representing total PKB/Akt expression, as well as a graph showing its fold stimulation (compared to the first loaded control that was assigned a value of 1) in controls and diet induced obese (DIO) animals.

3.3.2.2.2 Effect on PKB/Akt phosphorylation

Following 16 week of diet, there was no significant difference in PKB/Akt phosphorylation between untreated DIOs and untreated control animals as well as when treated DIOs were compared to treated controls, following 4 weeks of treatment with the GSK-3 inhibitor (figure 3.51). However, PKB/Akt phosphorylation was significantly higher in treated DIOs than untreated DIO animals ($^{\#}p= 0.0079$), while there was no significant difference between treated and untreated control animals (figure 3.51).
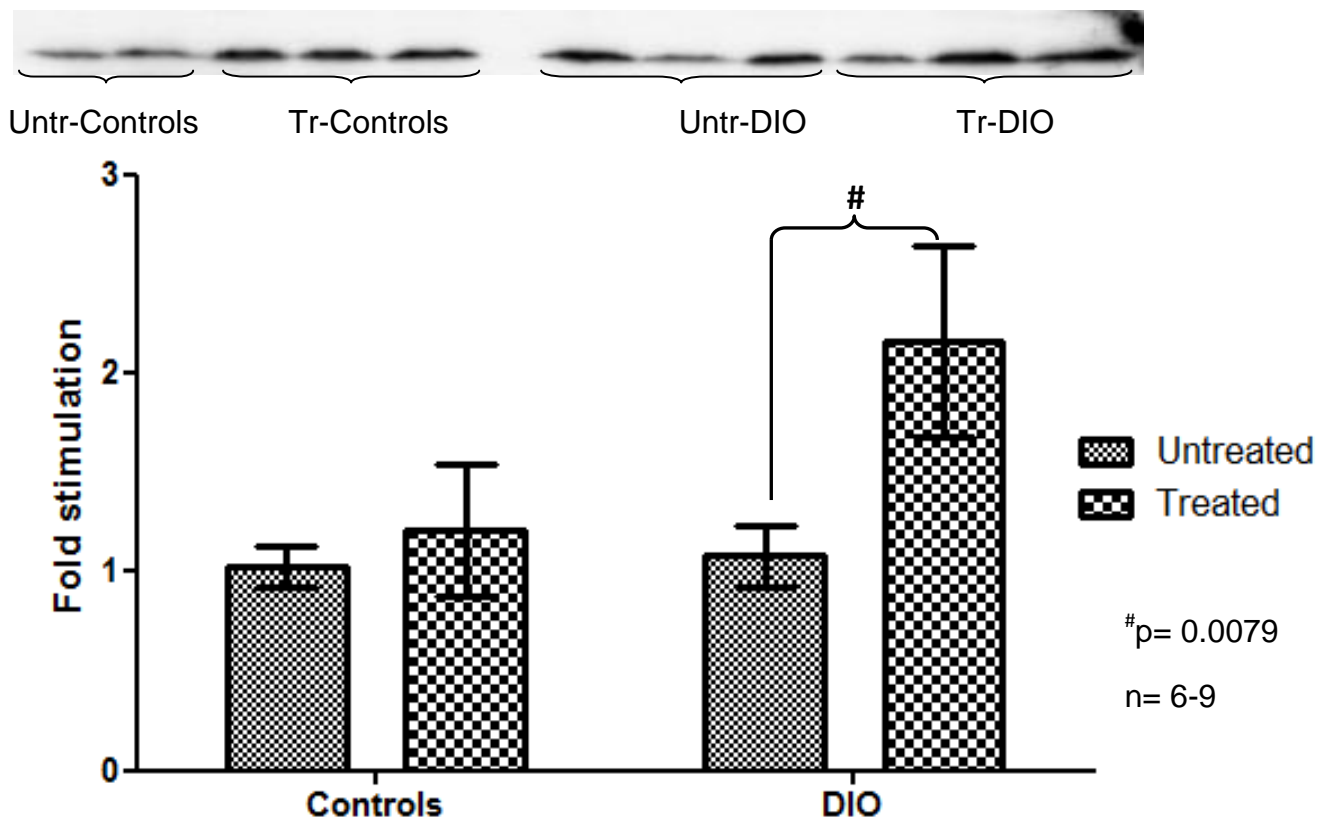
Figure 3.51: *Phosphorylated PKB/Akt*. Shown is the Western blot representing phosphorylated PKB/Akt, as well as a graph showing its fold stimulation (compared to the first loaded control that was assigned a value of 1) in controls and diet induced obese (DIO) animals.

3.3.2.2.3 Phospho/Total (P/T) ratio of PKB/Akt protein

After 16 weeks of diet, there was no significant difference in P/T ratios when untreated DIOs and untreated control animals were compared. However, following 4 weeks of treatment with GSK-3 inhibitor, P/T ratios of PKB/Akt were significantly higher in treated DIOs when compared with treated control animals ([##]p= 0.0174), as well as when treated DIOs were compared to untreated DIO animals ([#]p<0.0001) (figure 3.52). There was also no significant difference between treated and untreated control animals (figure 3.52).
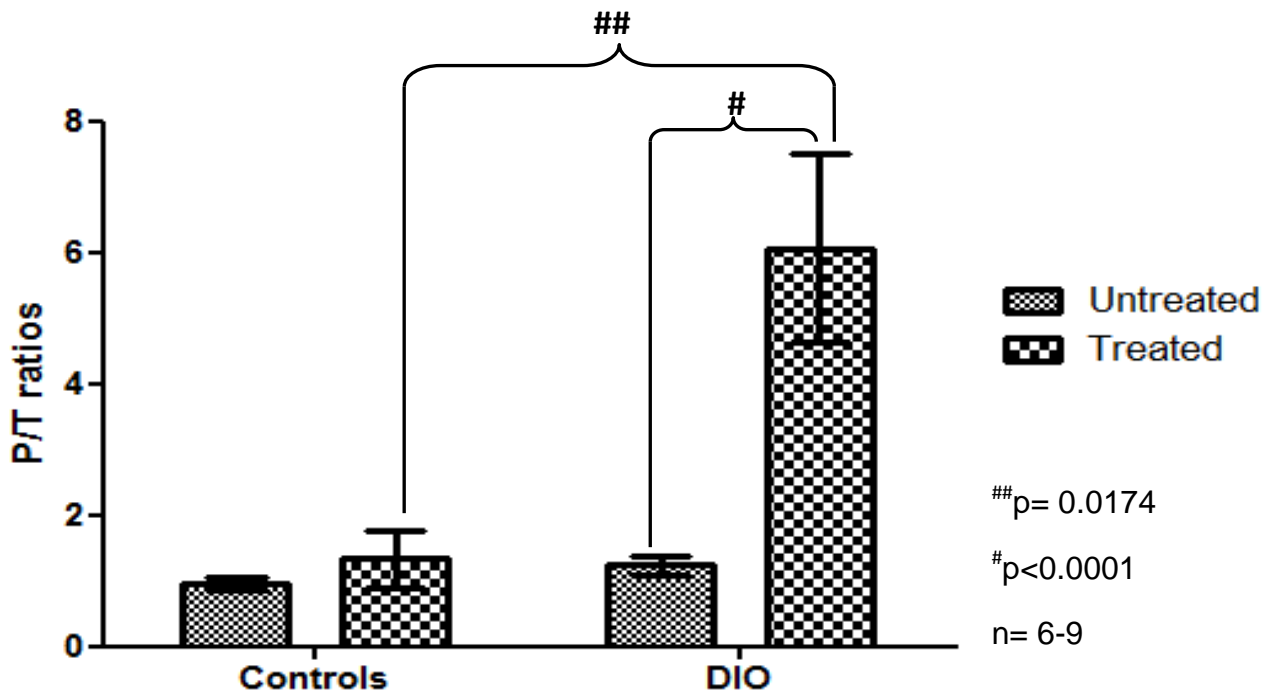
Figure 3.52: *PKB/Akt (P/T ratio).* Shown are the phospho/total ratios of both control and diet induced obese (DIO) animals.

3.3.2.3 **Effect on total IRS-1 expression**

Following 16 weeks on diet, total IRS-1 expression was significantly downregulated in untreated DIOs when compared to untreated controls (**p= 0.0089) (figure 3.53). In addition, after four weeks of treatment with GSK-3 inhibitor, IRS-1 protein was also significantly downregulated in treated DIOs as compared to treated controls (##p= 0.0388) as well as when treated DIOs were compared to untreated DIO animals (#p= 0.0388). However, there was no significant difference between treated and untreated controls (figure 3.53).
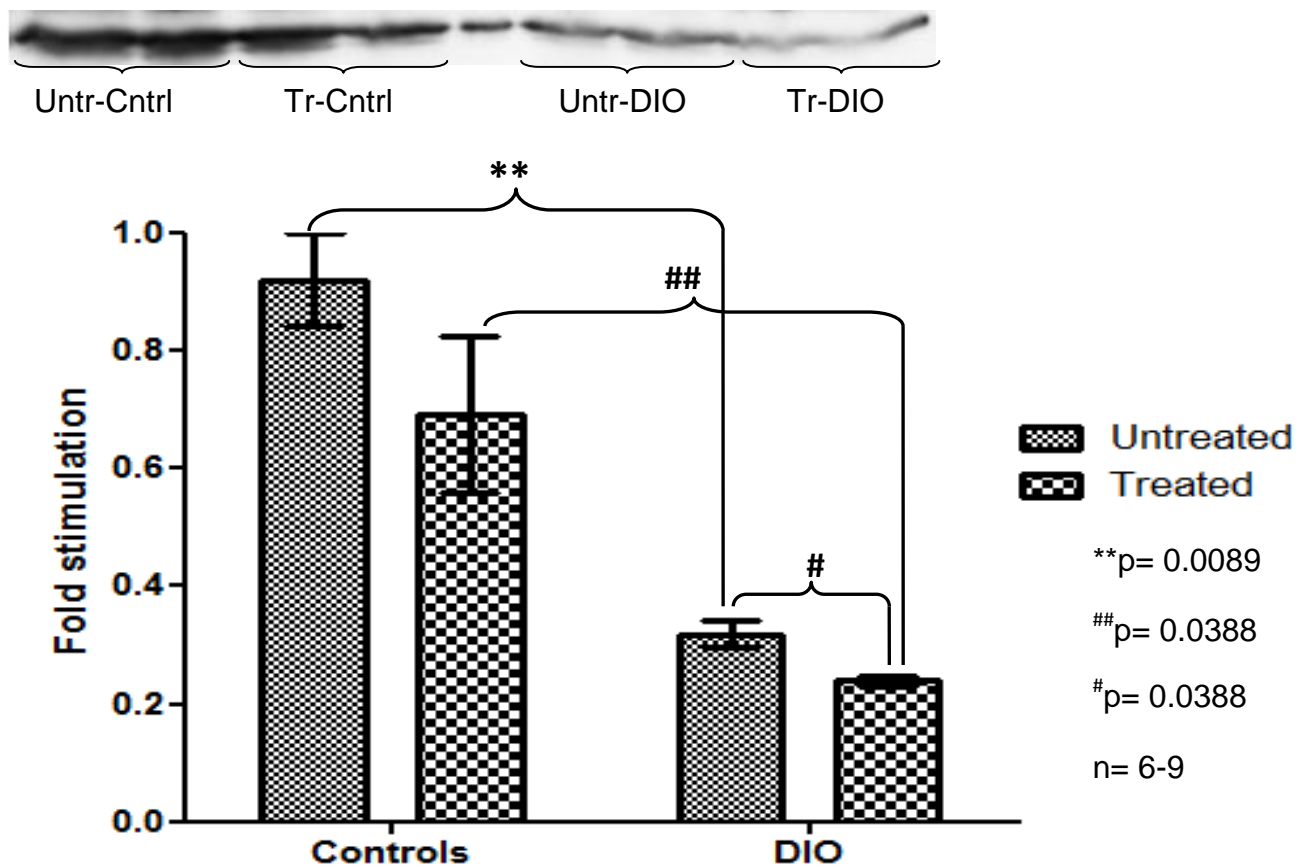
Figure 3.53: *Total IRS-1 protein.* Shown is the Western blot representing total IRS-1 expression as well as a graph showing its fold stimulation (compared to the first loaded control that was assigned a value of 1) in controls and diet induced obese (DIO) animals.

3.3.2.4 Effect on total IRS-2 expression

Following sixteen weeks of diet, the IRS-2 expression was significantly downregulated in untreated DIO animals as compared to untreated controls (**p= 0.0220) (figure 3.54). However, after four weeks of treatment with GSK-3 inhibitor, there was no significant difference between treated DIOs and treated control animals. In addition, IRS-2 expression was significantly upregulated in treated DIOs when compared to untreated DIOs ([#]p= 0.0075) as well as in treated controls when compared to untreated controls (*p= 0.0040) (figure 3.54).
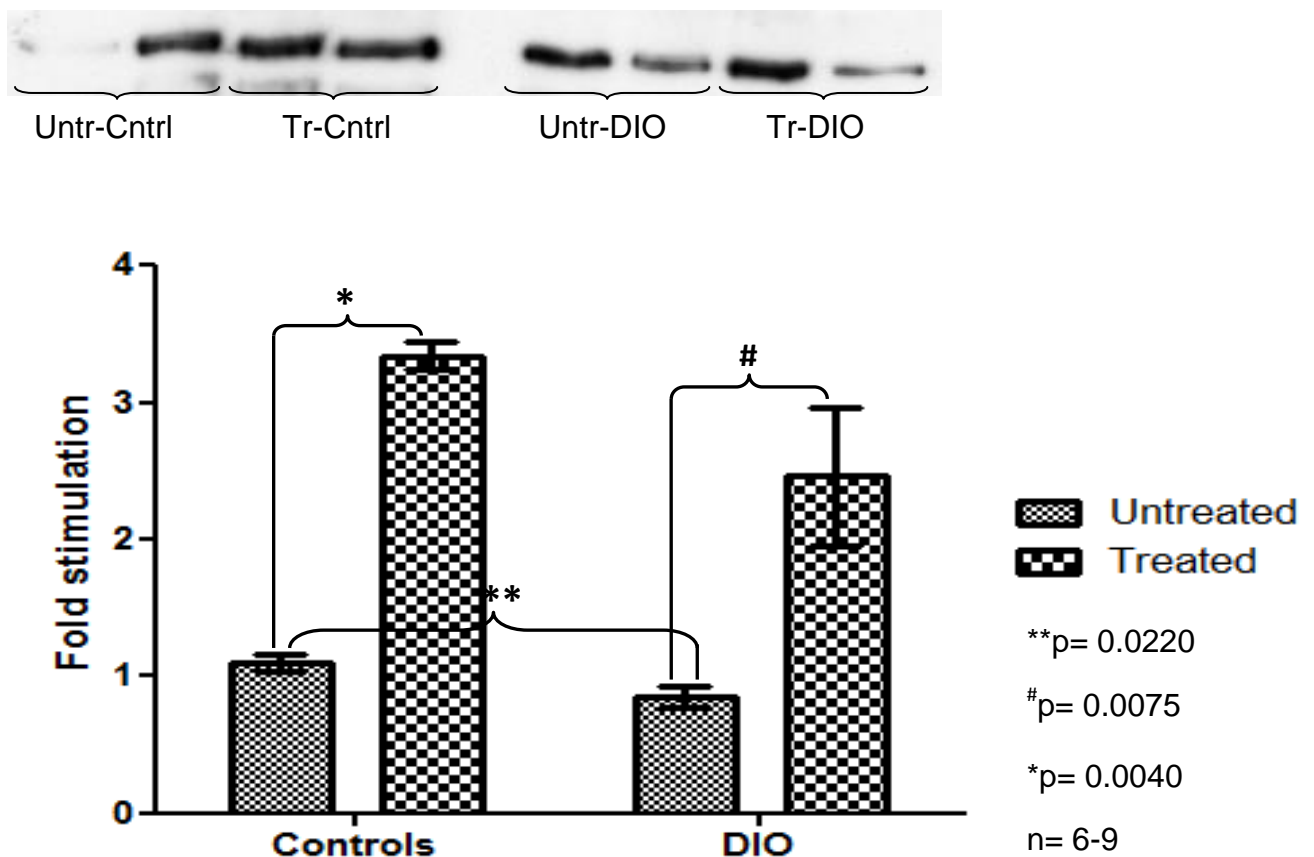
Figure 3.54: *Total IRS-2 protein*. Shown is the Western blot representing total IRS-2 expression as well as a graph showing its fold stimulation (compared to the first loaded control that was assigned a value of 1) in controls and diet induced obese (DIO) animals.

3.3.2.5 Effect on total SERCA-2a expression

After 16 weeks on diet, SERCA-2a expression was significantly downregulated in untreated DIOs as compared to untreated controls (**p= 0.0269) (figure 3.55). However, following four weeks of treatment with GSK-3 inhibitor, there was no significant difference in total SERCA-2a expression when treated DIO animals and treated controls were compared. In addition, there was also no significant difference between treated and untreated DIOs as well as when treated and untreated control animals were compared (figure 3.55).
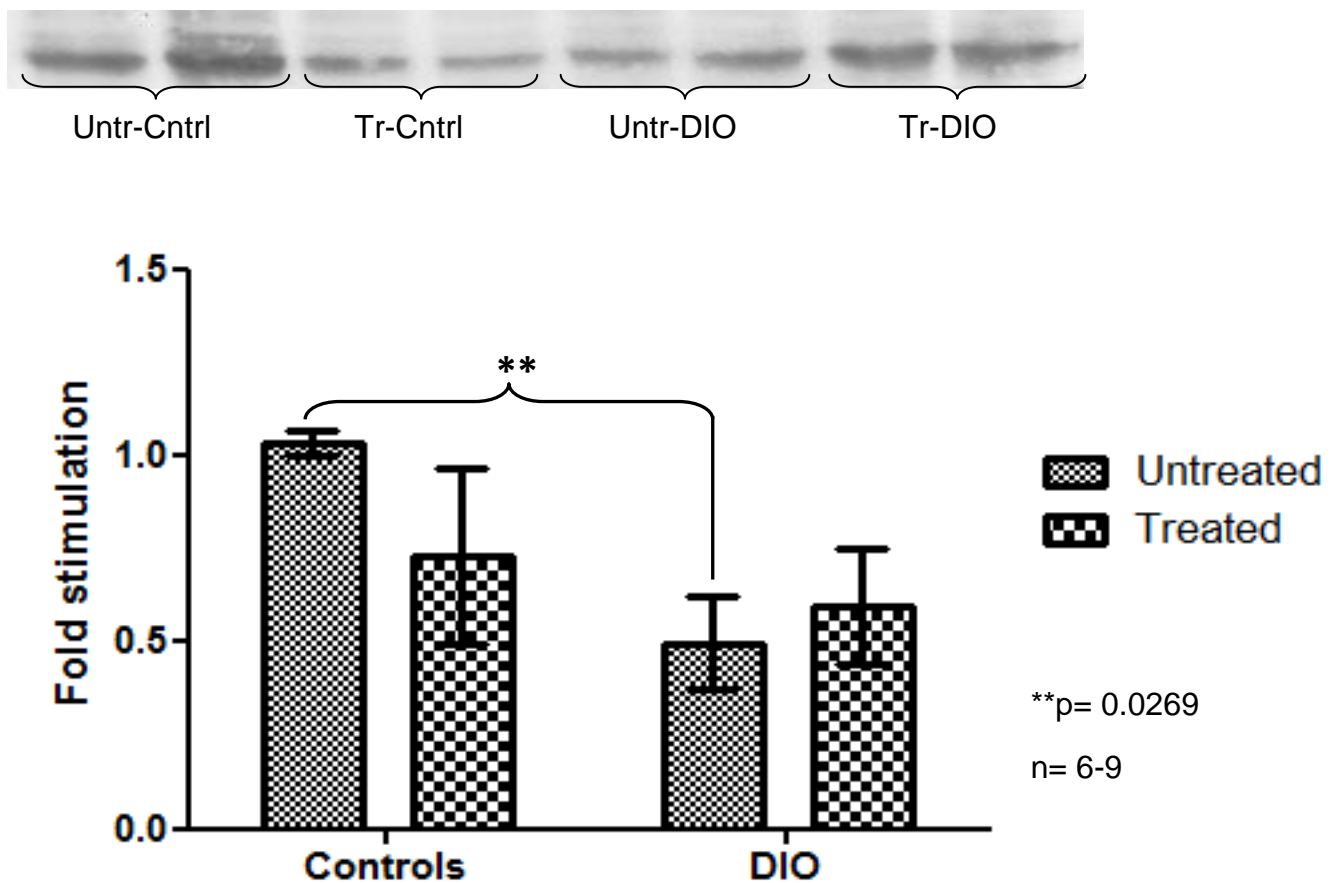
Figure 3.55: *Total SERCA-2a protein.* Shown is the Western blot representing total SERCA-2a expression as well as a graph showing its fold stimulation (compared to the first loaded control that was assigned a value of 1) in controls and diet induced obese (DIO) animals.

3.3.2.6 Effect on PLM protein

3.3.2.6.1 Total PLM protein

Following 16 weeks on diet, total PLM expression was significantly upregulated in untreated DIOs as compared to untreated control animals (**p= 0.0027). In addition, after four weeks of treatment with GSK-3 inhibitor, total PLM expression was also significantly upregulated in treated DIOs when compared to treated controls (figure 3.56). However, there were no significant differences in total PLM expression between treated and untreated DIOs as well as when treated and untreated control animals were compared (figure 3.56).
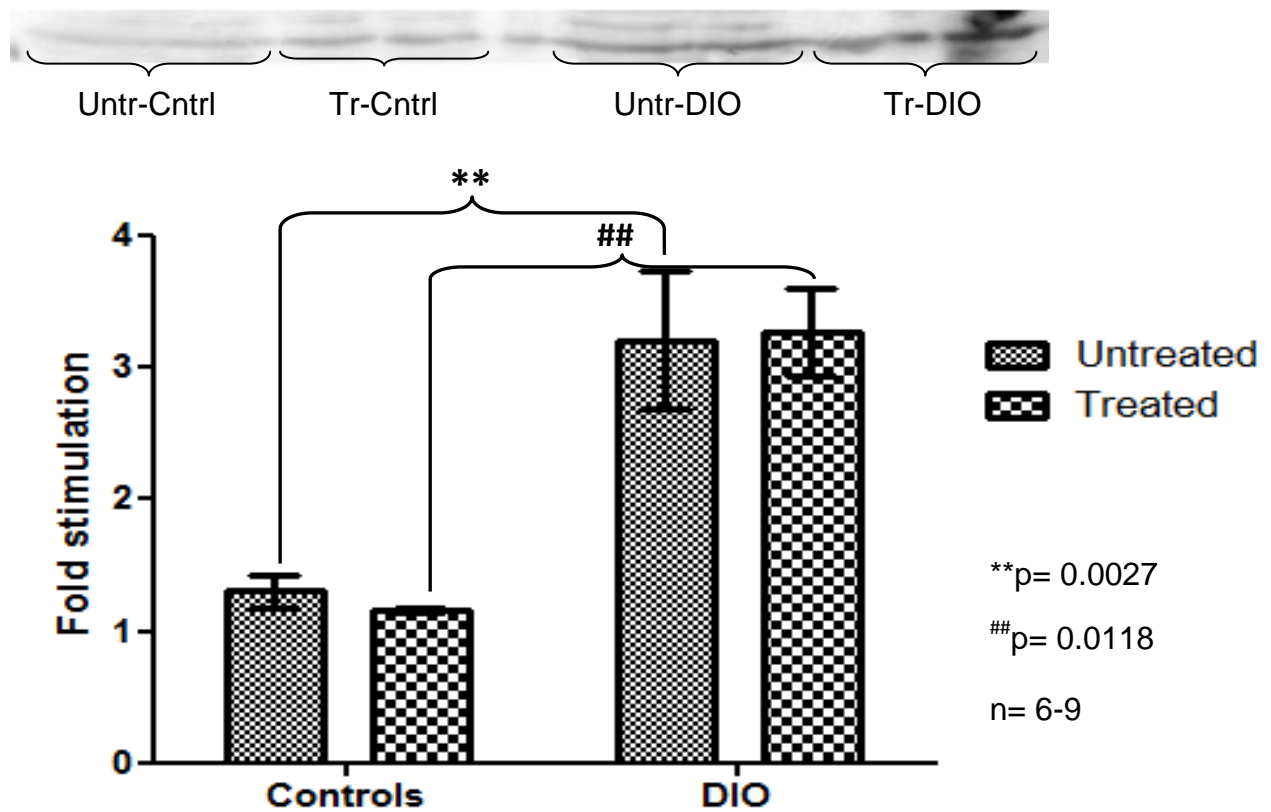
Figure 3.56: *Total PLM*. Shown is the Western blot representing total PLM expression as well as a graph showing its fold stimulation (compared to the first loaded control that was assigned a value of 1) in controls and diet induced obese (DIO) animals.

3.3.2.6.2 Effect on phospholamban (PLM) phosphorylation

Following 16 weeks on diet, PLM phosphorylation was lesser in untreated DIOs than untreated control animals (**p= 0.0177). However, after four weeks of treatment with GSK-3 inhibitor, there was no significant difference in phosphorylated PLM protein when treated DIOs and treated control animals were compared (figure 3.57). PLM phosphorylation was significantly higher in treated DIOs than untreated DIO animals (#p= 0.0249). There was no significant difference in phosphorylated PLM when treated and untreated control animals were compared (figure 3.57).
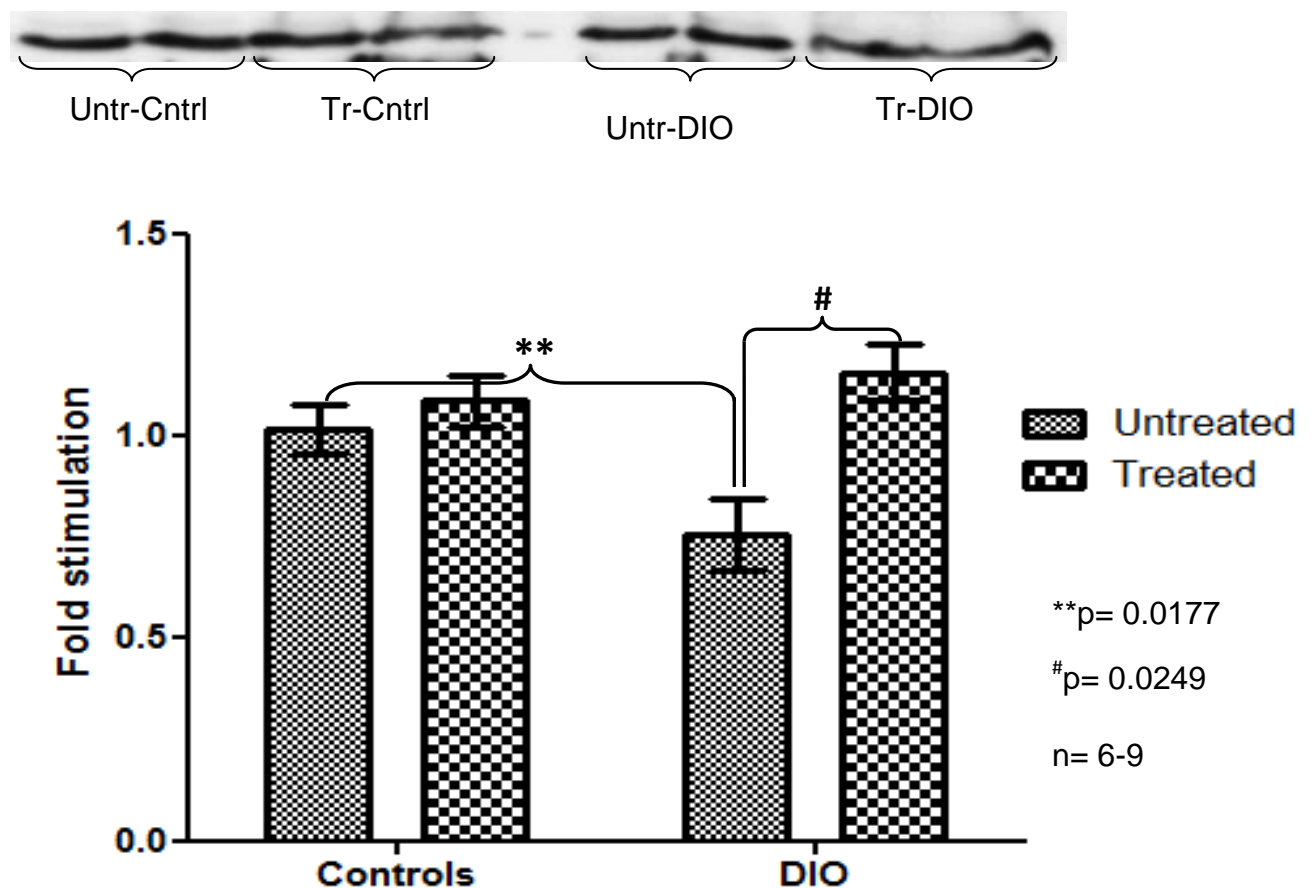
Figure 3.57: *Phosphorylated PLM.* Shown is the western blot representing phosphorylation of *PLM* protein as well as a graph showing its fold stimulation (compared to the first loaded control that was assigned a value of 1) in both treated (Tr) and untreated (Untr) animals.

3.3.2.6.3 Phospho/Total (P/T) ratio of PLM protein

The P/T ratios of PLM were significantly lower in untreated DIO animals than untreated controls (**p= 0.0005) as well as in treated DIOs when compared to treated control animals (##p= 0.0118) (figure 3.58). However, there was no significant difference in P/T ratios of PLM when treated and untreated DIO animals are compared. In addition, there was also no significant difference between treated and untreated controls (figure 3.58).
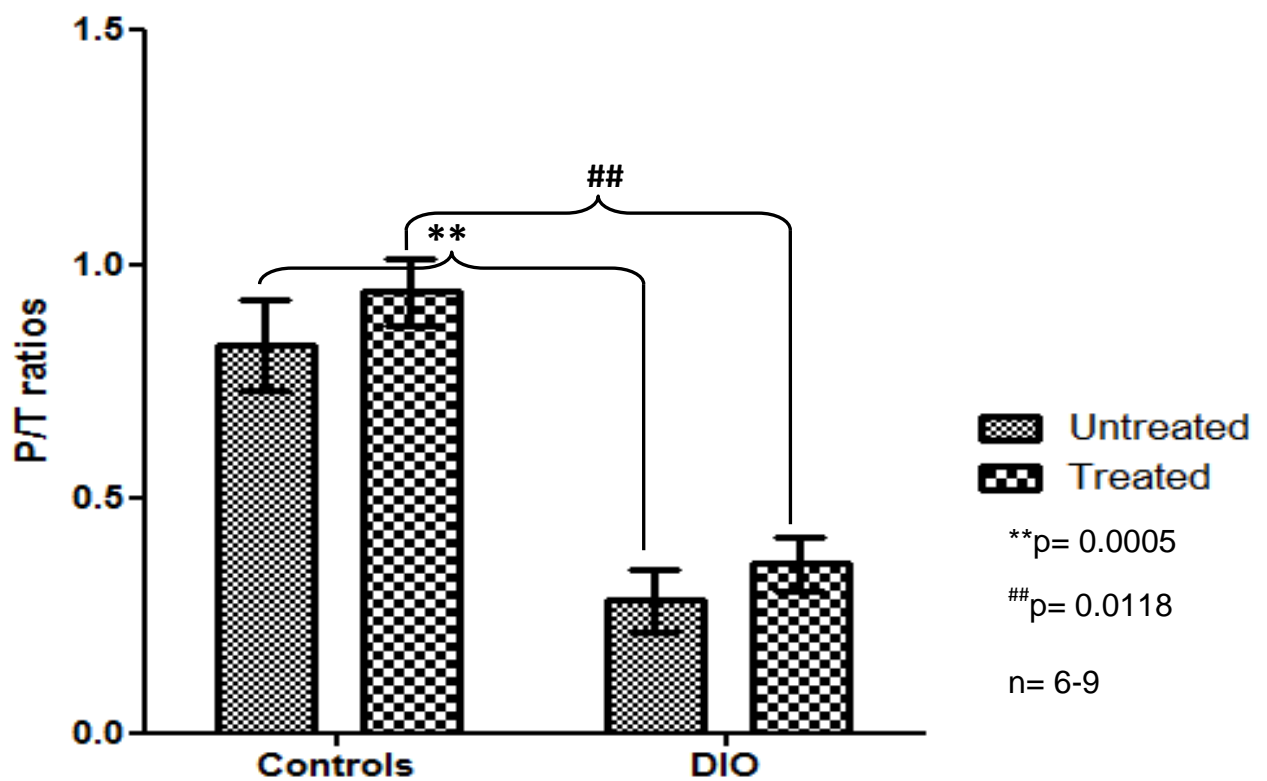
Figure 3.58: *Phospho/Total ratio of PLM.* Shown are the Phospho/Total ratios of PLM in both treated and untreated DIO and control animals.

3.3.3 Effect on Calcium ATPase activity

Following 16 weeks on diet, calcium ATPase activity was significantly lower in untreated DIOs when compared to untreated controls (**p= 0.0007). In addition, after four weeks of treatment with GSK-3 inhibitor, calcium ATPase activity was still lower in treated DIO animals as compared to treated controls ($^{\#\#}$p= 0.0296) (figure 3.59). However, there was no significant difference in calcium ATPase activity when comparing treated and untreated DIOs as well as when treated and untreated control animals were compared (figure 3.59).
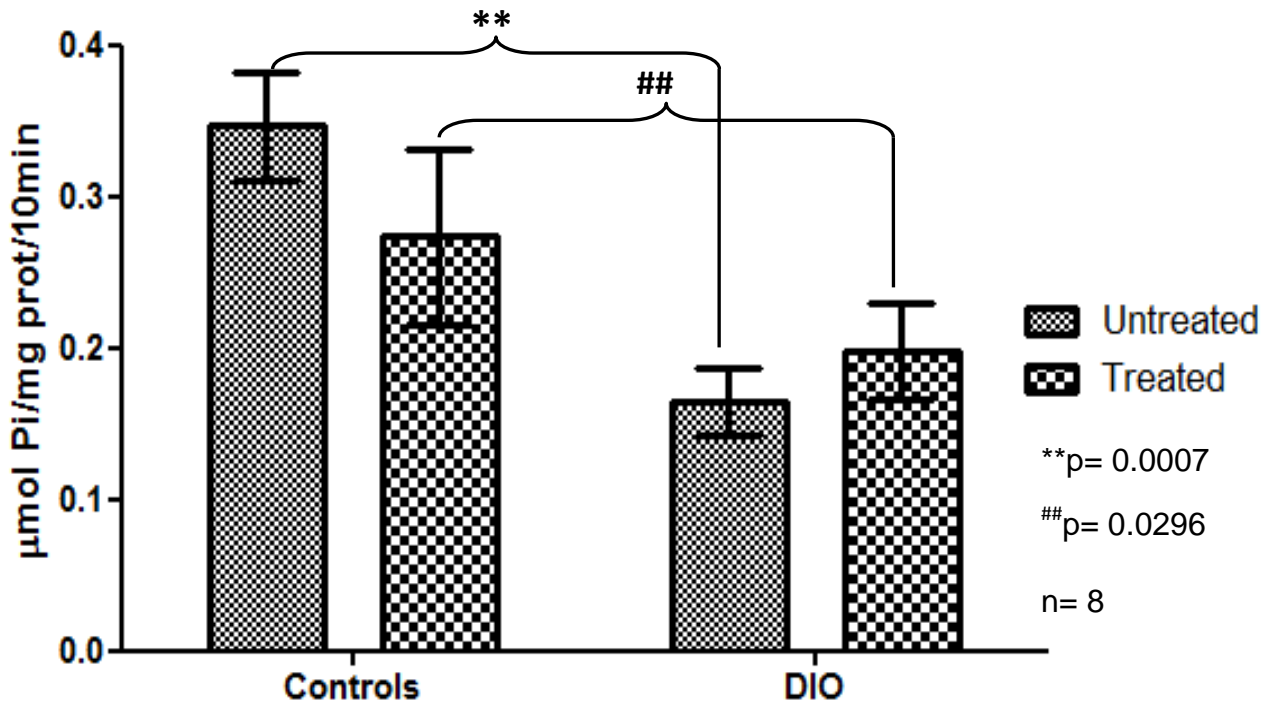
Figure 3.59: *Calcium ATPase activity.* Shown are the activities of both treated and untreated controls and DIO animals as determined by the amount of inorganic phosphate (P_i) produced.

CHAPTER 4

DISCUSSION AND CONCLUSION

4.1 **Discussion**

The primary aim of the current study was to determine the role of GSK-3 protein in the development of cardiomyopathy associated with obesity and insulin resistance. It has been well established that obesity plays a role in myocardial dysfunction (Poirier et al. 2005). The poor myocardial function in obesity has been attributed to metabolic abnormalities such as dyslipidemia, glucose intolerance, insulin resistance and is associated with impaired myocardial Ca^{2+} handling (Lopaschuk et al. 2007, Chess and Stanley 2008).

The current study focused on changes in DIO animals that may affect myocardial contractility. To achieve the aims of the present study, the well characterized rat model of diet induced obesity (DIO) was used to determine whether GSK-3 and its substrate proteins (IRS-1, IRS-2, PKB/Akt, SERCA-2a and PLM) are dysregulated. We first characterized GSK-3 and its substrate proteins at 8 weeks to determine early effects especially on SERCA-2a expression. We then again determined whether GSK-3 or its down-stream substrates are dysregulated at 16 weeks. The 8 and 16 weeks time points were both considered as baseline, in order to, after the treatment with a GSK-3 inhibitor, determine whether GSK-3 plays a role in the observed changes and whether these changes may be reversible.

4.1.1 Animal model (Biometric parameters)

The animal model was developed by feeding the animals with a rat chow diet supplemented with sucrose and condensed milk, while control animals were fed a normal rat chow diet for a period of 8 or 16 weeks. Thus DIO animals consumed more energy per day than the controls. It has been well established that a long term positive imbalance between energy intake and expenditure results in obesity and insulin resistance (review by Sethi and Vidal Puig 2007). In addition, a high sucrose containing diet administered to animals have been associated with a variety of effects including obesity, insulin resistance, hyperinsulinaemia and hyperglycaemia depending on the model (Reaven et al. 1979; Soria et al. 2001; Fukuchi et al. 2004, Kamgang et al. 2005). In the current study, at both 8 (figure 3.1-2) and 16 (figure 3.14-15) weeks, DIO animals were significantly bigger than the control animals and had increased intra-peritoneal fat depots. This indicates that the DIO animals were indeed abdominally obese and possibly insulin resistant. Insulin resistance was not measured at this time point; however, it was measured in both treated and untreated animals following treatment with GSK-3 inhibitor (section 4.1.3.3).

4.1.2 Expression and phosphorylation of proteins at baseline (8 and 16 weeks)

4.1.2.1 8 weeks time point

Following 8 weeks on diet, there was no significant difference in expression and basal phosphorylation of GSK-3 (figure 3.3-7), PKB/Akt (figure 3.8-10) and total IRS-2 (figure 3.12) proteins. GSK-3 protein has been shown to be elevated in tissues of insulin resistant obese rodent models of type 2 diabetes (review by Henriksen and Dokken 2006). However, total IRS-1 expression was significantly downregulated in DIO animals as compared to the age matched controls (figure 3.11).

127

We conclude that these animals are insulin resistant after only 8 weeks on diet, as the upstream located IRS-1 protein is downregulated four fold. Insulin binds to its receptor and stimulates IRS-1 protein, the activated IRS-1 protein then activates PKB/Akt via PI3K pathway (White 2002). In the present study, the downregulated IRS-1 protein may therefore impair activation of PKB/Akt protein, thus GSK-3 which is normally inhibited by PKB/Akt protein remains active. In addition, Kim et al. 1999 and Storgaard et al. 2001, also observed in skeletal muscle of type 2 diabetes mellitus patients and subjects with impaired glucose tolerance, insulin induced defects in IRS and PI3K expression but normal PKB/Akt activation. As the IRS-1 protein is downregulated, we thought that there may be other mechanisms or proteins that may take over the significant role of IRS-1. So we investigated the IRS-2 protein and we found that there was no significant difference in total IRS-2 expression between controls and DIO animals. It is therefore possible that IRS-2 may compensate for IRS-1 at this stage. The effect of insulin stimulation on this pathway has not been measured.

GSK-3 is known to control the expression of SERCA-2a protein (Michael et al. 2004), therefore we determined the total SERCA-2a expression. We found that total SERCA-2a expression was significantly downregulated by approximately 50% in hearts from DIO animals as compared to those coming from the control animals (figure 3.13). Although, SERCA-2a expression was down regulated in DIO animals, it was not associated with increased GSK-3 expression at this early stage, as was reported in previous studies (Michael et al. 2004).

4.1.2.2 **16 weeks time point**

Following 16 weeks of diet, there was still no significant difference in total GSK-3 protein (figure 3.16) as well as its basal phosphorylation (figure 3.17-20) between DIOs and the age matched control animals. Although there was no significant difference in total GSK-3 protein, there was a strong trend to elevated expression in DIO animals. Total PKB/Akt expression was significantly downregulated in DIO animals while there was no significant difference in its basal phosphorylation between control and DIO animals (figure 3.21-23). After 16 weeks of diet, DIO animals presented with decreased IRS-1 (figure 3.24) and IRS-2 (figure 3.25) protein expression. However, the PI3K associated activity of IRS-1/2 was not measured in the current study.

Previous studies, have reported that GSK-3 protein phosphorylates IRS-1 on a serine residue thus making it a poorer substrate for tyrosine phosphorylation by the insulin receptor thereby attenuating insulin signaling (Eldar-Finkelman and Krebs 1997). In addition, in studies in which PI3K activity associated to IRS-1 or IRS-2 have been performed side by side, a decrease in both IRS-1 and IRS-2 associated insulin stimulated PI3K activity has been observed in muscle biopsies from obese type 2 diabetic patients (Kim et al. 1999; Vollenweider et al. 2002; Bouzakri et al. 2003). Our observations therefore corroborate the observations of faulty signaling on the level of IRS in obesity and insulin resistance.

In type 2 diabetes mellitus, the first change in cardiac functioning is diastolic dysfunction (Cosson and Kevorkian 2003; Fang et al 2003). It has been shown that this dysfunction is induced by a decreased Ca^{2+} uptake by the myocardial sarcoplasmic reticulum as well as myocardial interstitial fibrosis (Dutta et al. 2002; Wold et al. 2005; Van Hoeven and Factor 1990). SERCA-2a plays a role in the Ca^{2+} uptake by the sarcoplasmic reticulum (Takeda 2010).

In the current study we therefore evaluated the expression and activity of the SERCA-2a protein. We found that the expression of SERCA-2a protein was significantly downregulated in DIO animals as compared to the age matched controls (figure 3.26). It has been reported that GSK-3 protein down regulates the expression of SERCA-2a by acting directly on its promoter (Michael et al. 2004). In our model, this early decreased SERCA-2a expression may have been caused by a different mechanism other than the actions of GSK-3. It has been well established that corticosteroids also decrease mRNA levels of SERCA-2a protein, while it increase mRNA levels of SLN (Gayan-Ramirez et al. 2000). However, the levels of corticosteroids were not measured in the current study.

In addition, it has been shown that the expression of SERCA-2a and PLM in the myocardium is dependent on the circulating concentration of tri-iodothyronin (T3) hormone (Nagai et al. 1989; Zarain-Herzberg et al. 1994; Holt et al. 1999). It has been well established that hyperthyroidism promotes an up regulation of SERCA-1a and down-regulation of SERCA-2a in red muscles of rodent animals (Nunes et al. 1985; Muller et al. 1994; Simonides et al. 2001; Arruda et al. 2003; Yamada et al. 2004). Arruda et al. 2005, using hyperthyroid rabbit skeletal muscle showed that the

Western blot analysis indicates a 6 fold increase in SERCA-1a expression and a 50% decrease in SERCA-2a expression. In the current study, the levels of thyroid hormone were not measured, so it may have also played a role in SERCA-2a down regulation.

The activity of SERCA-2a is negatively regulated by PLM protein (Tada et al. 1974; Munch et al. 2000). Thus we also investigated the expression of PLM and we found that hearts from DIO animals had significantly increased total PLM expression while its phosphorylation was decreased (figure 3.27-29). Our results therefore showed that PLM protein was upregulated and more active in DIO animals. Thus SERCA-2a was also affected by changes in PLM expression and phosphorylation. An unidentified mechanism may have decreased the content of SERCA-2a in the cardiac muscle cell, at the same time PLM may have decreased its activity. To further confirm this, we investigated the activity of the SERCA-2a protein, and we found that the SERCA-2a activity was significantly lower in DIO animals as compared to the controls (figure 3.30). The lower SERCA-2a activity in DIO animals was associated with the decreased SERCA-2a expression and increased total PLM expression. It has been previously shown that, the SERCA-2a activity is under inhibitory control of PLM (James et al. 1989; Kimura et al. 1996), while phosphorylation of PLM reactivates it (Tada et al. 1975).

Using the *in vivo* perfused isolated hearts, we investigated the contractile ability of hearts from both DIO and control animals and their ability to with stand low flow ischemia. In the current study, hearts were stabilized for 30 minutes, subjected to low flow ischemia (0.2 ml/min) for 25 minutes followed by 30 minutes of reperfusion. We monitored their contractility during and after low flow ischemia to give an indication of contractile ability and the recovery of contraction. We found no significant difference in systolic pressure (figure 3.31), diastolic pressure (figure 3.32), LVDevP (figure 3.33), PCDP (figure 3.37B), EIDP (figure 3.37C), TPC (figure 3.37A) and the rate of coronary flow (figure 3.38) when DIO and control animals were compared. The heart rate (figure 3.34) and rate pressure product (figure 3.35) were significantly lower in DIO animals than the age matched controls at baseline. However, there was no significant difference at reperfusion.

Results indicated that the RPP of DIO animals was lower than control animals at baseline, however, there was no significant difference after low flow ischemia. In addition, during low flow ischemia, DIO animals had a longer time to onset of ischemic contracture than control animals (figure 3.36). This was quite surprising, as the SERCA-2a expression was downregulated in these DIO animals, one would expect poor recovery in DIO animals. In addition, several studies conducted on animal models of heart failure and human failing hearts, suggested that alterations in SR Ca^{2+} handling are a critical feature of the hypertrophied or failing myocardium (review by Periasamy and Huke 2001). However, there is some contrasting evidence that state that life may be possible without SERCA-2a (review by Trafford et al. 2009). In addition, Andersson et al. 2009, using a novel inducible knockout of the SERCA-2 gene in adult mice, has shown that the hearts from these mice can

function in the near complete absence of SERCA-2. They discovered that despite a rapid decline in SERCA-2 protein levels to less than 5% of the control and a reduction of SR Ca^{2+} content by ~80%, the cardiac function is only modestly reduced (Andersson et al. 2009). In the current study, the retained contractile ability of hearts from DIO animals may be due to cardiac adaptive capacity. In addition, in the current study we only measured SERCA-2a expression and not SERCA-1a, other isoforms or the ryanodine receptor. However, it has been suggested that SERCA-1a does not only compete with SERCA-2a for functional site in the SR, it may also play a compensatory role when SERCA-2a isoform is downregulated (review by Periasamy and Huke 2001).

4.1.3 16 weeks plus treatment with GSK-3 inhibitor

GSK-3 protein was first discovered as a regulator of glycogen synthase thus playing a role in glycogen synthesis (Embi et al. 1980). However, abnormally high activities of GSK-3 protein has been implicated in several pathological disorders which include type 2 diabetes, neuron degenerative and affective disorders (Eldar-Finkelman et al. 2010). This led to the development of new generations of inhibitors with specific clinical implications to treat diseases such as type 2 diabetes, Alzheimer's disease and mood disorders (Martinez 2008). However, there is currently no clinical data available on long term GSK-3 inhibition, while preclinical data strongly support its important future role (review by Huisamen and Lochner 2010). In addition, there is very little data available on heart research (review by Huisamen and Lochner 2010). In the current study we treated the animals with the specific GSK-3 inhibitor that target the ATP binding site, in order to determine whether GSK-3 protein plays a role in changes observed at 8 and 16 weeks time points (baseline) and whether these

changes may be reversible. We investigated its effect on body weight, IP fat, ventricular weight, tibia length, fasting blood glucose, plasma insulin levels, protein expression and phosphorylation, as well as Calcium ATPase activity.

4.1.3.1 **Effect of the inhibitor on body weight (BW) and IP fat mass**

In the current study, we found that the DIO animals were significantly bigger than the controls (figure 3.39). This increased body mass was positively associated with increased intra-peritoneal fat mass (figure 3.40). However, when comparing treated and untreated groups, we found that treated controls were significantly bigger than untreated controls while treated DIO animals were significantly smaller than untreated DIOs (figure 3.39). Both treated and untreated DIO animals had increased IP fat as compared to treated and untreated control animals (figure 3.40). However, there was no significant difference in IP fat when treated and untreated DIOs were compared as well as between treated and untreated control animals (figure 3.40). As compared to the baseline results, treatment decreased the body weight of DIOs while it significantly increased the body weight of control animals. There should be other mechanisms triggered that may lead to a decreased body weight in DIO animals, that do not take place in control animals.

4.1.3.2 Effect of the inhibitor on ventricular weight (VW) and Tibia length (TL)

4.1.3.2.1 Effect on ventricular weight

Cardiac remodelling is one of the detrimental features associated with obesity (Abel et al. 2008, Chess and Stanley 2008). It has been reported that obesity may predispose the individual to fatal ventricular arrhythmias by inducing cardiac hypertrophy, which is an arrhythmogenic risk factor (Wolk 2000). In the current study, the ventricular weight was also measured to determine if the hearts were hypertrophied or not. We found that ventricles from DIO animals were significantly bigger than ventricles from control animals in both treated and untreated groups (figure 3.41). In addition, we found that ventricles from treated control animals were significantly bigger, while treated DIO animals had significantly smaller ventricles (figure 3.41). As the same results were observed in body weight, ventricular weight was positively associated with the body weight and this may indicate hypertrophy in hearts from DIO animals. This might be because the ventricles need to compensate for the higher volumetric load in the larger animals.

4.1.3.2.2 Effect on tibia length

Because body weight vs ventricular weight may cause false positive values for hypertrophy in DIO animals, as the ventricular weight may correlate with body weight. The tibia length was measured and we found no significant difference in tibia length in both treated and untreated animals (figure 3.42). Both diet and treatment did not have an influence in tibia length. Although there was no significant difference in tibia length, VW/TL ratio was significantly higher in untreated DIO as compared to untreated controls, an indication of hypertrophy in DIO animals. Hypertrophy in untreated DIOs may be due to a compensatory response as they have reduced

SERCA-2a activity. However, following the treatment with GSK-3 inhibitor, the VW/TL ratio was significantly higher in treated controls, while it was significantly lower in treated DIO animals (figure 3.43).

Therefore, inhibition of GSK-3 in a normal animal may lead to development of hypertrophy, while inhibition of GSK-3 activity in DIO animals did not exacerbate this hypertrophy. Haq et al. 2000 using lithium chloride (LiCl), also demonstrated that inhibition of GSK-3 activity leads to features of cardiac hypertrophy. In DIO animals, treatment with GSK-3 inhibitor improved or reversed cardiac hypertrophy. Recent evidence shows that GSK-3 functions as a negative regulator of cardiac hypertrophy (Haq et al. 2000; Badorff et al. 2002). In addition, it has been shown that insulin induced phosphorylation and inactivation of GSK-3 is impaired in diabetes and insulin resistance (Hardt and Sadoshima 2002). So this may not only contribute to impaired glycogen synthesis but also to enhanced protein synthesis, leading to the development of diabetic cardiomyopathy (Laviola et al. 2001)..

4.1.3.3 **Effect of the inhibitor on fasting blood glucose and insulin levels**

Among other functions of GSK-3 protein, it is well known to phosphorylate and inactivate glycogen synthase, a rate limiting enzyme of glycogenesis, thus playing a role in blood glucose homeostasis (Parker et al. 1983, Roach 1990, Zhang et al. 1993). It has been well established that one of the major features of type II diabetes mellitus is the impairment of both basal and insulin stimulated glucose metabolism in peripheral tissues (Patel et al. 2004). In addition, it has been shown that the muscle tissue from type II diabetic patients has reduced glycogen deposition as compared to normal tissues, which is correlated with decreased glycogen synthase activity,

increased GSK-3 activity and impaired insulin responsiveness (Shulman et al. 1990, Cline et al. 1994). In the current study, animals were treated with specific GSK-3 inhibitor and the fasting blood glucose and plasma insulin levels were measured to determine if the inhibitor improved them. As expected, we found that the untreated DIO animals had significantly higher fasting blood glucose levels (figure 3.44), an indication of pre-diabetic state. These animals were not diabetic, as the cut off point indicating diabetes is 8 Mmol/L. Although, the treatment with GSK-3 inhibitor had no effect on fasting blood glucose levels, the significant difference measured in untreated groups was not seen after treatment (figure 3.44).

A variety of chemically distinct selective and specific GSK-3 inhibitors have also been shown to improve insulin action both *in vivo* in animal models of insulin resistance (Cline et al. 2002; Henriksen and Dokken 2006) and *in vitro* in tissues and cultured cells (Ring et al. 2003; Coghlan et al. 2000; Nikoulina et al. 2002). For that reason, fasting plasma insulin levels were also measured and we found that the untreated DIO animals had significantly higher levels of insulin, indicating insulin resistance in these animals (figure 3.45). These higher insulin and glucose levels in untreated DIO animals showed that the experimental animals were indeed pre-diabetic and insulin resistant. Following the treatment with the GSK-3 inhibitor, the insulin levels were still significantly higher in DIO animals, showing that the treatment could not improve whole-body insulin resistance. This is underscored by the unchanged HOMA insulin resistant (IR) index (figure 3.46).

In the current study, the diet influenced both plasma glucose and insulin levels, while treatment had no effect. However, previous *in vitro* studies of cultured human skeletal muscle chronically treated with GSK-3 inhibitors (CHIR98014 and CHIR98023), have shown a significant increase in both basal and insulin stimulated glucose uptake (Nikoulina et al. 2000). In the current study, this was not supported. This might be because of the difference between *in vitro* and *in vivo* treatment with the inhibitor. However, amongst other studies, Ciaraldi et al. 2010, also showed that a reduction in GSK-3β expression had no statistical significant effect on basal glucose uptake in muscle cells. However, only a modest increase glucose uptake was observed when control cells were exposed to acute insulin stimulation (Ciaraldi et al. 2010). In addition, Henriksen and Teachey, 2007 also reported that, in the absence of insulin, no effects of GSK-3 inhibition were detected on glucose transport.

4.1.3.4 Effect of the inhibitor on protein expression and phosphorylation

4.1.3.4.1 Effect on GSK-3 expression and phosphorylation

In order to inhibit a specific protein kinase with a drug, the drug should either decrease its expression, modulate its phosphorylation, or compete for substrate or the ATP binding site (Van Wauwe and Haefner 2003). In the current study, following the treatment with GSK-3 inhibitor, we found no significant difference in total GSK-3 expression in both treated and untreated animals (figure 3.47). As mentioned earlier, one of the mechanisms of inhibiting this protein is to increase its phosphorylation. We also investigated GSK-3 phosphorylation and we found that GSK-3 phosphorylation was significantly increased in treated controls, while there was no significant difference in treated DIO animals (figure 3.48-9). However, a trend

towards increased GSK-3 phosphorylation was observed in treated DIO animals (figure 3.48-9). This increase in phosphorylation of GSK-3 in treated control animals may play a role in the activity of the protein.

Since the GSK-3 inhibitor used in this study competes for the ATP binding site; there may not be a decrease in total GSK-3 expression. However, besides competing for the ATP biding site, we showed that in control animals the treatment inhibited GSK-3 through phosphorylation, we also speculate that the increased tendency observed in treated DIO animals may have been just enough to inhibit the GSK-3 protein. In addition, other studies using GSK-3 inhibitor 4-benzyl-2-methyl-1, 2, 4-thiadiazolidine-3, 5-dione (TDZD-8) have shown increased GSK-3 serine-9 phosphorylation consistent with inactivation of the kinase (Gao et al. 2008). However, the other way to measure the extent of GSK-3 inhibition is to measure the activity of glycogen synthase (GS) as GSK-3 directly regulates its activity (MacAulay et al. 2005). The activity of GS was not measured in the current study.

4.1.3.4.2 Effect on PKB/Akt, IRS-1 and IRS-2 proteins

4.1.3.4.2.1 Effect on PKB/Akt expression and phosphorylation

In insulin sensitive cells, insulin binds to its receptor and activates IRS-1 or IRS-2 protein which then stimulates PKB/Akt via PI3K pathway (Saltiel and Pessin 2003; Shepherd 2005). The activated PKB/Akt protein is known to directly phosphorylate GSK-3 protein on its serine residue thus inhibiting it (Lawrence and Roach 1997). It has also been shown that *in vivo*, PKB/Akt does not only regulate GSK-3 activity but also directly interact with GSK-3 as both proteins can be co-immunoprecipitated (van Weeren et al. 1998). Since GSK-3 and PKB/Akt can interact with each other, we

139

investigated the effect of GSK-3 inhibition on expression and phosphorylation of PKB/Akt protein.

We found that total PKB/Akt was significantly down regulated in untreated DIO animals as compared to untreated controls (figure 3.50). Treatment with GSK-3 inhibitor decreased total PKB/Akt even further in treated DIO animals (figure 3.50). In addition, the treatment significantly increased PKB/Akt phosphorylation in DIO animals but had no effect in control animals (figure 3.51-2). This and the elevated P/T ratio indicate that PKB/Akt was more active in treated DIO animals, thus possibly contributing to the inhibition of GSK-3 activity. It may also reflect the higher level of IRS-2 expression. In contrast to the observed changes, Nikoulina et al. 2001, reported that following the treatment with GSK-3 inhibitor, PKB/Akt expression was unaltered indicating the specificity of the inhibitor. This might also be model specific as Nikoulina et al. 2001, worked in skeletal muscle cell cultures taken from patients.

4.1.3.4.2.2 Effect on IRS-1 expression

It has been shown that the treatment of muscle cell cultures from type II diabetic human subjects with a GSK-3 inhibitor (Chiron) increases the expression of IRS-1 protein, suggesting that GSK-3 may participate in the post-transcriptional regulation of insulin signaling components (Nikoulina et al. 2002). In the current study, we found that the total IRS-1 expression was significantly downregulated in untreated DIO animals (figure 3.53). However, the treatment with GSK-3 inhibitor decreased total IRS-1 expression further in DIO animals while it had no effect in control animals (figure 3.53).

We conclude that GSK-3 was not involved in down regulation of IRS-1 protein in our model. Instead GSK-3 inhibition further lowered IRS-1 expression. However, it was reported that GSK-3 phosphorylates IRS-1 on a serine residue and inhibits its activity (Eldar-Finkelman and Krebs 1997), (which was not measured in the current study), having no effect on its expression. In addition, Ciaraldi et al. 2010, also reported that IRS-1 expression was unaltered in skeletal muscle cell culture, following knock down of GSK-3β. However, in contrast to that, it has been reported that the longer term exposure of human muscle cell cultures to the GSK-3 inhibitor is associated with upregulation of IRS-1 and downregulation of GSK-3 protein expression (Nikoulina et al. 2002).

4.1.3.4.2.3 Effect on IRS-2 expression

Since IRS-1 expression was still depressed in DIO animals, the effect on IRS-2 expression was investigated. We found that untreated DIO animals had decreased IRS-2 expression (figure 3.54). However, following the treatment with GSK-3 inhibitor, IRS-2 expression was significantly upregulated in both treated DIOs and control animals (figure 3.54). This indicates that the treatment with the GSK-3 inhibitor significantly increased IRS-2 expression in both control and DIO animals while it had no effect on IRS-1 expression. Our results show that GSK-3 protein may act as a regulator of IRS-2 expression. In support to that, Nikoulina et al. 2002, suggested that GSK-3 may participate in the post-transcriptional regulation of insulin signaling components. The results also show that IRS-2 may compensate for reduced IRS-1 activity in DIO animals.

4.1.3.4.3 Effect on SERCA-2a and PLM proteins

4.1.3.4.3.1 Effect on SERCA-2a expression

In heart, GSK-3 plays several important roles such as in negative regulation of hypertrophy. On the other hand, its inhibition during ischemia and reperfusion (I/R) has been implicated as cardioprotective (Omar et al. 2010). Furthermore, GSK-3 protein has also been shown to play a role in myocardial contractility by directly down regulating the expression of SERCA-2a thereby leading to an inability to normalize cytosolic Ca^{2+} in diastole (Michael et al. 2004). SERCA-2a plays an important role in the uptake of calcium from the cytosol back to the SR during myocardial relaxation, thus it is considered as a primary regulator of the Ca^{2+} levels and myocardial contractility (Schimdt et al. 2001). However, it has been shown that SERCA-2a expression is down regulated in diabetic and insulin resistant rodents (Pearce et al. 2004 and Michael et al. 2004).

In the current study, the animals were treated with the GSK-3 inhibitor to investigate whether SERCA-2a expression and activity will be improved after the treatment. We found that SERCA-2a expression was significantly downregulated in untreated DIO animals (figure 3.55). Following treatment with the GSK-3 inhibitor, SERCA-2a expression was unchanged in DIO animals (figure 3.55). However, there was a tendency towards an increase in SERCA-2a levels in treated DIOs as compared to untreated DIO animals. From the negative results of the inhibitor on SERCA-2a expression, we conclude that other unidentified role players are possibly involved in regulation of SERCA-2a expression in this model. It is also possible that the exact mix of protective kinases required for protection is model and species dependent (Murphy and Steenbergen 2008).

In contrast to the results found in the current study, previous studies such as those of Michael et al. 2004 using transgenic mice, showed that the gene transfer of GSK-3β(SA9) containing a Ser-9 to Ala mutation that prevents inactivation of GSK-3β by serine-9 phosphorylation thus increasing GSK-3 activity, significantly reduced the expression of SERCA-2a protein. They then inhibited GSK-3β with Lithium Chloride (LiCl), to determine whether the inhibition of SERCA-2a expression was reversible or not. They showed that LiCl completely reversed the inhibition of SERCA-2a mRNA expression by GSK-3β (SA9) (Michael et al. 2004). LiCl however, is not a specific drug.

4.1.3.4.3 **Effect on PLM expression and phosphorylation**

In the current study, we also investigated the effect of GSK-3 inhibition on expression of PLM protein, which is known to regulate the activity of SERCA-2a (James et al. 1989; Asahi et al. 2003). We found that the expression of PLM protein was significantly upregulated in untreated DIO animals (figure 3.56). Following the treatment with the GSK-3 inhibitor, PLM expression was still upregulated to the same extent in DIO animals, therefore the treatment had no effect on PLM expression (figure 3.56). In addition, PLM phosphorylation was significantly decreased in untreated DIO animals (figure 3.57). However, the treatment with GSK-3 inhibitor significantly increased the phosphorylation of PLM protein in treated DIOs while it had no effect in control animals (figure 3.57-8). Although PLM expression was upregulated in DIO animals the treatment increased its phosphorylation thus rendering it less active. To the best of our knowledge, there are very few studies reporting changes in PLM expression following treatment with the GSK-3 inhibitor. Michael et al. 2004, using GSK-3β transgenic mice, showed that the expression of

PLM was unaltered in GSK-3β transgenic mice and its serine-16 phosphorylation was only modestly reduced. From the change in PLM phosphorylation, we expected an improvement in the SR Ca^{2+}-ATPase activity.

4.1.3.5 **Effect on calcium ATPase activity (SERCA-2a activity)**

It has been well established that SERCA-2a activity is positively associated with increased SERCA-2a expression and decreased PLM expression or increased PLM phosphorylation (Vittorini et al. 2007). In the present study, following the treatment with GSK-3 inhibitor, we measured the calcium ATPase activity. We found that the calcium ATPase activity was significantly decreased in untreated DIO animals (figure 3.59). Treatment with the GSK-3 inhibitor had no effect on calcium ATPase activity (figure 3.59). However, there was a trend towards an increase in SERCA-2a activity in treated DIO animals. In addition, the phosphorylation of PLM was increased almost 2 fold in DIO animals, so SERCA-2a activity may have increased *in vivo*, because we only used isolated SR membranes therefore the regulation by PLM was probably absent. Previous studies showed that GSK-3 inhibition reduced both diastolic and systolic Ca^{2+} overload, an indication of increased SERCA-2a activity, and this has been proposed as a strategy to improve post ischemic cardiomyocyte survival following ischemia and reperfusion, thus playing a role in cardioprotection (Murphy and Steenbergen 2005; Omar et al. 2010).

4.2 **Conclusion**

Our original hypothesis was that, GSK-3 protein and its substrate proteins play a role in the development of cardiomyopathy associated with obesity and insulin resistance. We wanted to determine whether GSK-3 and its substrate proteins are dysregulated in obese and insulin resistant animals. In the current study, we first showed that yes, indeed, the consumption of high calorie diet as well as an imbalance between energy intake and expenditure lead to increased body weight (obesity), and insulin resistance in male Wistar rats. This lead to the disruption of insulin signaling pathway, characterized by alterations in proteins involved such as IRS-1, IRS-2, PKB/Akt and GSK-3 at baseline. However, GSK-3 inhibition improved IRS-2 expression while it had no effect on IRS-1. So we conclude that GSK-3 may play a role in regulation of IRS-2 expression but not in IRS-1. However, IRS-2 may compensate for IRS-1 activity. In addition, GSK-3 inhibition also increased PKB/Akt phosphorylation. We showed that DIO animals developed cardiac hypertrophy at 16 weeks. However, we showed that GSK-3 inhibition may reverse cardiac hypertrophy in DIO animals, thus acting as a negative regulator of hypertrophy, although it exarcerbated development of hypertrophy in control animals.

We also showed that SERCA-2a was significantly downregulated while its regulatory protein PLM was upregulated in DIO animals indicating that these animals developed cardiomyopathy as early as 8 weeks on diet. The increased tendency of GSK-3 at both 8 and 16 weeks may have played a role in down regulation of SERCA-2a expression. However, there was no change in SERCA-2a expression after the treatment with the GSK-3 inhibitor, so we cannot conclude whether GSK-3 protein played a role in observed changes. However, the tendency towards increase

in SERCA-2a expression and increased PLM phosphorylation in treated DIO animals is promising. As we did not conclusively showed that the GSK-3 inhibitor, at the dose prescribed by the pharmaceutical company and with an oral administration route, was 100% effective to actually inhibit GSK-3 activity, further studies need to be conducted.

4.3 Limitations of this study

In the current study, only male Wistar rats were used. These animals were only fed a high calorie diet. The current study only focused on the insulin signaling pathway, especially on GSK-3 protein. There may be other pathways involved in the regulation of SERCA-2a as well as in the development of cardiomyopathy. Inhibition of downstream substrates of GSK-3 needs to be demonstrated conclusively. Unfortunately, a limited amount of inhibitor for *in vivo* studies was supplied.

4.4 Future studies

To confirm the effectiveness of the inhibitor *in vivo*, we will investigate the expression and phosphorylation of glycogen synthase protein. Glycogen synthase is a downstream substrate of GSK-3, which plays a role in regulation of glycogen synthesis (MacAulay et al. 2005). We expect to find decreased insulin stimulated phosphorylation. We would also like to investigate the effect of the GSK-3 protein on myocardial contractility using low flow ischemia and reperfusion. In addition, we would like to directly treat the hearts from DIO and control animals with GSK-3 inhibitor just before low flow ischemia. We will then carefully monitor these hearts during ischemia and at reperfusion to see if there are any changes as compared to untreated hearts.

REFERENCES

1. Abel ED, Litwin SE, Sweeney G. Cardiac remodeling in obesity. Physiol Rev. 2008 Apr; 88(2):389-419.

2. Abel ED, Peroni O, Kim JK, Kim YB, Boss O, Hadro E, Minnemann T, Shulman GI, Kahn BB. Adipose-selective targeting of the GLUT4 gene impairs insulin action in muscle and liver. Nature. 2001 Feb 8; 409(6821):729-33.

3. Adeghate E. Molecular and cellular basis of the aetiology and management of diabetic cardiomyopathy: a short review. Mol Cell Biochem. 2004 Jun; 261(1-2):187-91.

4. Alberti KG, Zimmet PZ. Definition, diagnosis and classification of diabetes mellitus and its complications. Part 1: diagnosis and classification of diabetes mellitus provisional report of a WHO consultation. Diabet Med. 1998 Jul; 15(7):539-53.

5. Alessi DR, Downes CP, The role of PI 3-kinase in insulin action, Biochim. Biophys. Acta 1436 (1998) 151–164.

6. Alessi DR, James SR, Downes CP, Holmes AB, Gaffney PR, Reese CB, Cohen P. Characterization of a 3-phosphoinositide-dependent protein kinase which phosphorylates and activates protein kinase B alpha. Curr Biol. 1997 Apr 1; 7(4):261-9.

7. Ali A, Hoeflich KP, Woodgett JR. Glycogen synthase kinase-3: properties, functions, and regulation. Chem Rev. 2001 Aug; 101(8):2527-40.

8. Andersson KB, Birkeland JA, Finsen AV, Louch WE, Sjaastad I, Wang Y, Chen J, Molkentin JD, Chien KR, Sejersted OM, Christensen G. Moderate

heart dysfunction in mice with inducible cardiomyocyte-specific excision of the Serca2 gene. J Mol Cell Cardiol. 2009 Aug; 47(2):180-7.

9. Andjelković M, Alessi DR, Meier R, Fernandez A, Lamb NJ, Frech M, Cron P, Cohen P, Lucocq JM, Hemmings BA. Role of translocation in the activation and function of protein kinase B. J Biol Chem. 1997 Dec 12; 272(50):31515-24.

10. Aneja A, Tang WH, Bansilal S, Garcia MJ, Farkouh ME. Diabetic cardiomyopathy: insights into pathogenesis, diagnostic challenges, and therapeutic options. Am J Med. 2008 Sep; 121(9):748-57.

11. Anger M, Samuel JL, Marotte F, Wuytack F, Rappaport L, Lompré AM. The sarco(endo)plasmic reticulum Ca^{2+}-ATPase mRNA isoform, SERCA 3, is expressed in endothelial and epithelial cells in various organs. FEBS Lett. 1993 Nov 8; 334(1):45-8.

12. Arruda AP, Da-Silva WS, Carvalho DP, De Meis L. Hyperthyroidism increases the uncoupled ATPase activity and heat production by the sarcoplasmic reticulum Ca^{2+}-ATPase. Biochem J. 2003 Nov 1; 375(Pt 3):753-60.

13. Arruda AP, Oliveira GM, Carvalho DP, De Meis L. Thyroid hormones differentially regulate the distribution of rabbit skeletal muscle $Ca^{(2+)}$-ATPase (SERCA) isoforms in light and heavy sarcoplasmic reticulum. Mol Membr Biol. 2005 Nov-Dec; 22(6):529-37.

14. Asahi M, Kimura Y, Kurzydlowski K, Tada M, MacLennan DH. Transmembrane helix M6 in sarco(endo)plasmic reticulum Ca^{2+}-ATPase forms a functional interaction site with phospholamban. Evidence for physical interactions at other sites. J Biol Chem. 1999 Nov 12; 274(46):32855-62.

15. Asahi M, Kurzydlowski K, Tada M, MacLennan DH. Sarcolipin inhibits polymerization of phospholamban to induce superinhibition of sarco(endo)plasmic reticulum Ca^{2+}-ATPases (SERCAs). J Biol Chem. 2002 Jul 26; 277(30):26725-8.

16. Asahi M, Nakayama H, Tada M, Otsu K. Regulation of sarco(endo)plasmic reticulum Ca2+ adenosine triphosphatase by phospholamban and sarcolipin: implication for cardiac hypertrophy and failure. Trends Cardiovasc Med. 2003 May; 13(4):152-7.

17. Badorff C, Ruetten H, Mueller S, Stahmer M, Gehring D, Jung F, Ihling C, Zeiher AM, Dimmeler S. Fas receptor signaling inhibits glycogen synthase kinase 3 beta and induces cardiac hypertrophy following pressure overload. J Clin Invest. 2002 Feb; 109(3):373-81.

18. Balaban RS. Cardiac energy metabolism homeostasis: role of cytosolic calcium. J Mol Cell Cardiol. 2002 Oct; 34(10):1259-71.

19. Balendran, A., Casamayor, A., Deak, M., Paterson, A., Ga¡ney, P., Currie, R., Downes, C.P. and Alessi, D.R. (1999) Curr. Biol. 9, 393^404. WANG Q, SOMWAR R, BILAN PJ,1 ZHI LIU,1 JIN J et al. Protein Kinase B/Akt Participates in GLUT4 Translocation by Insulin in L6 Myoblasts. MOLECULAR AND CELLULAR BIOLOGY, June 1999, p. 4008–4018

20. Balke CW, Shorofsky SR. Alterations in calcium handling in cardiac hypertrophy and heart failure. Cardiovasc Res. 1998 Feb; 37(2):290-9.

21. Barach JP, Wikswo JP Jr. The effect of action potential propagation on a numerical simulation of a cardiac fiber subjected to secondary external stimulus. Comput Biomed Res. 1991 Oct; 24(5):435-52.

22. Barry SP, Townsend PA, Latchman DS, Stephanou A. Role of the JAK-STAT pathway in myocardial injury. Trends Mol Med. 2007 Feb; 13(2):82-9. Epub 2006 Dec 27.

23. Bayascas JR, Alessi DR. Regulation of Akt/PKB Ser473 phosphorylation. Mol Cell. 2005 Apr 15; 18(2):143-5.

24. Beeson M, Sajan MP, Daspet JG, Luna V, Dizon M, Grebenev D, Powe JL, Lucidi S, Miura A, Kanoh Y, Bandyopadhyay G, Standaert ML, Yeko TR, Farese RV. Defective Activation of Protein Kinase C-z in Muscle by Insulin and Phosphatidylinositol-3,4,5,-(PO(4))(3) in Obesity and Polycystic Ovary Syndrome. Metab Syndr Relat Disord. 2004 Spring; 2(1):49-56.

25. Beeson M, Sajan MP, Dizon M, Grebenev D, Gomez-Daspet J, Miura A, Kanoh Y, Powe J, Bandyopadhyay G, Standaert ML, Farese RV, Activation of protein kinase C-zeta by insulin and phosphatidylinositol-3,4,5-(PO4)3 is defective in muscle in type 2 diabetes and impaired glucose tolerance: amelioration by rosiglitazone and exercise, Diabetes 52 (2003) 1926–1934.

26. Berne RM, Levy MN. Cardiovascular Physiology. St Louis, Mo: Mosby Year Book; 1997

27. Berridge MJ. Cardiac calcium signaling. Biochem Soc Trans. 2003 Oct; 31(Pt 5):930-3.

28. Bers DM, Guo T. Calcium signaling in cardiac ventricular myocytes. Ann NY Acad Sci 2005; 1047:86– 98.

29. Bers DM, Pogwizd SM, Schlotthauer K. Upregulated Na/Ca exchange is involved in both contractile dysfunction and arrhythmogenesis in heart failure. Basic Res Cardiol. 2002a; 97 Suppl 1:I36-42.

30. Bers DM. Cardiac excitation-contraction coupling. Nature. 2002b Jan 10; 415(6868):198-205.

31. Bers DM. Macromolecular complexes regulating cardiac ryanodine receptor function. J Mol Cell Cardiol 2004; 37: 417–429.

32. Bers, DM. Excitation–Contraction Coupling and Cardiac Contractile Force. Vol. 2 ed. Dordrect, The Netherlands: Kluwer Academic Publishers; 2001

33. Bevan P. Insulin signaling. J Cell Sci. 2001 Apr; 114(Pt 8):1429-30.

34. Blankesteijn WM, van de Schans VA, ter Horst P, Smits JF. The Wnt/frizzled/GSK-3 beta pathway: a novel therapeutic target for cardiac hypertrophy. Trends Pharmacol Sci. 2008 Apr; 29(4):175-80.

35. Block BA, Imagawa T, Campbell KP, Franzini-Armstrong C. Structural evidence for direct interaction between the molecular components of the transverse tubule/sarcoplasmic reticulum junction in skeletal muscle. J Cell Biol. 1988 Dec; 107(6 Pt 2):2587-600.

36. Bobe R, Bredoux R, Corvazier E, Lacabaratz-Porret C, Martin V, Kovács T, Enouf J. How many Ca^{2+} ATPase isoforms are expressed in a cell type? A growing family of membrane proteins illustrated by studies in platelets. Platelets. 2005 May-Jun; 16(3-4):133-50.

37. Bøtker HE, Helligsø P, Kimose HH, Thomassen AR, Nielsen TT. Determination of high energy phosphates and glycogen in cardiac and skeletal muscle biopsies, with special reference to influence of biopsy technique and delayed freezing. Cardiovasc Res. 1994 Apr; 28(4):524-7.

38. Bottomley PA, Wu KC, Gerstenblith G, Schulman SP, Steinberg A, Weiss RG. Reduced myocardial creatine kinase flux in human myocardial infarction:

an in vivo phosphorus magnetic resonance spectroscopy study. Circulation. 2009 Apr 14; 119(14):1918-24.

39. Boudina S, Abel ED. Diabetic cardiomyopathy, causes and effects. Rev Endocr Metab Disord. 2010 Mar; 11(1):31-9.

40. Boudina S, Abel ED. Mitochondrial uncoupling: a key contributor to reduced cardiac efficiency in diabetes. Physiology (Bethesda). 2006 Aug; 21:250-8.

41. Bouzakri K, Roques M, Gual P, Espinosa S, Guebre-Egziabher F, Riou JP, Laville M, Le Marchand-Brustel Y, Tanti JF, Vidal H. Reduced activation of phosphatidylinositol-3 kinase and increased serine 636 phosphorylation of insulin receptor substrate-1 in primary culture of skeletal muscle cells from patients with type 2 diabetes. Diabetes. 2003 Jun; 52(6):1319-25.

42. Bradford MM. A rapid and sensitive method for the quantitation of microgram quantities of protein utilizing the principle of protein-dye binding. Anal Biochem. 1976 May 7; 72:248-54.

43. Brady MJ, Bourbonais FJ, Saltiel AR. The activation of glycogen synthase by insulin switches from kinase inhibition to phosphatase activation during adipogenesis in 3T3-L1 cells. J Biol Chem. 1998 Jun 5; 273(23):14063-6.

44. Brandl CJ, deLeon S, Martin DR, MacLennan DH. Adult forms of the Ca2+ATPase of sarcoplasmic reticulum. Expression in developing skeletal muscle. J Biol Chem. 1987 Mar 15; 262(8):3768-74.

45. Bray GA and Bouchard C. Handbook of obesity, Etiology and Pathophysiology. Dekker, Marcel Incorporated. 2004; 2: 1072-

46. Brette F, Orchard C. T-tubule function in mammalian cardiac myocytes. Circ Res. 2003 Jun 13; 92(11):1182-92.

47. Brown A. M., Lee K. S. and Powell T. Sodium current in single rat heart muscle cells. J. Physiol. 1981; 318: 479–500.

48. Buck CA, Horwitz AF. Cell surface receptors for extracellular matrix molecules. Annu Rev Cell Biol. 1987; 3:179-205.

49. Buja G, Estes NA 3rd, Wichter T, Corrado D, Marcus F, Thiene G. Arrhythmogenic right ventricular cardiomyopathy/dysplasia: risk stratification and therapy. Prog Cardiovasc Dis. 2008 Jan-Feb; 50(4):282-93.

50. Cai L, Kang YJ. Oxidative stress and diabetic cardiomyopathy: a brief review. Cardiovasc Toxicol. 2001; 1(3):181-93.

51. Carmeliet E. Intracellular $Ca^{(2+)}$ concentration and rate adaptation of the cardiac action potential. Cell Calcium. 2004 Jun; 35(6):557-73.

52. Cesario DA, Brar R, Shivkumar K. Alterations in ion channel physiology in diabetic cardiomyopathy. Endocrinol Metab Clin North Am. 2006 Sep; 35(3):601-10.

53. Cheatham B, Kahn CR. Insulin action and the insulin signaling network. Endocr Rev. 1995 Apr; 16(2):117-42.

54. Cheatham, B., C. J. Vlahos, L. Cheatham, L. Wang, J. Blenis, and C. R. Kahn. Phosphatidylinositol 3-kinase activation is required for insulin stimulation of pp70 S6 kinase, DNA synthesis, and glucose transporter translocation. Mol. Cell. Biol. 1994; 14:4902–4911.

55. Cherrington, A. D. Diabetes 1999, 48, 1198-1214.

56. Chess DJ, Stanley WC. Role of diet and fuel overabundance in the development and progression of heart failure. Cardiovasc Res. 2008 Jul 15; 79(2):269-78.

57. Chou KC. Molecular therapeutic target for type-2 diabetes. J Proteome Res. 2004 Nov-Dec; 3(6):1284-8.

58. Ciaraldi TP, Carter L, Mudaliar S, Henry RR. GSK-3beta and control of glucose metabolism and insulin action in human skeletal muscle. Mol Cell Endocrinol. 2010 Feb 5; 315(1-2):153-8.

59. Ciaraldi TP, Nikoulina SE, Bandukwala RA, Carter L, Henry RR. Role of glycogen synthase kinase-3 alpha in insulin action in cultured human skeletal muscle cells. Endocrinology. 2007 Sep; 148(9):4393-9.

60. Clara Bouchea,b,1,2, Ximena Lopeza,b,c,2,3, Amy Fleischmana,b,d, Aaron M. Cypessa,b, Sheila O'Sheaa, Darko Stefanovskie, Richard N. Bergmane, Eduard Rogatskyf, Daniel T. Steinf, C. Ronald Kahna,b,4, Rohit N. Kulkarnia,b, and Allison B. Goldfine. Insulin enhances glucose-stimulated insulin secretion in healthy humans| PNAS | March 9, 2010 |vol. 107 no. 10. 4770–4775

61. Clarke, J. F., P. W. Young, K. Yonezawa, M. Kasuga, and G. D. Holman. Inhibition of the translocation of GLUT1 and GLUT4 in 3T3-L1 cells by the phosphatidylinositol 3-kinase inhibitor, wortmannin. Biochem. J. 1994; 300: 631–635

62. Clement O. Bewaji[1] and Enitan A. Bababunmi. Jasmonates: Regulation of Ca^{2+}-ATPase and role in calcium homeostasis. Int. J. Biomed. & Hlth. Sci. 2008; 4: 4

63. Cline GW, Johnson K, Regittnig W, Perret P, Tozzo E, Xiao L, Damico C, Shulman GI. Effects of a novel glycogen synthase kinase-3 inhibitor on

insulin-stimulated glucose metabolism in Zucker diabetic fatty (fa/fa) rats. Diabetes. 2002 Oct; 51(10):2903-10.

64. Cline GW, Rothman DL, Magnusson I, Katz LD, Shulman GI. 13C-nuclear magnetic resonance spectroscopy studies of hepatic glucose metabolism in normal subjects and subjects with insulin-dependent diabetes mellitus. J Clin Invest. 1994 Dec; 94(6):2369-76.

65. Coffer PJ, Jin J, Woodgett JR. Protein kinase B (c-Akt): a multifunctional mediator of phosphatidylinositol 3-kinase activation. Biochem J. 1998 Oct 1; 335 (Pt 1):1-13.

66. Coghlan MP, Culbert AA, Cross DA, Corcoran SL, Yates JW, Pearce NJ, Rausch OL, Murphy GJ, Carter PS, Roxbee Cox L, Mills D, Brown MJ, Haigh D, Ward RW, Smith DG, Murray KJ, Reith AD, Holder JC. Selective small molecule inhibitors of glycogen synthase kinase-3 modulate glycogen metabolism and gene transcription. Chem Biol. 2000 Oct; 7(10):793-803.

67. Cohen P, Goedert M. GSK3 inhibitors: development and therapeutic potential. Nat Rev Drug Discov. 2004 Jun; 3(6):479-87.

68. Coraboeuf E. Some considerations about the cardiac action potential plateau. J Electrocardiol. 1969; 2(2):91-4.

69. Cosson S, Kevorkian JP. Left ventricular diastolic dysfunction: an early sign of diabetic cardiomyopathy? Diabetes Metab. 2003 Nov; 29(5):455-66.

70. Craig R, Lehman W. Crossbridge and tropomyosin positions observed in native, interacting thick and thin filaments. J Mol Biol. 2001 Aug 31; 311(5):1027-36.

71. Cross DA, Watt PW, Shaw M, van der Kaay J, Downes CP, Holder JC, Cohen P. Insulin activates protein kinase B, inhibits glycogen synthase

kinase-3 and activates glycogen synthase by rapamycin-insensitive pathways in skeletal muscle and adipose tissue. FEBS Lett. 1997 Apr 7; 406(1-2):211-5.

72. Dajani R, Fraser E, Roe SM, Young N, Good V, Dale TC, Pearl LH. Crystal structure of glycogen synthase kinase 3 beta: structural basis for phosphate-primed substrate specificity and autoinhibition. Cell. 2001 Jun 15; 105(6):721-32.

73. Dally S, Bredoux R, Corvazier E, Andersen JP, Clausen JD, Dode L, Fanchaouy M, Gelebart P, Monceau V, Del Monte F, Gwathmey JK, Hajjar R, Chaabane C, Bobe R, Raies A, Enouf J. Ca2+-ATPases in non-failing and failing heart: evidence for a novel cardiac sarco/endoplasmic reticulum Ca2+-ATPase 2 isoform (SERCA2c). Biochem J. 2006 Apr 15; 395(2):249-58.

74. Davis JP, Norman C, Kobayashi T, Solaro RJ, Swartz DR, Tikunova SB. Effects of thin and thick filament proteins on calcium binding and exchange with cardiac troponin C. Biophys J. 2007 May 1;92(9):3195-206.

75. De Meyts P, Whittaker J. Structural biology of insulin and IGF1 receptors: implications for drug design, Nat. Rev. Drug. Discov. 1 (2002) 769–783.

76. DeFronzo, R. A. and Ferrannini, E., Regulation of intermediary metabolism during fasting and feeding, In DeGroot, L.J. and Jameson, J.L. (Eds.). Endocrinology. W.B. Saunders Co., 368 Y. H. Lee and M. F. White Philadelphia. 2001; pp. 737-755.

77. Diehl JA, Cheng M, Roussel MF, Sherr CJ. Glycogen synthase kinase-3beta regulates cyclin D1 proteolysis and subcellular localization. Genes Dev. 1998 Nov 15; 12(22):3499-511.

78. Doble BW, Woodgett JR. GSK-3: tricks of the trade for a multi-tasking kinase. J Cell Sci. 2003 Apr 1; 116(Pt 7):1175-86.

79. Dode L, Vilsen B, Van Baelen K, Wuytack F, Clausen JD, Andersen JP. Dissection of the functional differences between sarco(endo)plasmic reticulum Ca2+-ATPase (SERCA) 1 and 3 isoforms by steady-state and transient kinetic analyses. J Biol Chem. 2002 Nov 22; 277(47):45579-91.

80. Doenst T, Bugger H, Schwarzer M, Faerber G, Borger MA, Mohr FW. Three good reasons for heart surgeons to understand cardiac metabolism. Eur J Cardiothorac Surg. 2008 May; 33(5):862-71.

81. Dong LQ, Liu F. PDK2: the missing piece in the receptor tyrosine kinase signaling pathway puzzle. Am J Physiol Endocrinol Metab. 2005 Aug; 289(2):E187-96.

82. du Toit EF, Smith W, Muller C, Strijdom H, Stouthammer B, Woodiwiss AJ, Norton GR, Lochner A. Myocardial susceptibility to ischemic-reperfusion injury in a prediabetic model of dietary-induced obesity. Am J Physiol Heart Circ Physiol. 2008 May;294(5):H2336-43.

83. Dutta K, Carmody MW, Cala SE, Davidoff AJ. Depressed PKA activity contributes to impaired SERCA function and is linked to the pathogenesis of glucose-induced cardiomyopathy. J Mol Cell Cardiol. 2002 Aug; 34(8):985-96.

84. Eckel RH, Grundy SM, Zimmet PZ. The metabolic syndrome. Lancet. 2005 Apr 16-22; 365(9468):1415-28.

85. Eldar-Finkelman H, Argast GM, Foord O, Fischer EH, Krebs EG. Expression and characterization of glycogen synthase kinase-3 mutants and their effect on glycogen synthase activity in intact cells. Proc Natl Acad Sci U S A. 1996 Sep 17; 93(19):10228-33.

86. Eldar-Finkelman H, Krebs EG. Phosphorylation of insulin receptor substrate 1 by glycogen synthase kinase 3 impairs insulin action. Proc Natl Acad Sci U S A. 1997 Sep 2; 94(18):9660-4.

87. Eldar-Finkelman H, Licht-Murava A, Pietrokovski S, Eisenstein M. Substrate competitive GSK-3 inhibitors - strategy and implications. Biochim Biophys Acta. 2010 Mar; 1804(3):598-603.

88. Eldar-Finkelman H. Glycogen synthase kinase 3: an emerging therapeutic target. Trends Mol Med. 2002 Mar; 8(3):126-32.

89. Elliott P, Andersson B, Arbustini E, Bilinska Z, Cecchi F, Charron P, Dubourg O, Kühl U, Maisch B, McKenna WJ, Monserrat L, Pankuweit S, Rapezzi C, Seferovic P, Tavazzi L, Keren A. Classification of the cardiomyopathies: a position statement from the European Society Of Cardiology Working Group on Myocardial and Pericardial Diseases. Eur Heart J. 2008 Jan; 29(2):270-6.

90. Embi N, Rylatt DB, Cohen P. Glycogen synthase kinase-3 from rabbit skeletal muscle. Separation from cyclic-AMP-dependent protein kinase and phosphorylase kinase. Eur J Biochem. 1980 Jun; 107(2):519-27.

91. Endemann G, Yonezawa K, Roth RA. Phosphatidylinositol kinase or an associated protein is a substrate for the insulin receptor tyrosine kinase. J Biol Chem. 1990 Jan 5; 265(1):396-400.

92. Faber GM, Rudy Y. Action potential and contractility changes in [Na$^+$](i) overloaded cardiac myocytes: a simulation study. Biophys J. 2000 May; 78(5):2392-404.

93. Fabiato A. Simulated calcium current can both cause calcium loading in and trigger calcium release from the sarcoplasmic reticulum of a skinned canine cardiac Purkinje cell. J Gen Physiol. 1985 Feb; 85(2):291-320.

94. Faissner A, Heck N, Dobbertin A, Garwood J. DSD-1-Proteoglycan/Phosphacan and receptor protein tyrosine phosphatase-beta isoforms during development and regeneration of neural tissues. Adv Exp Med Biol. 2006; 557:25-53.

95. Fang ZY, Yuda S, Anderson V, Short L, Case C, Marwick TH. Echocardiographic detection of early diabetic myocardial disease. J Am Coll Cardiol. 2003 Feb 19; 41(4):611-7.

96. Fatkin D, Otway R, Richmond Z. Genetics of dilated cardiomyopathy. Heart Fail Clin. 2010 Apr; 6(2):129-40.

97. Feher JJ, Davis MD. Isolation of rat cardiac sarcoplasmic reticulum with improved Ca2+ uptake and ryanodine binding. J Mol Cell Cardiol. 1991 Mar; 23(3):249-58.

98. Fiol CJ, Wang A, Roeske RW, Roach PJ. Ordered multisite protein phosphorylation. Analysis of glycogen synthase kinase 3 action using model peptide substrates. J Biol Chem. 1990 Apr 15; 265(11):6061-5.

99. Fiske CH and Subbarow Y. The colorimetric determination of phosphorus. J. Biol. Chem. 66 (1925), pp. 375–400.

100. Fonarow GC, Srikanthan P. Diabetic cardiomyopathy. Endocrinol Metab Clin North Am. 2006 Sep; 35(3):575-99

101. Forde JE, Dale TC. Glycogen synthase kinase 3: a key regulator of cellular fate. Cell Mol Life Sci. 2007 Aug; 64(15):1930-44.

102. Franca-Koh J, Yeo M, Fraser E, Young N, Dale TC. The regulation of glycogen synthase kinase-3 nuclear export by Frat/GBP. J Biol Chem. 2002 Nov 15; 277(46):43844-8.

103. Franco R, Bortner CD, Cidlowski JA. Potential roles of electrogenic ion transport and plasma membrane depolarization in apoptosis. J Membr Biol. 2006 Jan; 209(1):43-58.

104. Freychet P, Roth J, Neville Jr DM, Insulin receptors in the liver: specific binding of (125 I)insulin to the plasma membrane and its relation to insulin bioactivity, Proc. Natl. Acad. Sci. U. S. A. 68 (1971) 1833–1837.

105. Fröjdö S, Vidal H, Pirola L. Alterations of insulin signaling in type 2 diabetes: A review of the current evidence from humans, Biochimica et Biophysica Acta 1792 (2009) 83–92

106. Fruman DA, Cantley LC. Phosphoinositide 3-kinase in immunological systems. Semin Immunol. 2002 Feb; 14(1):7-18.

107. Fukuchi S, Hamaguchi K, Seike M, Himeno K, Sakata T, Yoshimatsu H. Role of fatty acid composition in the development of metabolic disorders in sucrose-induced obese rats. Exp Biol Med (Maywood). 2004 Jun; 229(6):486-93.

108. Fuster V; Hurst JW. Hurst's the heart. McGraw-Hill Professional. 2004; pp. 1884–.ISBN 9780071432252. http://books.google.com/books?id=eWQAJDrVV7gC&pg=PA1884. Accessed 11 November 2010.

109. Gao HK, Yin Z, Zhou N, Feng XY, Gao F, Wang HC. Glycogen synthase kinase 3 inhibition protects the heart from acute ischemia-reperfusion injury

via inhibition of inflammation and apoptosis. J Cardiovasc Pharmacol. 2008 Sep; 52(3):286-92.

110. Garland PB, Randle PJ. Regulation of glucose uptake by muscles. 10. Effects of alloxan-diabetes, starvation, hypophysectomy and adrenalectomy, and of fatty acids, ketone bodies and pyruvate, on the glycerol output and concentrations of free fatty acids, long-chain fatty acyl-coenzyme A, glycerol phosphate and citrate-cycle intermediates in rat heart and diaphragm muscles. Biochem J. 1964 Dec; 93(3):678-87.

111. Gary W. Cline,[1] Kirk Johnson,[2] Werner Regittnig,[1] Pascale Perret,[1] Effie Tozzo,[2] Linda Xiao,[2] Christine Damico,[2] and Gerald I. Shulman. Effects of a Novel Glycogen Synthase Kinase-3 Inhibitor on Insulin-Stimulated Glucose Metabolism in Zucker Diabetic Fatty (fa/fa) Rats. Diabetes2002; 51:2903–2910.

112. Gayan-Ramirez G, Vanzeir L, Wuytack F, Decramer M. Corticosteroids decrease mRNA levels of SERCA pumps, whereas they increase sarcolipin mRNA in the rat diaphragm. J Physiol. 2000 Apr 15; 524 Pt 2:387-97.

113. Gertz EW, Wisneski JA, Stanley WC, Neese RA. Myocardial substrate utilization during exercise in humans. Dual carbon-labeled carbohydrate isotope experiments. J Clin Invest. 1988 Dec; 82(6):2017-25.

114. Goalstone ML, Draznin B. Insulin signaling. West J Med. 1997 Sep; 167(3):166-73.

115. Golfman L, Dixon IM, Takeda N, Lukas A, Dakshinamurti K, Dhalla NS. Cardiac sarcolemmal Na^+-Ca^{2+} exchange and Na^+-K^+ ATPase activities and gene expression in alloxan-induced diabetes in rats. Mol Cell Biochem. 1998 Nov; 188(1-2):91-101.

116. Goodwin GW, Ahmad F, Doenst T, Taegtmeyer H. Energy provision from glycogen, glucose, and fatty acids on adrenergic stimulation of isolated working rat hearts. Am J Physiol. 1998 Apr; 274(4 Pt 2):H1239-47.

117. Goodwin GW, Taylor CS, Taegtmeyer H. Regulation of energy metabolism of the heart during acute increase in heart work. J Biol Chem. 1998 Nov 6; 273(45):29530-9.

118. Gordon AM, Homsher E, Regnier M. Regulation of contraction in striated muscle. Physiol Rev. 2000 Apr; 80(2):853-924.

119. Griffin MA, Sen S, Sweeney HL, Discher DE. Adhesion-contractile balance in myocyte differentiation. J Cell Sci. 2004 Nov 15; 117(Pt 24):5855-63.

120. Grimes CA, Jope RS. The multifaceted roles of glycogen synthase kinase 3β in cellular signaling. Prog Neurobiol. 2001 Nov; 65(4):391-426.

121. Grundleger ML, Thenen SW. Decreased insulin binding, glucose transport, and glucose metabolism in soleus muscle of rats fed a high fat diet. Diabetes. 1982 Mar; 31(3):232-7.

122. Grundy SM. Obesity, metabolic syndrome, and cardiovascular disease. J Clin Endocrinol Metab. 2004 Jun; 89(6):2595-600.

123. Grynberg A, Demaison L. Fatty acid oxidation in the heart. J Cardiovasc Pharmacol. 1996; 28 Suppl 1:S11-7.

124. Gual P, Le Marchand-Brustel Y, Tanti J. Positive and negative regulation of glucose uptake by hyperosmotic stress. Diabetes Metab. 2003 Dec; 29(6):566-75.

125. Gual P, Le Marchand-Brustel Y, Tanti JF. Positive and negative regulation of insulin signaling through IRS-1 phosphorylation. Biochimie. 2005 Jan; 87(1):99-109.

126. Györke S, Carnes C. Dysregulated sarcoplasmic reticulum calcium release: potential pharmacological target in cardiac disease. Pharmacol Ther. 2008 Sep; 119(3):340-54.

127. Haffner SM. The prediabetic problem: Development of non-insulindependent diabetes mellitus and related abnormalities. J Diabetes Complications. 1997; 11:69–76.

128. Hajduch E, Litherland GJ, Hundal HS. Protein kinase B (PKB/Akt)-a key regulator of glucose transport? FEBS Lett. 2001 Mar 16; 492(3):199-203.

129. Hanada M, Feng J, Hemmings BA. Structure, regulation and function of PKB/AKT--a major therapeutic target. Biochim Biophys Acta. 2004 Mar 11; 1697(1-2):3-16.

130. Hao-Kao Gao, MD, PhD,* Zhong Yin, MD, PhD,* Ning Zhou, MD, PhD,* Xu-Yang Feng, MD, PhD,* Feng Gao, MD, PhD, and Hai-Chang Wang, MD, PhD*.Glycogen Synthase Kinase 3 Inhibition Protects the Heart From Acute Ischemia-Reperfusion Injury Via Inhibition of Inflammation and Apoptosis. J Cardiovasc PharmacolTM 2008; 52:286–292.

131. Haq S, Choukroun G, Kang ZB, Ranu H, Matsui T, Rosenzweig A, Molkentin JD, Alessandrini A, Woodgett J, Hajjar R, Michael A, Force T. Glycogen synthase kinase-3beta is a negative regulator of cardiomyocyte hypertrophy. J Cell Biol. 2000 Oct 2; 151(1):117-30.

132. Hardt SE, Sadoshima J. Glycogen synthase kinase-3beta: a novel regulator of cardiac hypertrophy and development. Circ Res. 2002 May 31; 90(10):1055-63.

133. Harris DA, Das AM. Control of mitochondrial ATP synthesis in the heart. Biochem J. 1991 Dec 15; 280 (Pt 3):561-73

134. Hartigan JA, Johnson GV. Transient increases in intracellular calcium result in prolonged site-selective increases in Tau phosphorylation through a glycogen synthase kinase 3beta-dependent pathway. J Biol Chem. 1999 Jul 23; 274(30):21395-401.

135. Hasenfuss G. Alterations of calcium-regulatory proteins in heart failure. Cardiovasc Res. 1998 Feb; 37(2):279-89.

136. Hayat SA, Patel B, Khattar RS et al. Diabetic cardiomyopathy: mechanisms, diagnosis and treatment. Clinical Science2004 Dec; 107(6): 539–557.

137. Henriksen EJ, Dokken BB. Role of glycogen synthase kinase-3 in insulin resistance and type 2 diabetes. Curr Drug Targets. 2006 Nov; 7(11):1435-41.

138. Henriksen EJ, Kinnick TR, Teachey MK, O'Keefe MP, Ring D, Johnson KW, Harrison SD. Modulation of muscle insulin resistance by selective inhibition of GSK-3 in Zucker diabetic fatty rats. Am J Physiol Endocrinol Metab. 2003 May; 284(5):892-900.

139. Henriksen EJ, Teachey MK. Short-term in vitro inhibition of glycogen synthase kinase 3 potentiates insulin signaling in type I skeletal muscle of Zucker Diabetic Fatty rats. Metabolism. 2007 Jul; 56(7):931-8.

140. Henry RR, Abrams L, Nikoulina S, Ciaraldi TP. Insulin action and glucose metabolism in nondiabetic control and NIDDM subjects. Comparison using human skeletal muscle cell cultures. Diabetes. 1995 Aug; 44(8):936-46.

141. Hicks R. Combating childhood obesity. Health. 2006

142. Hill JO, Peters JC: Environmental contributions to the obesity epidemic. Science 1998, 280:1371-1374.

143. Hinoi T, Yamamoto H, Kishida M, Takada S, Kishida S, Kikuchi A. Complex formation of adenomatous polyposis coli gene product and axin facilitates

glycogen synthase kinase-3 beta-dependent phosphorylation of beta-catenin and down-regulates beta-catenin. J Biol Chem. 2000 Nov 3; 275(44):34399-406.

144. Hirotani S, Zhai P, Tomita H, Galeotti J, Marquez JP, Gao S, Hong C, Yatani A, Avila J, Sadoshima J. Inhibition of glycogen synthase kinase 3beta during heart failure is protective. Circ Res. 2007 Nov 26; 101(11):1164-74.

145. Hoeflich KP, Luo J, Rubie EA, Tsao MS, Jin O, Woodgett JR. Requirement for glycogen synthase kinase-3beta in cell survival and NF-kappaB activation. Nature. 2000 Jul 6; 406(6791):86-90.

146. Holt E, Sjaastad I, Lunde PK, Christensen G, Sejersted OM. Thyroid hormone control of contraction and the Ca^{2+}-ATPase/phospholamban complex in adult rat ventricular myocytes. J Mol Cell Cardiol. 1999 Mar; 31(3):645-56.

147. Hooper PL. Insulin Signaling, GSK-3, Heat Shock Proteins and the Natural History of Type 2 Diabetes Mellitus: A Hypothesis. Metab Syndr Relat Disord. 2007 Sep;5(3):220-30

148. Hooper SL, Hobbs KH, Thuma JB. Invertebrate muscles: thin and thick filament structure; molecular basis of contraction and its regulation, catch and asynchronous muscle. Prog Neurobiol. 2008 Oct; 86(2):72-127.

149. Hryshko LV, Philipson KD. Sodium-calcium exchange: recent advances. Basic Res Cardiol. 1997; 92 Suppl 1:45-51.

150. Hsueh WA, Law RE, Do YS. Integrins, adhesion, and cardiac remodeling. Hypertension. 1998 Jan; 31(1 Pt 2):176-80.

151. Huisamen B, Lochner A. GSK-3 protein and the heart: friend or foe? SAHeart 2010; 7:48-57

152. Hulot JS, Jouven X, Empana JP, Frank R, Fontaine G. Natural history and risk stratification of arrhythmogenic right ventricular dysplasia/cardiomyopathy. Circulation. 2004 Oct 5; 110(14):1879-84.

153. Hunt SA, Abraham WT, Chin MH, Feldman AM, Francis GS, Ganiats TG, Jessup M, Konstam MA, Mancini DM, Michl K, Oates JA, Rahko PS, Silver MA, Stevenson LW, Yancy CW, Antman EM, Smith SC Jr, Adams CD, Anderson JL, Faxon DP, Fuster V, Halperin JL, Hiratzka LF, Jacobs AK, Nishimura R, Ornato JP, Page RL, Riegel B; American College of Cardiology; American Heart Association Task Force on Practice Guidelines; American College of Chest Physicians; International Society for Heart and Lung Transplantation; Heart Rhythm Society. ACC/AHA 2005 Guideline Update for the Diagnosis and Management of Chronic Heart Failure in the Adult: a report of the American College of Cardiology/American Heart Association Task Force on Practice Guidelines (Writing Committee to Update the 2001 Guidelines for the Evaluation and Management of Heart Failure): developed in collaboration with the American College of Chest Physicians and the International Society for Heart and Lung Transplantation: endorsed by the Heart Rhythm Society. Circulation. 2005 Sep 20; 112(12):e154-235.

154. Hunter SJ, Garvey WT. Insulin action and insulin resistance: Diseases involving defects in insulin receptors, signal transduction, and the gluco [35] transport effector system. Am J Med 1998; 105:331–345,

155. Hypertrophic Cardiomyopathy Association, P.O. Box 306 Hibernia NJ 07842. Telephone: 2009; (973) 983-7429; http://www.4hcm.org/. Accessed: 06/2010

156. Hypertrophic Cardiomyopathy Association. Genetics and HCM. 2009; http://www.4hcm.org/hcm/genetics/3061.html. Accessed: 06/2010.

157. Inesi G, Hua S, Xu C, Ma H, Seth M, Prasad AM, Sumbilla C. Studies of Ca^{2+} ATPase (SERCA) inhibition. J Bioenerg Biomembr. 2005 Dec; 37(6):365-8.

158. Jackson RT, Rashed M, Saad-Eldin R. Rural–urban differences in weight, body image, and dieting behavior among adolescent Egyptian schoolgirls. International journal of food sciences and nutrition, 2003, 54(1):1–11.

159. James P, Inui M, Tada M, Chiesi M, Carafoli E. Nature and site of phospholamban regulation of the Ca2+ pump of sarcoplasmic reticulum. Nature. 1989 Nov 2; 342(6245):90-2.

160. Juhaszova M, Zorov DB, Kim SH, Pepe S, Fu Q, Fishbein KW, Ziman BD, Wang S, Ytrehus K, Antos CL, Olson EN, Sollott SJ. Glycogen synthase kinase-3beta mediates convergence of protection signaling to inhibit the mitochondrial permeability transition pore. J Clin Invest. 2004 Jun; 113(11):1535-49.

161. Junqueira, L. C., J. Carneiro,a nd J. A. Long. 1992. Basic Histology.7 th ed. LangeM edicalP ublications, Los Altos. 66-131

162. Kabuta T, Take K, Kabuta C, Hakuno F, Takahashi S. Differential subcellular localization of insulin receptor substrates depends on C-terminal regions and importin beta. Biochem Biophys Res Commun. 2008 Dec 19; 377(3):741-6.

163. Kadambi VJ, Kranias EG. Phospholamban: a protein coming of age. Biochem Biophys Res Commun. 1997 Oct 9; 239(1):1-5.

164. Kahn CR, White MF. The insulin receptor and the molecular mechanism of insulin action. J Clin Invest. 1988 Oct; 82(4):1151-6.

165. Kamgang R, Mboumi RY, N'dillé GP, Yonkeu JN. Cameroon local diet-induced glucose intolerance and dyslipidemia in adult Wistar rat. Diabetes Res Clin Pract. 2005 Sep; 69(3):224-30.

166. Kamisago M, Sharma SD, DePalma SR, Solomon S, Sharma P, McDonough B, Smoot L, Mullen MP, Woolf PK, Wigle ED, Seidman JG, Seidman CE. Mutations in sarcomere protein genes as a cause of dilated cardiomyopathy. N Engl J Med. 2000 Dec 7; 343(23):1688-96.

167. Kandel ES, Skeen J, Majewski N, Di Cristofano A, Pandolfi PP, Feliciano CS, Gartel A, Hay N. Activation of Akt/protein kinase B overcomes a G(2)/m cell cycle checkpoint induced by DNA damage. Mol Cell Biol. 2002 Nov; 22(22):7831-41.

168. Karnik AA, Fields AV, Shannon RP. Diabetic cardiomyopathy. Curr Hypertens Rep. 2007 Dec; 9(6):467-73.

169. Kaski JP, Elliott P. The classification concept of the ESC Working Group on myocardial and pericardial diseases for dilated cardiomyopathy. Herz. 2007; 32(6):446–451.

170. Kaski JP, Elliott P; ESC Working Group. The classification concept of the ESC Working Group on myocardial and pericardial diseases for dilated cardiomyopathy. Herz. 2007 Sep; 32(6):446-51.

171. Kasper, Denis L. et al. Harrison's Principles of Internal Medicine, 16th edn. McGraw-Hill 2005. ISBN 0-07-139140-1. http://en.wikipedikia.org/wiki/Cardiomyopathy acessed: 11/2010

172. Kass RS. The channelopathies: novel insights into molecular and genetic mechanisms of human disease. J Clin Invest. 2005 Aug; 115(8):1986-9.

173. Katz AM. Molecular basis of calcium channel blockade. Am J Cardiol. 1992 Apr 30; 69(13):17E-22E.

174. Katz EB, Steinhelper ME, Delcarpio JB, Daud AI, Claycomb WC, Field LJ. Cardiomyocyte proliferation in mice expressing alpha-cardiac myosin heavy chain-SV40 T-antigen transgenes. Am J Physiol. 1992 Jun; 262(6 Pt 2):H1867-76.

175. Kelekar A, Chang BS, Harlan JE, Fesik SW, Thompson CB. Bad is a BH3 domain-containing protein that forms an inactivating dimer with Bcl-XL. Mol Cell Biol. 1997 Dec; 17(12):7040-6.

176. Kelly B, Chapman K, King L, Hardy L, Farrell L. Double standards for community sports: promoting active lifestyles but unhealthy diets. Health Promot J Austr. 2008a Dec; 19(3):226-8.

177. Kelly T, Yang W, Chen CS, Reynolds K, He J. Global burden of obesity in 2005 and projections to 2030. Int J Obes (Lond). 2008b Sep; 32(9):1431-7.

178. Kerouz NJ, Hörsch D, Pons S, Kahn CR. Differential regulation of insulin receptor substrates-1 and -2 (IRS-1 and IRS-2) and phosphatidylinositol 3-kinase isoforms in liver and muscle of the obese diabetic (ob/ob) mouse. J Clin Invest. 1997 Dec 15; 100(12):3164-72.

179. Kim YB, Nikoulina SE, Ciaraldi TP, Henry RR, Kahn BB. Normal insulin-dependent activation of Akt/protein kinase B, with diminished activation of phosphoinositide 3-kinase, in muscle in type 2 diabetes. J Clin Invest. 1999 Sep; 104(6):733-41.

180. Kimura Y, Asahi M, Kurzydlowski K, Tada M, MacLennan DH. Phospholamban domain Ib mutations influence functional interactions with the Ca2+-ATPase isoform of cardiac sarcoplasmic reticulum. J Biol Chem. 1998 Jun 5; 273(23):14238-41.

181. Kimura Y, Kurzydlowski K, Tada M, MacLennan DH. Phospholamban regulates the Ca2+-ATPase through intramembrane interactions. J Biol Chem. 1996 Sep 6; 271(36):21726-31.

182. Klabunde RE. Non-pacemaker potentials: Cardiovascular Physiology concepts. 1998-2010. http://www.cvphysiology.com/Arrhythmias/A006.htm, accessed: 09/2010.

183. Klein PS, Melton DA. A molecular mechanism for the effect of lithium on development. Proc Natl Acad Sci U S A. 1996 Aug 6; 93(16):8455-9.

184. Kosti RI, Panagiotakos DB. The epidemic of obesity in children and adolescents in the world. Cent Eur J Public Health. 2006 Dec; 14(4):151-9.

185. Krook A, Kawano Y, Song XM, Efendić S, Roth RA, Wallberg-Henriksson H, Zierath JR. Improved glucose tolerance restores insulin-stimulated Akt kinase activity and glucose transport in skeletal muscle from diabetic Goto-Kakizaki rats. Diabetes. 1997 Dec; 46(12):2110-4.

186. Kumar AS, Naruszewicz I, Wang P, Leung-Hagesteijn C, Hannigan GE. ILKAP regulates ILK signaling and inhibits anchorage-independent growth. Oncogene. 2004 Apr 22; 23(19):3454-61.

187. Kumar R, Singh VP, Baker KM. Kinase inhibitors for cardiovascular disease. J Mol Cell Cardiol. 2007 Jan; 42(1):1-11.

188. Laviola L, Belsanti G, Davalli AM, Napoli R, Perrini S, Weir GC, Giorgino R, Giorgino F. Effects of streptozocin diabetes and diabetes treatment by islet

transplantation on in vivo insulin signaling in rat heart. Diabetes. 2001 Dec; 50(12):2709-20.

189. Lawrence JC Jr, Roach PJ. New insights into the role and mechanism of glycogen synthase activation by insulin. Diabetes. 1997 Apr; 46(4):541-7.

190. Lehman W, Galińska-Rakoczy A, Hatch V, Tobacman LS, Craig R. Structural basis for the activation of muscle contraction by troponin and tropomyosin. J Mol Biol. 2009 May 15; 388(4):673-81.

191. Lehnart SE, Schillinger W, Pieske B, Prestle J, Just H, Hasenfuss G. Sarcoplasmic reticulum proteins in heart failure. Ann N Y Acad Sci. 1998 Sep 16; 853:220-30.

192. Leost M, Schultz C, Link A, Wu YZ, Biernat J, Mandelkow EM, Bibb JA, Snyder GL, Greengard P, Zaharevitz DW, Gussio R, Senderowicz AM, Sausville EA, Kunick C, Meijer L. Paullones are potent inhibitors of glycogen synthase kinase-3beta and cyclin-dependent kinase 5/p25. Eur J Biochem. 2000 Oct; 267(19):5983-94

193. Liberman Z, Eldar-Finkelman H. Serine 332 phosphorylation of insulin receptor substrate-1 by glycogen synthase kinase-3 attenuates insulin signaling. J Biol. Chem. 2005 Feb 11; 280(6):4422-8.

194. Lomedico P, Rosenthal N, Efstratidadis A, Gilbert W, Kolodner R, Tizard R. The structure and evolution of the two nonallelic rat preproinsulin genes. Cell. 1979 Oct; 18(2):545-58.

195. Lopaschuk GD, Folmes CD, Stanley WC. Cardiac energy metabolism in obesity. Circ Res. 2007 Aug 17; 101(4):335-47.

196. Luo W, Chu G, Sato Y, Zhou Z, Kadambi VJ, Kranias EG. Transgenic approaches to define the functional role of dual site phospholamban phosphorylation. J Biol Chem. 1998 Feb 20; 273(8):4734-9.

197. Lytton J, Westlin M, Burk SE, Shull GE, MacLennan DH. Functional comparisons between isoforms of the sarcoplasmic or endoplasmic reticulum family of calcium pumps. J Biol Chem. 1992 Jul 15; 267(20):14483-9.

198. Ma K, Cheung SM, Marshall AJ, Duronio V. PI(3,4,5)P3 and PI(3,4)P2 levels correlate with PKB/akt phosphorylation at Thr308 and Ser473, respectively; PI(3,4)P2 levels determine PKB activity. Cell Signal. 2008 Apr; 20(4):684-94.

199. Maack C, O'Rourke B. Excitation-contraction coupling and mitochondrial energetics. Basic Res Cardiol. 2007 Sep; 102(5):369-92.

200. MacAulay K, Blair AS, Hajduch E, Terashima T, Baba O, Sutherland C, Hundal HS. Constitutive activation of GSK3 down-regulates glycogen synthase abundance and glycogen deposition in rat skeletal muscle cells. J Biol Chem. 2005 Mar 11; 280(10):9509-18.

201. MacLennan DH, Brandl CJ, Korczak B, Green NM. Amino-acid sequence of a Ca^{2+} Mg^{2+}-dependent ATPase from rabbit muscle sarcoplasmic reticulum, deduced from its complementary DNA sequence. Nature. 1985 Aug 22-28; 316(6030):696-700.

202. MacLennan DH, Kimura Y, Toyofuku T. Sites of regulatory interaction between calcium ATPases and phospholamban. Ann N Y Acad Sci. 1998 Sep 16; 853:31-42.

203. MacLennan DH, Rice WJ, Green NM. The mechanism of Ca^{2+} transport by sarco(endo)plasmic reticulum Ca^{2+}-ATPases. J Biol Chem. 1997 Nov 14; 272(46):28815-8.

204. Manning BD, Cantley LC. AKT/PKB signaling: navigating downstream. Cell. 2007 Jun 29; 129(7):1261-74.

205. Markou T, Cullingford TE, Giraldo A, Weiss SC, Alsafi A, Fuller SJ, Clerk A, Sugden PH. Glycogen synthase kinases 3alpha and 3beta in cardiac myocytes: regulation and consequences of their inhibition. Cell Signal. 2008 Jan; 20(1):206-18.

206. Maron BJ, McKenna WJ, Danielson GK, Kappenberger LJ, Kuhn HJ, Seidman CE, Shah PM, Spencer WH 3rd, Spirito P, Ten Cate FJ, Wigle ED; Task Force on Clinical Expert Consensus Documents. American College of Cardiology; Committee for Practice Guidelines. European Society of Cardiology. American College of Cardiology/European Society of Cardiology clinical expert consensus document on hypertrophic cardiomyopathy. A report of the American College of Cardiology Foundation Task Force on Clinical Expert Consensus Documents and the European Society of Cardiology Committee for Practice Guidelines. J Am Coll Cardiol. 2003 Nov 5; 42(9):1687-713.

207. Maron BJ, Towbin JA, Thiene G, Antzelevitch C, Corrado D, Arnett D, Moss AJ, Seidman CE, Young JB; American Heart Association; Council on Clinical Cardiology, Heart Failure and Transplantation Committee; Quality of Care and Outcomes Research and Functional Genomics and Translational Biology Interdisciplinary Working Groups; Council on Epidemiology and Prevention. Contemporary definitions and classification of the cardiomyopathies: an

American Heart Association Scientific Statement from the Council on Clinical Cardiology, Heart Failure and Transplantation Committee; Quality of Care and Outcomes Research and Functional Genomics and Translational Biology Interdisciplinary Working Groups; and Council on Epidemiology and Prevention. Circulation. 2006 Apr 11; 113(14):1807-16.

208. Maron, BJ, and Salberg, L. Hypertrophic Cardiomyopathy: For Patients, Their Families, and Interested Physicians. Malden, MA: Futura Media Services, 2001. Accessed 10/2010

209. Martin GR, Timpl R. Laminin and other basement membrane components. Annu Rev Cell Biol. 1987; 3:57-85.

210. Martinez A. Preclinical efficacy on GSK-3 inhibitors: towards a future generation of powerful drugs. Med Res Rev. 2008 Sep; 28(5):773-96.

211. Matsumoto F, Makino K, Maeda K, Patzelt H, Maéda Y, Fujiwara S. Conformational changes of troponin C within the thin filaments detected by neutron scattering. J Mol Biol. 2004 Sep 24; 342(4):1209-21.

212. Mazzanti L, Rabini RA, Faloia E, Fumelli P, Bertoli E, De Pirro R. Altered cellular Ca^{2+} and Na^+ transport in diabetes mellitus. Diabetes. 1990Jul; 39(7):850-4.

213. Mazzanti M, DeFelice LJ. Ca channel gating during cardiac action potentials. Biophys J. 1990 Oct; 58(4):1059-65.

214. Medeiros-Neto, G., Halpern, A. and Bouchard, C. Progress in Obesity Research: 9, John Libbey Eurotext, Esher. 2003

215. Meijer L, Flajolet M, Greengard P. Pharmacological inhibitors of glycogen synthase kinase 3. Trends Pharmacol Sci. 2004 Sep; 25(9):471-80.

216. Meijer L, Skaltsounis AL, Magiatis P, Polychronopoulos P, Knockaert M, Leost M, Ryan XP, Vonica CA, Brivanlou A, Dajani R, Crovace C, Tarricone C, Musacchio A, Roe SM, Pearl L, Greengard P. GSK-3-selective inhibitors derived from Tyrian purple indirubins. Chem Biol. 2003 Dec; 10(12):1255-66.

217. Meyer M, Schillinger W, Pieske B, Holubarsch C, Heilmann C, Posival H, Kuwajima G, Mikoshiba K, Just H, Hasenfuss G, et al. Alterations of sarcoplasmic reticulum proteins in failing human dilated cardiomyopathy. Circulation. 1995 Aug 15; 92(4):778-84.

218. Michael A, Haq S, Chen X, Hsich E, Cui L, Walters B, Shao Z, Bhattacharya K, Kilter H, Huggins G, Andreucci M, Periasamy M, Solomon RN, Liao R, Patten R, Molkentin JD, Force T. Glycogen synthase kinase-3beta regulates growth, calcium homeostasis, and diastolic function in the heart. J Biol Chem. 2004 May 14; 279(20):21383-93.

219. Millipore. RAT/MOUSE GROWTH HORMONE ELISA KIT 96-Well Plate (Cat. #EZRMGH-45K). 2008

220. Minamisawa S, Hoshijima M, Chu G, Ward CA, Frank K, Gu Y, Martone ME, Wang Y, Ross J Jr, Kranias EG, Giles WR, Chien KR. Chronic phospholamban-sarcoplasmic reticulum calcium ATPase interaction is the critical calcium cycling defect in dilated cardiomyopathy. Cell. 1999 Oct 29; 99(3):313-22.

221. Miron IM. Functional consequences of complete gsk-3 ablation in mouse embryonic fibroblasts. A thesis submitted in conformity with the requirements for the degree of Master of Science, Graduate Department of Medical Biophysics in the University of Toronto. 2008.

222. Mlinar B, Marc J, Janez A, Pfeifer M. Molecular mechanisms of insulin resistance and associated diseases. Clin Chim Acta. 2007 Jan; 375(1-2):20-35.

223. Mootha VK, Arai AE, Balaban RS. Maximum oxidative phosphorylation capacity of the mammalian heart. Am J Physiol. 1997; 272:H769–775.

224. Morisco C, Seta K, Hardt SE, Lee Y, Vatner SF, Sadoshima J. Glycogen synthase kinase 3beta regulates GATA4 in cardiac myocytes. J Biol Chem. 2001 Jul 27; 276(30):28586-97.

225. Moule SK, Welsh GI, Edgell NJ, Foulstone EJ, Proud CG, Denton RM. Regulation of protein kinase B and glycogen synthase kinase-3 by insulin and beta-adrenergic agonists in rat epididymal fat cells. Activation of protein kinase B by wortmannin-sensitive and -insensitive mechanisms. J Biol Chem. 1997 Mar 21; 272(12):7713-9.

226. Mukherjee R, Spinale FG. L-type calcium channel abundance and function with cardiac hypertrophy and failure: a review. J Mol Cell Cardiol. 1998 Oct; 30(10):1899-916.

227. Muller A, van der Linden GC, Zuidwijk MJ, Simonides WS, van der Laarse WJ, van Hardeveld C. Differential effects of thyroid hormone on the expression of sarcoplasmic reticulum $Ca^{(2+)}$-ATPase isoforms in rat skeletal muscle fibers. Biochem Biophys Res Commun. 1994 Sep 15; 203(2):1035-42.

228. Münch G, Bölck B, Brixius K, Reuter H, Mehlhorn U, Bloch W, Schwinger RH. SERCA2a activity correlates with the force-frequency relationship in human myocardium. Am J Physiol Heart Circ Physiol. 2000 Jun; 278(6):H1924-32.

229. Murphy E, Steenbergen C. Does inhibition of glycogen synthase kinase protect in mice? Circ Res. 2008 Aug 1; 103(3):226-8.

230. Murphy E, Steenbergen C. Inhibition of GSK-3beta as a target for cardioprotection: the importance of timing, location, duration and degree of inhibition. Expert Opin Ther Targets. 2005 Jun; 9(3):447-56.

231. Myers MG Jr, Sun XJ, White MF. The IRS-1 signaling system. Trends Biochem Sci. 1994 Jul; 19(7):289-93.

232. Myers MG Jr, White MF. New frontiers in insulin receptor substrate signaling. Trends Endocrinol Metab. 1995 Aug; 6(6):209-15.

233. Nagai R, Zarain-Herzberg A, Brandl CJ, Fujii J, Tada M, MacLennan DH, Alpert NR, Periasamy M. Regulation of myocardial Ca^{2+}-ATPase and phospholamban mRNA expression in response to pressure overload and thyroid hormone. Proc Natl Acad Sci U S A. 1989 Apr; 86(8):2966-70.

234. Nánási PP, Varró A, Lathrop DA. Action-potential duration and contractility in canine cardiac tissues: action of inotropic drugs. Gen Pharmacol. 1998 Sep; 31(3):415-8.

235. Nandi A, Kitamura Y, Kahn CR, Accili D. Mouse models of insulin resistance. Physiol Rev. 2004 Apr; 84(2):623-47.

236. National Diabetes Information Clearinghouse, National Institute of Diabetes and Digestive and Kidney Diseases – NDIC. NIH Publication No. 09–4893 October 2008. diabetes.niddk.nih.govndic@info.niddk.nih.gov. accessed: 10/2010

237. National Heart, Lung, and Blood Institute. Diseases and Conditions Index. Types of cardiomyopathy. 2009;

http://www.nhlbi.nih.gov/health/dci/Diseases/cm/cm_types.html. accessed: 10/2010

238. Negretti N, O'Neill SC, Eisner DA. The relative contributions of different intracellular and sarcolemmal systems to relaxation in rat ventricular myocytes. Cardiovasc Res. 1993 Oct; 27(10):1826-30.

239. National institute of health (NIH) PUBLICATION NO. 98-4083. The Evidence Report. SEPTEMBER 1998; www.nhlbi.nih.gov/guidelines/obesity/ob_gdlns.pdf. accessed: 10/2010

240. Nikoulina SE, Ciaraldi TP, Carter L, Mudaliar S, Park KS, Henry RR. Impaired muscle glycogen synthase in type 2 diabetes is associated with diminished phosphatidylinositol 3-kinase activation. J Clin Endocrinol Metab. 2001 Sep; 86(9):4307-14.

241. Nikoulina SE, Ciaraldi TP, Mudaliar S, Carter L, Johnson K, Henry RR. Inhibition of glycogen synthase kinase 3 improves insulin action and glucose metabolism in human skeletal muscle. Diabetes. 2002 Jul; 51(7):2190-8.

242. Nikoulina SE, Ciaraldi TP, Mudaliar S, Mohideen P, Carter L, Henry RR. Potential role of glycogen synthase kinase-3 in skeletal muscle insulin resistance of type 2 diabetes. Diabetes. 2000

243. Noble ME, Endicott JA, Johnson LN. Protein kinase inhibitors: insights into drug design from structure. Science. 2004 Mar 19; 303(5665):1800-5.

244. Nunes MT, Bianco AC, Migala A, Agostini B, Hasselbach W. Thyroxine induced transformation in sarcoplasmic reticulum of rabbit soleus and psoas muscles. Z Naturforsch C. 1985 Sep-Oct; 40(9-10):726-34.

245. O'Brien, R. M.; Granner D. K. Biochem. J. 1991, 278, 609-619.

246. Odermatt A, Taschner PE, Scherer SW, Beatty B, Khanna VK, Cornblath DR, Chaudhry V, Yee WC, Schrank B, Karpati G, Breuning MH, Knoers N, MacLennan DH. Characterization of the gene encoding human sarcolipin (SLN), a proteolipid associated with SERCA1: absence of structural mutations in five patients with Brody disease. Genomics. 1997 Nov 1; 45(3):541-53.

247. Omar MA, Wang L, Clanachan AS. Cardioprotection by GSK-3 inhibition: role of enhanced glycogen synthesis and attenuation of calcium overload. Cardiovasc Res. 2010 Jun 1; 86(3):478-86.

248. Opie LH. The metabolic vicious cycle in heart failure. Lancet 2004; 364:1733– 4

249. Ormerod JO, Ashrafian H, Frenneaux MP. Impaired energetics in heart failure, a new therapeutic target. Pharmacol Ther. 2008 Sep; 119(3):264-74.

250. Ormerod JOM, Ashrafian H, Frenneaux MP. Impaired energetics in heart failure — A new therapeutic target. Pharmacology & Therapeutics. 2008; 119: 264–274

251. Park KW, Yang HM, Youn SW, Yang HJ, Chae IH, Oh BH, Lee MM, Park YB, Choi YS, Kim HS, Walsh K. Constitutively active glycogen synthase kinase-3beta gene transfer sustains apoptosis, inhibits proliferation of vascular smooth muscle cells, and reduces neointima formation after balloon injury in rats. Arterioscler Thromb Vasc Biol. 2003 Aug 1; 23(8):1364-9.

252. Parker PJ, Caudwell FB, Cohen P. Glycogen synthase from rabbit skeletal muscle; effect of insulin on the state of phosphorylation of the seven phosphoserine residues in vivo. Eur J Biochem. 1983 Jan 17; 130(1):227-34.

253. Patel DS, Dessalew N, Iqbal P, Bharatam PV. Structure-based approaches in the design of GSK-3 selective inhibitors. Curr Protein Pept Sci. 2007 Aug; 8(4):352-64.

254. Patel S, Doble B, Woodgett JR. Glycogen synthase kinase-3 in insulin and Wnt signaling: a double-edged sword? Biochem Soc Trans. 2004 Nov; 32(Pt 5):803-8.

255. Paulsson M. Basement membrane proteins: structure, assembly, and cellular interactions. Crit Rev Biochem Mol Biol. 1992; 27(1-2):93-127.

256. Pearce NJ, Arch JR, Clapham JC, Coghlan MP, Corcoran SL, Lister CA, Llano A, Moore GB, Murphy GJ, Smith SA, Taylor CM, Yates JW, Morrison AD, Harper AJ, Roxbee-Cox L, Abuin A, Wargent E, Holder JC. Development of glucose intolerance in male transgenic mice overexpressing human glycogen synthase kinase-3β on a muscle-specific promoter. Metabolism. 2004 Oct; 53(10):1322-30.

257. Periasamy M, Bhupathy P, Babu GJ. Regulation of sarcoplasmic reticulum Ca^{2+} ATPase pump expression and its relevance to cardiac muscle physiology and pathology. Cardiovasc Res 2008; 77: 265–273.

258. Periasamy M, Huke S. SERCA pump level is a critical determinant of Ca^{2+} homeostasis and cardiac contractility. J Mol Cell Cardiol. 2001 Jun; 33(6):1053-63.

259. Periasamy M, Kalyanasundaram A. SERCA pump isoforms: their role in calcium transport and disease. Muscle Nerve. 2007 Apr; 35(4):430-42.

260. Periasamy M, Reed TD, Liu LH, Ji Y, Loukianov E, Paul RJ et al. Impaired cardiac performance in heterozygous mice with a null mutation in the

sarco(endo)plasmic reticulum Ca^{2+}-ATPase isoform 2 (SERCA2) gene. J Biol Chem. 1999; 274:2556–62

261. Perry SV. Vertebrate tropomyosin: distribution, properties and function. J Muscle Res Cell Motil. 2001; 22(1):5-49.

262. Peskoff A, Langer GA. Calcium concentration and movement in the ventricular cardiac cell during an excitation-contraction cycle. Biophys J. 1998 Jan; 74(1):153-74.

263. Philipson KD. The cardiac Na^+-Ca^{2+} exchanger: dependence on membrane environment. Cell Biol Int Rep. 1990 Apr; 14(4):305-9.

264. Plyte SE, Hughes K, Nikolakaki E, Pulverer BJ, Woodgett JR. Glycogen synthase kinase-3: functions in oncogenesis and development. Biochim Biophys Acta. 1992 Dec 16; 1114(2-3):147-62.

265. Poirier P, Després JP. [Impact of obesity in contemporary cardiology]. Med Sci (Paris). 2005 Dec; 21 Spec No: 3-9.

266. Poornima IG, Parikh P, Shannon RP. Diabetic cardiomyopathy: the search for a unifying hypothesis. Circ Res. 2006 Mar 17; 98(5):596-605.

267. Puoane T, Steyn K, Bradshaw D, Laubscher R, Fourie J, Lambert V, Mbananga N. Obesity in South Africa: the South African demographic and health survey. Obes Res. 2002 Oct; 10(10):1038-48.

268. Ramaswamy S, Nakamura N, Vazquez F, Batt DB, Perera S, Roberts TM, Sellers WR. Regulation of G1 progression by the PTEN tumor suppressor protein is linked to inhibition of the phosphatidylinositol 3-kinase/Akt pathway. Proc Natl Acad Sci U S A. 1999 Mar 2; 96(5):2110-5.

269. Rao R, Hao CM, Redha R, Wasserman DH, McGuinness OP, Breyer MD. Glycogen synthase kinase 3 inhibition improves insulin-stimulated glucose

metabolism but not hypertension in high-fat-fed C57BL/6J mice. Diabetologia. 2007 Feb; 50(2):452-60.

270. Rayment I, Holden HM, Whittaker M, Yohn CB, Lorenz M, Holmes KC, Milligan RA. Structure of the actin-myosin complex and its implications for muscle contraction. Science. 1993 Jul 2; 261(5117):58-65.

271. Reaven GM, Chang H, Hoffman BB, Azhar S. Resistance to insulin-stimulated glucose uptake in adipocytes isolated from spontaneously hypertensive rats. Diabetes. 1989 Sep; 38(9):1155-60.

272. Reaven GM. Bantin lecture 1988: Role of insulin resistance in human disease. Diabetes 37:1595–1607, 1988.

273. Reaven GM. Effect of variations in carbohydrate intake on plasma glucose, insulin, and triglyceride responses in normal subjects and patients with chemical diabetes. Adv Exp Med Biol. 1979; 119:253-62.

274. Richardson P, McKenna W, Bristow M, Maisch B, Mautner B, O'Connell J, Olsen E, Thiene G, Goodwin J, Gyarfas I, Martin I, Nordet P. Report of the 1995 World Health Organization/International Society and Federation of Cardiology Task Force on the Definition and Classification of cardiomyopathies. Circulation. 1996 Mar 1; 93(5):841-2.

275. Ring DB, Johnson KW, Henriksen EJ, Nuss JM, Goff D, Kinnick TR, Ma ST, Reeder JW, Samuels I, Slabiak T, Wagman AS, Hammond ME, Harrison SD. Selective glycogen synthase kinase 3 inhibitors potentiate insulin activation of glucose transport and utilization in vitro and in vivo. Diabetes. 2003 Mar; 52(3):588-95.

276. Roach PJ. Control of glycogen synthase by hierarchal protein phosphorylation. FASEB J. 1990 Sep; 4(12):2961-8.

277. Robinson TF, Factor SM, Sonnenblick EH. The heart as a suction pump. Sci Am. 1986 Jun; 254(6):84-91.

278. Rodriguez P, Kranias EG. Phospholamban: a key determinant of cardiac function and dysfunction. Arch Mal Coeur Vaiss. 2005 Dec; 98(12):1239-43.

279. Rothenberg PL, Lane WS, Karasik A, Backer J, White M, Kahn CR. Purification and partial sequence analysis of pp185, the major cellular substrate of the insulin receptor tyrosine kinase. J Biol Chem. 1991 May 5; 266(13):8302-11.

280. Ruben PC. Action Potentials: Generation and Propagation. J. Wiley, 2001; 10: 1038

281. Rubler S, Dlugash J, Yuceoglu YZ, Kumral T, Branwood AW, Grishman A. New type of cardiomyopathy associated with diabetic glomerulosclerosis. Am J Cardiol. 1972 Nov 8; 30(6):595-602.

282. Rylatt DB, Aitken A, Bilham T, Condon GD, Embi N, Cohen P. Glycogen synthase from rabbit skeletal muscle. Amino acid sequence at the sites phosphorylated by glycogen synthase kinase-3, and extension of the N-terminal sequence containing the site phosphorylated by phosphorylase kinase. Eur J Biochem. 1980 Jun; 107(2):529-37

283. Ryves WJ, Dajani R, Pearl L, Harwood AJ. Glycogen synthase kinase-3 inhibition by lithium and beryllium suggests the presence of two magnesium binding sites. Biochem Biophys Res Commun. 2002 Jan 25; 290(3):967-72.

284. Sachse FB, Moreno AP, Abildskov JA. Electrophysiological modeling of fibroblasts and their interaction with myocytes. Ann Biomed Eng. 2008 Jan; 36(1):41-56.

285. Saltiel AR, Kahn CR. Insulin signaling and the regulation of glucose and lipid metabolism. Nature. 2001 Dec 13; 414(6865):799-806.

286. Saltiel AR, Pessin JE. Insulin signaling in microdomains of the plasma membrane. Traffic. 2003 Nov; 4(11):711-6.

287. Saltiel, A.R. New perspectives into the molecular pathogenesis and treatment of type 2 diabetes. Cell 2001; 104, 517–529

288. Schmidt AG, Edes I, Kranias EG. Phospholamban: a promising therapeutic target in heart failure? Cardiovasc Drugs Ther. 2001 Sep; 15(5):387-96.

289. Schmidt AG, Gerst M, Zhai J, Carr AN, Pater L, Kranias EG, Hoit BD. Evaluation of left ventricular diastolic function from spectral and color M-mode Doppler in genetically altered mice. J Am Soc Echocardiogr. 2002 Oct; 15(10 Pt 1):1065-73.

290. Schmidt AG, Gerst M, Zhai J, Carr AN, Pater L, Kranias EG, Hoit BD. Evaluation of left ventricular diastolic function from spectral and color M-mode Doppler in genetically altered mice. J Am Soc Echocardiogr. 2002 Oct; 15(10 Pt 1):1065-73.

291. Schmidt HD, Koch M. Influence of perfusate calcium concentration on the inotropic insulin effect in isolated guinea pig and rat hearts. Basic Res Cardiol. 2002 Jul; 97(4):305-11.

292. Sears CE, Ashley EA, Casadei B. Nitric oxide control of cardiac function: is neuronal nitric oxide synthase a key component? Philos Trans R Soc Lond B Biol Sci. 2004 Jun 29; 359(1446):1021-44.

293. Sethi JK, Vidal-Puig AJ. Thematic review series: adipocyte biology. Adipose tissue function and plasticity orchestrate nutritional adaptation. J Lipid Res. 2007 Jun; 48(6):1253-62.

294. Shah A, Shannon RP. Insulin resistance in dilated cardiomyopathy.Rev Cardiovasc Med 2003; 4 Suppl 6:S50 –7.

295. Shannon TR, Chu G, Kranias EG, Bers DM. Phospholamban decreases the energetic efficiency of the sarcoplasmic reticulum Ca pump. J Biol Chem. 2001 Mar 9; 276(10):7195-201.

296. Shattock MJ. Phospholemman: its role in normal cardiac physiology and potential as a druggable target in disease. Curr Opin Pharmacol. 2009 Apr; 9(2):160-6.

297. Shaw PC, Davies AF, Lau KF, Garcia-Barcelo M, Waye MM, Lovestone S, Miller CC, Anderton BH. Isolation and chromosomal mapping of human glycogen synthase kinase-3 alpha and -3 beta encoding genes. Genome. 1998 Oct; 41(5):720-7.

298. Shepherd PR. Mechanisms regulating phosphoinositide 3-kinase signaling in insulin-sensitive tissues. Acta Physiol Scand. 2005 Jan; 183(1):3-12.

299. Shulman GI, Rothman DL, Jue T, Stein P, DeFronzo RA, Shulman RG. Quantitation of muscle glycogen synthesis in normal subjects and subjects with non-insulin-dependent diabetes by 13C nuclear magnetic resonance spectroscopy. N Engl J Med. 1990 Jan 25; 322(4):223-8.

300. Silverman BZ, Fuller W, Eaton P, Deng J, Moorman JR, Cheung JY, James AF, Shattock MJ. Serine 68 phosphorylation of phospholemman: acute isoform-specific activation of cardiac Na/K ATPase. Cardiovasc Res. 2005 Jan 1; 65(1):93-103.

301. Simmerman HK, Collins JH, Theibert JL, Wegener AD, Jones LR. Sequence analysis of phospholamban. Identification of phosphorylation sites and two major structural domains. J Biol Chem. 1986 Oct 5; 261(28):13333-41.

302. Simmerman HK, Jones LR. Phospholamban: protein structure, mechanism of action, and role in cardiac function. Physiol Rev. 1998 Oct; 78(4):921-47.

303. Simonides WS, Thelen MH, van der Linden CG, Muller A, van Hardeveld C. Mechanism of thyroid-hormone regulated expression of the SERCA genes in skeletal muscle: implications for thermogenesis. Biosci Rep. 2001 Apr; 21(2):139-54.

304. Simpson L, Li J, Liaw D, Hennessy I, Oliner J, Christians F, Parsons R. PTEN expression causes feedback upregulation of insulin receptor substrate 2. Mol Cell Biol. 2001 Jun; 21(12):3947-58.

305. Sodjinou R, Agueh V, Fayomi B, Delisle H. Obesity and cardio-metabolic risk factors in urban adults of Benin: relationship with socio-economic status, urbanisation, and lifestyle patterns. BMC Public Health. 2008 Mar 4; 8:84.

306. Sordahl LA, McCollum WB, Wood WG, Schwartz A. Mitochondria and sarcoplasmic reticulum function in cardiac hypertrophy and failure. Am J Physiol. 1973 Mar; 224(3):497-502.

307. Soria A, D'Alessandro ME, Lombardo YB. Duration of feeding on a sucrose-rich diet determines metabolic and morphological changes in rat adipocytes. J Appl Physiol. 2001 Nov; 91(5):2109-16.

308. South African National Standard: The Care and Use of Experimental Animals Standards SA. SANS 10386:200X – Latest version (2008)

309. Sparrow LG, McKern NM, Gorman JJ, Strike PM, Robinson CP, Bentley JD, Ward CW. The disulfide bonds in the C-terminal domains of the human insulin receptor ectodomain. J Biol Chem. 1997 Nov 21; 272(47):29460-7.

310. Spittaels K, Van den Haute C, Van Dorpe J, Geerts H, Mercken M, Bruynseels K, Lasrado R, Vandezande K, Laenen I, Boon T, Van Lint J,

Vandenheede J, Moechars D, Loos R, Van Leuven F. Glycogen synthase kinase-3beta phosphorylates protein tau and rescues the axonopathy in the central nervous system of human four-repeat tau transgenic mice. J Biol Chem. 2000 Dec 29; 275(52):41340-9.

311. Spudich JA, Huxley HE, Finch JT. Regulation of skeletal muscle contraction. II. Structural studies of the interaction of the tropomyosin-troponin complex with actin. J Mol Biol. 1972 Dec 30; 72(3):619-32.

312. Stambolic V, Ruel L, Woodgett JR. Lithium inhibits glycogen synthase kinase-3 activity and mimics wingless signaling in intact cells. Curr Biol. 1996 Dec 1; 6(12):1664-8.

313. Stanley JR, Woodley DT, Katz SI, Martin GR. Structure and function of basement membrane. J Invest Dermatol. 1982 Jul; 79 Suppl 1:69s-72s.

314. Stanley WC, Recchia FA, Lopaschuk GD. Myocardial substrate metabolism in the normal and failing heart. Physiol Rev. 2005 Jul; 85(3):1093-129.

315. Stokoe D, Stephens LR, Copeland T, Gaffney PR, Reese CB, Painter GF, Holmes AB, McCormick F, Hawkins PT. Dual role of phosphatidylinositol-3,4,5-trisphosphate in the activation of protein kinase B. Science. 1997 Jul 25; 277(5325):567-70.

316. Storgaard H, Song XM, Jensen CB, Madsbad S, Björnholm M, Vaag A, Zierath JR. Insulin signal transduction in skeletal muscle from glucose-intolerant relatives of type 2 diabetic patients [corrected]. Diabetes. 2001 Dec; 50(12):2770-8. Erratum in: Diabetes 2002 Feb; 51(2):552.

317. Svetlana E. Nikoulina,[1,2] Theodore P. Ciaraldi,[1,2] Sunder Mudaliar,[1,2] Leslie Carter,[1,2] Kirk Johnson,[3] and Robert R. Henry[1,2]. Inhibition of

Glycogen Synthase Kinase 3 Improves Insulin Action and Glucose Metabolism in Human Skeletal Muscle. Diabetes 2002; 51:2190–2198.

318. Sweadner KJ, Donnet C. Structural similarities of Na,K-ATPase and SERCA, the Ca^{2+}-ATPase of the sarcoplasmic reticulum. Biochem J. 2001 Jun 15; 356(Pt 3):685-704.

319. Tada M, Kirchberger MA, Katz AM. Phosphorylation of a 22,000-dalton component of the cardiac sarcoplasmic reticulum by adenosine 3':5'-monophosphate-dependent protein kinase. J Biol Chem. 1975 Apr 10; 250(7):2640-7.

320. Tada M, Kirchberger MA, Repke DI, Katz AM. The stimulation of calcium transport in cardiac sarcoplasmic reticulum by adenosine 3':5'-monophosphate-dependent protein kinase. J Biol Chem. 1974 Oct 10; 249(19):6174-80.

321. Tada M, Toyofuku T. Molecular regulation of phospholamban function and expression. Trends Cardiovasc Med. 1998 Nov; 8(8):330-40.

322. Tada M, Yamada M, Kadoma M, Inui M, Ohmori F. Calcium transport by cardiac sarcoplasmic reticulum and phosphorylation of phospholamban. Mol Cell Biochem. 1982 Jul 23; 46(2):73-95.

323. Taegtmeyer H, Hems R, Krebs HA. Utilization of energy-providing substrates in the isolated working rat heart. Biochem J. 1980 Mar 15; 186(3):701-11.

324. Taegtmeyer H. Switching metabolic genes to build a better heart. Circulation 2002;106:2043–

325. Tajsharghi H. Thick and thin filament gene mutations in striated muscle diseases. Int J Mol Sci. 2008 Jun; 9(7):1259-75. Epub 2008 Jul 16.

326. Takeda N. Cardiac disturbances in diabetes mellitus. Pathophysiology. 2010 Apr; 17(2):83-8

327. Territo PR, French SA, Dunleavy MC, Evans FJ, Balaban RS. Calcium activation of heart mitochondrial oxidative phosphorylation: rapid kinetics of mVO2, NADH, AND light scattering. J Biol Chem. 2001 Jan 26; 276(4):2586-99.

328. Thiene G, Corrado D, Basso C. Revisiting definition and classification of cardiomyopathies in the era of molecular medicine. Eur Heart J. 2008 Jan; 29(2):144-6. Epub 2007 Dec 22.

329. Thirone AC, Huang C, Klip A. Tissue-specific roles of IRS proteins in insulin signaling and glucose transport. Trends Endocrinol Metab. 2006 Mar; 17(2):72-8.

330. Tikunova SB, Rall JA, Davis JP. Effect of hydrophobic residue substitutions with glutamine on Ca^{2+} binding and exchange with the N-domain of troponin C. Biochemistry. 2002 May 28; 41(21):6697-705.

331. Timpl R. Molecular aspects of basement membrane structure. Prog Clin Biol Res. 1985; 171:63-74.

332. Toriumi C, Imai K. Determination of insulin in a single islet of Langerhans by high-performance liquid chromatography with fluorescence detection. Anal Chem. 2002 May 15; 74(10):2321-7.

333. Toyofuku T, Kurzydlowski K, Tada M, MacLennan DH. Amino acids Lys-Asp-Asp-Lys-Pro-Val402 in the Ca^{2+}-ATPase of cardiac sarcoplasmic reticulum are critical for functional association with phospholamban. J Biol Chem. 1994 Sep 16; 269(37):22929-32.

334. Trafford AW, Lederer WJ, Sobie EA. Keeping the beat: life without SERCA--is it possible? J Mol Cell Cardiol. 2009 Aug; 47(2):171-3.

335. Van Hoeven KH, Factor SM. A comparison of the pathological spectrum of hypertensive, diabetic, and hypertensive-diabetic heart disease. Circulation. 1990 Sep; 82(3):848-55.

336. Van Obberghen E, Baron V, Delahaye L, Emanuelli B, Filippa N, Giorgetti-Peraldi S, Lebrun P, Mothe-Satney I, Peraldi P, Rocchi S, Sawka-Verhelle D, Tartare-Deckert S, Giudicelli J. Surfing the insulin signaling web. Eur J Clin Invest. 2001 Nov; 31(11):966-77.

337. Van Wauwe J, Haefner B. Glycogen synthase kinase-3 as drug target: from wallflower to center of attention. Drug News Perspect. 2003 Nov; 16(9):557-65.

338. van Weeren PC, de Bruyn KM, de Vries-Smits AM, van Lint J, Burgering BM. Essential role for protein kinase B (PKB) in insulin-induced glycogen synthase kinase 3 inactivation. Characterization of dominant-negative mutant of PKB. J Biol Chem. 1998 May 22; 273(21):13150-6.

339. Vanhaesebroeck B, Alessi DR. The PI3K-PDK1 connection: more than just a road to PKB. Biochem J. 2000 Mar 15; 346 Pt 3:561-76.

340. Vetter R, Rehfeld U, Reissfelder C, Weiss W, Wagner KD, Günther J, Hammes A, Tschöpe C, Dillmann W, Paul M. Transgenic overexpression of the sarcoplasmic reticulum Ca^{2+}ATPase improves reticular Ca^{2+} handling in normal and diabetic rat hearts. FASEB J. 2002 Oct; 16(12):1657-9.

341. Vittorini S, Storti S, Parri MS, Cerillo AG, Clerico A. SERCA2a, phospholamban, sarcolipin, and ryanodine receptors gene expression in

children with congenital heart defects. Mol Med. 2007 Jan-Feb; 13(1-2):105-11.

342. Vollenweider P, Ménard B, Nicod P. Insulin resistance, defective insulin receptor substrate 2-associated phosphatidylinositol-3' kinase activation, and impaired atypical protein kinase C (zeta/lambda) activation in myotubes from obese patients with impaired glucose tolerance. Diabetes. 2002 Apr; 51(4):1052-9.

343. Wahler GM. Cardiac action potentials.Cell. Heart Physiology and Pathophysiology. Chapter 10, 2001b; Fourth edition: 199-211.

344. Wahler GM. Cardiac action potentials.Cell. Physiology sourcebook. A molecular approach. Chapter 52, 2001a; Third edition: 887-98.

345. Wahler GM. Developmental increases in the inwardly rectifying potassium current of rat ventricular myocytes. Am J Physiol. 1992 May; 262(5 Pt 1):C1266-72.

346. Walker CA, Spinale FG. The structure and function of the cardiac myocyte: a review of fundamental concepts. J Thorac Cardiovasc Surg. 1999 Aug; 118(2):375-82.

347. Wang CC, Goalstone ML, Draznin B. Molecular mechanisms of insulin resistance that impact cardiovascular biology. Diabetes. 2004 Nov; 53(11):2735-40.

348. Waters SB, Pessin JE. Insulin receptor substrate 1 and 2 (IRS1 and IRS2): what a tangled web we weave. Trends Cell Biol. 1996 Jan;6(1):1-4.

349. Waters SB, Yamauchi K, Pessin JE. Functional expression of insulin receptor substrate-1 is required for insulin-stimulated mitogenic signaling. J Biol Chem. 1993 Oct 25; 268(30):22231-4.

350. Waters SB, Yamauchi K, Pessin JE. Functional expression of insulin receptor substrate-1 is required for insulin-stimulated mitogenic signaling. J Biol Chem. 1993 Oct 25; 268(30):22231-4.

351. Weber CR, Piacentino V 3rd, Ginsburg KS, Houser SR, Bers DM. Na$^+$-Ca^{2+} exchange current and submembrane [Ca^{2+}] during the cardiac action potential. Circ Res. 2002 Feb 8; 90(2):182-9.

352. Weir GC, Bonner-Weir S. Five stages of evolving beta-cell dysfunction during progression to diabetes. Diabetes. 2004 Dec; 53 Suppl 3:S16-21.

353. Wells JC, Cole TJ, Treleaven P. Age-variability in body shape associated with excess weight: the UK National Sizing Survey. Obesity (Silver Spring). 2008 Feb; 16(2):435-41.

354. Wexler RK, Elton T, Pleister A, Feldman D. Cardiomyopathy: an overview. Am Fam Physician. 2009 May 1; 79(9):778-84.

355. White MF, Maron R, Kahn CR. Insulin rapidly stimulates tyrosine phosphorylation of a Mr-185,000 protein in intact cells. Nature. 1985 Nov 14-20; 318(6042):183-6.

356. White MF. IRS proteins and the common path to diabetes. Am J Physiol Endocrinol Metab. 2002 Sep; 283(3):E413-22.

357. Whitehead JP, Clark SF, Urso B, James DE. Signaling through the insulin receptor. Curr Opin Cell Biol. 2000 Apr; 12(2):222-8.

358. Whitmer JT, Kumar P, Solaro RJ. Calcium transport properties of cardiac sarcoplasmic reticulum from cardiomyopathic Syrian hamsters (BIO 53.58 and 14.6): evidence for a quantitative defect in dilated myopathic hearts not evident in hypertrophic hearts. Circ Res. 1988 Jan; 62(1):81-5.

359. Williams JH. Contractile apparatus and sarcoplasmic reticulum function: effects of fatigue, recovery, and elevated Ca2+. J Appl Physiol. 1997 Aug; 83(2):444-50.

360. Williams R, Ryves WJ, Dalton EC, Eickholt B, Shaltiel G, Agam G, Harwood AJ. A molecular cell biology of lithium. Biochem Soc Trans. 2004 Nov; 32(Pt 5):799-802.

361. Wold LE, Dutta K, Mason MM, Ren J, Cala SE, Schwanke ML, Davidoff AJ. Impaired SERCA function contributes to cardiomyocyte dysfunction in insulin resistant rats. J Mol Cell Cardiol. 2005 Aug; 39(2):297 -307.

362. Wolk R. Arrhythmogenic mechanisms in left ventricular hypertrophy. Europace. 2000 Jul; 2(3):216-23.

363. Woodcock EA, Matkovich SJ. Cardiomyocytes structure, function and associated pathologies. International Journal of Biochemistry & Cell Biology. 2005; 37: 1746–1751

364. Woodgett JR, Plyte SE, Pulverer BJ, Mitchell JA, Hughes K. Roles of glycogen synthase kinase-3 in signal transduction. Biochem Soc Trans. 1993 Nov; 21(4):905-7.

365. Woodgett JR. Judging a protein by more than its name: GSK-3. Sci STKE. 2001 Sep 18; 2001(100):re12.

366. Woodgett JR. Molecular cloning and expression of glycogen synthase kinase-3/factor A. EMBO J. 1990 Aug; 9(8):2431-8.

367. Woodgett JR. Physiological roles of glycogen synthase kinase-3: Potential as a therapeutic target for diabetes and other disorders. Curr Drug Targets Immune Endocr Metabol Disord 2003; 3: 281–290.

368. Woodgett JR. Regulation and functions of the glycogen synthase kinase-3 subfamily. Semin Cancer Biol. 1994 Aug; 5(4):269-75.

369. Wuytack F, Papp B, Verboomen H, Raeymaekers L, Dode L, Bobe R, Enouf J, Bokkala S, Authi KS, Casteels R. A sarco/endoplasmic reticulum Ca^{2+}-ATPase 3-type Ca^{2+} pump is expressed in platelets, in lymphoid cells, and in mast cells. J Biol Chem. 1994 Jan 14; 269(2):1410-6.

370. Xavier IJ, Mercier PA, McLoughlin CM, Ali A, Woodgett JR, Ovsenek N. Glycogen synthase kinase 3beta negatively regulates both DNA-binding and transcriptional activities of heat shock factor 1. J Biol Chem. 2000 Sep 15; 275(37):29147-52.

371. Yamada T, Inashima S, Matsunaga S, Nara I, Kajihara H, Wada M. Different time course of changes in sarcoplasmic reticulum and myosin isoforms in rat soleus muscle at early stage of hyperthyroidism. Acta Physiol Scand. 2004 Jan; 180(1):79-87.

372. Yamada, N. et al. Increased risk factors for coronary artery disease in Japanese subjects with hyperinsulinemia or glucose intolerance. Diabetes Care 1994; 17, 107–114

373. Yang ZZ, Tschopp O, Baudry A, Dümmler B, Hynx D, Hemmings BA. Physiological functions of protein kinase B/Akt. Biochem Soc Trans. 2004 Apr; 32(Pt 2):350-4.

374. Young ME, McNulty P, Taegtmeyer H. Adaptation and maladaptation of the heart in diabetes: part II: potential mechanisms. Circulation 2002; 105:1861–70.

375. Zarain-Herzberg A, Marques J, Sukovich D, Periasamy M. Thyroid hormone receptor modulates the expression of the rabbit cardiac sarco (endo) plasmic reticulum Ca^{2+}-ATPase gene. J Biol Chem. 1994 Jan 14; 269(2):1460-7.

376. Zaza A. Control of the cardiac action potential: The role of repolarization dynamics. J Mol Cell Cardiol. 2010 Jan; 48(1):106-11.

377. Zellner JL, Spinale FG, Eble DM, Hewett KW, Crawford FA Jr. Alterations in myocyte shape and basement membrane attachment with tachycardia-induced heart failure. Circ Res. 1991 Sep; 69(3):590-600.

378. Zhang W, DePaoli-Roach AA, Roach PJ. Mechanisms of multisite phosphorylation and inactivation of rabbit muscle glycogen synthase. Arch Biochem Biophys. 1993 Jul; 304(1):219-25.

379. Zhao W, Uehara Y, Chu G, Song Q, Qian J, Young K, Kranias EG. Threonine-17 phosphorylation of phospholamban: a key determinant of frequency-dependent increase of cardiac contractility. J Mol Cell Cardiol. 2004 Aug; 37(2):607-12.

380. Zvaritch E, Backx PH, Jirik F, Kimura Y, de Leon S, Schmidt AG, Hoit BD, Lester JW, Kranias EG, MacLennan DH. The transgenic expression of highly inhibitory monomeric forms of phospholamban in mouse heart impairs cardiac contractility. J Biol Chem. 2000 May 19; 275(20):14985-91.